HERIOT WATT UNIVERSITY

Studies on the WFDC-domain-containing Protein, Carcinin

Suzanne Suleiman

A thesis submitted for the degree of

Doctor of Philosophy

School of Energy, Geoscience, Infrastructure and Society

Heriot-Watt University

Edinburgh, UK

February, 2018

Abstract

The whey acidic four-disulphide core (WFDC) domain-containing proteins are a diverse group of antimicrobials and/or anti-proteases, widespread throughout animal taxa. Carcinin was the first WFDC-domain containing protein to be isolated from a marine invertebrate on the basis of its antibacterial properties, and is the prototypic member of a large WFDC family, designated as the crustins. The previous research conducted on carcinin did not sufficiently reveal its vital role, despite its high abundance in haemolymph. In addition, the vast majority of reported crustins were investigated by studying gene transcripts and/or producing the recombinant peptide via simple bacterial expression systems. These approaches did not give the required knowledge regarding the biological role of these peptides that were assumed to be multifunctional. The present study aimed to optimise a purification method to increase the yield of the isolated pure carcinin. A specific polyclonal antibody was raised against the native peptide, being the first specific antibody against crustin to be employed to investigate the immune staining in various tissues and organs. In addition, the native purified carcinin was employed in functional studies to investigate its involvement in host defence reactions. Carcinin was detected mainly in the haemocytes, and was secreted from these cells to support the immunological functions of various tissues. A unique deposition of carcinin was detected in the gonads and the eyestalk, showing a distinct presence through different maturation stages and its importance for the regenerating tissues. Carcinin was found to affect the viability of bacterial cells by inducing pore formation. Furthermore, carcinin was shown to support phagocytosis as an opsonin, and to aid the elimination of unwanted particles including bacteria and defective cells. This study succeeded in revealing the multifunctionality of carcinin, and emphasized the importance of utilising the native protein in the characterization of novel antimicrobial peptides.

To my family

Acknowledgments

First of all, I owe my deepest gratitude to my primary supervisor, Dr Elisabeth Dyrynda in Heriot-Watt University for her continuous support and motivation of my Ph.D, and for allowing me to grow as a research scientist. Her guidance helped me at all times of research and writing of this thesis. Without her immense knowledge, advice and patience, it would not have been possible to complete this project.

Secondly, I would like to express my sincere appreciation to my co-supervisor Dr Valerie Smith (University of St. Andrews) for her priceless help and advice. I greatly appreciate her insightful discussions and suggestions, and her answers to my questions. Her support has been essential to all parts of this project.

I would also like to deeply thank Prof. Peter Morris (Heriot-Watt University) for his huge support. In particular his kindness in allowing me to carry out part of my research in his lab. Without this, an essential section of this project would not have materialised.

Special thanks to my previous colleague Dr. Calum Robb (Edinburgh University) for his great help in lab techniques and experiments, especially at the beginning of my PhD.

In addition, I acknowledge the help of many members of staff at Heriot-Watt University, namely Mrs Margaret Stobie for her assistance in maintenance of the aquarium facility, preparation of tissue sections, and microscopy techniques; Dr Jane Polglase and Dr Loris Fossier for their advice and help with thaustochytrid culture; Prof. Ted Henry and Dr Alastair Lyndon for their advice in statistical analysis; Dr David Brown and Mr Mark Leonard for their support in scanning electron microscopy experiments; Prof. Stephen Euston for help with confocal microscopy; Ms Saioa Ilincheta for her help with the bacterial cultures; Mr Sean McMenamy for supplying the experimental animals; Mr McMenamy and Mr Mohammad Ali Salik for advice in interpreting mass spectrometry results.

I am also grateful for the financial support of my sponsor, the Capacity Building Project between the Ministry of Higher Education in Syria and the British Council. Likewise, I deeply appreciate the Heriot-Watt alumni office for granting me an Alumni Office bursary in 2014. I would also like to thank the International Society for Developmental

& Comparative Immunology for providing a bursary allowing me to attend their 13th Congress in 2015 at Murcia, Spain.

Furthermore, very warm regards to all my friends and all the lovely people I met in this wonderful country. Thank you for standing by me and for all the precious moments that help me carry on despite all stressful times.

Finally, my warmest thanks go to my family members; mainly a great big heartfelt thank you to my husband for his unconditional love and support throughout all the years of my PhD study. My little angel, Natalie, I could not imagine all those years without her being my soul mate. My brother and sisters, thanks for all your love and devotion. My parents, thanks for all your great sacrifices and all you have done for me throughout my life.

Thanks immensely to everyone who believed in me.

Suzanne.

Declaration statement

ACADEMIC REGISTRY

Research Thesis Submission

Name*:*	Suzanne Suleiman		
School:	EGIS		
Version: *(i.e. First, Resubmission, Final)*	Final submission	Degree Sought:	Ph.D

Declaration

In accordance with the appropriate regulations I hereby submit my thesis and I declare that:

1) the thesis embodies the results of my own work and has been composed by myself
2) where appropriate, I have made acknowledgement of the work of others and have made reference to work carried out in collaboration with other persons
3) the thesis is the correct version of the thesis for submission and is the same version as any electronic versions submitted*.
4) my thesis for the award referred to, deposited in the Heriot-Watt University Library, should be made available for loan or photocopying and be available via the Institutional Repository, subject to such conditions as the Librarian may require
5) I understand that as a student of the University I am required to abide by the Regulations of the University and to conform to its discipline.
6) I confirm that the thesis has been verified against plagiarism via an approved plagiarism detection application e.g. Turnitin.

* *Please note that it is the responsibility of the candidate to ensure that the correct version of the thesis is submitted.*

Signature of Candidate*:*		Date:	

Submission

Submitted By *(name in capitals):*	SUZANNE SULEIMAN
Signature of Individual Submitting:	
Date Submitted:	

For Completion in the Student Service Centre (SSC)

Received in the SSC by *(name in capitals):*			
Method of Submission *(Handed in to SSC; posted through internal/external mail):*			
E-thesis Submitted (**mandatory for final theses)**			
Signature:		Date:	

Table of Contents

List of Tables

List of Figures

List of abbreviations and symbols

$^{o}/_{oo}$	parts per thousand
3D	three-dimensional
5-HT	5-hydroxytriptamine
β-GBP	β-1,3-glucan-binding protein
™	trademark
x *g*	multiples of gravity
Ab	antibody
AGH	androgenic gland hormone
ALF(s)/ALPF(s)	anti-lipopolysaccharide factor(s)
AMP(s)	antimicrobial peptide(s)
ANOVA	analysis of variance
AP	alkaline phosphate
APD	antimicrobial peptide database
BCIP	5-bromo-4-chloroindolyl phosphate
BLAST	basic local alignment search tool
BSA	bovine serum albumin
cDNA	complementary DNA
CFU	colony-forming unit
Da	unified atomic mass unit or dalton
DAB	3,3′-diaminobenzidine
DAPI	4',6-diamidino-2-phenylindole
dH2O	distilled water
DMSO	dimethylsulfoxide
DNA	deoxyribonucleic acid
DOc	degenerating oocytes
DSCAM	Down syndrome cell adhesion molecules
dsRNA	double stranded RNA
DTT	1,4-Dithiothreitol
EDTA	ethylenediaminetetraacetic acid
Eppin	epididymal protease inhibitor
EST	expressed sequence tag
ETosis	extracellular trap formation
FDC	four-disulphide core

FITC	fluorescein isothiocyanate
FPLC	fast protein liquid chromatography
GC(s)	granular cell(s)
gDNA	genomic DNA
GIH	gonad-inhibiting hormone
GSI	gonado-somatic index
H2A	histone H2A
H&E	haematoxylin and eosin
HC(s)	hyaline cell(s)
HDL	high density lipoprotein
HE4	human epididymis protein 4
HGNC	HUGO gene nomenclature committee
HIV-1	human immunodeficiency virus -1
HLS	haemocyte lysate solution
HMDS	hexamethyldisilazane
HPLC	high performance liquid chromatography
HUGO	human genome organisation
ICC	immunocytochemistry
IHC	immunohistochemistry
IL-8	Interleukin-8
InEPTs	invertebrate extracellular phagocyte traps
kDa	kilo Dalton
Ku-wap-fusins	kunitz waprin fusion protein
LGBP	lipopolysaccharide- and β-1,3-glucan-binding protein
LPS	lipopolysaccharide
MAC	marine anticoagulant
MC-BHB	Mar Chiquita—brain heart broth medium
MIC	minimum inhibitory concentration
MIH	moult-inhibiting hormone
ML-15	salt-modified Leibovitz’s L-15 medium
MO	mandibular organ
mOc	mature oocyte
MOIH	mandibular organ-inhibiting hormone
MPO	myeloperoxidase
mRNA	messenger RNA

N	number of replicates
NADPH	the reduced form of nicotinamide adenine dinucleotide phosphate
NBT	nitroblue tetrazolium
NCBI	National Center for Biotechnology Information
NE	neutrophil elastase
NET(s)	neutrophil extracellular trap(s)
NETosis	neutrophil extracellular traps formation
NFκB	nuclear factor kappa-light-chain-enhancer of activated B cells
nL9C-ESI-MSMS	nano-scale liquid chromatographic electrospray tandem mass spectrometry
Oc	oocyte
OD	optical density
P	probability
PAb	polyclonal Ab
PAMPs	pathogen associated molecular patterns
PBS	phosphate buffered saline
PFA	paraformaldehyde
PI3	proteinase inhibitor 3
PMA	phorbol 12-myristate 13-acetate
PMSF	phenylmethanesulfonyl fluoride
ppA	phenoloxidase activating enzyme
ProH(s)	pro-haemocyte(s)
proPO	prophenoloxidase
PRRs	pattern recognition receptors
PXN	peroxinectin
RNA	ribonucleic acid
RNAi	RNA interference
ROS	reactive oxygen species
R-P HPLC	reverse-phase high performance liquid chromatography
SDS	sodium dodecyl sulphate
SDS/PAGE	sodium dodecyl sulphate polyacrylamide gel electrophoresis
SEM	scanning electron microscopy
SGC(s)	semi-granular cell(s)
SLPI	secretory leukocyte protease inhibitor
SSPB	salt amended sodium phosphate buffer

SD	standard deviation
TBS	Towbin buffer with SDS
TEMED	tetramethylethylenediamine
TGF- β	tumour growth factor-β
TNF-α	tumour necrosis factor-α
Tukey HSD	Tukey honestly significant difference
UmodL1	uromodulin like 1
UV	ultraviolet
VGNC	vertebrate gene nomenclature committee
VLDL	very low density lipoprotein
WAP	whey acidic protein
WFDC	whey/four-disulphide core
XO	medulla terminalis ganglionic X-organ
XO/SG	the X organ/sinus gland complex

Publications and Presentations

Publications

Suleiman, S., Smith, V. J. and Dyrynda, E. A. (2017) Unusual tissue distribution of carcinin, an antibacterial crustin, in the crab, *Carcinus maenas*, reveals its multi-functionality. *Developmental and Comparative Immunology* 76, 274-284.

Suleiman. S, Smith. V. J, Dyrynda. E. A. Carcinin, a whey four-disulphide core (WFDC) domain-containing-protein, plays multiple roles in the defence responses to bacteria in the decapod crustacean, *Carcinus maenas*. In prep, to be submitted to *Developmental and Comparative Immunology*.

Poster Presentations

Suleiman, S., Smith, V. J. and Dyrynda, E. A. (2015) Immunological and other functions of WAP (whey acidic protein) domain containing proteins in decapod Crustaceans, *XIII Congress of the International Society of Developmental and Comparative Immunology*, Murcia, Spain, 28 Jun - 3 Jul.

Suleiman, S., Smith, V. J. and Dyrynda. E. A. (2014) The Multifunctionality of WAP (whey acidic protein) domain containing protein from the shore crab *Carcinus maenas*, *Postgraduate Student Conference***,** School of Life Sciences, Heriot-Watt University, Edinburgh, UK, 12 Dec-14 Dec.

Chapter 1

General Introduction

1.1. The whey/four-disulphide core (WFDC)-domain-containing proteins

The present work explored the localisation and possible functions of a WAP/WFDC-domain containing protein in a marine invertebrate, namely, the crab, *Carcinus maenas*. This group of proteins is extremely widespread throughout taxa and very diverse in terms of structure and function, with much unknown about them, particularly outside mammalian species. Therefore, the primary goal of this project was to obtain more knowledge about the WFDC-domain containing protein, carcinin, which was the first to be discovered from a marine invertebrate (Relf *et al.*, 1999).

The name whey acidic protein (WAP) came from the discovery of these proteins in milk, with the major whey protein from mouse milk being designated as the prototypical peptide of this family. The mouse peptide was first described by Piletz *et al*. in 1981 as an acidic, cysteine rich peptide with 14 kDa molecular weight. The domain, however, is not restricted to milk, and WFDC domain proteins are found throughout the animal kingdom and in many different molecules. Hennighausen and Sippel in 1982 found that the WFDC domain was shared among proteins from several diverse sources, including wheat germ agglutinin, snake venom neurotoxin, ragweed pollen allergen and neurophysin.

Through surveying a large number of four-disulphide core (FDC) domains in a wide range of species, Ranganathan *et al.* (1999) designated the structure of this domain in the PROSITE database (entry number PS51390), as having eight-conserved cysteines, as per the following:

C_1-(X*n*)-C_2-(X*n*)-C_3-(X5)-C_4-(X5)-C_5-C_6-(X3,X4)-C_8

(X represents any amino acid residue, n is the number of the X residues).

The WFDC-domain-containing protein family was described by Bingle (2011) as a group of polypeptides which share at least one characteristic cysteine-rich domain composed of 40-50 amino acids with a conserved arrangement. The cysteine residues are coiled into disulphide bridges in a conservative manner in all proteins of this family. The number of cysteine residues, and the subsequent intra-molecular disulphide bridges, is not consistent among peptides of this family. For example, the second cysteine is

absent in mouse UmodL1 (Di Shiavi *et al*., 2005), although like other similar peptides, still considered a genuine WFDC protein because of the preservation of the remaining cysteine residues (Bingle, 2011).

Over recent years, the number of WFDC sequences reported has risen considerably, with more than 6000 identified in the last six years alone. According to GenBank® nucleotide sequences, there are 8017 hits for 'WAP domain' at the time of writing, including 7837 from the animal kingdom (Figure 1.1). The high numbers of newly discovered sequences reflect the increasing interest in this protein family. According to the HUGO Gene Nomenclature Committee (HGNC), there are 18 known genes encoding WFDC proteins in humans (http://www.genenames.org/), reviewed by Bingle and Vyakarnam (2008). Among these, only a few have been extensively studied at the protein level, namely; secretory leukocyte peptidase inhibitor (SLPI), trappin/elafin, WFDC2 and eppin (Table 1.1). Outside of humans, 22 WFDC genes have been identified in other mammals according to the Vertebrate Gene Nomenclature Committee (VGNC) (http://vertebrate.genenames.org/). What is clear from the distribution across animal taxa is that over half the sequences lodged in GenBank® come from mammals, yet only 22% from invertebrates. Although invertebrates comprise over 95% of all known animal species, the apparently low percentage is probably reflective of research effort devoted to the different groups. This is further illustrated by comparing distribution amongst only invertebrate phyla (Fig. 1.1B), where over 50% of sequences are recorded from arthropods. This phylum includes economically important (crustacean) and medically important (insect) groups, thus again is likely to be mirroring research intensity.

Due to the large diversity of this family, adapting a particular grouping model has proved difficult. According to Smith (2011), WFDC-domain containing proteins in lower vertebrates/invertebrates could be categorized into five sub-groups: (i) waprins; (ii) chelonianins (both isolated from reptiles); (iii) perlwapins; (iv) lustrin A (both from molluscs); and (v) crustins from crustaceans. This classification depends mainly on the species from which peptides were isolated, in addition to the identified protein structure. The key characters and functions of these proteins are summarized in Table 1.2.

A

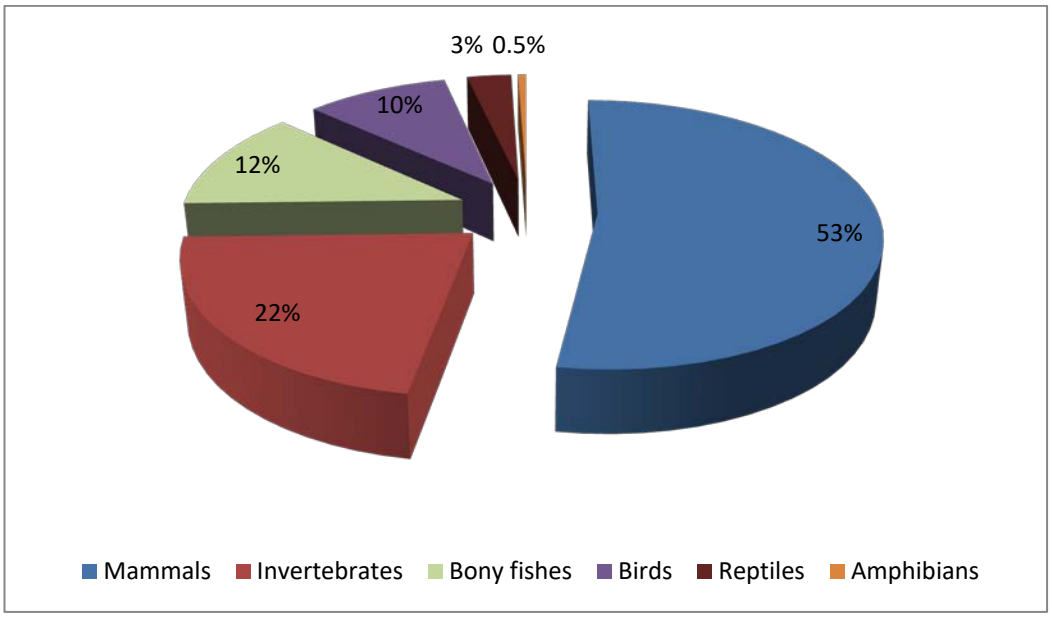

B

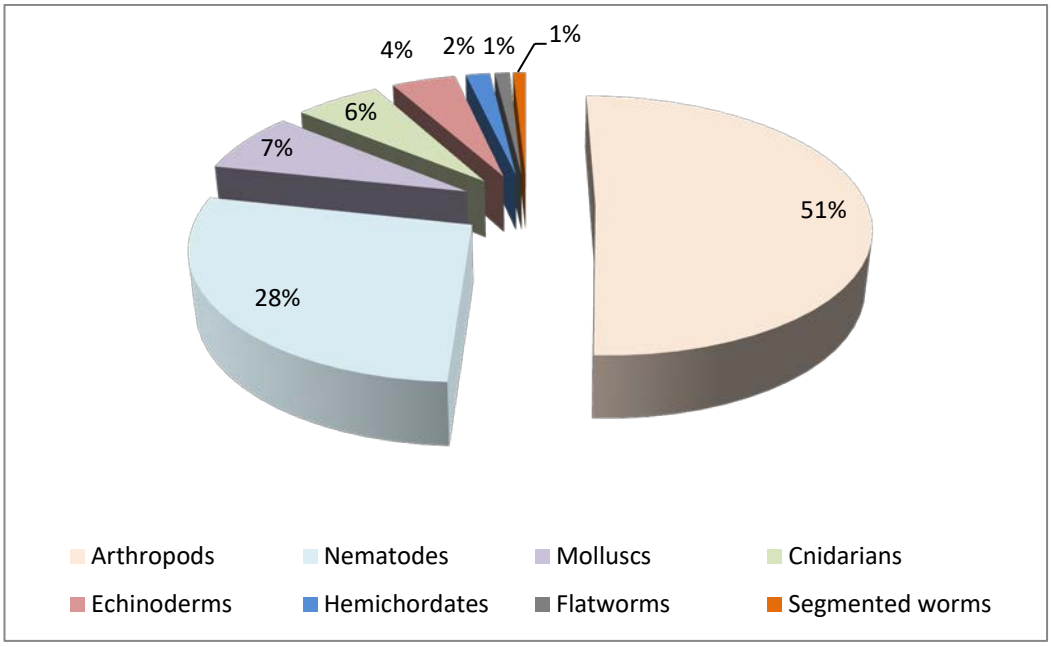

Figure 1.1: Percentages of hits for 'WAP domain' in the GenBank® Nucleotide Sequence Database in different taxa in the animal kingdom (A) and in invertebrates (B). Data is based on 6121 hits for vertebrates, and 1716 hits for invertebrates, correct at time of writing.

Table 1.1: Summary of the best-studied WFDC-domain containing proteins in humans.

WFDC protein		Functional domains	Localisation/expression	Activity and function	Key references
SLPI **MW (kDa)** **No amino acids**	 11.7 107	Two WFDC domains	Mucosal epithelial cells, macrophages and neutrophils	Antibacterial, protease inhibitor antifungal, anti-inflammatory. Interferes with signal transduction pathways, and regulates extracellular chromatin trap formation	Thompson and Ohlsson, 1986 Wiedow *et al*., 1998 Mihaila and Tremblay, 2001 Taggart *et al*., 2005 Fahey and Wira, 2002 Curvelo *et al.*, 2014 Mikami *et al*., 2015
Elafin/ PI3 **MW (kDa)** **No amino acids**	 6 117	Single WFDC domain	Psoriatic skin, bronchial secretions, macrophages and neutrophils	Inhibits neutrophil elastase and proteinase-3, has antimicrobial and immunomodulatory roles	Wiedow *et al.*, 1990 Sallenave *et al.*, 1994 Simpson *et al*., 1999 Mihaila and Tremblay 2001 Guyot *et al*., 2005 Williams *et al*., 2006 Moreau *et al*., 2008
HE4/ WFDC2 **MW (kDa)** **No amino acids**	 25 124	Two WFDC domains	Human epididymis, lung, kidney, salivary gland, also in cancerous tissues, such as ovary and lung cancers	Interacts with trypsin, chymotrypsin, prostate specific antigen, proteinase K, and papain. Recombinant peptide binds Gram-positive and Gram-negative bacterial cells, with a bacteriostatic effect against *S. aureus*. Anti-inflammatory	Schummer *et al*., 1999 Bingle *et al.*, 2002 Bingle *et al*., 2006 Galgano *et al*., 2006 Chhikara *et al.*, 2012 O'neal *et al*., 2013 Hua *et al*., 2014 Orfanelli *et al*., 2014
Eppin **MW (kDa)** **No amino acids**	 15.3 133	Kunitz domain in addition to the WFDC domain	Epididymis and testis, spermatozoa surface.	Antimicrobial peptide, inhibits elastase, supresses sperm motility, with possible role as a male contraceptive	Richardson *et al.* 2001 Yenugu *et al*., 2004 Wang *et al.*, 2007a & b O'Rand *et al*., 2009

Table 1.2: WFDC protein sub-groups in lower vertebrates/invertebrates. Adapted from Smith (2011).

WFDC proteins	Animal	Protein	Activity	Functional domains	Key reference
Waprins Nucleotide* sequences No. amino-acids	Snakes 208 66-84	Venom	Envenomation, antibacterial	WFDC Kunitz domain Ku-wap-fusins**	Torres *et al.*, 2003 Pahari *et al.*, 2007 Doley *et al.*, 2010
Chelonianins Nucleotide* sequences No. amino-acids	Reptile: fish, shrimp, whipworm 27 110	Egg white of turtle	? assumed proteinase inhibitory	WFDC Kunitz domain	Seemuller *et al.*, 1986 Chen *et al.*, 2005
Perlwapins Nucleotide* sequences No. amino-acids	Molluscs, Fish 68 134	Shell matrix	Regulation of Ca^{+2} deposition in shell formation	WFDC domain	Treccani *et al.*, 2006
Lustrin A Nucleotide* sequences No. amino-acids	Molluscs 913 1,428	Shell nacre	Assumed to be multifunctional, and to protect the shell matrix	WFDC domain Complex composition of cysteine rich and proline rich motifs and glycine-serine loops	Shen *et al.*, 2007
Crustins Nucleotide* sequences No. amino-acids	Crustaceans ants 118 88-197	Haemocytes	Antimicrobial/ protease inhibitors	1 or 2 WFDC domains. Gly-rich domain Pro-arg rich domain (See Figure 1.5)	Smith *et al.*, 2008

* No. of hits in GenBank® database, at time of writing

** WAP domain is merged into a Kunitz-like domain

Despite the great diversity of these proteins, two main activities stand out, i.e. their protease inhibitory (McKnight *et al.,* 1991) and/or antimicrobial effect (Couto *et al.,* 1993). Proteins from mammalian milk play a regulatory role in growth and differentiation of mammary gland epithelial cells, by inhibition of elastase-type serine proteases (Nukumi et al., 2007a). The same mechanism was also found to supress breast cancer cells (Nukumi et al., 2007b). Non-milk WFDC proteins have a wide range of functions according to the number of WFDC domains and existence of other functional domains as well. Apart from the cysteine residues, the remaining amino acids in the peptides are diverse, giving rise to the assumption that their functional role is linked to the WFDC domain (Bingle, 2011). However, individual proteins with an anti-protease property exhibit an ability to interact with proteases due to the presence of the protease inhibitory loop, identified by examining their three-dimensional (3D) structure. For example, elafin has a central β-sheet with two external parts interconnected by the proteinase inhibitory loop (Francart *et al*., 1997), while SLPI has its protease inhibitory loop near the C-terminus (Eisenberg *et al*., 1990).

Of the proteins described from humans, they are most frequently found in immune cells and tissues such as epithelial cells (e.g. SLPI and elafin; Bingle *et al*., 2001 and Williams *et al*., 2006), and in reproductive tissues (e.g. the epididymal protease inhibitor [eppin] Richardson *et al*., 2001). In addition, genes of *SLPI, WFDC2,* the *proteinase inhibitor 3 (PI3*) (elafin) are predominant in lung tissue, which strongly indicates an importance in pulmonary immunity (reviewed by Small *et al*., 2017). However, the human peptide genes also show an association with cancer cells, such as *WFDC1* (Larsen *et al*., 2000) and *WFDC2* (Bingle *et al*., 2006). In fact, McAlhany *et al*. (2003) stated that *WFDC1* acts as a tumour suppressor by regulating tumour growth factor-β (TGF- β). The main features of the human peptides are summarized in Table (1.2), however, they all share protease inhibitory and antibacterial properties.

Although the number of nucleotide sequences is high in non-mammalian groups, much less detail is known of the proteins' functions. In snake venom of the taipan, *Oxyuranus microlepidotus*, the isolated omwaprin exhibits antibacterial activity against Gram-positive bacteria *in vitro,* with a possible destabilizing effect on bacterial cell walls (Nair *et al*., 2007). However, none of the reported waprins to date has shown any

ability to inhibit proteases (Inagaki, 2015). The biological functions of the chelonianins is still under-explored, although an ability to inhibit trypsin/subtilisin endopeptidase was reported by Seemuller *et al*. (1986). In invertebrates, the WFDC proteins share the antimicrobial/anti-protease functions with the ones from vertebrates. However, the possibility of other roles for these peptides was raised, largely due to the diversity and organizational differences between the invertebrate groups. Invertebrates rely entirely on innate immunity and many species undergo metamorphosis through numerous developmental stages, with some species experiencing moulting of the cuticle as they grow. Thus, the appearance of other functions of this vast group of proteins in invertebrates is highly possible. For example, perlwapins are believed to bind calcium in abalone shell, inhibiting its deposition, and thus controlling the growth of calcite layers within the nacre (Treccani *et al*., 2006). Kuballa and Elizur (2008) reported a possible role of the crustin *pl*crustin from the crab, *Portunus pelagicus*, in cuticle hardening during moulting. The function of lustrin A is still uncertain, but because of its structural complexity it is assumed to act in a multifunctional way, and is posited to have a role in preventing the degradation of shell matrix by protease inhibition (Shen *et al*., 1997).

Amongst invertebrates, crustins are the best described and most studied group of the WFDC family. Similarly to the mammalian WFDC domain proteins, crustin transcripts have been most commonly identified in the key immunological tissues. In particular, the transcripts were largely detected in the circulating haemocytes, the main mediators of immune responses, strongly indicating a role in innate immunity. Crustin studies will be reviewed in more detail in Section (1.3.1), but in brief, they have been shown to be important immunological effectors in crustaceans.

In summary, WFDC proteins are widely spread throughout the animal kingdom and display a diverse range of biological roles. The WFDC domain is highly conserved among members of this family, and its structure is tight and stable because of the presence of intra-molecular disulphide bridges. What is known, to date, about WFDC proteins is their protease inhibitory and antibacterial properties, together with their main distribution in cells and tissues of the immune, reproductive and respiratory systems. However, more functional studies are required, in particular *in vivo*, in order to gain

more insight into the role of WFDC proteins as a whole. The fact that this group of peptides are widely present in invertebrates make them ideal for *in vivo* experimental studies, as many species are easily available, with no ethical restrictions on their use as experimental models. For this reason, the next section will review the immunity of crustaceans, one of the most important groups of marine invertebrates, and where one of the largest WFDC sub-groups, namely crustins, was identified and studied.

1.2. Crustaceans and their Immune System

The Crustacea are a vast, diverse subphylum of arthropods (Ahyong *et al*., 2011), with more than 67,000 known terrestrial and marine species, ranging in size between < 0.1 mm in length for the ectoparasite, *Stygotantulus stocki*, to > 3.8 m in the Japanese spider crab. *Macrocheira kaempferi*. Crustaceans occupy varied niches from tidal zones to thermal vents, with a large fossil record back to the middle Cambrian age (Briggs, 1978). The majority are either marine or freshwater, with only a small number of terrestrial species. Marine crustaceans are abundant, with the group including some parasites, such as sea lice and fish lice (Covich and Thorp, 1991).

The taxon is ecologically and economically important, with more than 10 million tons of decapod crustaceans (especially shrimp, crab and prawn species) obtained via fishing or farming as an important food source for humans ("FIGIS: Global Production Statistics 1950–2007". Food and Agriculture Organization). In contrast, non-decapods such as krill, although not fished for food, are vital elements of the food chain as their biomass is one of the largest in marine ecosystems (Nicol and Endo, 1997). On the other hand, some crustacean species, e.g. crayfish and crabs, are regarded as invasive animals in some countries. For example, the shore crab, *Carcinus maenas*, is a hardy predator that can cause damage to coastal ecosystems in North America and Canada (Pickering and Quijon, 2011). It was also reported to badly affect juvenile lobster growth by competing for food sources (Rossong *et al*., 2005). Crustaceans are also emerging as important experimental model animals due to their wide availability, with no ethical restrictions on their handling, bleeding and manipulation.

Like all invertebrates, crustaceans lack the complex adaptive, antibody-mediated arm of the immune system with its specific immunological memory (Cerenius *et al*., 2010).

Despite this, they have survived through a long evolutionary history, even though their open circulation is in intimate contact with the pathogen-heavy marine environment. The cellular and humoral parts of the innate immune system of crustaceans are highly capable of identifying and responding to non-self threats accordingly. Cell-mediated reactions such as phagocytosis, degranulation, encapsulation and extracellular trap formation are conducted mainly by the circulating haemocytes (Smith, 2016). These mechanisms are augmented by the release of soluble factors, mostly generated and secreted by the haemocytes, to achieve the right and effective immunological reaction (Cerenius *et al*., 2010).

1.2.1. Crustacean Haemocytes

The immune cells of crustaceans, referred to as haemocytes, were first described in the shore crab, *C. maenas*, by Smith and Ratcliffe (1978). The three sub-populations among mature haemocytes are: (i) hyaline cells (HCs): representing ca. 80% of the total haemocyte population, and around 10-17 µm diameter. They appear ovoid or spindle shaped when in culture conditions, and produce pseudopodial extensions when attached to foreign surfaces like glass. Cytochemical stains show the cells appearing basophilic, with the cytoplasm nearly devoid of granules; (ii) semi-granular cells (SGCs) comprise *ca* 10% of haemocytes, and are ovoid with diameters between 12-20 µm. The SGCs possess cytoplasmic granules, which are fragile and tend to degranulate *in vitro* with the release of their granule contents into the extracellular matrix (Smith and Ratcliffe, 1978); (iii) granular cells (GCs) feature denser and larger cytoplasmic granules than the SGCs, and measure approximately the same size or slightly larger, and are more resistant to lysis (Söderhäll and Smith, 1983). They form around 15% of the total haemocyte population (Smith, 2016). Both SGCs and GCs are not observed to attach and spread to the same extent as HCs when in contact with glass surfaces.

The immature cells, namely pro-haemocytes (ProHs), were first isolated by Roulston and Smith (2011) in the spider crab, *Hyas araneus.* They were enriched after induction of their release into the haemolymph by 24-hour pre-bleeding of animals. The ProHs measure 8-10 µm and represent less than 5% of the total haemocytes. Roulston and Smith described two subgroups of ProHs; granular and agranular, with the latter being

predominant and possibly being the precursors of the mature HCs, with the granular ProHs most likely developing into GCs and SGCs. Figure (1.2).

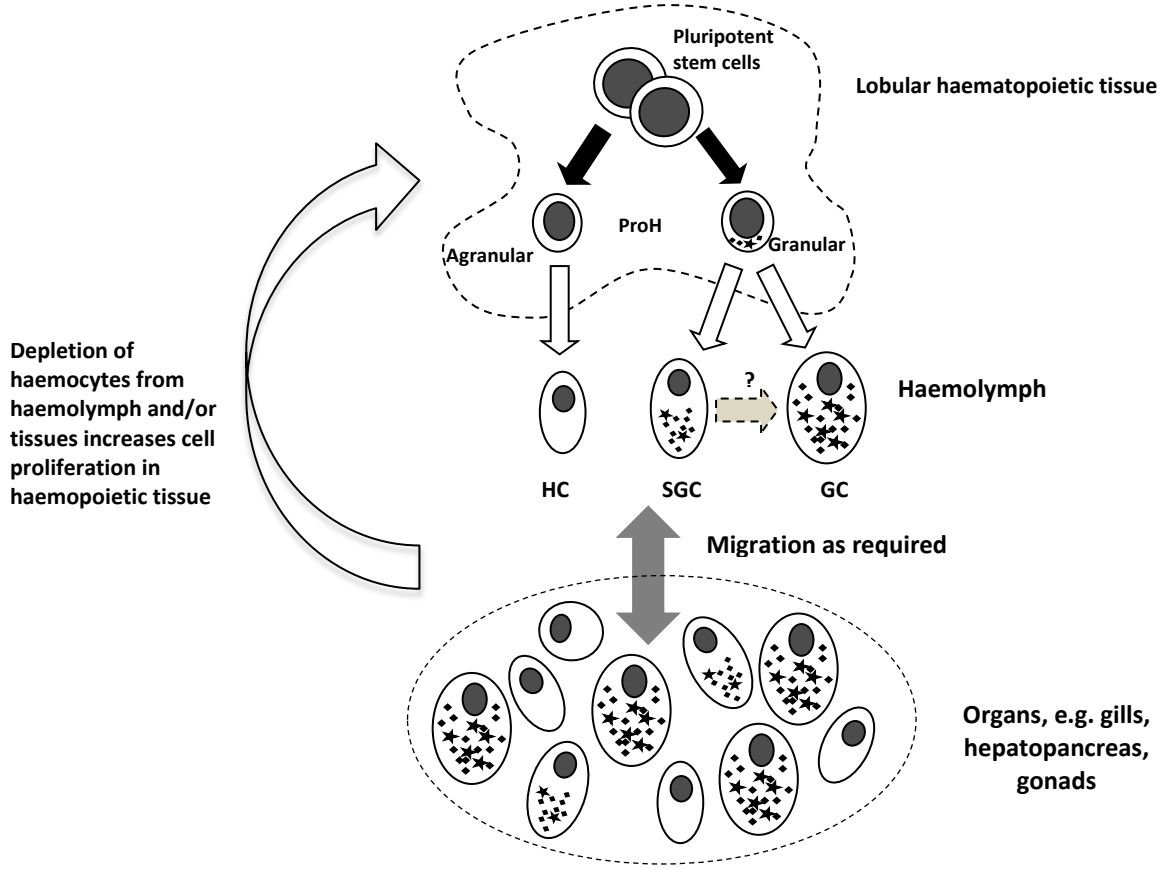

Figure 1.2: Hypothetical scheme depicting the likely maturation process of crab haemocytes. Based on observations in this thesis and from information from van de Braak *et al*. (2002) and Roulston and Smith (2011). It is believed that pluripotent stem cells in haemopoietic tissue give rise to two types of ProHs; agranular and granular. Agranular ProHs develop into mature HCs, while the granular type gives rise to both SGCs and GCs. It has been previously suggested that SGCs might develop into GCs, but this is currently unknown. Adapted from Smith *et al.* (2010). SGC=semi-granular cell, GC=granular cell, HC=hyaline cell, ProH=prohaemocyte.

1.2.2. Pattern recognition

The haemocytes identify pathogenic molecules known as pathogen associated microbial patterns (PAMPs) via specific cell-bound or humoral pattern recognition receptors (PRRs). PAMPs such as lipopolysaccharide or flagellin may be secreted from invading microbes, or present on the surfaces of bacterial cells (Janeway and Medzhitov, 2002; Medzhitov and Janeway, 2002). Many PRRs have been purified and investigated in crustaceans, such as β-glucan binding protein (β-GBP) that binds β -1,3-glucans from fungi (Duvic and Söderhall, 1990), and lipopolysaccharide- and β-1,3-glucan-binding protein (LGBP) that binds β -1,3-glycans and the lipopolysaccharide (LPS) (Lee *et al*., 2000). This interaction initiates intracellular signal cascades that end in a specific immune response such as degranulation, phagocytosis, or cellular death. Degranulation of granular haemocytes results in the release of more of the soluble immune effectors, such as AMPs and prophenoloxidase activating (proPO) system activators, thus enhancing the immune response (Smith, 2016).

Most recently, a new group of recognition receptors, the Down syndrome cell adhesion molecules (DSCAM) have been identified in some crustaceans such as the shrimp species, *Litopennaeus vannamei* (Chou *et al*., 2009), *Penaeus monodon* (Chou *et al*., 2011), and the crayfish, *Pacifastacus leniusculus* (Watthanasurorot *et al*., 2011). The lattermost publication, however, was retracted in 2016 because of concerns over image manipulation (Watthanasurorot *et al*., 2016). Since then, DSCAM has been identified in a second crayfish species, *Cherax quadricarinatus* (Ng *et al*., 2014). DSCAM are a highly variable family in arthropods, with more than 13 000 isoforms predicted for the water flea, *Daphnia magna*, 22 000 for *P. lenisculus* and over 30 000 for the mosquito, *Anopheles gambii* and the fruit fly, *Drosophila melanogaster* (Hauton, 2012). The receptors possess a transmembrane domain at the carboxyl end, but some are present as soluble forms, such as in *L. vannamei* (Chou *et al*., 2009) or as both soluble and membrane-bound, e.g. *P. monodon* (Chou *et al*., 2011). All DSCAM proteins share a conserved region comprising ten immunoglobulin-like domains and six fibrinogen-like domains. *In vivo* experiments in crustaceans revealed that the other variable parts of these molecules can be modified according to the type of challenge, e.g. viral or bacterial, thus contributing further to the diversity of this protein family (Brites *et al*., 2008; Chou *et al*., 2009).

1.2.3. Cellular responses

Phagocytosis is a highly conserved multi-phase process, in which phagocytic cells recognise foreign particles, engulf them into intracellular vacuoles known as the phagosomes, and subsequently clear them to the outside matrix. It has an important role, not only in immunity against invading organisms, but also in clearance of dead cells/cell debris (Jiravanichpaisal *et al*., 2006). In the shore crab, *C. maenas*, HCs are the phagocytic cell type (Smith and Ratcliffe, 1978). When tested *in vitro* using different bacteria, the percentage phagocytosis ranges between 2.40-14.7% according to the bacterial species (Smith and Ratcliffe, 1978). Phagocytosis is boosted by humoral proteins known as opsonins, which attach to foreign particles and thus facilitate their recognition and clearance by phagocytic cells. Two peptides from the crayfish, *P. lenisculus*, have been identified as opsonins, namely, peroxinectin (Johansson *et al*., 1999), and the masquerade-like protein (Huang *et al*., 2000). Peroxinectin is multifunctional, as besides opsonization (Thörnqvist *et al*., 1994), it also supports cell-cell attachment (Johansson and Söderhäll, 1988), induces degranulation (Johansson and Söderhäll, 1989) and encapsulation (Kobayashi *et al*., 1990), in addition to its role as a peroxidase (Johansson *et al*., 1995). Recently, Robb *et al*, (2014) showed that a homologue of this protein is present in the hyaline cells of the shore crab. The masquerade-like peptide is one of the PRRs of *P. leniusculus* which opsonises Gram-negative bacteria such as *E. coli*, and yeast (Huang *et al*., 2000).

Extracellular trap formation (ETosis) was first reported by Brinkmann *et al*. in 2004 as a controlled cell death pathway undergone by human neutrophils, which serves to trap bacteria. This trapping mechanism is initiated by chromatin decondensation, and followed by chromatin release to the extracellular domain to seize infectious agents. The trap itself becomes decorated with proteins such as antimicrobial peptides (AMPs) and certain enzymes such as elastase, thus concentrating the antimicrobial effect due to the confined space. In 2014, Robb *et al*. reported the release of uncondensed chromatin from the nuclei of *C. maenas* HCs and SGCs, a similar process to that first reported in human neutrophils a decade earlier by the group of Brinkmann and Zychlinsky. Robb *et al*. also demonstrated extracellular trap formation from cells of other invertebrates including the blue mussel, *Mytilus edulis* and the acoelomate sea anemone, *Actinia equina*. Designated as invertebrate extracellular phagocyte traps (InEPTs) to discriminate them from those of vertebrate cells, it was shown to be a fundamental,

highly conserved immune mechanism. It has now been proved to occur widely across non-vertebrate taxa, for example in slime moulds (Zhang *et al*., 2016), the shrimp, *Litopenaeus vannamei* (Ng *et al*., 2013), gastropods, (Lange *et al*., 2017) and the oyster, *Crassostrea gigas* (Poirier *et al*., 2014), with high levels of extracellular DNA also identified at plant root tips (Wen *et al*., 2009).

HCs and SGCs in *C. maenas* were shown to expel chromatin extracellularly upon challenge with the protein kinase C activator, phorbol myristate acetate (PMA), as well as lipopolysaccharide (LPS) and the marine pathogen, *Listonella anguillarum*, (Figure 1.3, a-h), (Robb *et al*., 2014). This mechanism was confirmed to be dependent on NADPH oxidase and the subsequent release of reactive oxygen species. Scanning electron microscopy (SEM) revealed that InEPTs occur with a similar morphology to that of NETosis in mammalian neutrophils, with nuclear membrane deterioration evident prior to chromatin discharge. The extended chromatin strands were decorated with globule-like structures, presumably the haemocyte proteins.

Importantly, the same study showed extracellular chromatin to play a part in encapsulation (Figure 1.3, i-k), a process by which haemocytes aggregate and form capsule-like clumps that sequester infectious agents. The chromatin was seen to form the main framework on which intact haemocytes can assemble and form effective clumps (Robb *et al*., 2014). These structures lodge in the haemal sinuses, such as gill lamellae, to be expelled later during the moult (Smith and Ratcliffe, 1980; White and Ratcliffe, 1982). Haemocytopaenia then occurs as large numbers of haemocytes migrate into haemal sinuses to form capsules/clumps, (Smith, 2016). This reduction in haemocyte numbers is compensated by an influx of newly formed ProHs from haematopoietic tissue, entering the circulation (Lin and Söderhäll, 2011; Roulston and Smith, 2011).

Robb *et al*. (2014) also confirmed the involvement of other proteins in InEPT formation and encapsulation. The histone H2A was detected by immuno-cyto and histo chemistry to co-localise with the DNA, thus the discharged chromatin upon stimulation serving to deliver a bactericidal agent. Histones were reported in 1958 to have significant

antibacterial activity (Hirsch, 1958), and are currently well known as unconventional antibacterial effectors (Smith *et al*., 2010). Interestingly, the adhesive protein, peroxinectin was also detected extracellularly *in vitro* on expelled chromatin and *in vivo* in gill capsules (Robb *et al*., 2014). The peroxinectin also showed a distinct presence at different times during capsule formation, no doubt to assist cellular attachment, especially since its role in encapsulation had been reported earlier (Kobayashi *et al.*, 1990).

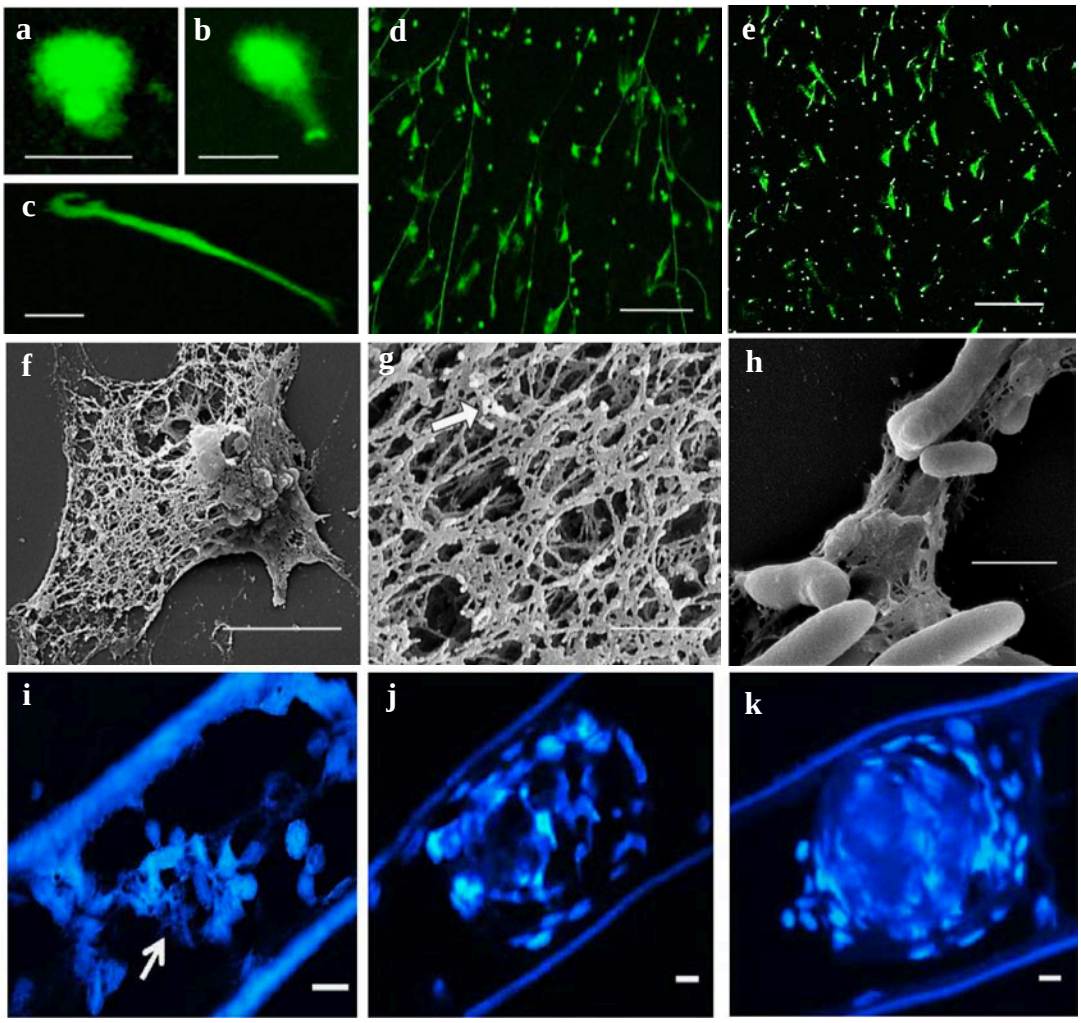

Figure 1.3: InEPTs formation in *C. maenas*. (**a-d**): InEPTs in HC population. HCs stained with Sytox green and stimulated with PMA show discharging extracellular chromatin 3 hours (**a)** and (**b**), and 24 hours (**c**) and (**d**) post stimulation, scale bar in (**a**), (**b**) and (**c**) = 30 µm, in (**d**): 300 µm. (**e**) InEPTs in SGC population stimulated and stained, as above. (**f)** and **(g**): SEM images of InETPs induced from HCs, details are illustrated in (**g**) with arrow indicating granules deposited on the extracellular chromatin meshes. (**h**): SEM image showing extracellular chromatin released from *L. anguillarum*-stimulated HC, entrapping bacterial cells. (**i-k**): DAPI stained gill sections show InEPTs associated with encapsulation, one (**i**), three (**j**) and 24 (**k**) hours after LPS injection. In the 1-hour section, chromatin starts to discharge (as arrow indicates). After 3 hours, more extracellular chromatin is detected, mostly at the periphery of the forming clumps. After 24 hours, expelled chromatin is seen diffused inside the dense core of the mature capsule. Images reproduced from Robb *et al.* (2014) under the Creative Commons licence of Nature Publishing Group.

1.2.4. The prophenoloxidase activating system (proPO system)

The proPO system is an enzyme cascade system important in arthropod immunity (summarized in Figure 1.4), which has been likened to a primitive form of the vertebrate complement system. The proPO system comprises numerous proteins and enzymes contained in haemocyte granules, which are present there in an inactive form. As well as the proPO enzyme itself, a number of serine protease inhibitors act as regulatory factors to avoid activation of this system when not required (Cerenius and Söderhäll, 2004). The activation of the system is induced by the presence of PAMPs, which initiates a serine protease cascade, leading to the activation of proPO and ending with the formation of melanin (Aspán and Söderhäll, 1991). The ProPO system is responsible for generating several cytotoxic by-products as well as melanin itself, which contributes directly to encapsulating pathogens. Once triggered, the activated components of the system contribute to different cellular processes via opsonization, generation of toxic oxygen metabolites, wound healing and encapsulation. (Söderhäll and Cerenius, 1998). (Figure 1.4).

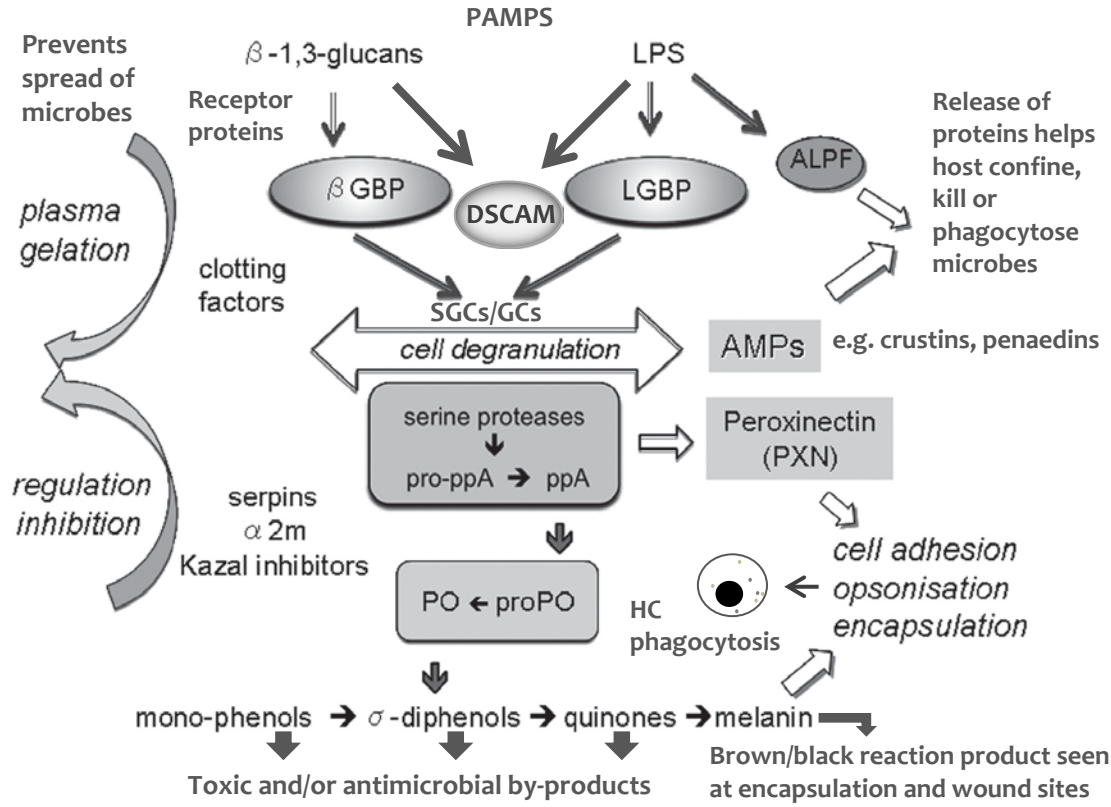

Figure 1.4: Summary of the ProPO involvement in crustacean immune reactions. Pattern recognition initiates immune response by binding of PAMPs, e.g. β-1, 3 glucans and LPS with PRRs, such as βGBP, LGBP, DSCAM and anti-lipopolysaccharide binding protein (ALPF). This results in degranulation of GCs and SGCs and the subsequent release of granule contents, such as antimicrobial peptides (AMPs) that, in addition to ALPF, contribute to the microbial killing. Granules also contain the adhesive protein peroxinectin (PXN) that enhances cell attachment and contributes to capsule formation, in addition to its role as an opsonin. Immune response is also manifested with the activation of the proPO system, triggered by secretion of serine proteases from granular haemocytes. These enzymes convert pro-phenoloxidase activating enzyme (pro-ppA) into phenoloxidase activating enzyme (ppA), which in turn mediates the activation of PO. This oxidizes mono-phenols, ending by the formation of melanin that further contributes to various immune responses such as encapsulation. This system is controlled by factors that are also secreted via degranulation, including protease inhibitors, such as serpins and kazal inhibitors, and α-2 macroglobulin. Degranulation also results in plasma gelation, caused by the release of clotting factors, that prevents spreading of microbes. Adapted from Smith *et al*. (2003).

1.2.5. Antimicrobial peptides (AMPs)

Immune responses are associated/ augmented with the release of small peptides with natural anti-infective effects. These molecules, known as antimicrobial peptides, are known in crustaceans to be produced by granules of SG and G haemocytes, and are released via degranulation upon exposure to certain stimulants. AMPs are widespread throughout the animal kingdom and are commonly defined as small (10 kDa or 50 amino-acid residues), cationic, amphipathic proteins. They possess broad-spectrum antimicrobial activity, killing or inhibiting the growth of microbial cells including Gram-positive and negative bacteria, fungi, parasites and even viruses (reviewed by Ganz, 2003; Brogden 2005; Smith and Dyrynda 2015). AMPs have commonly been isolated from key immunological tissues, with indications of them being synthesized within the granules of defensive cells such as human phagocytes (Hirsch 1956). Amongst the first groups of animal AMPs to be characterized were the defensins from mammalian leucocytes (Ganz *et al*., 1985) followed by cecropins from insects (Steiner *et al*., 1981) and magainins from amphibians (Zasloff, 1987). The number of AMPs has increased very considerably since and they are now considered fundamental and ancient immune weapons, not only as part of innate immunity, but also as a support to components of the adaptive immune system.

With the rapid growth of this field, especially after the development of amino acid sequence prediction tools, the peptides have been categorized into groups for better understanding of them. A number of databases have been created, including the Antimicrobial Peptide Database and data analysis system (APD), which details AMP nomenclature, classification, prediction and much more (http://aps.unmc.edu/AP/main.php) (Wang *et al.*, 2016). The classification on the APD website grouped these peptides on basis of their biological action (antibacterial, anti-fungal, anti-viral, anti-parasitic, anti-protist, etc).

Although AMPs are often described as cationic compounds, some are anionic, such as maximin H5 from amphibians (Lai *et al*., 2002) and dermcidin from humans (Schittek *et al*., 2001). Some AMPs are categorized by their amino acid composition, for example proline-rich AMPs such as abaecin and glycine-rich AMPs such as hymenoptaecin from honeybees (Boman, 1995), and cysteine-rich AMPs, e.g.

tachyplesins from horseshoe crab (Kawabata *et al*., 1996) and crustins from crustaceans (Smith *et al*., 2008). Some reported AMPs are part of larger protein structures, for example lactoferricin from lactoferrin (Kuwata *et al*., 1998). AMPs can also be classified according to their structure, and a number of studies have defined the secondary/tertiary structure of these peptides, mainly to understand their mechanism of action. The two main categorizations are (i) linear peptides which take on an α helix structure, e.g. cecropins from insects (Andersson *et al*., 2003) and magainins from amphibians (Vaz Gomes *et al.*, 1993) and (ii) cysteine-rich AMPs, with stable disulphide bridges creating β-sheet structures, such as protegrins from porcine leukocytes (Fahrner *et al.*, 1996), and defensins from humans, insects and plants.

The potential antimicrobial effect of AMPs is influenced by their physiochemical properties such as their size, net charge, amphipathy and hydrophobicity. The overall charge of AMPs enables them to be electrostatically attracted to bacterial cells (Brodgen, 2005). AMPs can incorporate within the structure of the bacterial wall by interacting with the negatively charged lipid bilayers, causing the formation of trans-membrane pores that lead to cell lysis (Brodgen, 2005). However, AMPs were reported as well to be able to diffuse inside the bacterial cell without disturbing the bacterial membrane, to inhibit some vital bacterial processes like synthesis of bacterial wall or nucleic acids, or inhibit certain enzymes, mostly proteases (Brodgen, 2005).

Research into AMPs also relates to their exploitation, either as therapeutic antibiotic agents, or as alternatives to antibiotics in aquaculture (reviewed by Destoumieux-Garzón *et al*., 2016), hence the interest in AMPs from diverse species. AMPs have been considered as substitutes for antibiotics, with some reaching clinical trials (Pacor *et al*., 2002; Andres *et al*., 2004; Kang *et al*., 2014; Cheung *et al*, 2015). An important example is the defensin homologue from a saprophytic fungus, plectasin, which was effective against antibiotic resistant *Streptococcus pneumoniae* (Mygind *et al*., 2005). Some AMPs can control the inflammatory response as immune modulators, for example, the ALPF from the shrimp, *P. monodon,* which was seen to interact with murine macrophages *in vitro*, and display anti-tumour activity against HeLa cells (Lin *et al*., 2010, a and b). AMPs use in aquaculture has also been considered, although less so in comparison with medicinal exploitation. A good example of this is the usage of

tachyplesin in the pearl industry, where it has been used in combination with exopolysaccharides as a filming agent to improve oyster survival post-grafting and increase their quality (Guezennec *et al.*, 2013).

1.3. Crustacean AMPs

The main types of AMPs in crustaceans were reviewed by Smith and Dyrynda (2015). The first AMP was isolated from haemocytes of *C. maenas* by Schnapp *et al*. (1996) as a proline-rich peptide, designated as Bac-C. Many other peptides have been described and classified since, of which crustins and penaeidins form the major groups. Penaeidins are described as proline and cysteine-rich cationic antimicrobials, with molecular weight between 5-7 kDa. There are 305 identified penaeidin nucleotide sequences according to the Genbank® Nucleotide Sequences Database at time of writing. The first penaedin protein was characterized by Destoumieux *et al*. in 1997 in the shrimp, *L. vannamei*. Penaeidins have two functional domains; one is a proline-arginine rich domain at the N-terminus, and the other is a cysteine-rich domain at the C-terminus. Penaeidins were reported to be strongly antibacterial against Gram-positive bacteria, with MIC values ranging between 0.6-5 µM (Tassanakajon *et al*., 2011). They also possess antifungal activity, related mainly to their ability to bind chitin (Destoumieux *et al.*, 2000), in addition to a possible chemoattractant function (Song and Li, 2014).

A third, smaller group of crustaceans AMPs includes the anti-lipopolysaccharide factors (ALFs), first identified in amoebocytes of the chelicerate horseshoe crabs, *Limulus polyphemus* and *Tachypleus tridentatus* (Tanaka *et al*., 1982; Ohashi *et al*., 1982). These small peptides (10-12 kDa) have LPS binding sites and broad antimicrobial activity against Gram-positive and negative bacteria with MIC values reported between 0.0095–50 µM (Rosa *et al*., 2013; Tassanakajon *et al*., 2011). Several other individual peptides, not belonging to any known families, have also been identified. These include peptides such as arasin-1, hyastatin and scygonadin (reviewed by Smith & Dyrynda, 2015) and are considered in more detail where appropriate in later chapters.

1.3.1. Crustins

The crustin AMP family have been mainly recorded from decapod crustaceans, in addition to other groups like Pleocyemata and Dendrobranchiata (Smith and Dyrynda, 2015), as well as non-crustacean groups like ants (Zhang and Zhu, 2012). To date, the crustins are the largest group of WFDC-domain containing proteins amongst invertebrates. They possess at least one WFDC domain at their carboxyl terminus, and contain other peptide enriched regions, such as proline-rich and glycine-rich areas. At the time of writing, there are 113 crustin sequences identified in the Genbank® Protein Database (https://www.ncbi.nlm.nih.gov), and 119 in the Genbank® Nucleotides Database (https://www.ncbi.nlm.nih.gov) (Figure 1.5).

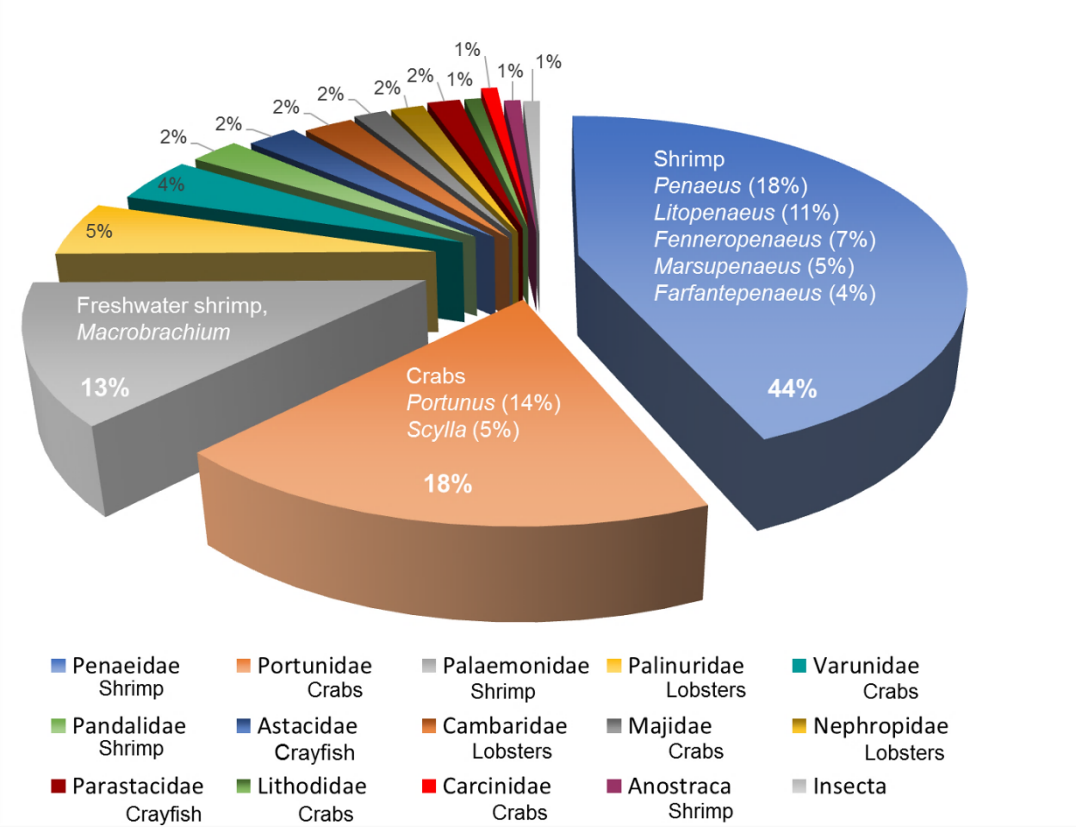

Figure 1.5: Percentage distribution of crustin sequences across the taxonomic families of the Pancrustacea, according to Genbank® Nucleotide Database. Data are based on 119 crustin sequences, correct at time of writing.

Apart from the WFDC domain, other regions in crustin structure appeared to be diverse, like the N-terminus, which means that crustins do not show the same degree of conservation as other AMPs (Smith, 2011). The arrangement of the region in-between the signal and the WFDC domain varies, but is still unique for some sub-groups within the Decapoda, which made it possible to consider it as a special criterion to designate crustins into types. Smith *et al*., (2008) described three main types of crustins, however, a type IV was added later and described by having a double WFDC domain. Figure (1.6) summarizes the crustin types.

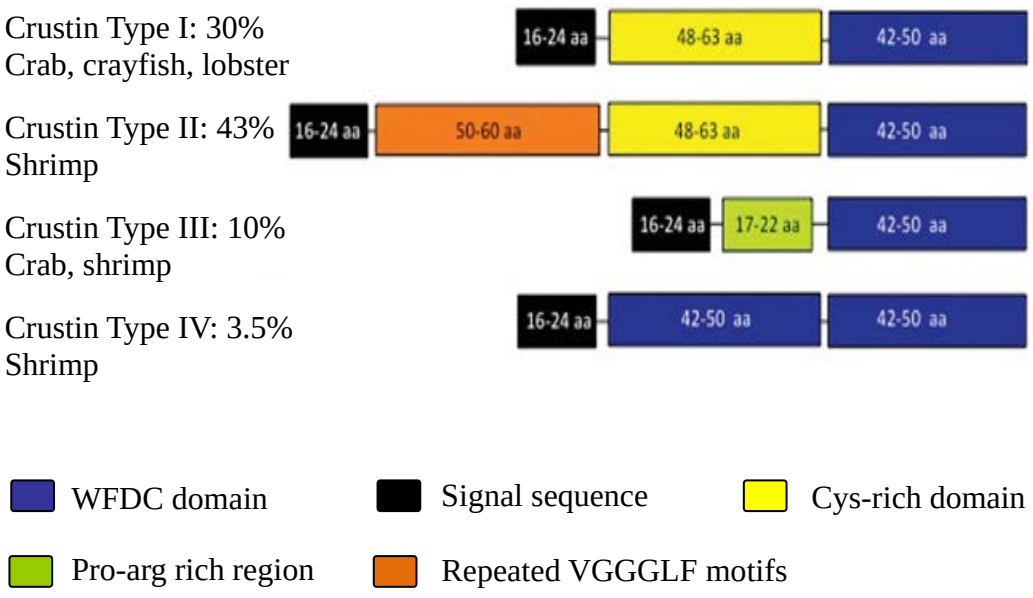

Figure 1.6: Crustin types. Type I crustins present in animals such as crabs, crayfish and lobster and characterized by the cysteine-rich region at the N-terminus. Type II crustin found mainly in shrimp contain an additional glycine –rich sequence, in additional to the cysteine-rich domain at the N-terminus. Type III crustins present in crab and shrimp species possess only proline and arginine-rich region near their signal sequence. Type IV crustin are found in shrimp species and characterized by double WFDC domain. Adapted from Smith, 2011.

Over one hundred crustin sequences had been identified in the literature (Table 1.3), with 20 from the shrimp, *Penaeus monodon,* 15 from *M. japonicus* and 12 from *Litopenaeus vannamei,* (Table 1.3). According to the scheme of Smith et al (2008), 30% of reported crustins belong to Type I, 43% to Type II, and only 10% from Type III. A few crustins with a double WFDC domain have been classed as Type IV of which examples include *Mj*-DWD from *Marsupenaeus japonicas,* *Fc*-DWD from *Fenneropenaeus chinensis,* and *Es*-DWD1 from *Eriocheir sinensis* (Chen *et al*., 2008, Du *et al*., 2009, Li *et al*., 2013). Some remaining sequences have not been categorized according to the Smith *et al,* (2008) classification.

Among all published studies, 95% of crustins were cloned, characterized and sequenced by studying the crustin transcripts, without isolating the native peptide. The vast majority of crustins had their genes detected in haemocytes, which seem to be the primary site for crustin synthesis. Very few crustin transcripts were first obtained from tissues other than haemocytes, exceptions being the crustin *Pm*5 from *Penaeus monodon,* which was detected in the gill and eyestalk (Vatanavicharn *et al*.,2009) and the crustin PET- 15, which seemed to be present mainly in the epithelium of the olfactory organ in *Panulirus argus* (Stoss *et al*., 2004). Following identification in haemocytes of a given species, gene expression has then subsequently been investigated in tissues such as gills, heart, hepatopancreas and intestine: for example *Lv* SWD from *L. vannamei* (Visetnan *et al.*, 2017), *Mj*Cru I-1 from *M. japonicus* (Liu *et al*., 2015), *Cq*Crs from the red claw crayfish, *Cherax quadricarinatus* (Yu 2016), and *Pc*-SWD from the red swamp crayfish, *Procambarus clarkii* (Du *et al*., 2010). A smaller number of studies have detected transcripts in other tissues; e.g. the epidermis (Cru*Ha* 1 and 2 from the spider crab, *Hyas araneus,* Sperstad *et al*., 2009 a), the eyestalk (*Pt*crustin 2 and 3 from the swimming crab, *Portunus trituberculatus,* Cui *et al*., 2012), the gonads (*Fc*-crus 3 from the Chinese white shrimp *Fenneropenaeus chinensis,* Sun *et al.*, 2010), the haematopoietic tissues (*Pl*crustin 2 from the freshwater crayfish *P. leniusculus,* Jiravanichpaisal *et al*., 2007), and nervous tissue (*Pj* C1, 2 from the Japanese spiny lobster, *Panulirus japonicus,* Pisuttharachai *et al*., 2009).

Of the total number of crustin studies, around 40% investigated antibacterial and/or functional roles of the proteins. Of these, the recombinant protein was used, most

commonly expressed in bacterial systems, for example Zhang *et al.* (2007a & b); Supungul *et al*. (2008); Mu *et al*. (2011). Recently, the yeast *Pichia pastoris* has been used to produce Crus *Pm*1 and 7 from *P. monodon* (Arayamethakorn *et al*., 2017), and *Pc*Cru from *Procambarus clarkia* (Liu *et al*., 2016). Of the functional studies conducted on native and recombinant peptides, 37 crustins (around 32% of the identified sequences) were found to be antibacterial, mostly effective against Gram-positive strains only, with fewer active against only Gram-negative or both Gram types. It was also notable that the minimum inhibitory concentrations (MIC) were generally lower than those of other AMPs (reviewed by Smith and Dyrynda, 2015). To date, the mechanism by which crustins interact with and affect bacterial strains is poorly understood, with few studies addressing this. So far, crustin binding to bacterial cells has been investigated using gel electrophoresis and western blotting (Du *et al*., 2015; Yu *et al*., 2016), without visualising any resultant damage. Apart from this, only one study aimed to examine the crustin-bacteria interaction by scanning electron microscopy and immunohistochemistry (Liu *et al*., 2015).

Among antibacterial crustins, 10 also exhibit an inhibitory effect against proteases (e.g. Du *et al*., 2009; Jiang *et al*., 2013; Jiang *et al*., 2015), which was put forward as an explanation to their antibacterial effect. Some crustins have shown anti-fungal activity, e.g. both native crustins Cru*Ha*1,2 from the spider crab, *Hyas araneus* (Sperstad *et al*., 2009 a), and the recombinant *Cq*Crs from *Cherax quadricarinatus* (Yu *et al*., 2016). Antiviral activity has largely not been addressed, although a few crustins have been classified as such. However, the relevant studies were based on gene expression changes upon viral challenge, rather than testing the effectiveness of the peptide itself, e.g. Chen *et al*. (2008); Antony *et al*. (2011 a & b); Jiang *et al.* (2015). Indications of activity against eukaryotic cells by testing haemolytic and cytotoxic activity have also not been widely investigated, with none of the crustins used having this property (Battison *et al*., 2008; Mu *et al*., 2010; Jayesh *et al*., 2016). This may indicate that crustins are most likely to interact with and affect the viability of prokaryotic cells, rather than eukaryotic ones.

Many crustin studies have focussed on assessing their response either to microbial challenge, or to the effects of immune stimulants, the latter being a widely discussed

and somewhat controversial area of crustacean research. The majority of bacterial challenge studies have used injection of different *Vibrio* strains (e.g Vargas-Albores *et al*., 2004; Du *et al*., 2015; Visetnan *et al.*, 2017), with occasional challenge by oral administration (Soonthornchai *et al*., 2010). Fungal challenge has been used only rarely, e.g. Shockey *et al*. (2009) who challenged the shrimp *L. vannamei* with the fungus *Fusarium oxysporum*. Given the severe effects that White Spot Syndrome Virus (WSSV) has on the crustacean aquaculture industry, viral challenge has been used widely in recent years (e.g García *et al*., 2009; Du *et al.*, 2010; Antony *et al*., 2011 b). Many researchers have employed stimulation with PAMPS as immune-stimulants; for example, Wang *et al*. (2008) challenged *L. vannamei* by feeding animals with β-1, 3 glucan, however, no changes in either Crustin I or P were detected. In contrast, Li *et al*. (2013) stimulated the Chinese mitten crab, *Eriocheir sinensis*, with glucans, LPS and peptidoglycans, and observed up-regulation in expression of the crustin *Es*DWD1 following challenge.

However, results arising from microbial challenge or immune stimulation are ambiguous, with no specific pattern of gene expression of crustins observed upon stimulation. While some studies reported up-regulation of a crustin upon stimulation with specific type of bacteria, such as *Vibrio* strains, (e.g. Du *et al*., 2015; Visetnan *et al*., 2017) others showed down-regulation (e.g. Supungul *et al*., 2004; Vargas-Albores *et al*., 2004) or even no changes in gene expression (e.g. Sperstad *et al.*, 2010). In most of the studies, no explanation was given, as mostly no additional research was conducted to interpret gene expression results, for example performing total and differential haemocyte counts, protein localisation or functional studies. In addition, there was no indication to the mechanism that the crustin interacts with the microbe, either as direct action or by mediating other immune responses.

Some studies have aimed to detect crustins' roles and changes in different developmental stages. For example, Zhang *et al.* (2010) detected transcripts of *Pl* crustin in the midphase of embryonic development, and did not detect any noticeable changes in expression following bacteria immersion. Kuballa and Elizur in 2008 investigated the role of crustin-like genes in different moult stages of *Portunus pelagicus*. These authors reported increased levels of expression in inter- and pre-moult

stages, and decreased expression in post moult and ecdysis, which raised the possibility of a role in regulating calcium deposition in the hard cuticle. Other studies have investigated other possible contributions of crustin in managing stress conditions such as elevated ambient ammonia levels; for example Yue *et al*. (2010 a) detected a decrease in *Pt*crustin expression levels in the haemocytes upon exposure to 20 mg mL^{-1} of ammonia. Brockton *et al*. (2008) tested the effects of unusual temperature regimes and high osmolarity in the expression of carcinin in *C. maenas* haemocytes, while a similar study considered the influence of heat and high salt levels on the expression of Crus *Pm* 5 in *P.monodon* (Vatanavicharn *et al*., 2009). Recently, new *in vivo* approaches have been utilised; RNA interference has been employed in some shrimp species for knocking down crustin expression by injecting double stranded RNA (dsRNA). This study by Liu *et al*. (2016) found increased mortality rates upon infection with *A. hydrophilia* in *Procambarus clarkia* subjected to crustin knock-down.

1.3.1.1. Carcinin

The first member of the crustin family was purified and studied by Relf *et al.* in 1999 and designated later by Smith and Chisholm (2001) as carcinin, although its presence as an unnamed peptide had been observed since 1996 by Schnapp *et al*. Carcinin is an 11.5 kDa crustin, present in the GCs of the shore crab *C. maenas*. It was found to be cationic and hydrophobic, and unusually, maintained its antibacterial effectiveness in high temperatures up to 100 ºC (Relf *et al*., 1999). Carcinin is characterized by the presence of one WFDC domain, with 30% similarity to SLPI between BLAST and FASTA as reported by Relf *et al*. (1999). The antibacterial spectrum of carcinin only acted against Gram-positive marine/salt-tolerant bacteria, some of which are fish/shellfish pathogens, e.g. *Aerococcus viridans var homari*. The native carcinin required high osmolarity for its antibacterial activity, which may be needed to stabilize its structural conformation. Otherwise, it could be an indication that carcinin interacts with bacterial cell walls in those areas involved in resistance to high-salt conditions (Relf *et al.*, 1999). Carcinin activity was reported to be prompt but short (Brockton *et al*., 2007) with an average half-life of 10-30h. The secreted mature active peptide resulting from proteolytic cleavage is prone to rapid degradation, which is essential to protect crab tissues from its harmful effect.

At the gene level, a study in the shore crab by Towle and Smith (2006) detected carcinin transcripts in a wide range of crab tissues including gills, hepatopancreas, hypodermis, brain, testis, muscle, heart, and antennal gland (GenBank accession numbers DW585033, DW585032), although that did not make clear whether the transcripts arose from haemocytes or other cell types. Brockton *et al*. (2007) obtained the full-length cDNA of carcinin and reported its similarity to β-defensins, whereupon carcinin conformation was assumed to include a β –sheet or a loop structure. However, the results of injecting *C. maenas* with bacteria had an unexpected effect on the transcription levels of carcinin. There was no increase in carcinin gene expression even 48-hour post injection of the heat-killed *Planococcus citreus* (Brockton *et al*., 2008). In contrast, a remarkable reduction in the number of circulating haemocytes was observed, explained by their involvement in the encapsulation process to combat bacterial infection. Apart from this, expression of carcinin appeared to change when the animals were under stress, e.g. being elevated when temperature was changed to mimic environmentally extreme degrees. In addition, its antibacterial effect reached its maximum levels at the same extreme temperatures, though haemocyte counts were detected in their lowest levels (Brockton *et al*., 2008).

Table 1.3: Summary of the most studied crustin peptides.

Species	Crustin name/Type	Study approach	Key reference
P. monodon	Crustin *Pm*1-10/II SWD*Pm*1-3/III	Gene expression study for characterization and localisation in healthy, bacterially and virally challenged animals. Expression of recombinant peptides for functional studies.	Supungul *et al*., 2004 Amparyup *et al*., 2008 a Donpudsa *2014* Arayamethakorn *et al*., 2017
L. vannamei	Crustins *Lv* 1-6 Crustins *Ls* 1-3/II Crustins I, P/II *Lv*SWD/III	Gene expression study for characterization and localisation in healthy and bacterial/ viral /PAMP challenged animals. Expression of recombinant peptides for functional studies. RNAi	Bartlett *et al*., 2002 Vargas-Albores *et al*., 2004 Shockey *et al*., 2009 Visetnan *et al*., 2017
M. japonicus	*Mj*crustin-like peptide 1-5/II Crustin-like peptide *Mj*CRS/II *Mj*-DWD/IV *Mj*Cru I,1-5/I	Gene expression study for characterization and localisation in healthy and bacterial/ viral /PAMPs challenged animals. Expression of recombinant peptides for functional studies. RNAi	Rattanachai *et al*., 2004 Chen *et al*., 2008 Hipolito *et al*., 2014 Liu *et al*., 2015 Jiang *et al*., 2015
F. chinensis	Cru*Fc*/II *Fc*-DWD/IV *Fc*-Crus1,2/II *Fc*-Crus3/I	Gene expression study for characterization and localisation in healthy and bacterial/ viral /PAMPs challenged animals. Expression of recombinant peptides for functional studies.	Zhang *et al*., 2007 a & b Du *et al*., 2009 Sun *et al*., 2010
P. trituberculatus	*Pt*Crustin 1-3/I	Gene expression study for characterization and localisation in healthy and bacterial challenged animals. Expression of recombinant peptides (in yeast) for functional studies.	Yue *et al.*, 2010a Yue *et al.*, 2010b Liu *et al.*, 2011

E. sinensis	*CrusEs*/I Crus*Es*2/III *ES*-DWD1/IV	Gene expression study for characterization and localisation in healthy and bacterial/ PAMPs challenged animals. Expression of recombinant peptides for functional studies.	Mu *et al.*, 2010 Mu *et al.*, 2011 Li *et al.*, 2013
P. japonica	*Pj*-crus Ia, Ib/I *Pj*-crus II/II *Paj*-Crus Ic, Id, Ie, If/I *Paj*-Crus IIb and IIc/II	Gene expression study for characterization and localisation in healthy and bacterial challenged animals	Kim *et al*., 2012 Kim *et al*., 2013
P. leniusculus	*Pl*crustin1-2/I *Pl*crustin3/III	Gene expression study for characterization and localisation in healthy and bacterial challenged animals, in moulting animals, and during embryonic development. Expression of recombinant peptides.	Jiravanichpaisal *et al.*, 2007 Kuballa and Elizur, 2008 Donpudsa *et al.*, 2010 Zhang *et al*., 2010
H. americanus	CAP-2/? Hoa-crustin/I	Native peptide Gene expression for characterization and localisation in healthy and bacterial challenged animals	Battison *et al.*, 2008 Christie *et al.*, 2007 Clark *et al.*, 2013
H. araneus	Cru*Ha*1, 2/I Crustin *Ha*1, *Ha*2	Native peptides, gene expression study for characterization and localisation in healthy animals Gene expression for localisation study in bacterial challenged animals	Sperstad *et al.*, 2009 a Sperstad *et al.*, 2010
S. paramamosain/ serrata	Crus*Sp*/I	Gene expression for characterization and localisation in healthy animals. Recombinant peptide.	Imjongjirak *et al.*, 2009 Afsal *et al.*, 2011
C. maenas	Carcinin/I	Native peptide for antibacterial assay Gene expression in healthy individuals Gene expression in bacterial challenged animals Recombinant expression Native peptide for *in vivo* localisation via ICC, IHC, *in vitro* functional study	Relf *et al*., 1999 Towle and Smith, 2006 Brocton *et al.*, 2007 Brockton *et al.*, 2008 Suleiman *et al.*, 2017, and the current thesis

1.4. Hypothesis and scientific aims

The fact that carcinin is present in high levels in the haemocytes of *C. maenas* makes it intriguing that it is revealed only as a weak, narrow-spectrum antibacterial peptide. Since the animal invests so heavily in making large quantities of the peptide, this gives rise to the hypothesis that carcinin plays other biological roles in the animal besides a purely antimicrobial function. Since the studies of Brockton *et al*., no further studies have been conducted to unveil the novelty of this peptide, and whether it contributes to other immunological or non-immunological functions in the animal.

The aims of this project are:

1. To optimize the carcinin purification method in order to gain adequate amounts of the native peptide in reasonable time, and use the purified carcinin to produce specific polyclonal antibody (PAb).

2. To investigate the presence of the carcinin in tissues of healthy individuals of the shore crab *C. maenas*.

3. To study changes in carcinin localisation arising from biological events, such as gonadal maturation, moulting and in regenerating tissues.

4. To investigate the antibacterial mechanism of carcinin, it’s interaction with bacterial cells and possible opsonisation property.

5. To examine association of carcinin with chromatin extracellular trap formation by phagocytes.

Chapter 2
Carcinin Purification and Antibody Production

2.1. Introduction

The first objective of the present study was to purify the native carcinin from the haemocytes of *C. maenas*. Proteomic studies have recently gained significant roles in diverse research disciplines of marine animals and aquaculture (Campos *et al.,* 2013, Chandramouli, 2016). However, of the many crustin sequences (more than one hundred) now reported from different species (see Table 1.3, Chapter 1), gene expression has been the predominant approach to characterize and localise the majority of crustins, with haemocytes the most common cell type used for mRNA extraction and cDNA cloning (e.g., Bartlett *et al*., 2002, Supungul *et al*., 2008, Yue *et al*., 2010 b, Antony *et al*., 2010, Afsal *et al*., 2011, Afsal *et al*., 2013). There is no doubt that genetic methods are rapid and effective ways to obtain an enormous amount of data regarding protein sequences and phylogeny. However, it is important to consider that genetic data may fail to reflect accurately the localisation, abundance and biological roles of proteins. Protein function is also hugely correlated with its three-dimensional structure, which can be altered during different protein interactions (Hong *et al*., 2006).

Of 83 published studies regarding crustins, around 33 reports (*ca* 40%) have utilized recombinant proteins, paired with gene expression analyses (e.g. Zhang *et al*., 2007a & b, Supungel *et al*., 2008, Mu *et al*., 2011), or as the sole approach (e.g. Banerjee *et al.,* 2015, Jayesh *et al*., 2016). Gene expression analysis gives a general idea if a protein is expressed in an organ, without specifying the particular tissue that contains this protein, or giving any idea of whether the protein is originally produced in a certain organ, or delivered there by haemocytes (see Chapter 3 for more detail). In addition, studies to date have limited crustin detection to organs like gills, hepatopancreas, and muscles, ignoring the possible role that crustin might serve in other organs like gonads and nerve tissues. It is now clear that genome expression studies can aid more understanding of protein functions if paired with research based on studying the structure, properties and biological role of proteins.

Since the original purification of carcinin by Relf *et al* (1999), only four crustins have been purified and studied as native proteins: CAP-2 isolated by Battison *et al,* (2008) from haemocytes of the lobster, *H. americanus,* Cru*Ha*1 *and* Cru*Ha*2; two crustin isoforms isolated from haemocytes of the spider crab, *H. araneus* (Sperstad *et al.,* 2009

a); and a crustin from the granular haemocytes of the mangrove crab *E. tetragonum* (Sivakamavalli *et al*., 2015).

Many crustin studies aimed to produce the peptide in order to carry out functional studies, using mostly bacterial expression systems. The produced recombinant crustins have been employed in a number of biological assays to investigate crustin's anti-microbial spectrum (Supungul *et al.*, 2008, Mu *et al*., 2011, Banerjee *et al*., 2015, Jayesh *et al*., 2016, Yu *et al*., 2016) and other biological functions, like protease inhibitory properties (Chen *et al*., 2008), and/or haemolytic assays (Jayesh *et al.*, 2016). It is crucial however, when expressing a peptide using cell machinery, to take into account the peptide characteristics that dictate the optimal expression system that needs to be used. This was not the case with most crustins, as the majority of researchers used only one approach, the *E. coli* expression system, because of the high growth rate of the bacterium, its low cost and ease of usage.

The drawbacks of using bacterial expression systems are correlated with the lack of efficient post-translational modification on the protein product occurring in eukaryotic cells, such as glycosylation, phosphorylation, acylation, methylation, and most importantly, the formation of disulphide bridges (Walsh and Jefferis, 2006), which is essential for crustin function. If the recombinant crustins produced from bacterial systems were not processed and folded to form the unique structure of the WFDC domain, then their biological activity would be influenced profoundly. Moreover, a radical altering of peptide solubility can result from misfolding. This is associated with the formation of inclusion bodies, which in turn might cause the release of undesirable contaminants, mostly endotoxins, from bacterial cytoplasm during cell disruption for extracting the protein product (Cavallaro *et al.*, 2011). Another thing that should be considered that the bacterially expressed peptide has the amino acid N-formylmethionine instead of methionine as an the initial amino acid in the peptides produced by eukaryotic cells, which besides affecting protein structure, might induce an immune response if the peptide is to be used *in vivo* (Fu *et al.*, 2006). In addition, the cytotoxic effect of the produced AMP on the viability of the expressing bacterial cells should be considered.

However, some studies have tended recently to consider these drawbacks of the bacterial expression systems, and turn to use more complicated cellular machinery such as yeast (Liu *et al*., 2016, Arayamethakorn *et al.*, 2017). Yeast expression systems are also cost-effective, and still considered as simple and undemanding. Folding and modification of the produced peptide is more likely to occur similarly to that in the source organism (Idiris *et al*., 2010, Mattanovich *et al*., 2012). However, the glycosylation mechanism in yeast differs considerably from higher eukaryotes, which can still affect protein solubility, half-life and interactions (Hossler *et al*., 2009, De Pourcq *et al*., 2010). Insect cells were considered recently as an alternative to yeast and bacterial systems. Peptides produced in insect cells undergo signal peptide cleavage and disulphide bridge formation, in addition to proteolytic processing (Kollewe and Vilcinskas, 2013). However, though the glycosylation pattern is still different from mammalian cells (Harrison and Jarvis 2006), which was considered as a weakness for producing mammalian peptides, it does not differ from the mechanism occurring in other invertebrates, including crustaceans, which means insect expression systems are the ultimate cellular machinery for recombinant expression of crustacean peptides. Mammalian cells are the ideal systems for human recombinant peptide production in terms of post-translational processing, though culture conditions are complex and demand specialized techniques (Zhu and Hatton, 2017).

The original purification of carcinin was done by two steps of high performance liquid chromatography (HPLC); the first used an ion-exchange column, and the second used the reverse-phase high performance liquid chromatography (R-P HPLC) (Relf *et al.*, 1999). However, in this study, a modified protocol based on Fast Liquid Protein Chromatography (FPLC) was used instead. FPLC is a special type of chromatography, which serves mainly to purify large biomolecules such as proteins and DNA, and uses liquid buffered mobile phases. This procedure also involved two steps of purification; the first utilized ion separation via cation exchange resins, and the second was based on size exclusion chromatography. The procedure was used due to its availability, and because it is being used in a wide and successful manner to purify proteins.

Besides purifying the protein of interest and optimizing the purification method to achieve high yield of the purified peptide, the current study aimed to raise a specific antibody (Ab) for later use to localise the protein. In addition, different protein sub-

cellular localisation prediction methods are available on the Internet. Therefore, these were used to test the sub-cellular location, prior to investigating carcinin localisation *in vitro* and *in vivo*. These methods utilize amino acid sequence of a protein to predict its sub-cellular localisation, according to a specific signal included in the amino acid sequence that could be identified by certain compartment membranes (O'Rourke *et al*., 2005, Binder *et al*., 2014). The easy application and availability of these methods enabled their use in the present study to shed more light on carcinin localisation within cell compartments.

The aims of this chapter were:

1. To develop a modified method to purify larger quantities of carcinin from *C. maenas* haemocytes.
2. To confirm the identity of the protein by mass spectroscopy and use the purified protein to produce a specific antibody for use in future experiments.
3. To predict carcinin sub-cellular localisation on the basis of its amino acid sequence, using prediction software available on the web.

2.2. Materials and Methods

2.2.1. Animals

Specimens of adult intermoult (stage C4) crabs (carapace width *ca* 50- 75 mm) of *C. maenas* were obtained by creeling from the Forth Estuary, Scotland. Crabs were maintained in seawater tanks at ambient temperature (*ca* 10 ± 3° C) and water salinity of *ca* 32.5 ± 1.5 $^{o}/_{oo}$ for no longer than one week until use, as in Robb *et al.* (2014). All animals were fed twice per week with commercial fish pellets or fresh mussels. Only healthy animals were used for haemolymph extraction.

2.2.2. Reagents

Unless otherwise mentioned, all chemicals were purchased from Sigma-Aldrich. Solutions were prepared using distilled (dH2O) or Millipore water, followed by filtering through 0.2 μm cellulose acetate sterile syringe filters (VWR, Leicestershire, UK)

2.2.3. Carcinin purification

2.2.3.1. Preparation of cell lysate

Haemocyte lysate solution (HLS) was prepared from groups of between 24 and 50 crabs at a time, according to a method modified from Relf *et al.* (1999). Prior to bleeding, crabs were chilled by placing them at -20 ºC for a maximum of 10 minutes, then swabbing the bleeding site with 70% ethanol. Haemocytes were extracted by withdrawing 2 mL haemolymph per crab from the arthrodial membrane between the merus and carpus segments of the crab claw (Smith and Ratcliffe, 1978), into 3 mL of ice-cold marine anticoagulant (MAC) (Söderhäll and Smith, 1983) supplemented with the protease inhibitor phenylmethanesulfonyl fluoride (PMSF: dissolved in dimethyl sulfoxide at a final concentration of 1 mM). The haemolymph samples were pooled and then centrifuged at 1,900 x *g* for 10 min (4 ^{o}C). After discarding the supernatant, the cell pellet was re-suspended in twice the volume of 50 mM sodium phosphate buffer (pH 6.5) containing 1 mM PMSF at 4 ^{o}C. The haemocytes were then disrupted to release cell contents by repeated bursts (4-5 times each for 30 seconds) on a vortexer, with the cells cooled on ice for five minutes after each burst. The disrupted haemocytes were finally centrifuged at 40,000 x *g* (4 ^{o}C) for 22 min. The resulting HLS was

collected and protein concentration was calculated using the Bradford assay (Bradford, 1976).

2.2.3.2. FPLC procedure

In order to optimise carcinin purification, carcinin was purified from the HLS by fast liquid protein chromatography (FPLC) on a ÄKTA FPLC system (GE Healthcare Life Sciences, Buckinghamshire, UK). Around 10 mL of HLS was loaded onto a Mono S 5/50 GL cation exchange column (GE Healthcare Life Sciences) equilibrated with 50 mM sodium phosphate buffer at pH 6.5. This was eluted with 50 mM sodium phosphate buffer (pH 6.5) containing 1M NaCl. The salt gradient was increased from 0-100% over 20 min. Fractions of 1 mL were collected and the protein concentration in each was determined by the Bradford assay (Bradford, 1976). Fractions containing high levels of protein were subject to further purification on a Superose 6 10/300 GL gel filtration column (GE Healthcare Life Sciences). Equilibration and elution were again performed using 50 mM sodium phosphate buffer (pH 6.5).

2.2.4. Sodium dodecyl sulphate polyacrylamide gel electrophoresis (SDS/PAGE)

SDS/PAGE was performed according to Schägger and von Jagow (1987); In brief, a discontinuous multiple polyacrylamide gel was made of separating (resolving) gel (T: 16.5%, C: 3%), spacer gel (T: 10%, C: 3%) and stacking gel on top (T: 4%, C: 3%) (Bio-Rad). Gel combinations were mixed, and just prior to gel pouring, 10% ammonium persulfate and tetramethylethylenediamine (TEMED) were added to initialize gel polymerization in 0.5% and 0.05% percentages of total gel volume, respectively. Protein samples (cell lysate, haemolymph plasma [1:10 dilution] and purified fractions) were mixed in a 1:1 ratio with 54 mg mL^{-1} of 1,4-Dithiothreitol (DTT) in Laemmli buffer (Bio-Rad), and heated for 3 minutes at 90 °C for protein denaturation. An average of 5 μg of denatured protein in each sample was loaded onto the gels, in addition to 10 μL of SDS/PAGE protein marker (Precision Plus Protein™ All Blue Prestained Protein Standard, Bio-Rad, Hertfordshire, UK). Gels were run using a Mini-Protean Tetra Cell System and PowerPac™ HC power supply (Bio-Rad) for 35 minutes at 200 volts. Migrated bands were stained with Coomassie Brilliant Blue R-250 (Bio-Rad), except for gels prepared for western blotting and imaged via the ChemiDoc XRS+ system (Bio-Rad).

2.2.5. Mass spectrometry procedure

Protein identity of fractions with molecular weight matching that expected for carcinin was confirmed by Nano-scale liquid chromatographic electrospray tandem mass spectrometry (nLC-ESI-MSMS). Gel bands with molecular weight *ca* 11-12 kDa were excised manually with a sterile razor and each one placed in a sterile Eppendorf tube containing 1 mL of 0.22 Millipore water before sending for MSMS analysis. Mass spectrometry was performed at the BBSRC Mass Spectrometry and Proteomics Facility Unit (University of St Andrews, St Andrews, Scotland). Briefly, bands were subject to in-gel digestion according to Shevchenko *et al.* (1996), using ProGest Investigator in-gel digestion robot (Diglab). After cutting the gel into 1 mm cubes, each one was subjected to de-staining with acetonitrile, reduction and alkylation, before digestion with trypsin at 37° C. Formic acid (10%) was used to extract the peptides.

For nLC-ESI-MSMS analysis, and after peptide concentration with SpeedVac (ThermoSavant), separation was performed on an Acclaim PepMap 100 C18 trap and an Acclaim PepMAp RSLC C18 column (ThermoFisher Scientific, Paisley, UK) via a nono LC Ultra 2D plus loading pump and nanoLC as-2 auto sampler (Eskigent). Elution of peptides was carried out by pumping a gradient of increasing acetonitrile with 1% formic acid. The eluent was sprayed into a Triple TOF 5600 electrospray tandem mass spectrometer (ABSciex) and analyzed in Information Dependent Acquisition (IDA) mode. The generated mass spectra were used to search the NCBInr database Aug 2013 with no species restriction using the Mascot algorithm (Matrix Science). As a cleavage enzyme, trypsin was used, in addition to carbamidomethyl as a fixed modification of cysteine and methionine oxidation and deamidation of glutamines and asparagine as variable modifications.

2.2.6. Carcinin antibody production

This study aimed to produce a polyclonal rabbit antibody (Ab) from 1 mg of purified freeze-dried carcinin by a commercial company (Davids Biotechnologie, Regensburg, Germany), as the first specific Ab to be raised against native crustin. In brief, rabbits were immunized with carcinin 5 times during a 63-day period and the resultant antibody purified by affinity purification by the company. Following receipt of the antibody, Western blotting was carried out to test for reactivity in HLS, FPLC fractions and cell-free haemolymph samples. SDS/PAGE was carried out as before (Section 2.2.4), but

without Coomassie blue staining. After electrophoresis, the gel was washed with distilled water then both gel and the 0.45µm nitrocellulose blotting membrane (Bio-Rad), were equilibrated with transfer buffer (TBS: Towbin buffer with SDS: 25 mM Tris, 192 mM glycine, 20% methanol (v/v), 0.025–0.1% SDS, pH 8.3) for 15 minutes. After soaking fibre pads and filter papers in the transfer buffer, a sandwich cassette was assembled in a Mini Trans-Blot® Cell (Bio-Rad) and the transfer was done at 20 volts for 2.5 hours. After blotting, the nitrocellulose membrane was washed for 10 minutes with TTBS washing buffer (20 mM Tris-HCl, 500 mM NaCl, 0.05% Tween 20, pH 7.5) and blocked over night with 3% bovine serum albumin (BSA) solution in TBS on a rocker (Techne Seesaw Mini SSM4; Bibby Scientific, USA).

Both the anti-carcinin polyclonal Ab, and rabbit pre-immune serum were diluted in 3% BSA solution in TTBS in different ratios: 1:10000, 1:50000 and 1:00000. Primary incubation was for 1.5 hours, followed by washing three times each for five minutes with TTBS. Goat anti-rabbit alkaline phosphatase (AP) tagged secondary Ab was added in the same dilutions as above and incubated for a further 1.5 hours. Another 3 washes as before were carried out before adding the alkaline phosphatase substrate solution. This comprised 100 µL of 5-bromo-4-chloroindolyl phosphate (BCIP) solution (15 mg BCIP in 1 mL dimethylsulfoxide [DMSO]) plus 100 µL nitroblue tetrazolium (NBT) solution (30 mg NBT in 70% DMSO/30% distilled water) added to 10 mL AP colour development buffer (MgCl2 0.233 g, Tris base 12.1 g, dH2O 800 mL, pH 9.5). After the signal developed, the nitrocellulose membrane was washed with TBS, and imaged using the ChemiDoc XRS+ system (Bio-Rad). Three controls were included, namely: (i) no primary nor secondary Ab; (ii) secondary Ab only; (iii) pre-immune rabbit serum substituted for the primary Ab. Controls (i) and (ii) used buffer in place of the relevant Ab.

2.2.7. Carcinin sub-cellular localisation prediction

The amino acid sequence of carcinin was obtained from GenBank library, NCBI (carcinin [Carcinus maenas] GenBank: CAD20734.1). The FASTA format was uploaded on three protein sub-cellular localisation general prediction tools: CELLO (Yu *et al*., 2006) (http://cello.life.nctu.edu.tw/), Protein Prowler (Bodén and Hawkins, 2005) (http://bioinf.scmb.uq.edu.au:8080/pprowler_webapp_1-2/), and MultiLoc (Sun *et al*., 2005, Casadio *et al*., 2008) (http://abi.inf.uni-tuebingen.de/Services/MultiLoc/).

2.3. Results

2.3.1. Carcinin purification

Total protein concentrations measured by Bradford assay ranged between 4-5 mg mL^{-1} in HLS crude samples. Cation exchange FPLC samples with protein concentrations between 1-3.5 $mg.mL^{-1}$ were loaded onto a gel filtration FPLC column. Carcinin was successfully purified, appearing in fractions 19 and 20 (Figures 2.1, 2.2) with identity confirmed using SDS-PAGE and mass spectroscopy (Figure 2.3, Figure 2.4, i, ii).

Carcinin concentrations in the purified fractions measured between 200-600 µg mL^{-1}, depending on the total number of crabs bled, with percentage yield of the purified carcinin ranged between 5-12%. Carcinin purity was revealed by SDS/PAGE (Figure 2.3) as only carcinin bands were seen in fractions 19 and 20, and confirmed by mass spectrometry (Figure 2.4). Sadly, and due to carcinin's observed property to stick to nitrocellulose membrane, all efforts taken to concentrate purified fraction did not succeed in obtaining higher yields of purified protein from an initial number of ca. 20 crabs, thus at later stages in the study, higher numbers of animals (50) were used for haemolymph extraction to obtain higher protein concentrations.

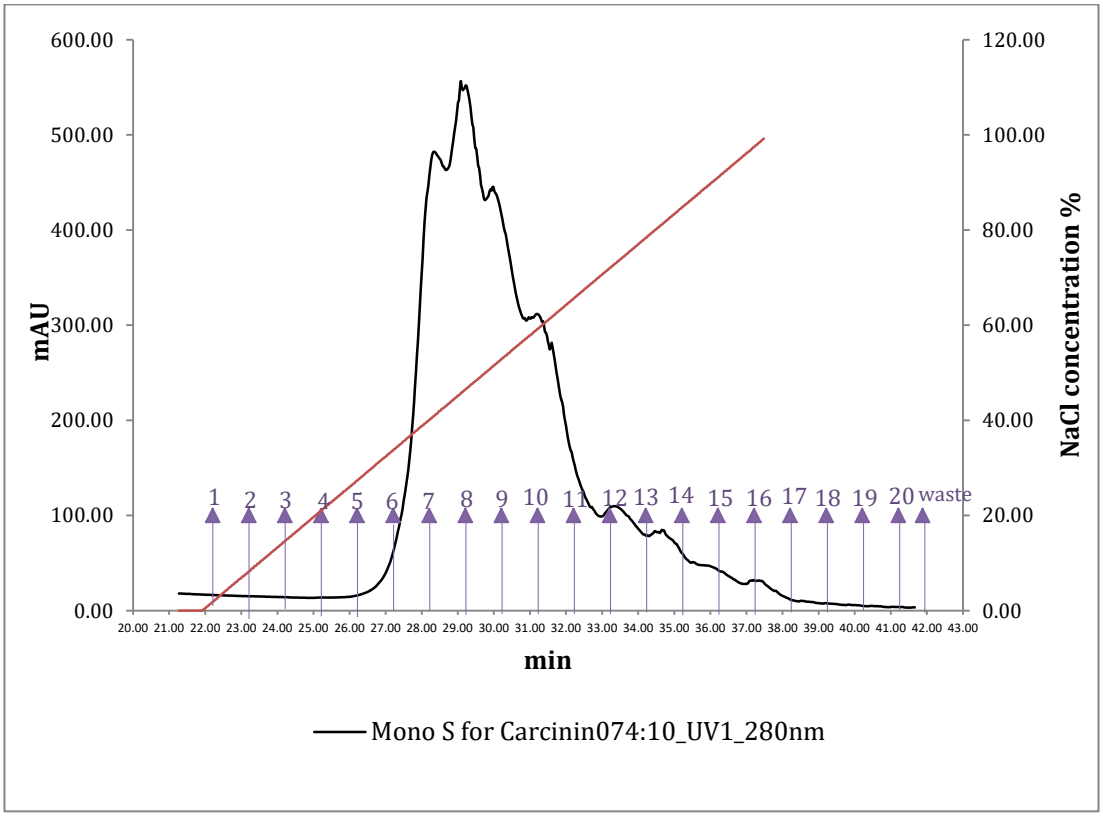

Figure 2.1: First step of carcinin purification from HLS of the shore crab, *C.maenas*, via FPLC Mono S cation exchange column. Chromatogram showing high protein concentration peaks in fractions 6-14, identified by UV detection (UVI 280 nm) and eluted with 40-85% NaCl (red line).

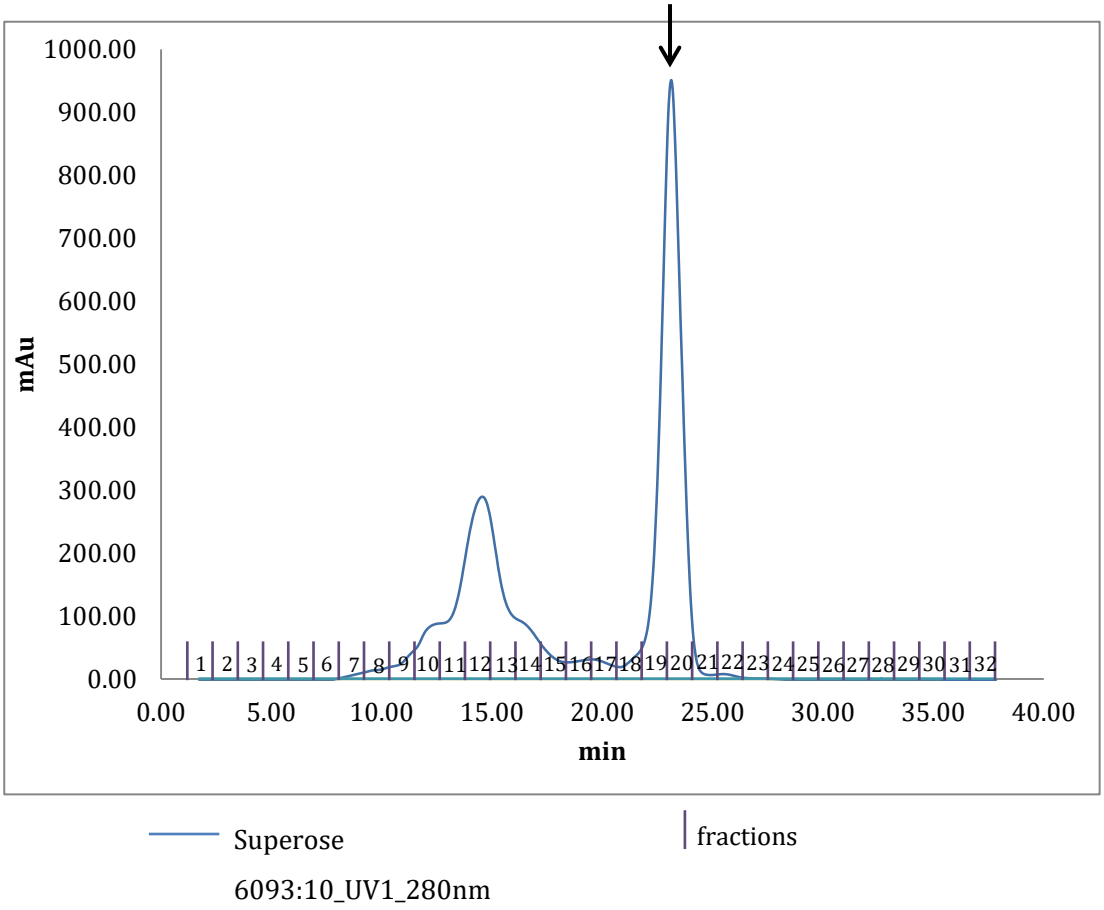

Figure 2.2: Second step of carcinin purification via Suprose gel filtration column. Chromatogram shows purified carcinin peaks in fractions 19 and 20 (arrow).

2.3.2. Confirmation of carcinin identity

Coomassie blue stained SDS/PAGE bands in FPLC fractions 19 and 20 had molecular masses of 11-12 kDa, matching that previously recorded for carcinin by Relf *et al.*, (1999), and Brockton *et al.,* (2007). The purified protein from fractions 19 and 20 appeared as a twin band consisting of closely migrated, but not identical double parts (Figure 2.3 a, c). No proteins of a similar molecular mass were observed in samples of cell-free haemolymph (Figure 2.3, b). The twin parts of the band were separately excised and subjected to mass spectrometry, which revealed that both parts corresponded to carcinin and had the same weight (Figure 2.4, i, ii), though one appeared to be more abundant, as revealed from band density on SDS/PAGE (Figure 2.3, a, c).

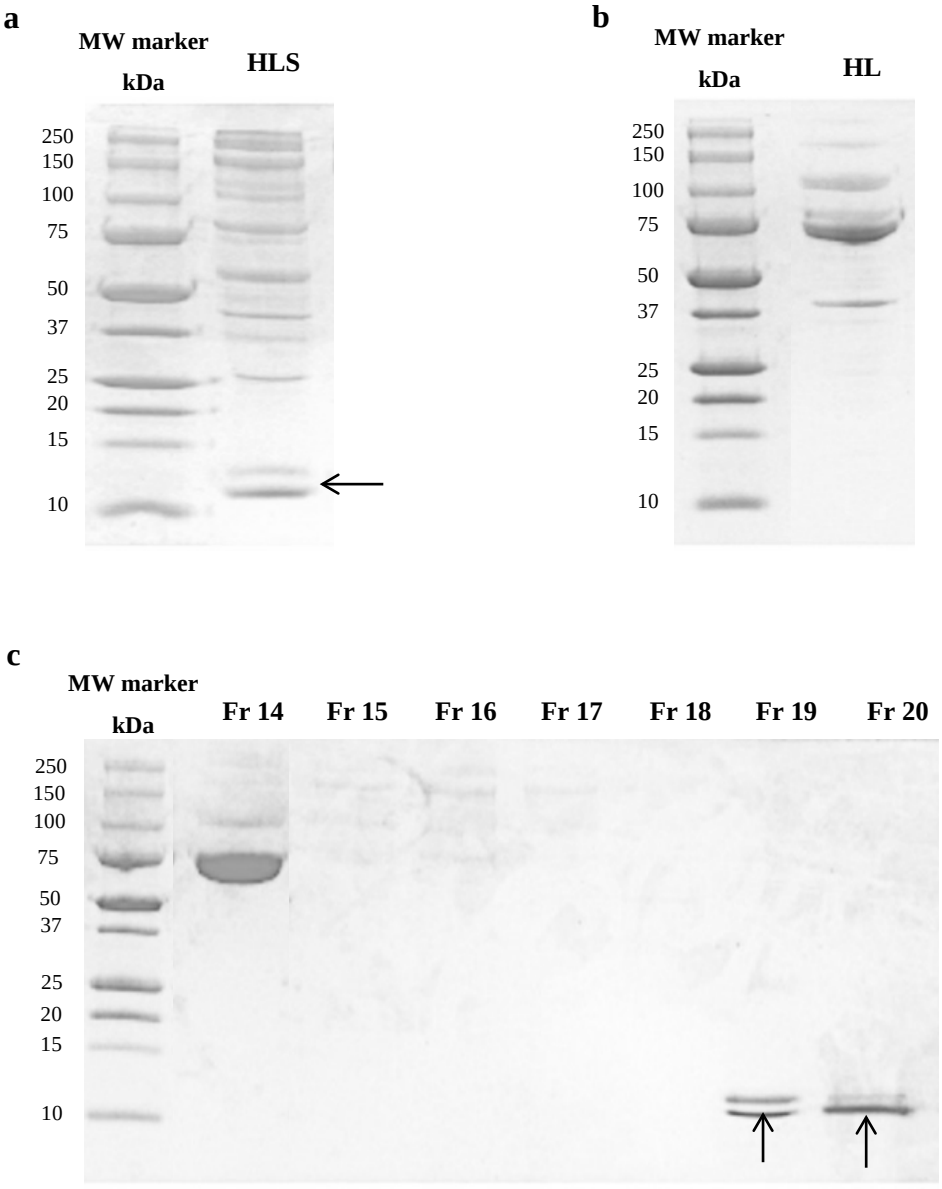

Figure 2.3: SDS/PAGE gels. (**a**): HLS sample run on SDS/PAGE shows twin band of between 11-12 kDa (arrow). (**b**): Cell-free haemolymph sample on SDS/PAGE reveals protein bands ranging between 40-200 kDa, with no band matching carcinin. (**c**): Lanes show fractions 14 to 20 collected after FPLC gel filtration. Fractions 19 and 20 depict two bands of carcinin of approximately 11.5 kDa, each has two parts with the upper band appearing less abundant in both fractions (arrows). Bands are produced from uploading 5 µg of protein per well. Fr=fraction, HL=cell-free haemolymph, HLS=haemocytes lysate solution.

i

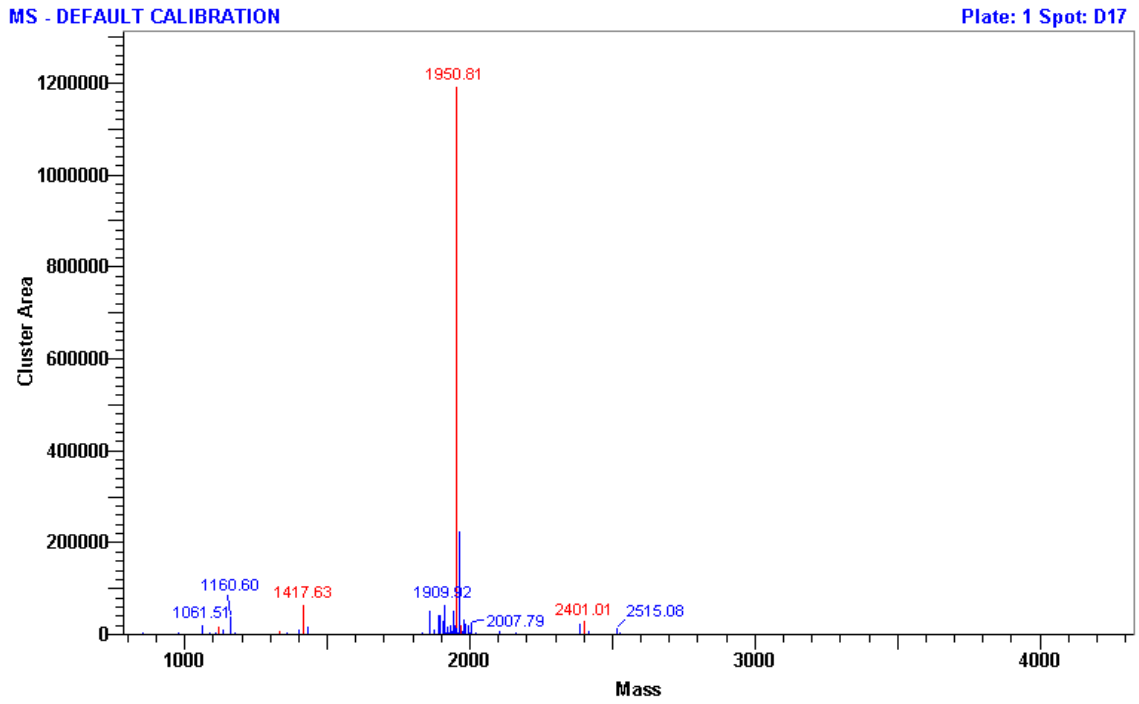

ii

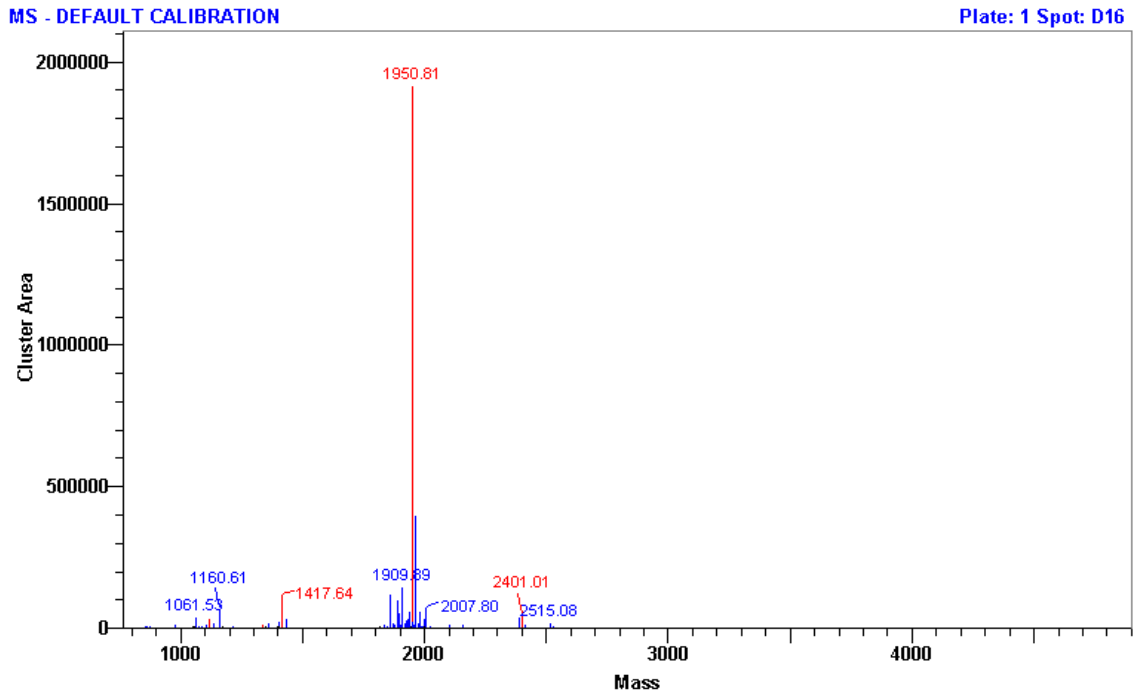

Figure 2.4: nLC-ESI-MSMS analysis of excised gel bands. Major peaks (in red) match carcinin protein profile from the NCBI database. For both graphs (**i**) and (**ii**), vertical axis represents abundancy, while horizontal axis represents mass to charge ratio.

2.3.3. Western blotting

Western blotting showed that the anti-carcinin polyclonal Ab bound to both parts of the carcinin bands depicted in fractions 19 and 20 as well as those present in HLS. No reactivity was observed with other proteins in the HLS samples, nor with any proteins in the cell-free haemolymph (Figure 2.5). The most effective staining was achieved with 1:50000 dilutions of both primary and secondary Abs. No reactivity was observed in any of the three controls.

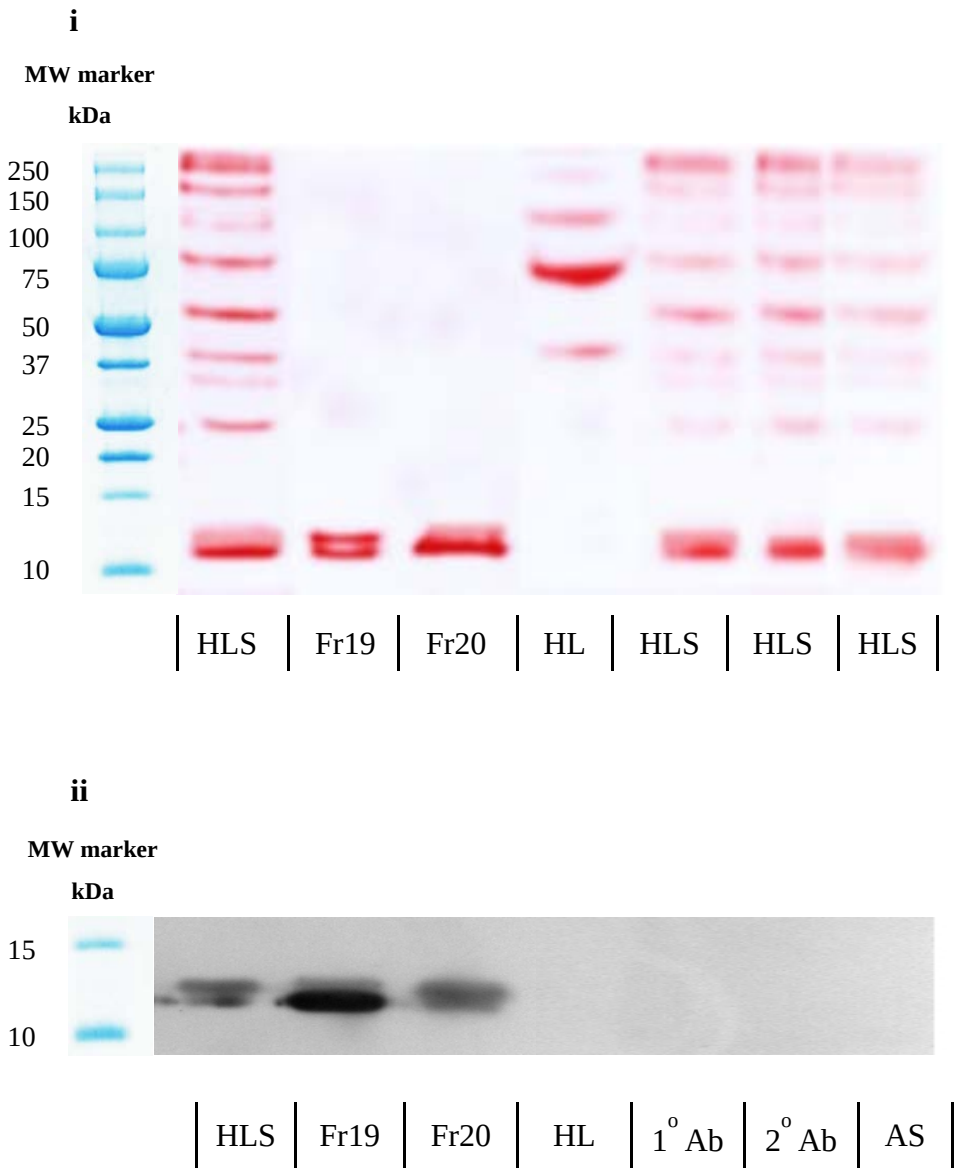

Figure 2.4: Western blot showing reactivity of the anti-carcinin polyclonal Ab. (**i**): Image of the blotted nitrocellulose membrane, stained with Ponceau S shows HLS, Fr19, Fr20 and HL bands. The three HLS samples run subsequently aim to test Abs specificity. (**ii**): Specific binding after western blotting using anti-carcinin Ab was observed in both purified carcinin fractions 19 and 20, as well as in carcinin bands from HLS samples. No reactivity was seen in cell-free haemolymph (HL) samples, any other peptides in HLS or the antibody controls. Bands are produced from loading 5 µg of protein per well. 1^{o} Ab= control with neither primary nor secondary Abs, 2^{o} Ab=no primary Ab, AS=antisera control.

2.3.4. Prediction of carcinin sub-cellular localisation

All three protein subcellular localisation prediction engines used in this study revealed that carcinin is a secretory (or extracellular) protein.

Table 2.1: CELLO results of carcinin sub-cellular localisation, indicating it to be an extracellular protein.

SeqID: gi|18157188|emb|CAD20734.1| carcinin [Carcinus maenas]				
Analysis Report:				
SVM	LOCALIZATION	Reability	RELIABILITY	
Amino Acid Comp.	Extracellular	0.669	0.669	
N-peptide Comp.	Extracellular	0.899	0.899	
Partitioned seq. Comp.	Extracellular	0.811	0.811	
Physico-chemical Comp.	Extracellular	0.985	0.985	
Neighboring seq. Comp.	Extracellular	0.773	0.773	
CELLO Prediction:				
	Extracellular	4.136*	4.136 *	
	Mitochondrial	0.202	0.202	
	Cytoplasmic	0.194	0.194	
	Nuclear	0.185	0.185	
	Chloroplast	0.149	0.149	
	Plasma Membrane	0.059	0.059	
	Lysosomal	0.020	0.020	
	ER	0.016	0.016	
	Vacuole	0.015	0.015	
	Peroxisomal	0.014	0.014	
	Golgi	0.005	0.005	
	Cytoskeletal	0.004	0.004	

	PProwler			PTS1Prowler
Sequence	SP	MTP	OTHER	Peroxisome
gi|18157188|emb|CAD20734.1|	**0.98**	**0.00**	**0.02**	**0.00**

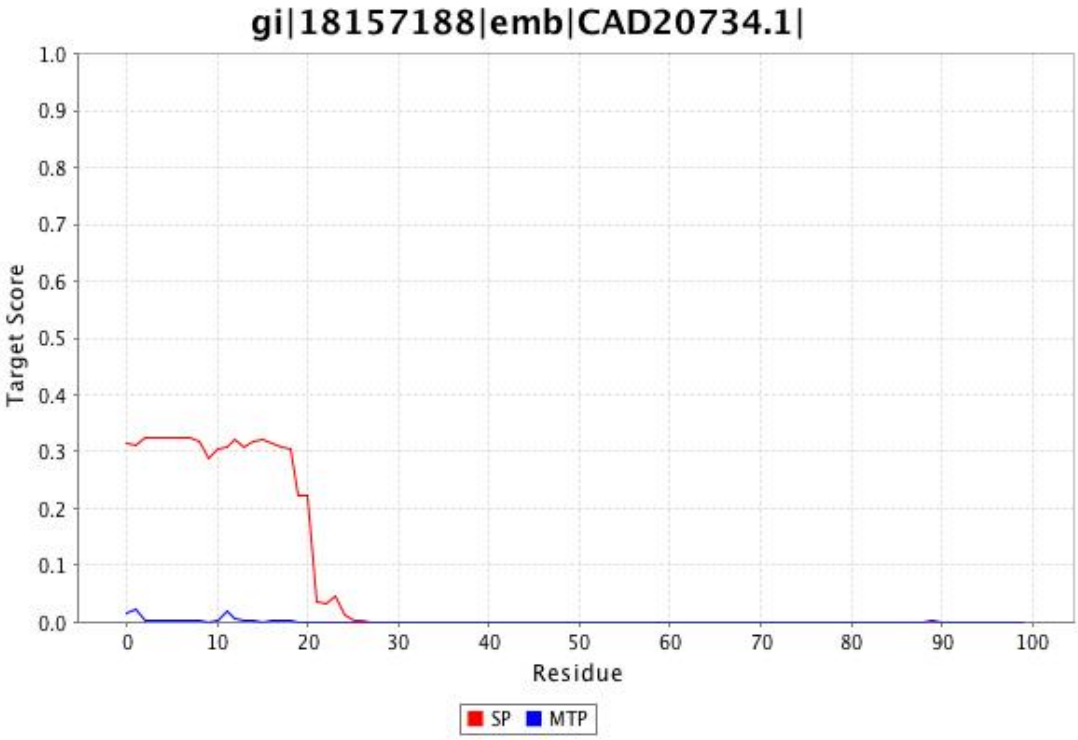

The targeting score of a residue indicates the predictor's belief that the residue is part of a targeting sequence directing the protein to a specified compartment (secretory pathway, mitochondria, or chloroplast). The score is calculated separately for each compartment.

SP: secretory pathway

MTP: mitochondria

Figure 2.6: Carcinin sub-cellular localisation predicated by Protein Prowler. Result shows carcinin as a secreted protein.

Table 2.2: Result of protein sub-cellular localisation prediction tool, MultiLoc, indicating that carcinin is an extracellular protein.

origin = animal

predictor = MultiLoc

ID	Predicted Location	Score
Seq 1	extracellular	0.99

Protein: gi|18157188|emb|CAD20734.1|carcinin[Car

Predicted Location: secretory pathway: 1.0

cytoplasmic: 0.0

nuclear: 0.0

mitochondrial: 0.0

2.4. Discussion

Understanding the structure and properties of carcinin is crucial for defining its function. The present study succeeded in extracting the native carcinin from the haemocytes of *C. maenas* via an FPLC procedure, which aided greatly to purify carcinin effectively. FPLC is a preferable procedure when purifying proteins from a crude cell lysate, since damaging factors such as high pressure and temperature, harsh solvents and extreme pH are not employed in FPLC. A high-pressure rate has been accused of altering protein structure and damaging its assembly (Runde, 2016). The large loops and high flow rate in the FPLC procedure enabled injection of larger sample volumes, which helped to gain higher yields of carcinin more quickly than HPLC. Moreover, the transparent glass columns in FPLC were not only biocompatible, but also allowed close observation of the process, including the presence of air bubbles that can affect separation efficiency. In addition, the software employed by the FPLC procedure was flexible and simple to use, and enabled the direct control of different parameters like flow rate, when necessary. Purified carcinin was of great importance in producing specific Ab, as well as employing the protein in a number of biological assays. Recruitment of natural carcinin assures its efficacy and leads to results that might be more accurate and trusted.

SDS/PAGE showed carcinin appearing as a small protein which migrated as a double band between 11 and 12 kDa. Both parts of the twin band were confirmed to match carcinin by mass spectrometry, indicating to 100% purity, and it is therefore possible that the bands may represent carcinin isoforms. This thought is supported by Brockton *et al.* (2007), who studied the full-length cDNA of carcinin and its matching genomic sequence. The study predicted carcinin to have six isoforms (GenBank accession nos. AJ237947, AJ427538, AJ821886, AJ821887, AJ821888 and AJ821889) in addition to a further two isoform sequences from gDNA sequencing. The study assumed that isoform diversity came from non-synonymous alteration on amino acid sequencing, occurring at distinct nucleotide loci either at the genomic and/or transcript level. These included residue 17 (nucleotide 49) at the leader sequence (one substitution), residue 22, and three possible amino acid substitutions at position 39 and 56, plus one substitution at position 63 in both translated cDNA and gDNA sequences. These isoforms might come from either transcription of different alleles and/or post-translational modification of individual transcripts.

The diversity of crustin genes has also been reported in other studies, indicating that one or more crustin isoforms are likely to occur (Afsal *et al*., 2013, Banerjee *et al* 2015, Vatanavicharn *et al.,* 2009). Though, the assumption that the observed twin band part might relate to carcinin isoforms raises some debate as neither Relf *et al.* (1999) nor Brockton *et al.* (2007) in their SDS/PAGE for purified and recombinant carcinin revealed the supposed isoform. Alternative splicing producing messenger RNA is the predominant cause for appearance of protein isoforms. It was reported recently that alternative splicing might have individual differences that produces different phenotypes (Hassan *et al.,* 2014). Carcinin isoforms might arise individually, thus it is possible that while some crabs may have particular isoforms for carcinin, others might not. Another explanation may relate to the number of crabs used in this study, which was larger than used by either Relf or Brockton and co-authors. Bleeding of fifty crabs led to a higher protein concentration in the crude sample thus some carcinin isoforms, which could have been at a relatively low concentration in the previous studies could then be detectable by SDS/PAGE. It is reasonable as well to consider that some cleavage might occur in protein formation while extracting carcinin in the current study, thus generating a second, slightly separated band to the principal carcinin one.

Sub-cellular prediction methods revealed carcinin as an extracellular or a secretory protein. In the oncoming chapters, experiments will reveal more details about the localisation of carcinin. Using its specific Ab, more evidence emerged to illustrate where carcinin is made and secreted, and how it exerts its action, this helping to unmask its biological role.

In conclusion, a key step to further understand the ambiguous biological role of carcinin was accomplished. The purification procedure was optimized to give larger yields of the purified native peptide. This enabled the production of a specific, polyclonal Ab for the native form of carcinin that was used later in a broad range of immunocytochemistry (ICC) and immunohistochemistry (IHC) procedures. It was of great importance as well that considerable amounts of purified native carcinin were employed in a number of biological assays aiming to define carcinin specific roles in various defence mechanisms, as will be described in the forthcoming chapters.

Chapter 3

Carcinin Localisation in Haemocytes and Tissues of *Carcinus maenas*

3.1. Introduction

Many recent studies have focussed on crustin gene expression in different tissues and quantifying expression changes following experimental challenge (e.g Hipolito *et al.*, 2014, Liu *et al.*, 2015, Yu *et al.*, 2016). Most of these studies have demonstrated crustin expression in haemocytes, but failed to show whether specific cell types and tissues of other organs also synthesize the protein (e.g. Imjongjirak *et al.,* 2009, Kim *et al.*, 2012 Arockiaraj *et al.,* 2013, Hipolito *et al.*, 2014). While gene expression in these tissues may change after injection of microorganisms or immune-stimulating compounds, no consistent pattern of crustin response emerges (reviewed by Smith and Dyrynda, 2015). Studies on *C. maenas*, including data obtained from an expressed sequence tag (EST) library, have not added significantly to knowledge of carcinin distribution and function (Brockton *et al*., 2007). Therefore, it is essential to identify the specific localisation of carcinin, not only to understand where and how carcinin exerts its effects, but also to contribute to a fuller comprehension of carcinin involvement in cell and tissue function. Thus, in addition to haemocytes, it is important to consider carcinin localisation in other body organs that play key roles in immune defence mechanisms.

In animals such as crustaceans with open circulations, i. e. where haemolymph flows freely through the body cavity and is pumped by the heart directly into the organs and tissues of the animal, in the absence of blood vessels, organs such as the gills, hepatopancreas and gonads are important contributors to overall defence. In *C. maenas*, there are nine pairs of gills, which are highly permeable tissues exposed to many invading organisms (Sawyer *et al.,* 1976). Thus in addition to their respiratory function, they need effective immune defence mechanisms to contain possible pathogens before they can spread further. The hepatopancreas (also referred to as the midgut gland) is a large bilateral organ that controls metabolic functions such as digestion, enzyme secretion, and nutrient absorption and storage. The rest of the digestive system, especially the gut, is also important in immunity as different pathogens commonly enter with food. It is important to consider that some insect AMPs were found to be secreted from the gut and contribute to anti-microbial defence there (Richman and Kafatos, 1997).

Other tissues less frequently considered for crustin localisation include the heart, gonads and eyestalk. In the crab, the heart is a single-chambered sac that maintains haemolymph circulation via muscle contraction, thus protecting this organ is vital. The reproductive system of the crab is controlled by glands at the base of the eyestalk, which drive the maturation of the testes and ovaries. Protection of these organs is therefore critical for the developing gametes, and later on, the growing embryos. Crabs are dioecious: the females have paired ovaries, which together with the sperm reception structures form the female reproductive system, connected to the outside via gonophores; the males have paired white to yellow elongate testes, connected to the external environment by the vas deferens and gonophores. Recently, anti-microbial proteins have been reported from the reproductive system of the mud crab, *Scylla serrata*, and found to play significant roles in protection during mating and embryo development (Xu *et al*, 2011 a & b). The eyestalk is also an essential organ, which is responsible not only for vision, but also controls different neuroendocrine processes (Quackenbush, 1986).

These organs were therefore chosen for examination of carcinin localisation, not only for their functional importance, but also because they were suitable for histological processing. Other tissues were not examined as their size and/or fragility meant that they were unlikely to remain intact during histological processing. Carcinin was localised using the carcinin- specific polyclonal antibody (PAb) raised against the native protein (see Chapter 2). Indirect immunocyto- (ICC) and histo- (IHC) chemistry techniques were performed, using secondary antibodies (Ab) conjugated with enzymes or fluorescent dyes, as appropriate. Phase, fluorescence and confocal microscopy were all employed in carcinin visualization, allowing the amplification of weak signals and visualization of small structures.

The aim of this chapter is:

1. To confirm carcinin localisation in whole and enriched haemocyte populations of *C. maenas*, using the produced specific polyclonal Ab.
2. To identify the extent of carcinin localisation in different organs of healthy, unstimulated *C. maenas* including gills, hepatopancreas, heart, midgut caecum, eyestalk and gonads.

3.2. Methods

3.2.1. Optimization of primary and secondary Abs concentration used for immunochemistry procedures

Preliminary experiments were carried out to define the optimum primary and secondary Ab concentrations to give the clearest signal without non-specific binding (Hofman and Taylor, 2013). This was done using haemocytes extracted into MAC as in Section (2.2.3.1), but without the addition of PMSF to the anti-coagulant. The diluted haemolymph was centrifuged on a Beckman Coulter Allegra^{TM} X-12R centrifuge (High Wycombe, UK) at 500 x *g* (4°C) for five minutes. The supernatant was discarded and the cells were washed with sterile 3.2% NaCl (5 minutes, 4 °C, 500 x *g*). Cells were then re-suspended in MAC, and cyto-centrifuged in a Shandon Cytospin 3 (Thermo-Fisher Scientific, UK) at room temperature, by adding 200 µL of cell suspension per cyto-centrifugation funnel. Additional MAC (300 µL) was added to each funnel just before centrifuging the haemocytes at 7x *g* for 3 minutes at room temperature onto clean glass slides. These slides were then subjected to fixation and immunocytochemistry as described in Section (3.2.3), testing primary and secondary antibodies in dilutions ranging between1:100 - 1:1000. The immunocytochemistry and immunohistochemistry procedures conducted in this study were adapted from Robb *et al*. (2014). Slides were examined using a compound microscope (Olympus BX40).

3.2.2. Haemocyte separation

Enriched sub-populations of haemocytes were separated using density gradient centrifugation, as described previously in Söderhäll and Smith, (1983). Percoll gradients were prepared by mixing 9 parts of Percoll (GE Healthcare Life Sciences) with one part of 32% NaCl to prepare a stock isotonic solution. The required Percoll density (either 60% or 40%) was obtained by further dilution with 3.2% NaCl, followed by centrifugation in a Beckman Coulter Avanti® J-26 XP centrifuge (High Wycombe, UK) at 25000 x *g* for 22 minutes (4°C) to make continuous gradients. Haemolymph (2 mL) was extracted as described in Section (2.2.3) and diluted in 3 mL of MAC (minus PMSF). This diluted haemolymph (2 mL) was loaded onto 9 mL of 60% continuous Percoll gradients and centrifuged at 3,000 x *g* for 10 min in a Beckman Coulter Allegra^{TM} X-12R centrifuge to generate bands of HCs, SGCs and GCs.

ProH populations were obtained and isolated via two-step density gradient centrifugation as in Roulston and Smith (2011). Briefly, 1 mL of haemolymph was withdrawn initially per crab to induce ProHs release into circulation from the haemopoietic tissue. A second haemolymph extraction (2 mL) from the same animal was made 24 hours later and this sample layered onto 60% continuous Percoll and centrifuged as above. The top layer of the HC cell band was carefully removed and placed on a second, 40% Percoll gradient. Centrifugation was then carried out under the same conditions used for the initial separation on the 60% gradient. ProHs appeared as a thin layer directly above the HCs band.

Cells from each enriched, separated haemocyte population were subject to brief washing (5 minutes, 4 °C, 500 x *g*) with 3.2% NaCl before re-suspension in MAC and adjustment of the cell number to *ca* 6.0 x 10^5 mL^{-1}. Cyto-centrifugation slides were prepared as above (Section 3.2.1), followed by fixation with 4% paraformaldehyde (PFA) in phosphate buffered saline (PBS) with 2% NaCl for 30 minutes prior to ICC.

3.2.3. Immunocytochemistry

For localisation of carcinin in whole and enriched haemocyte populations, cyto-centrifuged cell preparations were permeabilized with 0.1% Triton-X 100 in PBS. Blocking of endogenous peroxidase (for peroxidase labelled secondary antibody) was done by incubation with 3% hydrogen peroxide in PBS for 30 min, followed by 3×5 min washes with PBS. Blocking of endogenous antigens was performed using 10% goat serum added to 10% bovine serum albumin solution in PBS with 1-hour incubation. Glycine (0.1M) and ammonium chloride (50 mM) were also present in the blocking solution to quench auto-fluorescence when using fluorescent-tagged antibodies. Incubation with the primary antibody (1:100 dilution of anti-carcinin PAb) for 90 min was followed by a further 90 min incubation with the secondary Ab. The secondary antibody solution consisted of either 1:100 peroxidase tagged goat anti-rabbit Ab, or 1:100 FITC tagged goat anti-rabbit Ab (excitation 488 nm and emission 518 nm), alone or with 5 μM DRAQ5™ (BioStatus Ltd. Leicestershire, UK) (excitation 647 nm; emission 681 nm, pseudo-coloured blue) and 0.15 μM rhodamine phalloidin (Thermo Fisher Scientific, Paisley, UK) (excitation 540 nm; emission 565 nm) to identify F-actin. All Ab dilutions were made up with blocking solution and 3×5 min washes in PBS were performed between each step. For peroxidase detection,

slides were incubated with the peroxidase substrate 3,3-diaminobenzidine (DAB) diluted with 3% hydrogen peroxide (1:1) for 30 minutes or until the signal developed, before final washing. The slides were mounted with Vectashield mounting medium (with anti-fade agent) (Vector Laboratories, Peterborough, UK) for fluorescence detection, or Kaiser's aqueous mounting medium (water 52 mL, gelatin 8 g, glycerol 50 mL).

Control slides comprised (i) preparations without primary or secondary antibodies, (ii) slides incubated with secondary antibody only and (iii) preparations treated with rabbit serum instead of primary antibody and incubated with the secondary. For controls (i) and (ii), 3% bovine serum albumin in PBS was substituted for the relevant antibody solution. All slides were examined using either an Olympus BX40 for peroxidase-labelled slides, a Zeiss Axiophot fluorescence microscope for phase contrast and fluorescence labelling, or a Leica (DMIRE2) TCS2 confocal microscope (Leica Microsystems, Milton Keynes, UK) for multi-staining fluorescence labelling.

3.2.4. Fluorescence image processing and co-localisation analysis

Fluorescence images were captured by Zeiss ZEN digital imaging software for fluorescence microscopy or Leica software for confocal microscopy. Image processing was done using Image J (National Institutes of Health, USA). Analysis of fluorescence microscopy images was carried out to quantify carcinin co-localisation with other cellular markers (i.e. f actin, DNA). This approach was made due to the fact that interpretation of co-localisation images is highly subjective, while fluorescence images can be analysed quantitatively, as they are built from numbers (digital data) (Zinchuk *et al.*, 2007). Though this approach is common for protein localisation studies in mammalian cells, it has not been used before for any invertebrate studies, in particular for any of the studied crustins. Image J software was used to select 128×128 pixel area from a representative overlay fluorescence image then split into individual colour channels, each one saved as a text image. Each pixel was given a value from 0 to 255, proportional to the intensity of colour in the original fluorescence image. Microsoft Word was used to modify the text files previously generated by Image J, so that they could be read by Microsoft excel (replacing all tabs with manual line breaks). Following this, Excel was used for all calculations by using the IF function to provide the number of total pixels in each individual (e.g. green/red)

and combination (e.g. yellow/orange or cyan) colour. Percentages of the amount of carcinin that co-localises, or not, with the marker was calculated from the number of pixels in the individual or combination colours as well as the intensity of the fluorescence emission in each pixel. A scatter plot was then generated showing the distribution of individual colour pixels against their value.

3.2.5. Tissue processing

3.2.5.1. Tissue excising and fixation

Samples of gill, hepatopancreas, heart, hindgut, eyestalk and gonads were excised from adult crabs freshly killed by injection of 4 mL of 2.5% glutaraldehyde in 3.2% NaCl as in Robb *et al.* (2014). All tissues, except the eyestalks, were immediately fixed in fresh 2.5% glutaraldehyde for 24 h. The eyestalks, which in crab are partially calcified, required 48 h fixation in Davidson's solution (formalin 40%: 20 parts, glycerol: 10 parts, glacial acetic acid: 10 parts, ethanol 10%: 30 parts, seawater: 30 parts) rather than glutaraldehyde (Atwood *et al*., 2003). Fixed organs were immersed in 70% ethanol before full dehydration and clearing. Tissues were trimmed prior to processing (approximately 25×20×4 mm) to fit inside labelled plastic cassettes.

3.2.5.2. Tissue processing

The processing procedure used an ethanol gradient that gently and completely dehydrates samples to remove aqueous fixative and any tissue water content. This was followed by incubating samples in a clearing fluid (Histo-Clear as a xylene substitute) (National Diagnostics), which is totally miscible with the dehydrating alcohol and wax-embedding agent. Finally, the tissues were impregnated with molten wax prior to the final embedding stage in blocks of paraffin wax (Atwood *et al*., 2003).

Processing was performed overnight in an automated tissue processor (Shandon Duplex Tissue Processor) which automatically transferred the samples through the following solutions:

70% ethanol, 2 hours.

90% ethanol, 2 hours.

100% ethanol, 1 hour.

100% ethanol, 1 hour.

Histo-Clear, 1 hour.

Histo-Clear, 2 hours.
Histo-clear, 1 hour.
Molten wax, 2 hours, 60-65°C.
Molten wax, 1 hour, 60-65°C.

3.2.5.3. Wax embedding and tissue sectioning

Embedding was carried out on a Shandon Histocentre 2 embedding centre using stainless steel cassette moulds. The plastic cassettes were incorporated into the finished block which makes it more rigid for sectioning and ensures that the specimen always stays with its proper given label. The blocks were finally cooled on an integral cold plate and removed from the mould when the wax was set (Jamie and Nowacek, 2010).

Sections (5 μm thick) were cut using a LKB Historange (model 22180) rotary microtome, and then floated into a warm water bath at 40°C, (Electrothermal model MH8510) to smooth out the creases. The sections were subsequently lifted onto poly-L-lysine coated microscope slides (Thermo Scientific), and allowed to dry in a warm oven.

3.2.5.4. Haematoxylin and Eosin staining

Haematoxylin and eosin (H & E) staining was carried out to map tissue morphology. The fine structures on these slides were identified with reference to Johnston, (1980). Dried sections on slides were rehydrated by putting them through Histo-clear, followed by a decreasing ethanol gradient as specified below:

1. Histo-clear, 5 minutes
2. Histo-clear, 30 seconds
3. 100% ethanol 100%, 30 seconds
4. 90% ethanol, 30 seconds
5. 70% ethanol, 30 seconds
6. Distilled water (dH2O), 30 seconds

Slides were then stained with haematoxylin for 6 minutes followed by washing with tap water until water became clear. They were then placed in Scott's tap water (7g

sodium bicarbonate + 40g magnesium sulphate in 2000mL dH2O) for bluing. Eosin staining was for 15 seconds until a pink colour developed, followed by washing with tap water as above. Slides were then dehydrated (70% ethanol, 90% ethanol, 100% ethanol each for 30 seconds, Histo-clear for 30 seconds, then a second Histo-clear for 5 minutes), and mounted with Histomount (National Diagnostics) (Jamie and Nowacek, 2010).

3.2.6. Immunohistochemistry

Following rehydration and permeabilization as above (Section 3.2.5), slides were incubated with 1mM levamisol (Vector Laboratories, Peterborough, UK) in PBS to quench endogenous alkaline phosphate. Washing steps, endogenous antigen blockage and antibody incubation times were performed as above (Section 3.2.3). The secondary Ab for immunohistochemistry (goat anti-rabbit labelled with alkaline phosphatase) was used at 1:100 dilution and was chosen so that the substrate solution produced a colour distinct from any natural colouration in the tissues. Alkaline phosphatase substrate was prepared as above (Section 2.2.6), producing a deep blue-purple colour. Tissue sections were then washed, dehydrated and mounted as above (Section 3.2.5), prior to examination.

3.3. Results

3.3.1. Carcinin antibody dilution matrix

The antibody dilution matrix found that 1:100 dilutions for both primary and secondary antibody gave a strong signal for carcinin with no apparent background (data not shown). The optimum Ab concentrations in this experiment were higher than those used for western blotting (1:50,000). As the western blotting process involves protein denaturation, more binding sites become exposed and available to interact with the Ab, thus less Ab is needed to develop the signal.

3.3.2. Immunocytochemistry of carcinin: cellular and sub-cellular localisation in haemocytes

3.3.2.1. Peroxidase tagged carcinin secondary Ab detection

Examination of separated haemocytes using peroxidase tagged secondary Ab showed carcinin localisation in the granules of the SGCs and GCs (Figure 3.1, a and c). The majority of HCs were negative for carcinin, however, some showed faint staining at the cell periphery. Some SGCs were also present amongst the HCs (Figure 3.1, e), identified by their stained, cytoplasmic granules. This was expected, as while the separation method yields highly enriched HC populations (90% purity), a small number of SGCs are occasionally present at the bottom of the HC band. The initial ICC images confirmed that approximately 100% of granular and semi-granular haemocytes contain carcinin, while a percentage of 8.8% of HCs showed a fainter, peripheral localisation (Figure 3.2).

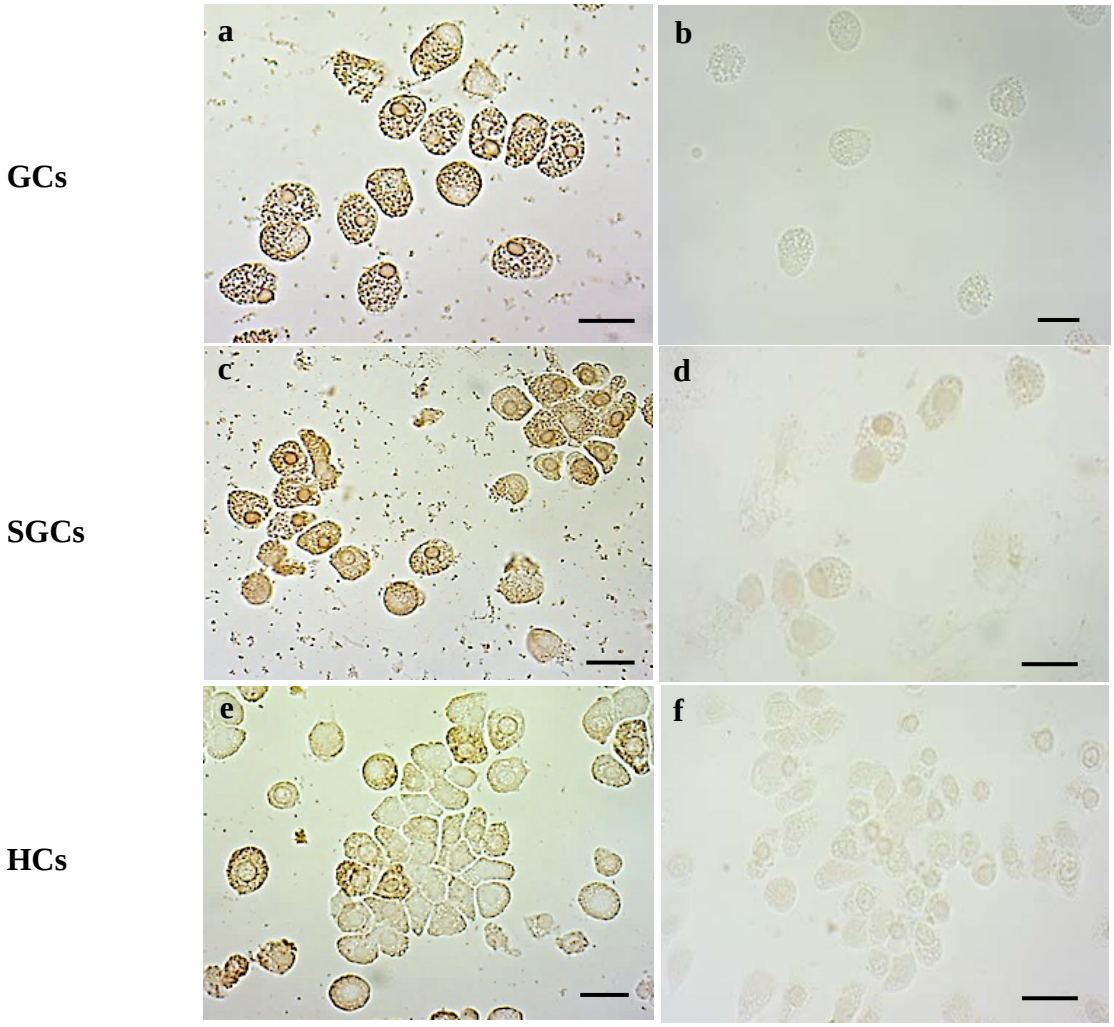

Figure 3.1: Initial detection of carcinin by peroxidase-tagged secondary Ab in separated haemocyte populations. Immunocytochemistry of GCs (**a**, **b**), SGCs (**c**, **d**) and HCs (**e**, **f**) from enriched populations, using carcinin specific Ab and peroxidase tagged secondary Ab. DAB is used as peroxidase substrate to indicate presence of carcinin by brown colouration. Carcinin is present in the cytoplasmic granules of both GCs (**a**) and SGCs (**c**). HCs are unstained, although a few contaminating SGCs are present and stained internally. A small proportion of hyaline cells show staining at the cell membrane (**e**, arrow). (**b**), (**d**) and (**f**) are anti-sera controls for GCs, SGCs and HCs, respectively. Scale bar 10μm.

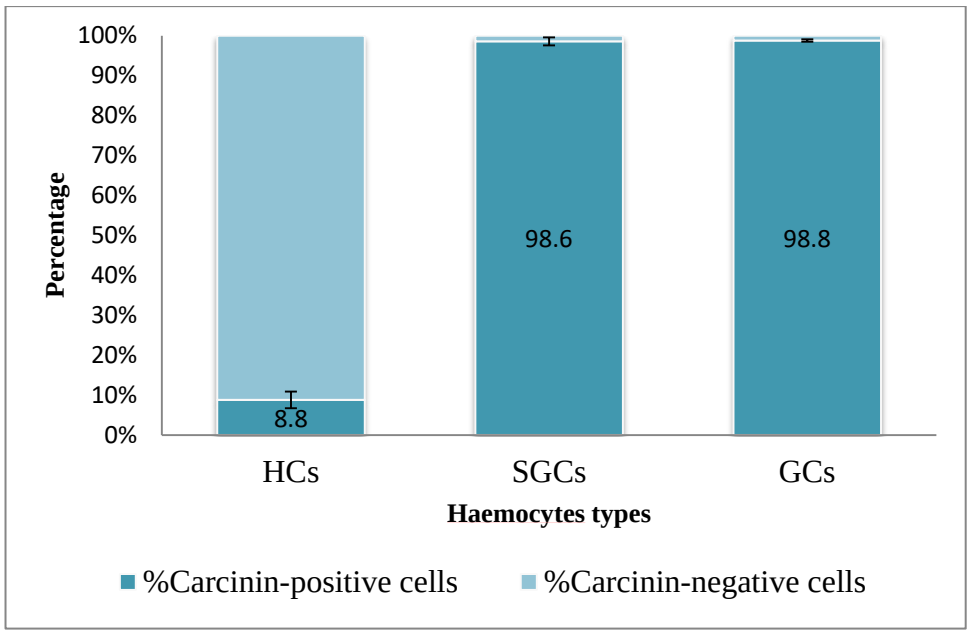

Figure 3.2: Percentages of carcinin positive cells in separated populations of HCs, SGCs and GCs. Carcinin signal is positive in 8.8% (± 2.1) of HCs, 98.6% (± 1) of SGCs and 98.8% (± 0.3) of GCs. Bars show standard deviation of the mean. Results are based on a total of six animals, with a minimum of 500 cells counted per animal.

3.3.2.2. FITC tagged carcinin secondary Ab detection

Fluorescence microscopy gave better resolution for carcinin localisation in the haemocyte populations. The presence of many large, carcinin-positive granules in the GCs gave a stronger signal compared to the SGCs, often to the point of obscuring the nucleus (Figure 3.3, a, d). The cytoplasmic contents of many HCs, in contrast, were unstained, although similarly to using a peroxidase-label, approximately 10% of the cells exhibited a positive signal for carcinin around their periphery (Figure 3.3, g-i), indicating carcinin on or outside the plasma membrane. The ProHs were unusual in that whilst the majority did not show positive staining for carcinin, a few displayed an intracellular signal (Figure 3.3, j-l).

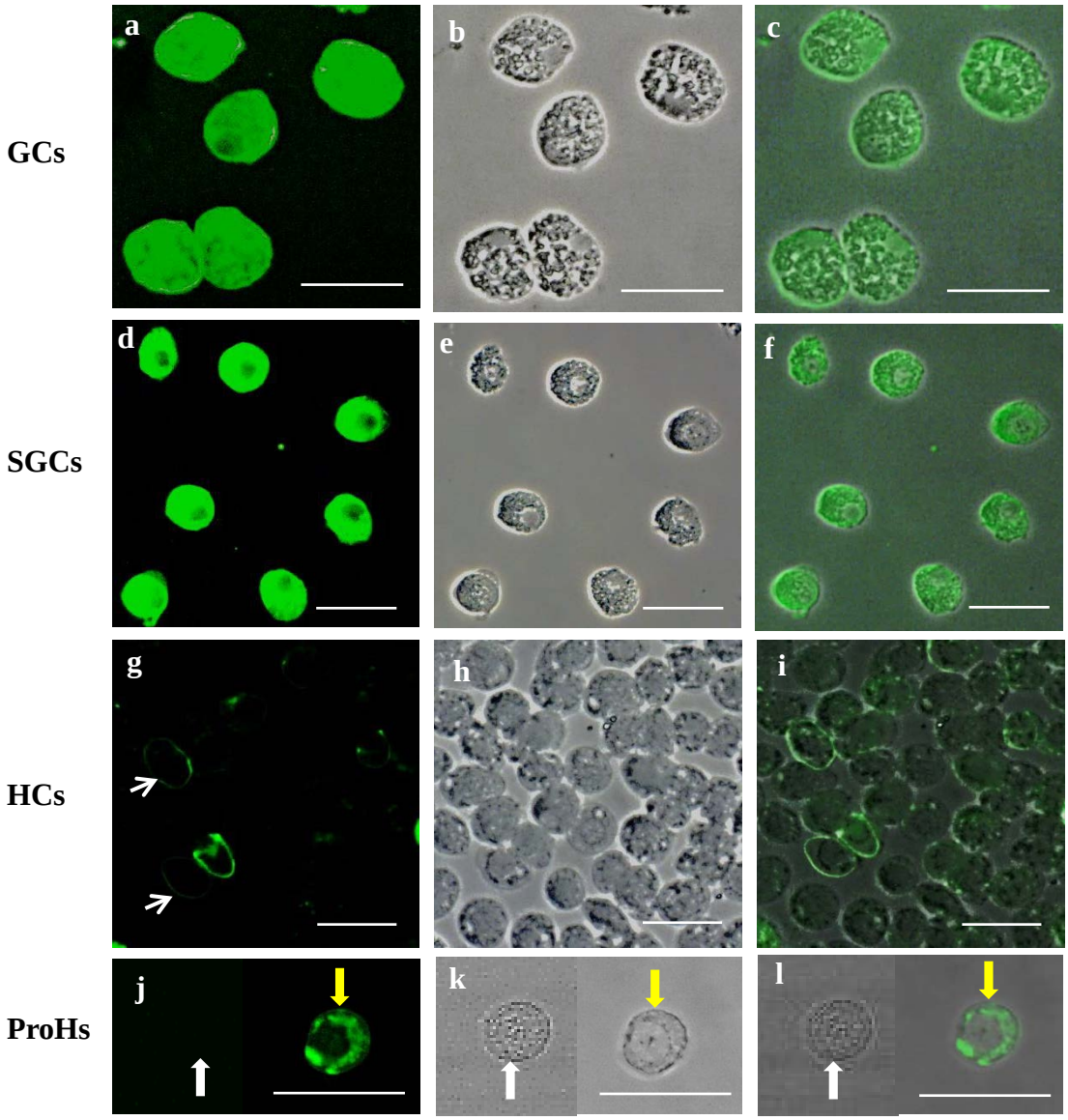

Figure 3.3: Immunocytochemical localisation of carcinin in separated *C.maenas* cell populations, using carcinin-specific antibody and goat-anti rabbit FITC-tagged secondary Ab. ICC displaying carcinin localisation (green fluorescence staining; (**a**, **d**, **g**, **j**), with corresponding phase contrast images (**b**, **e**, **h** and **k)** and overlay images (**c**, **f**, **i** and **l)** with GCs (**a-c**), SGCs (**d-f**), HCs (**g-i**) and ProHs (**j-l**). HC cytoplasm (**g-i**) is unstained although some HCs show staining around the cell periphery (white arrows). Isolated agranular ProHs with no staining for carcinin (**j-l**, white arrows), while a second, granular ProHs shows carcinin present in the cytoplasmic granules (**j-l**, yellow arrows). Scale bar 10µm.

3.3.2.3. Confocal microscopy detection

Examination using confocal microscopy confirmed that freshly harvested, un-separated haemocytes gave very strong signals in the cytoplasm of *ca* 15% of the cells, frequently obscuring the cytoplasm and sometimes the nucleus (Figure 3.4). A smaller proportion of the unseparated haemocytes (*ca* 10%) showed variable degrees of less intense and more granular staining, with the remainder (*ca* 75%) giving no signal at all (Figure 3.4). Based on the size, shape and relative proportion in the mix, the cell types correspond to the GCs, SGCs, and HCs, respectively. Within the unstained cell population a few haemocytes were small and had a thin ring of cytoplasm around the central nucleus, typical of agranular ProHs, with an extremely low proportion revealing small amounts of carcinin in the cytoplasm, suggesting they were granular ProHs (Figure 3.4).

As well as being present in the cytoplasmic granules, images from confocal microscopy also showed some GCs secreting the protein to the extracellular domain during degranulation (Figure 3.5, a-d). For SGCs, carcinin was also present in cytoplasmic granules (Figure 3.5, e-h), with the degree and intensity of the colour combination in overlay images reflecting the number and size of granules (Figure 3.5, h), (Figure 3.6, b). Again, carcinin was detectable in only some HCs but at the cell periphery (Figure 3.5, i-l). In positive HCs, the signal was associated with the cytoplasmic membrane or in small intracellular inclusions of the cytoplasm (Figure 3.6, c), where carcinin co-localised with F-actin (Figure 3.5, l). Confocal microscopy also supported the finding that ProHs exhibit two modes of staining: some cells stain positively within cytoplasm while others are devoid of the protein (Figure 3.5, m-p). Where present in the ProHs, carcinin appeared to be associated with small granular cytoplasmic inclusions (Figure 3,5 m-p, yellow arrow). Analysis of co-localisation (Figure 3.6) confirmed these observations. In GCs, SGCs and ProHs that have carcinin, co-localisation seemed to be full, while in carcinin-positive HC, carcinin appeared to present mainly on the cytoplasmic membrane (See appendix 1 for scatter plot representing total negative co-localisation between F-actin and DNA).

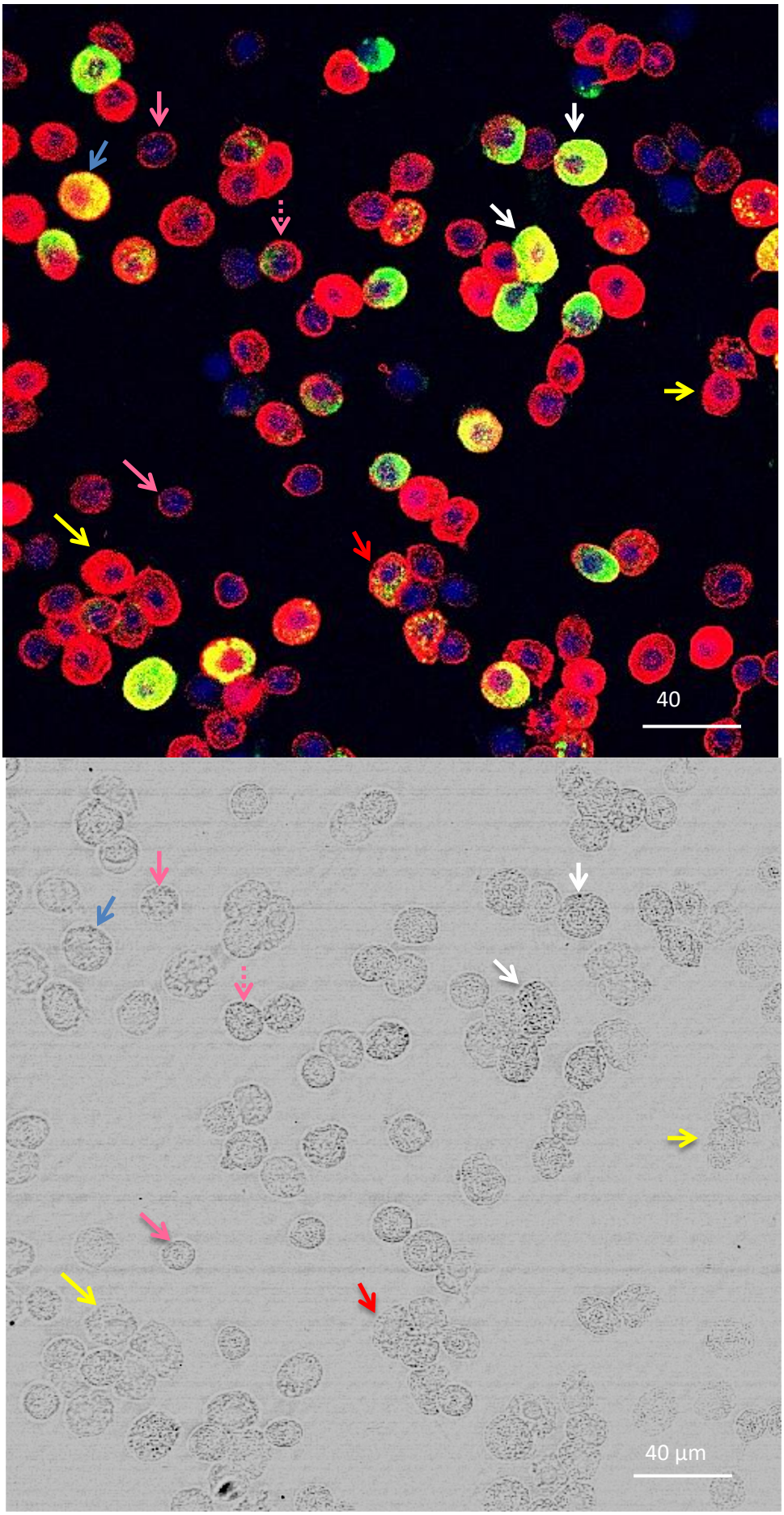
40
40 µm

Figure 3.4: Confocal microscopy images of un-separated haemocytes of *C.maenas*. (**a**): ICC overlay image with FITC tagged secondary Ab for carcinin (green), rhodamine phalloidin for F-actin (red), and DRAQ5™ for DNA (blue pseudocolour). (**b**): The corresponding phase contrast image, revealing cell shape, size, and differing granule proportion in the cytoplasm of different cell types. In the fluorescence image GCs appear with green/yellow stain at the cytoplasm (white arrows). SGCs have less intense colour for carcinin, varying from small patches of greenish colour in parts of the cytoplasm (red arrows), to cells with a more orange hue (blue arrows). Remaining cells are shown by the F-actin (red) and DNA (blue) with no green or yellow signal. These include HCs (yellow arrows) and ProHs (pink arrows) identified by their size and nuclear to cytoplasmic ratio. Among all these cells, one pro-haemocyte has a small amount of green staining in the cytoplasm (dashed pink arrow), indicating carcinin.

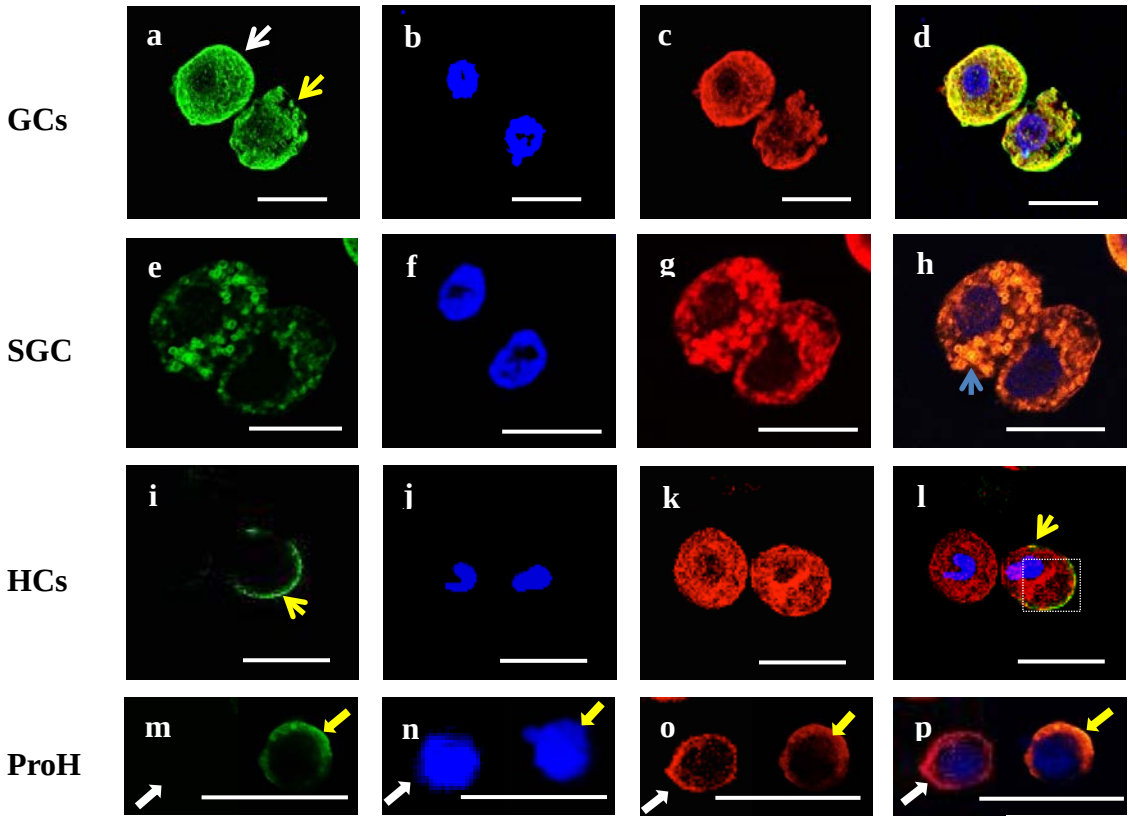

Figure 3.5: Carcinin subcellular localisation in separated haemocyte populations, pictured by confocal microscopy. GCs are in images (**a-d**), SGCs are in images (**e-h**), HCs are in images (**i-l**) and ProHs (**m-p**). Cells are stained, as detailed in the methods (green for carcinin in **a**, **e**, **l** and **m**, blue pseudocolour for DNA in **b**, **f**, **j** and **n**, red for F-actin in **c**, **g**, **k** and **o,** and the overlay image in **d**, **h**, **l** and **p**). In GCs images, the cell indicated by white arrow seems intact, with carcini green staining in granules inside the cytoplasm. The cell indicated by yellow arrow appears to be degranulating as the cytoplasmic membrane is disrupted and granules containing carcinin are being discharged to the extracellular domain. In both GCs, co-localisation with F actin overlaps and gives a yellow colour in the corresponding overlay image (**d**). SGCs appear with varying numbers of granules inside the cytoplasm, but still fewer on average than in GCs. SGCs with lower numbers of granules appear orange in the overlay image (**h**). Two HCs (**i-l**), with carcinin associated with cytoplasmic membrane in one cell (yellow arrow), while the other is unstained for carcinin. Overlay image (**l**) has carcinin on parts of the outer membrane. Two types of ProHs were noticed, agranular ProH with no carcinin (**m-p**, white arrow) and granular ProH with carcinin present in the cytoplasm (**m-p**, yellow arrow) and co-localised with F actin in orange colour combination (**m**, yellow arrow). Scale bar 10 μm.

Analysis of the previous overlay images gave a numerical idea of carcinin localisation within individual haemocyte populations. Analysis was made of at least ten images for each cell type. Analysis of GCs (Figure 3.6, a) illustrated full co-localisation between carcinin and F-actin (99%), with approximately equal red and green values for the majority of the pixels, resulting in a largely diagonal distribution in the scatter plot diagram. The scatter plot for SGCs was slightly different (Figure 3.6, b). While carcinin in SGCs was also seen fully co-localised with the F-actin (99%), the majority of the pixels have their green values less than the red ones. This can be interpreted as the carcinin signal being less intense in SGCs, with scatter plot revealing a shift in pixel distribution towards the red axis. Similarly, analysis of pixel distribution of granular ProH found similar results (Figure 3.6, d), which indicated that carcinin in these cells, although generated and co-localised with the F-actin, exists in relatively lower amounts than the mature GCs. When HC images were analysed (Figure 3.6, c), the detected carcinin signal represented by intensity of the green pixels, was low. The scatter plot revealed the majority of the dots to have red rather than green value. The calculated co-localisation percentage is low (16%), indicating that carcinin was present mostly on and surrounding the cytoplasmic membrane, with little diffusing inside.

GCs

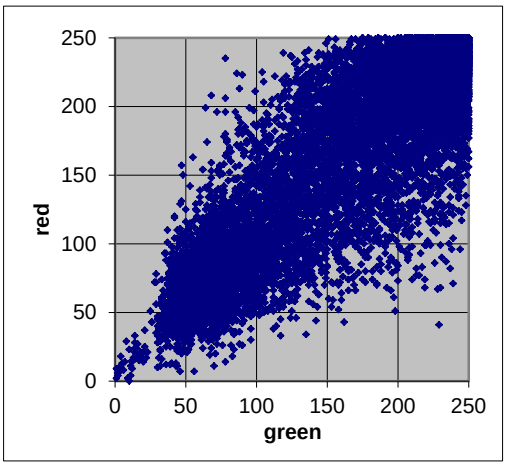

	Green	Red	Yellow	Black	Total
Total no. of pixels:	267	371	15521	225	16384
	1.6%	2.3%	96.%		
	G only	G in Y		R only	R in Y
Total pixel intensity:	18276	3069173		25981	3032411
	0.6%	99.4%		0.8%	99%

SGCs

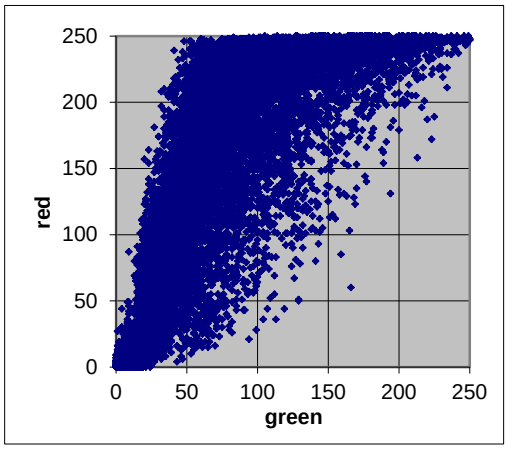

	Green	Red	Yellow	Black	Total
Total no. of pixels:	143	2261	8832	5148	16384
	1.3%	20.1%	78.6%		
	G only	G in Y		R only	R in Y
Total pixel intensity:	9248	976103		220142	1778226
	0.9%	99%		11%	89%

HCs

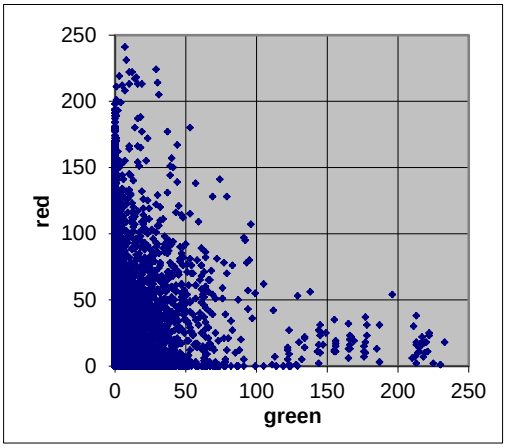

	Green	Red	Yellow	Black	Total
Total no. of pixels:	203	2579	59	13543	16384
	7.1%	90.8%	2%		
	G only	G in Y		R only	R in Y
Total pixel intensity:	22099	4249		231798	4466
	83.9%	16.1%		98%	1.9%

ProHs

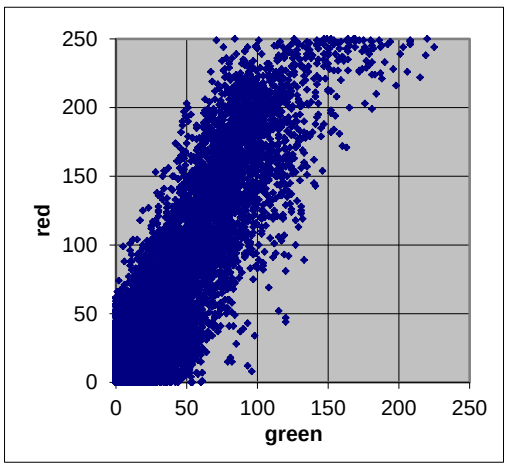

	Green	Red	Yellow	Black	Total
Total no. of pixels:	171	1694	3137	11382	16384
	3.4%	33.9%	62.7%		
	G only	G in Y		R only	R in Y
Total pixel intensity:	10205	301847		130090	509527
	3.3%	96.7%		20.3%	79.7%

Figure 3.6: Analysis of carcinin subcellular localisation in separated haemocytes populations. Scatter plots illustrate analysis of red and green pixel distribution in GCs (**a**), SGCs (**b**), HCs (**c**) and granular ProHs (**d**) overlay images. In scatter plot (a): most of the pixels are located in the central area of the plot, revealing that green pixels are intense, while in the scatter plot (b): less green pixel intensity is detected, resulting in the scatter plot shaping differently to the GCs, with pixel distribution shifted towards the red axis. (**a**) Indicates that 96% of total pixels in GCs overlay image are yellow, with 99% of carcinin co-localised with F-actin. (**b**) Shows that 87% of the total pixels in SGCs overlay image are from the combination colour, with 96% of carcinin co-localised with F-actin. (**c**) In HCs, co-localisation analysis of the area where carcinin is present (indicated by square in **Figure 3.5, l**) shows that yellow pixels are present in only 2.1% of the total pixels. Co-localisation percentage is 16%, which means that the majority of carcinin (84%) is actually on the cytoplasmic membrane, not penetrated into the cytoplasm, while the rest, presented by the co-localisation percentage (16%), infuses inside the hyaline cell. In (**d**), co-localisation analysis of the granular ProH indicates that 63% of pixels are from the combination colour, and 97% of carcinin co-localised with F-actin.

3.3.3. Histological localisation of carcinin

3.3.3.1. Gills

Figure (3.7, a) shows a longitudinal section from a single gill, illustrating its central stem, from which branches of secondary lamellae arise (Figure 3.7, a). The gill wall consists of a cuticle, which appeared purple in H & E staining. The internal gill surface is lined with epithelium (Figure 3.7, b), with large numbers of haemocytes diffusing throughout the secondary lamellae and the central stem (Figure 3.7, a, c). At higher magnification, different haemocyte types could be distinguished according to their size, and the presence and intensity of their cytoplasmic granules (Figure 3.7, c). Some granular and SGCs could be seen discharging their granules (Figure 3.7, d), thus delivering their contents to the gill.

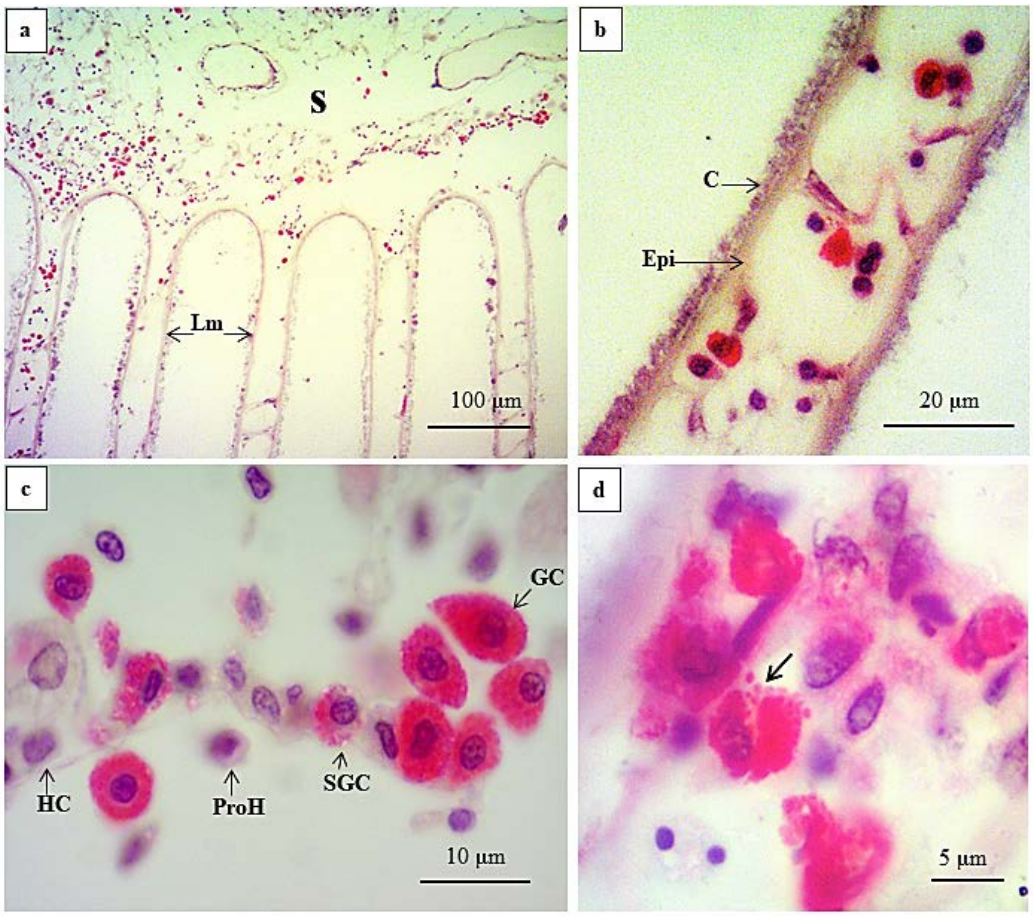

Figure 3.7: Longitudinal section of *C. maenas* gill stained with H & E. (**a**): Low magnification image of gill longitudinal section. (**b**): High magnification of part of gill secondary lamellae. (**c**): High magnification of gill central stem. (**d**): High magnification of granulating haemocytes in gill central stem. Images reveal gill

structure consisted of central stem (S) with branches of secondary lamellae (Lm), with large number of haemocytes have infiltrated gill's lamellae. In (**b**), the gill wall structure is composed of external cuticle (C) lined with epithelium (Epi) ranging in thickness in different parts of the wall. Different types of haemocytes including GCs with their intense content of cytoplasmic granules stained with deep pink, SGCs with fewer cytoplasmic granules, HCs and ProHs with no granules in their cytoplasm and differentiated by their size, as in image (**c**). Degranulation of some granular haemocytes is seen in image (**d**, arrow), with individual granules stained in deep pink are released, thus acting to deliver soluble content to other cells or structures in the gill.

Immunohistochemistry showed a clear signal for carcinin in circulating haemocytes diffusing through the gill (Figure 3.8, a, b), which was consistent with the staining seen in different haemocyte types *in vitro* (Section 3.3.2). Granular and SGCs were discernible by their degree of granular staining, with some (Figure 3.8, c) showing degranulation. Discharging granules were positive for carcinin, with the stain extending and spreading outside haemocytes, with some adjacent areas of the gill wall showing a paler colour (Figure 3.8, c). Similarly to the *in vitro* observations, some HCs in the gill showed carcinin associating with their plasma membrane (Figure 3.8, b). Of the few pro-haemocytes visible in the sections, the majority were not carcinin-positive. The gills were well populated with stained haemocytes, but there was no other conspicuous presence of carcinin apart from occasional pale colouration in the wall from nearby haemocytes (Figure 3.8, d).

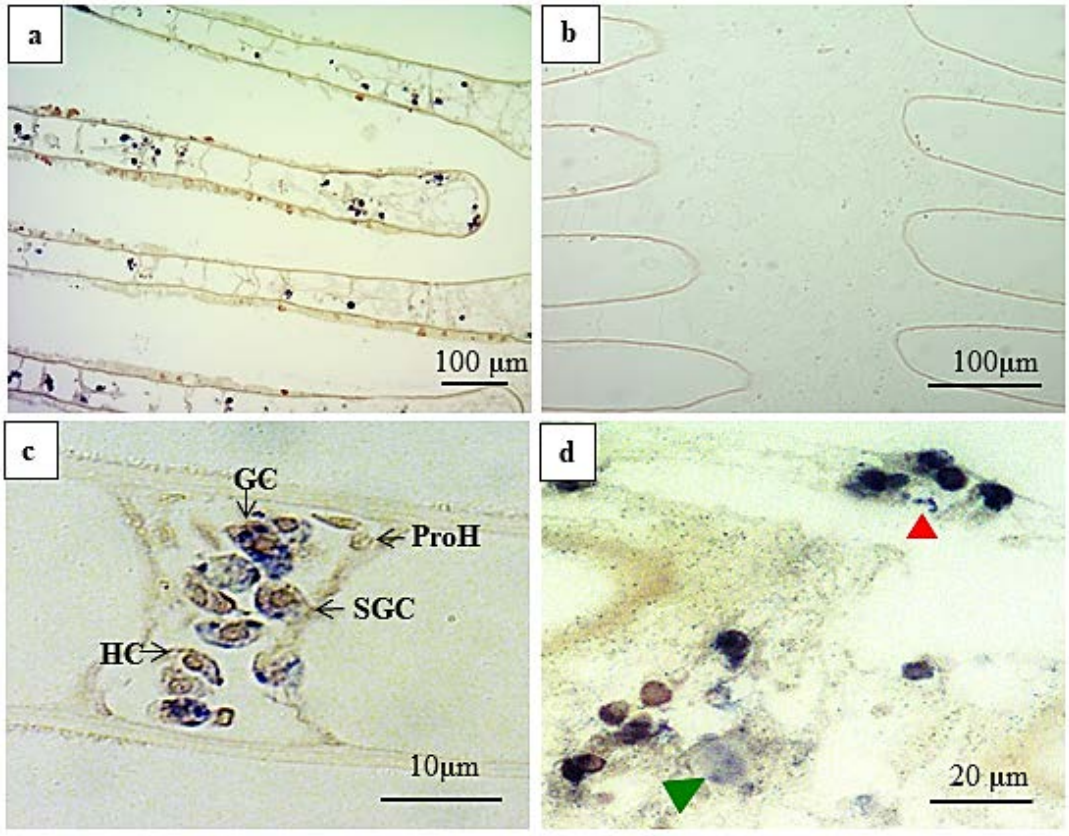

Figure 3.8: Carcinin in gills. (**a):** Low magnification image of longitudinal section of gill lamellae stained with carcinin specific Ab and goat-anti rabbit alkaline phosphatase tagged secondary Ab. (**b**): Antisera control shows no staining. (**c**): A group of different types of haemocytes assemble in gill lamellae. (**d**): High magnification of degranulating GCs in gill lamellae. Haemocytes are observed penetrating gill tissues, with some haemocytes stained deep purple with no other parts of the gill lamellae appear stained in any of the images. In image (**c**), GCs are almost fully-stained with deep purple in the cytoplasm, SGCs are partly stained in the cytoplasm, spindle shaped HC is stained on the cytoplasmic membrane, and agranular ProHs are unstained. GCs appear to release their cytoplasmic granules in image (**d**). Discharged granules are stained for carcinin (red arrowhead). Faint purple staining is noticed in other area (green arrow), and might be related to secreting soluble carcinin.

3.3.3.2. Hepatopancreas

Figure (3.9, a) shows the lobular structure of the hepatopancreas, comprising numerous small tubules and surrounded by a laminar connective tissue capsule. The epithelium of the tubules includes different cell types, with a basal membrane bordering the tubules and separating them from the haemal space. Haemal sinuses in the interstitial spaces between tubules are composed of connective tissue permeated with different types of haemocytes (Figure 3.9, b). Hepatopancreatic secretions are released into the lumen of the tubules that empty into the main collecting duct.

Immunohistochemistry revealed carcinin only in the haemocytes penetrating the interstitial connective tissues. No carcinin was detected in other parts of the tubules (Figure 3.10, a, b). Instead, localisation was confined to a thin line along the outer capsule of the organ in contact with the haemocoelic cavity (Figure 3.10, a, b). In some areas, carcinin stained parts of the connective tissue (Figure 3.10, c, d), where traces were seen in the haemal spaces around haemocytes. Although some dark spots were noticed in the epithelial part of the tubule (Figure 3.10, a), they were also present in the controls and do not appear to be related to carcinin (Figure 3.10, f). It is likely from the size, shape and appearance of these spots that they are calcium spherules, which are located in the cytoplasm, and store calcium and other materials in mature resorptive cells (R cells), a type of epithelial cell in the tubules which absorbs nutrients (Sousa *et al*., 2005).

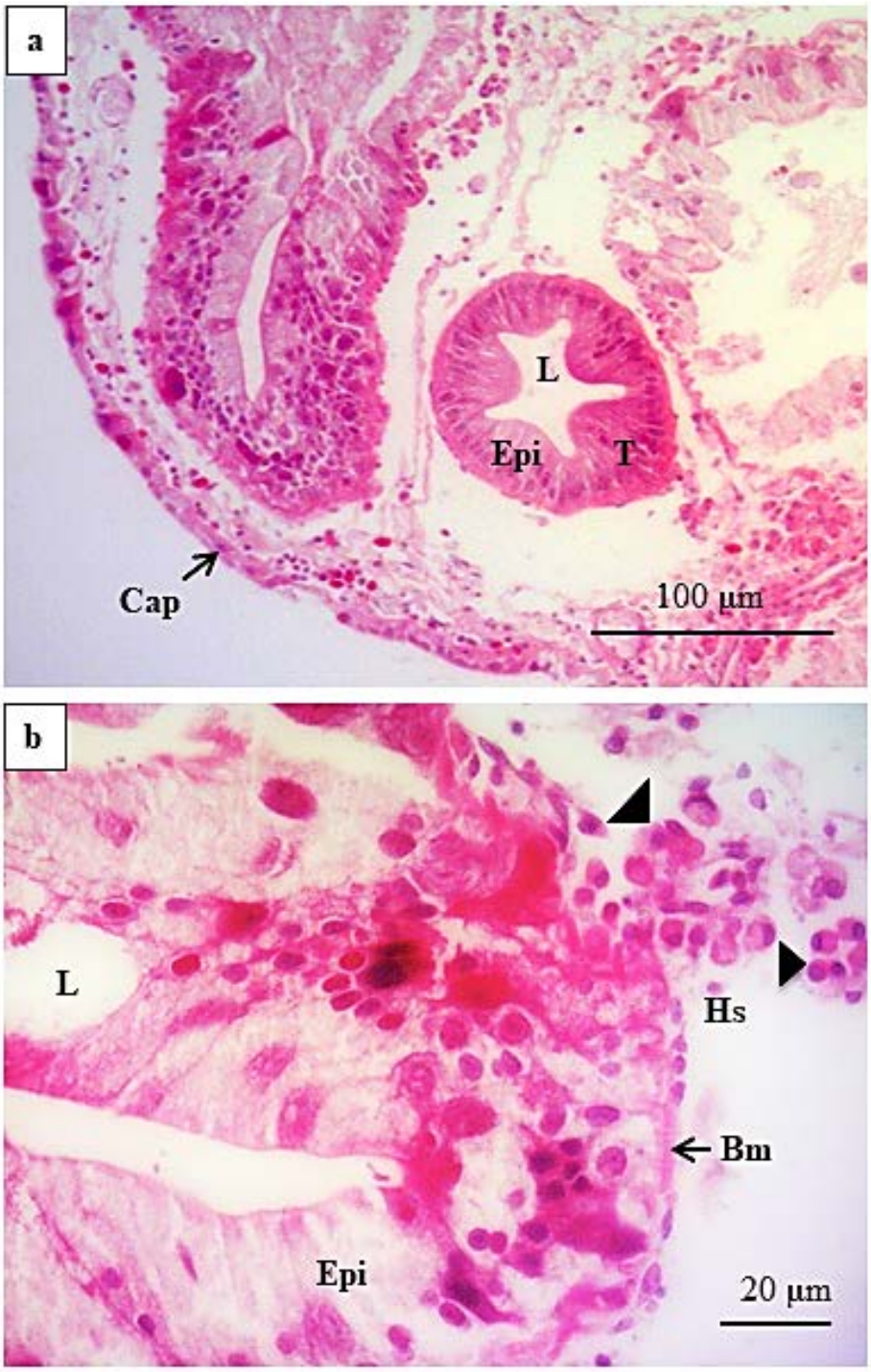

Figure 3.9: Hepatopancreas structure as seen stained with H & E. (**a**) Low magnification image of cross section of hepatopancreas. (**b**): High magnification of hepatopancreas tubule. Images illustrate hepatopancreas tubular structure. Hepatopancreas is surrounded by a capsule (Cap) as indicated, consisting of laminar connective tissues. The image (**b**) reveals tubule lumen (L) and epithelial matrix (Epi), and bordered by basal membrane (Bm). Haemal sinuses (Hs) occur between secretory tubules and contain haemocytes (arrow heads) that penetrate the connective tissues.

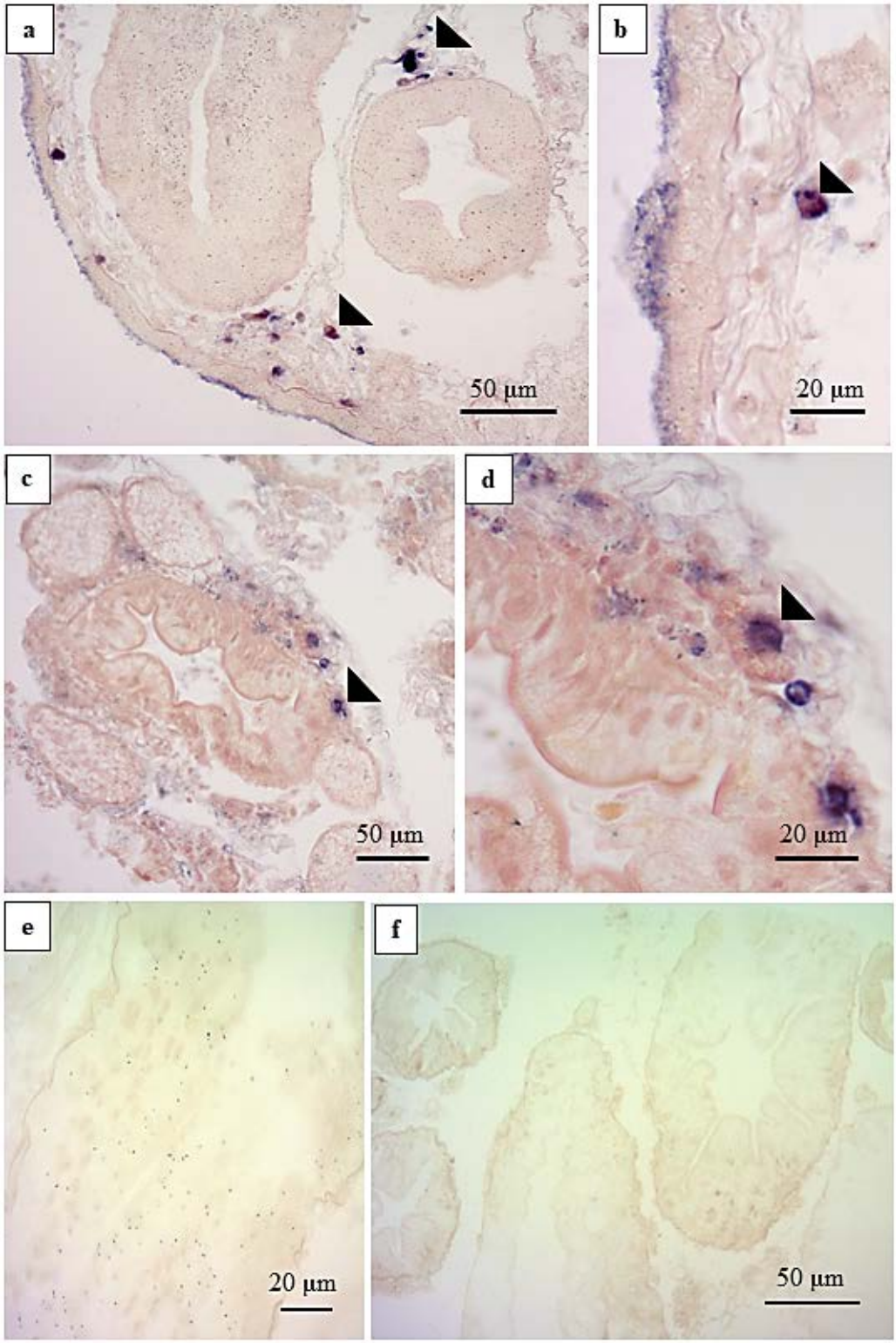

Figure 3.10: Carcinin in hepatopancreas. (**a**): Low magnification of hepatopancraes cross section stained with carcinin specific antibody and alkaline phosphatase tagged secondary Ab. (**b-d**): High magnification of parts of hepatopancreas structure, stained as above. (**e**): Control image (no primary or secondary Abs). (**f**): Antisera control. Al experimental and control images reveal natural colour of the hepatopancreas as dark

yellow to brown. Haemocytes in haemal sinuses showed strong signals for carcinin in all experimental IHC images (**a**-**d**) (arrow heads). Alkaline phosphatase staining is also evident in the hepatopancreas outer capsule (**a**) and (**b**) and appears strongly in haemocytes attached to the tubule basal membrane (**c**). Image (**d**) reveals thin film of staining outside haemocytes associated with connective tissues. The control image (**e**) shows dark little droplets in the epithelium of the tubule, most probably calcium spherules. The antisera control image (**f**) illustrates that staining is specific to carcinin.

3.3.3.3. Midgut caecum

Cross sections showed the midgut caecum characterized by a central lumen and a wall of circular and longitudinal muscles. The wall is lined with epithelium, in addition to a cuticle that overlays each group of longitudinal muscle (Figure 3.11, a). The distribution of carcinin followed a similar pattern to that of the hepatopancreas. The only positively stained cells were the haemocytes in the interstitial spaces (Figure 3.11, b, c). Although carcinin was released from some haemocytes (Figure 3.11, c), no distinct staining was noticed in other parts, probably due to the loss of some interstitial connective tissues during tissue processing. Carcinin was not evident in the other cells of this tissue.

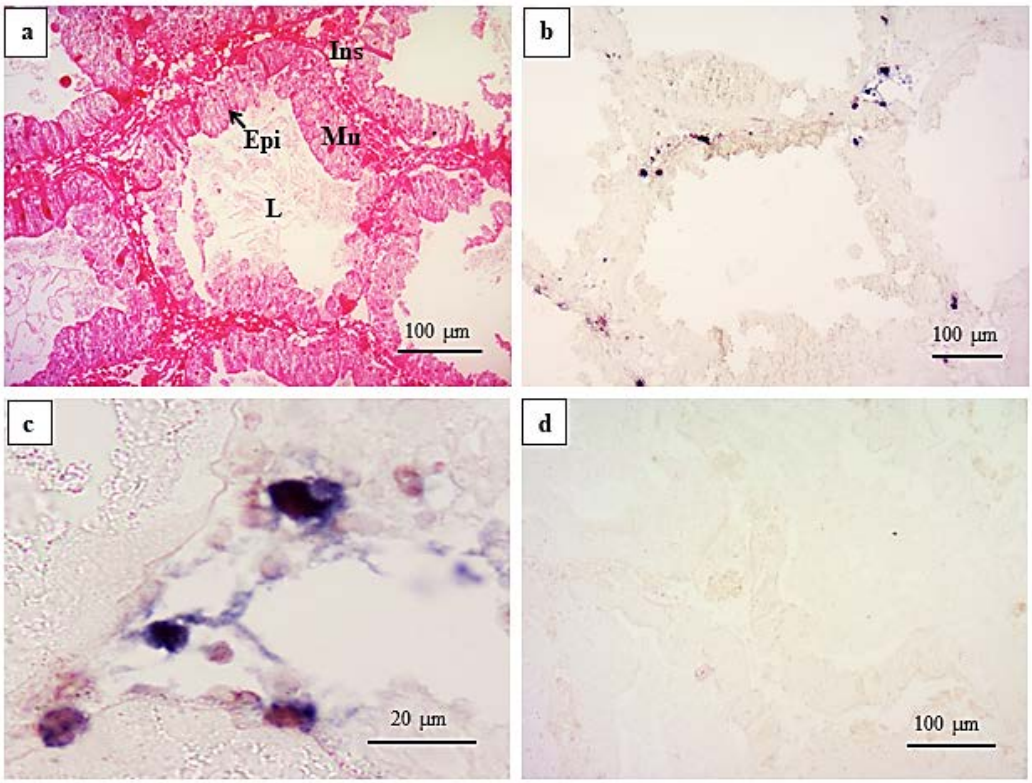

Figure 3.11: Midgut caecum structure and localisation of carcinin. (**a**): Cross section of midgut caecum stained with H & E. (**b**): Cross section of midgut caecum stained with AP tagged Ab. (**c**): High magnification of part of the interstitial space midgut caecum section. (**d**): Antisera control. Midgut caecum has a tubular structure, with a wall surrounding the central lumen (L) and consists of muscle cells (Mu) lined with epithelium (Epi). Interstitial space (Ins) contains connective tissue in addition to haemocytes, as detailed in H & E image (**a**). Immunohistochemical localisation of carcinin shows it evident in interstitial haemocytes, but no traces were observed in other parts of the section. The high magnification image (**c**) shows carcinin to be secreted from haemocytes.

3.3.3.4. Heart

Cross-sections of heart tissue revealed an extensive myocardium, separated by a basement membrane from the epicardium connective tissues (Figure 3.12, a). The epicardium does not have haemal lacunae, and since as it is very prone to disruption during dissection, haemocytes are notably visible in the disrupted area (Figure 3.12, a). Carcinin was absent from the heart musculature, with the only positive cells being the haemocytes within the epicardium (Figure 3.12, b, c). Some carcinin was being discharged, as faint staining was present in some areas of the epicardium (Figure 3.12, b). No other clear areas of alkaline phosphatase staining were evident.

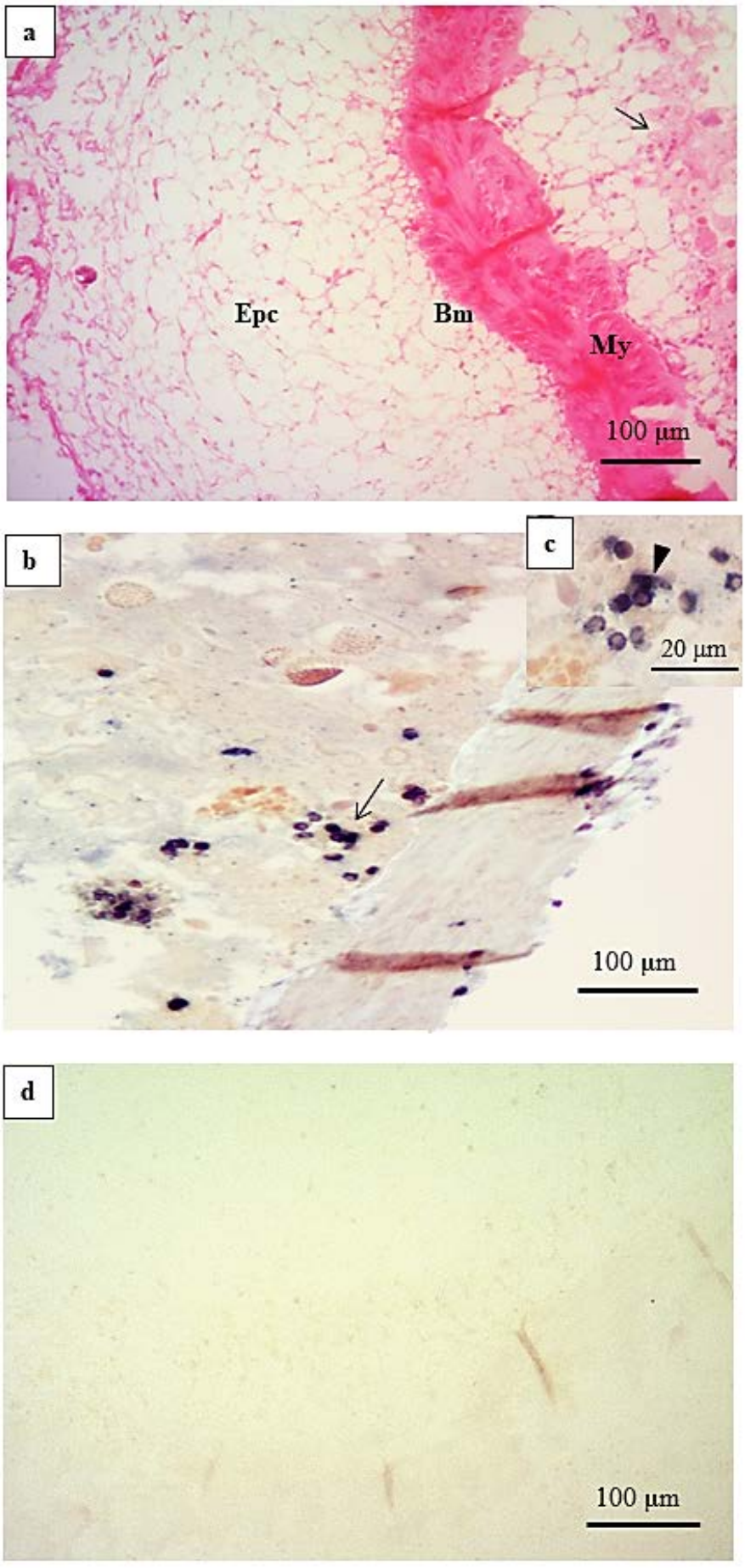
a
Epc
Bm
My
100 µm
b
c
20 µm
100 µm
d
100 µm

Figure 3.12: Heart structure in *C. maenas* and carcinin localisation. (**a**): Cross section of heart tissues stained with H & E. (**b)** and **(c**): IHC images of heart tissue stained with AP tagged carcinin AB. (**d**): Antisera control. Heart tissue is composed of myocardium (My) separated from epicardium connective tissue (Epc) with basal membrane (Bm). Epicardium is made up of connective tissues with some haemocytes apparent in disrupted areas (arrow). In IHC images, carcinin staining mainly appears in the haemocytes (arrow). Traces of alkaline phosphatase staining are noticed in some parts of epicardium connective tissue (arrow head). This staining is assumed to relate to secreted carcinin.

3.3.3.5. Eyestalk

The eyestalk is a bilateral, multifunctional organ with a complex structure (Figure 3.12, a). Each compound eye comprises numerous omnatidia enclosed by a thin convex cuticle and separated from the rest of the eyestalk by a basement membrane. More proximally, optic ganglia are present and contain several parts; peripherally is the lamina ganglionaris, which is entered by large bundles of optic nerve fibres. The medulla externa is adjacent, followed by the medulla interna, then the last ganglion, the medulla terminalis. The optic (or ocular) peduncle is formed where the medulla terminalis narrows, and is referred to as the optic nerve at the point it enters the brain. Importantly, the eyestalk contains the neuro-endocrine system, which is mainly represented by the so called 'X organ' located in the medulla terminalis. This secretes different hormones, such as the moult-inhibiting and gonad-inhibiting hormones that control other organs of the body. These secretions pass to the sinus gland between the medulla externa and medulla interna, which stores and releases them to circulation.

Ablation of eyestalks blocks the release and circulation of the neuro-secretory products in the animal (see Chapter 4). The initial removal of the eyestalks to investigate carcinin localisation occurred in the area proximal to the medulla terminalis in the ocular peduncle (Figure 3.13, b). The area shown in H & E stained cross sections (Figure 3.13, c) is at the proximal end of the eyestalk. The section is cut through a relatively thick part of the cuticle and shows the exocuticle, epicuticle and endocuticle. The endocuticle is underlain with epithelial cells associated with a brown-pigmented film. The space just underneath this is an artefact caused by tissue loss/shrinkage due

to processing and has been frequently recorded (Johnson, 1980). More centrally is an area of connective tissue infiltrated with some haemocytes (Figure 3.13, d)

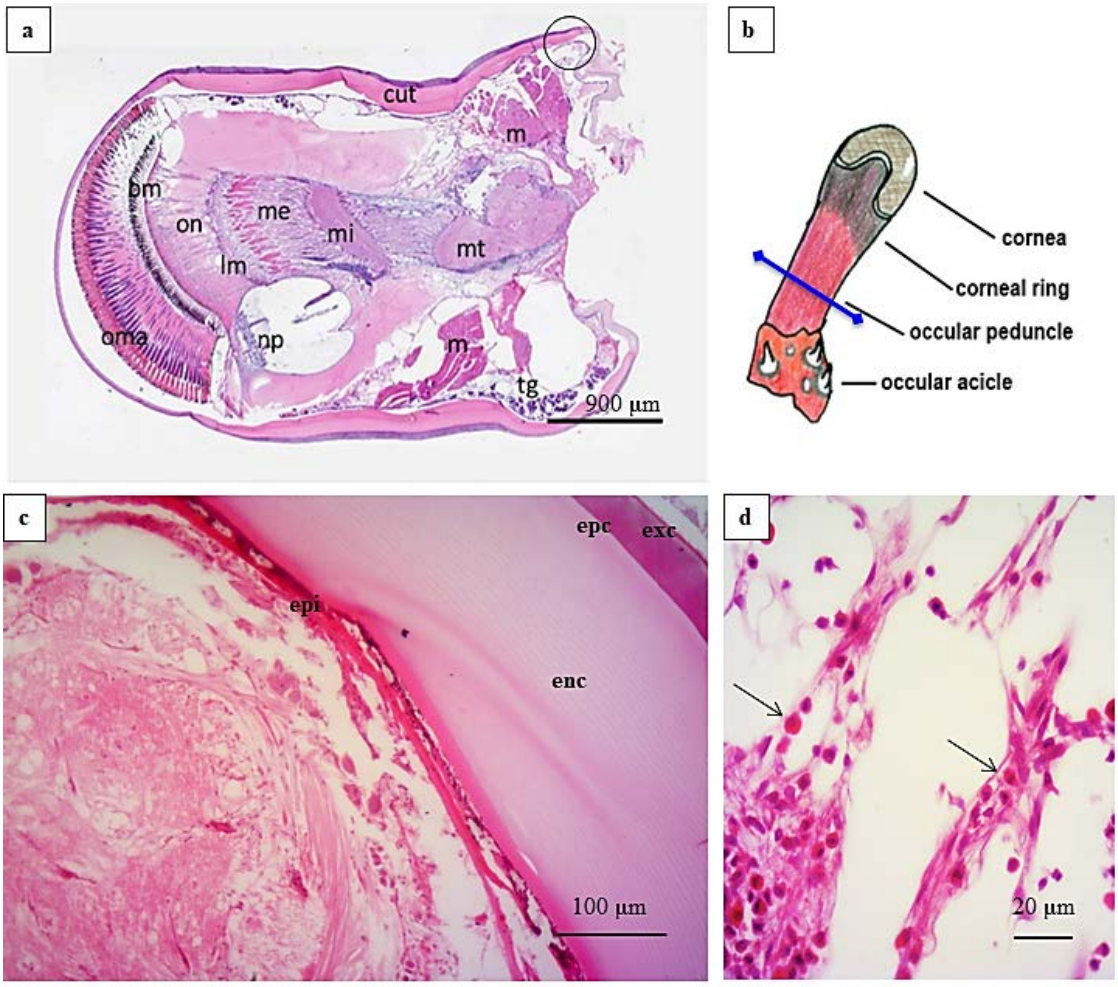

Figure 3.13: Eyestalk structure in crustaceans. (**a**): Longitudinal section of the American lobster, *Homarus americanus* eyestalk (low magnification), as a model of a crustacean eyestalk, stained with H & E. (**b**): Diagram showing the eyestalk of the hermit crab *Coenobita clypeatus*, adapted from Forest *et al.* (2000). (**c**): Cross section of the proximal end of the eyestalk of *C. maenas* stained with H & E. (**d**): High magnification of the connective tissues in the eyestalk, containing haemocytes indicated by arrows. The eyestalk is encased by a cuticle (cut) with increasing thickness on the lateral margins of the eye. The compound eye consists of an ommatidial region (oma), separated from the optic ganglia with basement membrane (bm). The optic ganglia are made up of the lamina ganglionaris (lm), which is the peripheral area. Next come medulla externalis (me), medulla internalis (mi), and medulla terminalis (mt), m = retractor muscle, np = nerve plexus, tg = tegmental glands, on= optic nerve. Image (**a**) was adapted from Shields and Boyd (2014). The

blue line in diagram image (**b**) indicates the approximate section site in the present study. In image (**c**) the cuticle is composed of the exocuticle (exc), epicuticle (epc) and endocuticle (enc) which represent the thick part of the cuticle. It is lined by epithelium (epi), which is adjacent to connective tissue with some haemocytes present

Carcinin localisation in the cross section revealed some positively stained haemocytes penetrating the connective tissue area (Figure 3.14, a, c). In addition, a positive signal was also detected in parts of the exocuticle (Figure 3.14, a), and in the endocuticle surrounding the eyestalk, where it appeared as a broad band of decreasing intensity towards the centre (Figure 3.14, a, b). The stained bands correspond with the growth bands laid down in the hard structures of different invertebrates, such as the endocuticle of crabs, and serve to estimate age (Kilada *et al.*, 2012).

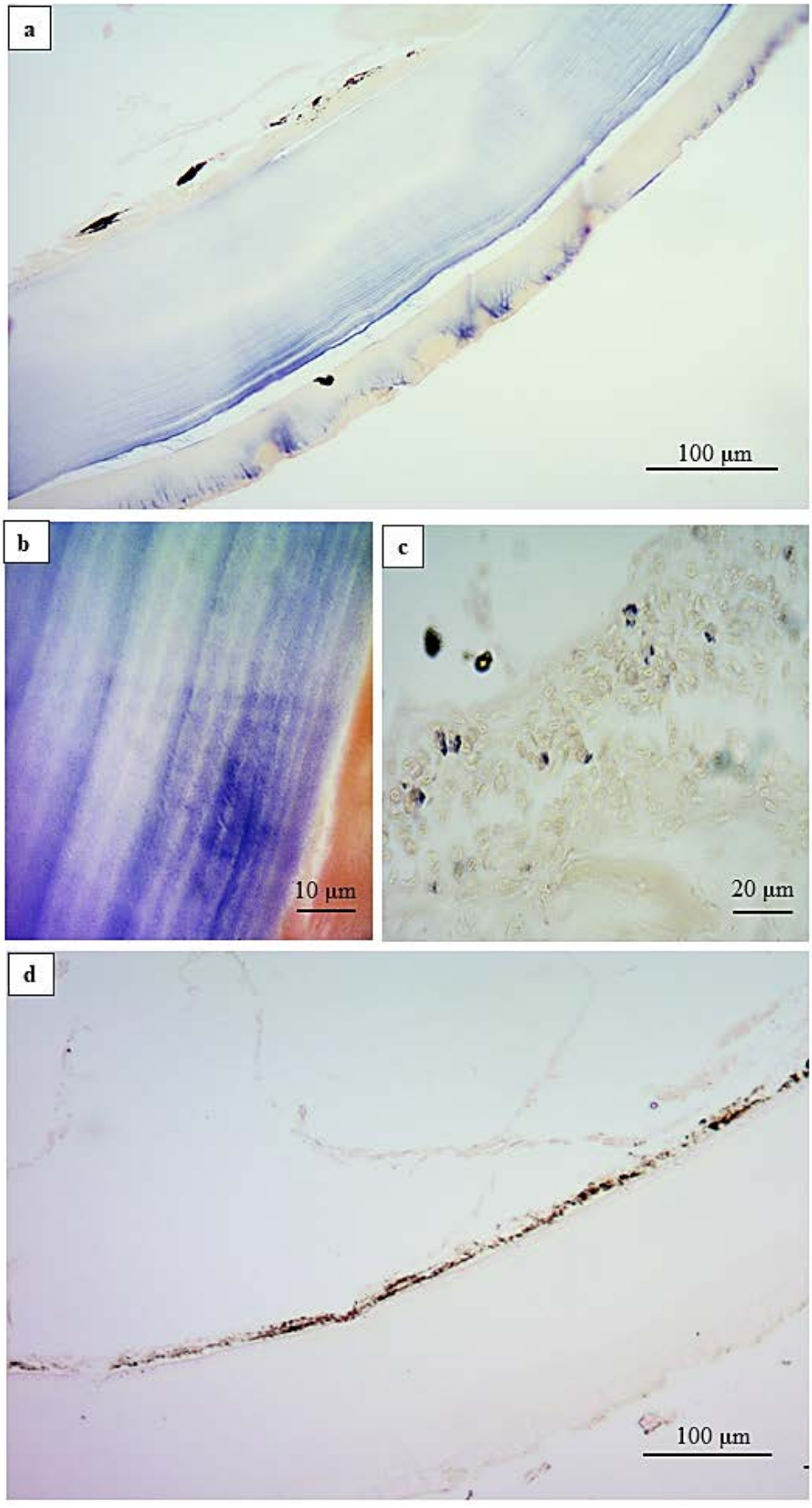
a
100 µm
b
10 µm
c
20 µm
d
100 µm

Figure 3.14: Carcinin localisation in the eyestalk of *C. maenas*. (**a**): Low magnification of the cross section of the proximal end of the eyestalk of *C. maenas* stained with carcinin-specific antibody and alkaline phosphatase tagged secondary Ab. (**b**): High magnification image of part of eyestalk endocuticle, stained as above. (**c**): High magnification image of the central part of cross section of the eyestalk, stained as above. (**d**): Antisera control. The low magnification image shows carcinin signal in parts of the exocuticle, as well as the endocuticle. Staining in endocuticle is shown as a gradient of stained lines, and is more intense near the periphery. These lines appear as concentric circles and match endocuticle growth bands. This staining seems not to be consistent throughout the cuticle, as it is more localised at rims of parallel lines with some having a darker signal than others, as shown in (**b**). Apart from the cuticle, only a few haemocytes are stained for carcinin, as seen in the high magnification of the connective tissue region in (**c**).

3.3.3.6. Ovary

The ovarian tissue is lobular, and enveloped by a thin capsule and epithelium (Figure 3.15, a) that defines the ovary shape in the haemocoel cavity. The youngest (primary) oocytes arise from oogonia via mitotic division in the germinal zone. Primary oocytes divide meiotically, and at the second meiosis, produce secondary oocytes classified into five types: early previtellogenic oocyte (Oc1), late previtellogenic oocyte (Oc2), early vitellogenic oocyte (Oc3), late vitellogenic oocyte (Oc4) and mature oocyte (mOc) (Figure 3.15, a, b). The developing oocytes increase in size and decrease in the nuclear: cytoplasmic ratio, and move from the germinal centre towards the periphery of the ovary (Sharifian *et al.*, 2015). Development of oocytes involves decreasing in the basophilic nature of the cytoplasm of previtellogenic oocytes (Oc1-Oc2) to more acidophilic (eosinophilic) cytoplasm in vitellogenic and mature oocytes (Oc3-4; Figure 3.15, a, b). The appearance and histological structure of ovaries in the present study suggested that they are in a proliferative stage. The interstitial space between oocytes is composed of connective tissue diffused by some haemocytes in addition to clusters of accessory cells (Figure 3.15, b). Accessory, or follicle, cells are seen either at the lobe periphery or flatten and surround each of the oocytes as they mature. Accessory cells play an important role in embryo development, by participating in yolk production or contributing to development of the chorionic membrane of the mature

ovum (Ryan, 1967). Recent studies suggest that accessory cells are associated with oocyte degeneration (Kim *et al.*, 2014). In the present study, some oocytes, especially in the peripheral region, showed vacuolation, with no apparent nucleus, and no distinctive staining for either eosin or haematoxylin (Figure 3.15, a). It is possible these are degenerating oocytes (DOc), as they match the description featured in Kim *et al*. (2014).

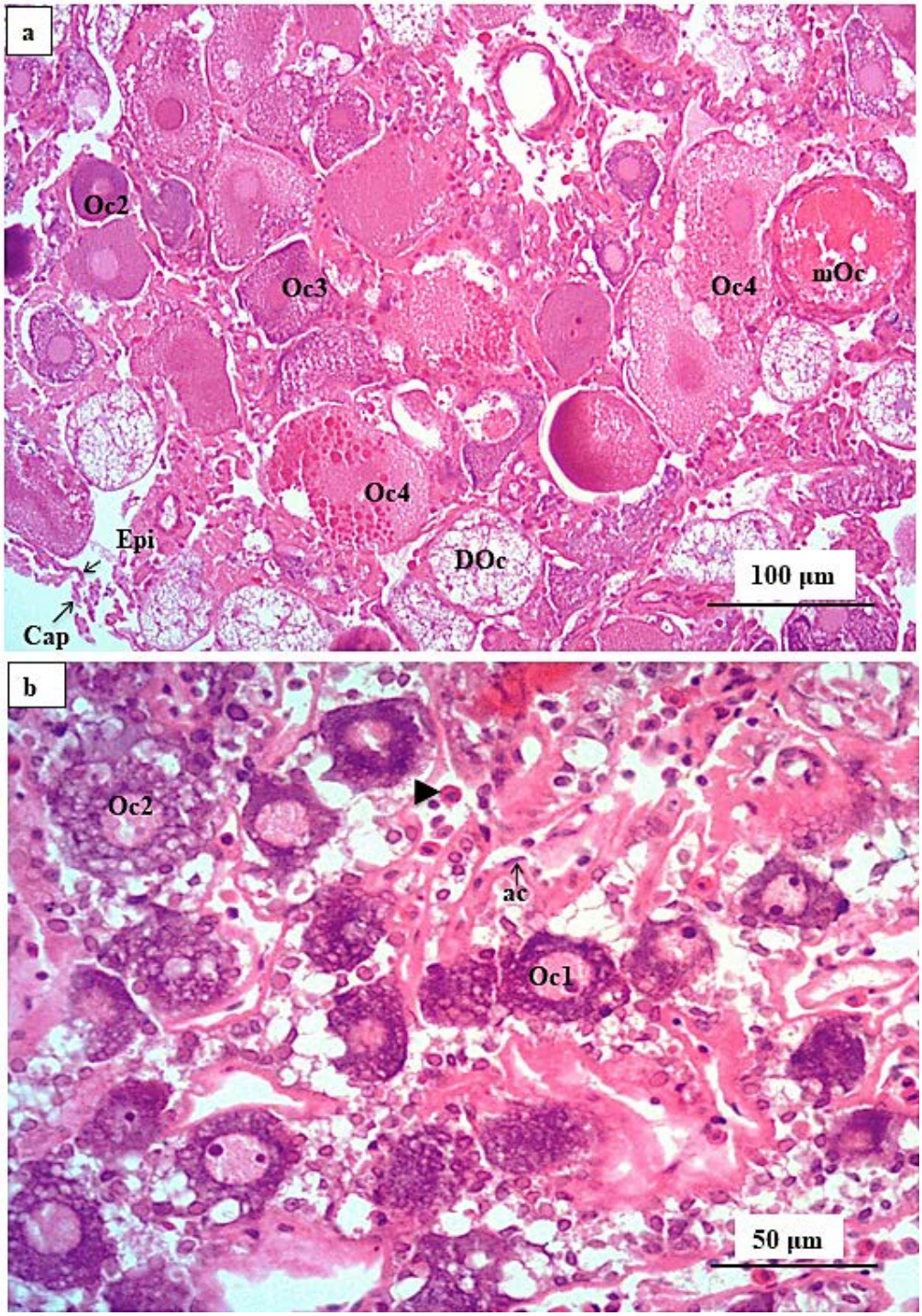

Figure 3.15: Structure of *C. maenas* ovary. (**a**): Cross section of peripheral area of the ovary stained with H & E. (**b**): Cross section of central area of the ovary stained with H & E. Ovarian section reveals different types of developing oocytes, previtellogenic oocytes are Oc1 and Oc 2, vitellogenic oocytes are Oc3 and Oc4. In all stages Oc1, 2 and 3, the nucleus is still visible, while in the mature oocyte (mOc) the nucleus has become obscure and the cytoplasm stained with deep pink due to its high content of yolk bodies. Some oocytes, especially near the periphery appeared vacuolated with no nucleus and only weak staining with H & E. These are believed to be degenerated oocytes (DOc). Ovary is surrounded by ovarian capsule (Cap) lined with epithelial cells (Epi). A single layer of epithelium surrounds each oocyte. The central area contains more previtellogenic oocytes (Oc1, 2) characterized with their basophilic cytoplasm and large nucleus. The high magnification illustrates more clearly the interstitial space filled with connective tissues and accessory cells (ac) and infiltrated with some haemocytes (arrow heads).

Carcinin localisation in the ovary exhibited very strong staining in the ovarian capsule, the thin pavement epithelium of the capsule and oocytes, and the connective tissue around the developing oocytes and their associated accessory cells in the germinal zone (Figure 3.16, 3.17). Patches of carcinin were also detected in the epithelium around some of the oocytes (Figure 3.17, a-c). Carcinin-positive cells were commonly observed in very close contact with the epithelium of some oocytes and appeared to be depositing stained granular material onto their surface (Figure 3.17, d). More remarkably, carcinin was further present in varying degrees within the cytoplasm of some oocytes near to the ovarian wall (Figure 3.16, a), as well as in the nuclei of more deeply stained oocytes (Figure 3.16, a). Carcinin was detected in some of the stage 2, 3 and 4 oocytes, with strongest staining seen in stages 3 and 4 (Figure 3.17, a, b). Visualization of the small stage 1 oocytes was difficult in unstained areas of section, but the lack of clear carcinin signals in any other parts of the ovary implies that they are likely to be devoid of carcinin.

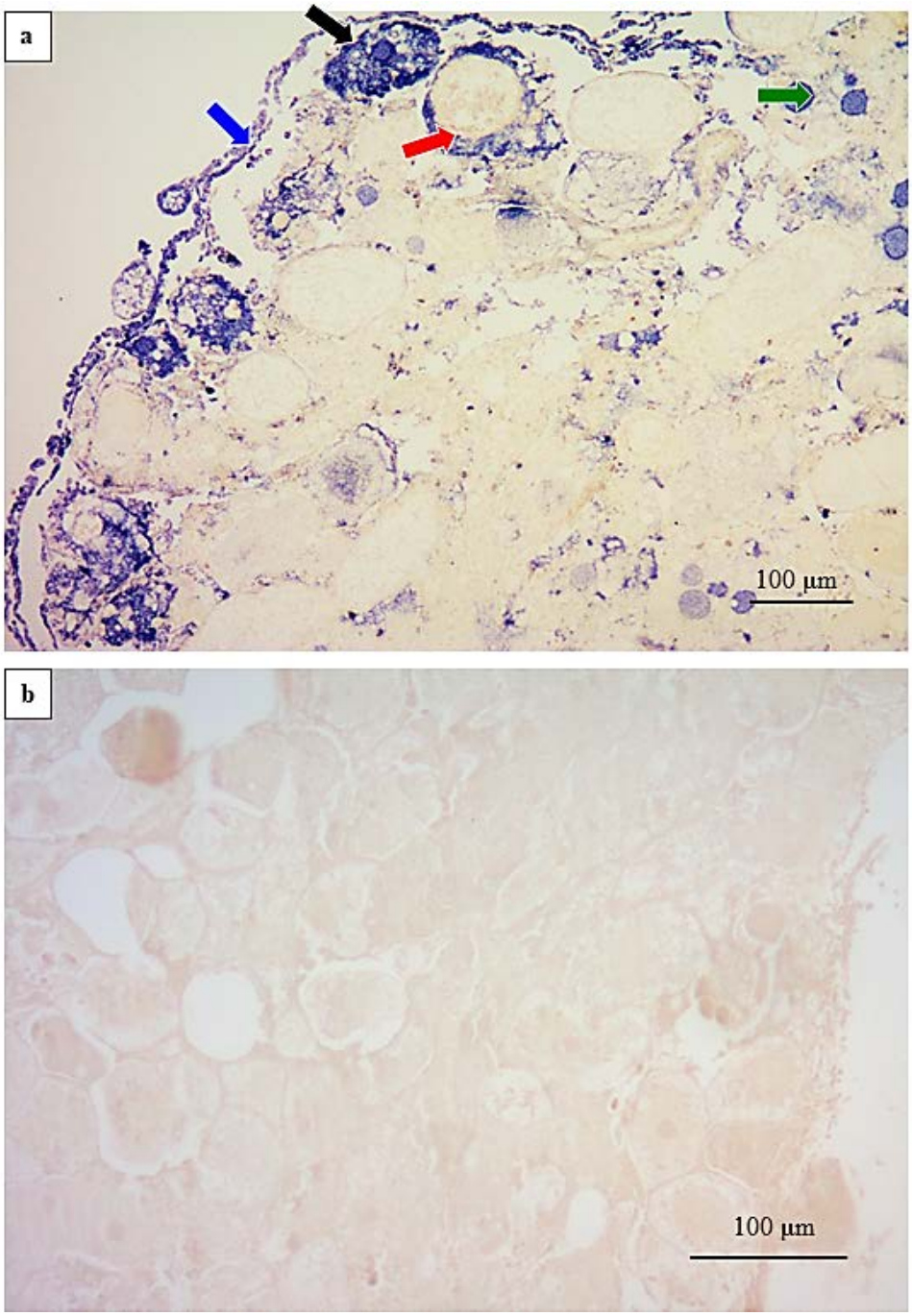

Figure 3.16: Low magnification image for carcinin distribution in *C. maenas* ovary. (**a**): Ovarian cross section stained with carcinin-specific antibody and alkaline phosphatase tagged secondary Ab. (**b**): Antisera control. Carcinin signal is detected in the outer ovarian capsule and epithelium (blue arrow). It is also present in some of the peripheral oocytes, mostly from vitellogenic stage, (black arrow) and stains the interstitial space surrounding them (red arrow). The nucleus of some oocytes is stained for carcinin (green arrows).

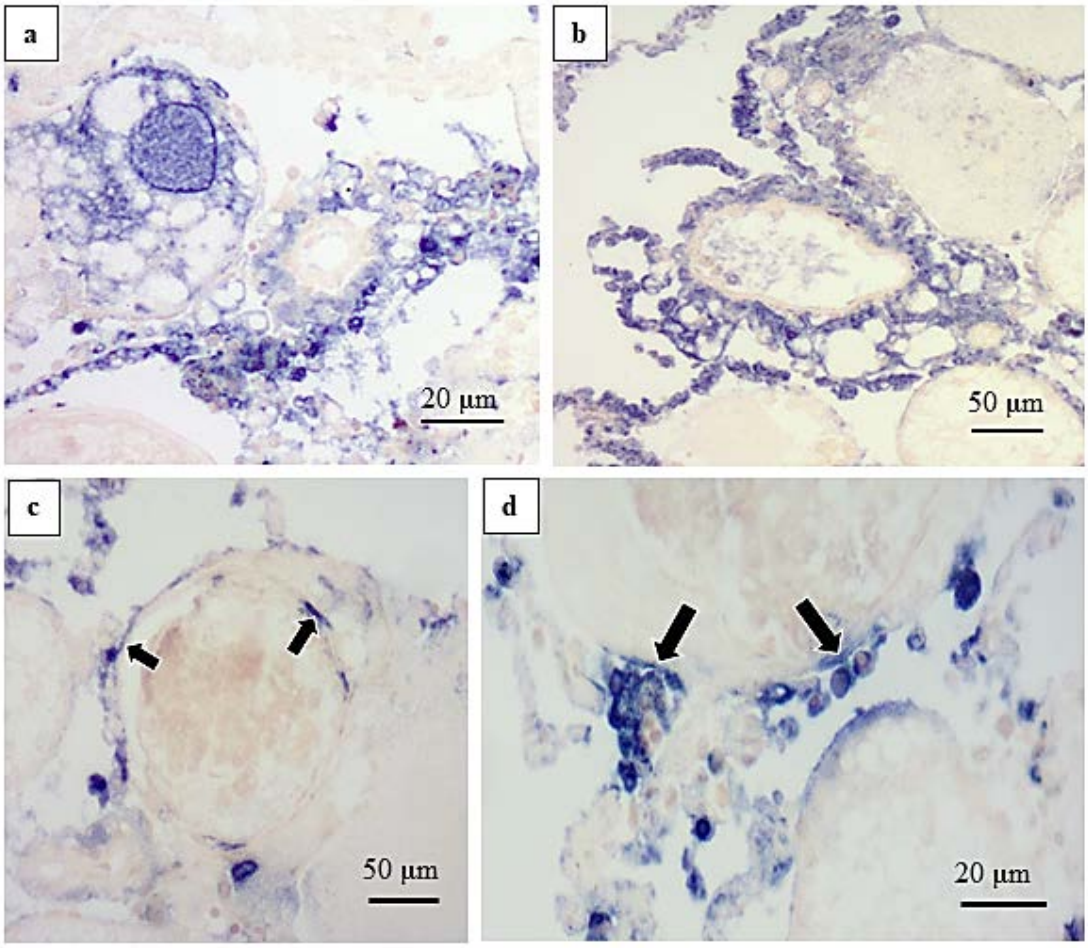

Figure 3.17: Details of carcinin signal in the ovary. High magnification images of carcinin signal in the ovarian central zone (**a**), connective tissues (**b**), and epithelium (**c**) and (**d**). Ovary's central zone is highly stained for carcinin, especially in cells around and associated with oocytes (**a**). Another signal is detectable in nucleus and cytoplasm of a developing oocyte. Carcinin signal appears in the epithelium and the thin film of tissue surrounding oocytes (**b**-**d**). Carcinin signal (indicated by arrows) presents in the epithelial cells around oocytes, in addition to some haemocytes in the interstitial space. High magnification highlights staining in the interstitial space with arrows indicating stained cells and possible release of carcinin to parts of oocyte epithelium (**d**).

3.3.3.7. Testis

The testis is encased by an outer capsule and consists of numerous lobules, each enclosed by a basal membrane (Figure 3.18). The barriers between lobes comprise connective tissue extensions from the outer capsule, in addition to haemal spaces. Sperm develop inside the lobes through spermatogenesis, which is initiated in spermatogonia, the large undifferentiated cells with sizeable nuclei present at the top of each lobe. Spermatogonia produce primary, then secondary spermatocytes through two mitotic divisions. Differentiation of the secondary ones is in the seminiferous tubules at the centre of each lobe. Meiotic division then occurs, producing spermatids that develop via sperminogenesis to mature sperm. Different stages of spermatogenesis and development, as well as changes in the shape of the tubules could be seen in the H & E stained sections (Figure 3.18). In some parts, the lobes appeared to be in a single state of development, while in others, various types of developing spermatocytes or spermatids were shown in a single lobe.

In the testis, a strong positive signal for carcinin was evident in the compact connective tissues in between the lobules (Figure 3.19, a) and in the epithelial layer that lines the mature sperm duct inside the developed lobule (Figure 3.19, b). Carcinin was also observed around the epithelium in some high magnification images (Figure 3.19, c, d). In developed lobules, the connective tissues appeared looser and the carcinin signal was still noticeable (Figure 3.19, b). Many carcinin-positive haemocytes were observed in the testis (Figure 3.19, a, b) but the spermatogonia, the spermatocytes and the spermatids were all negative, as confirmed by antisera control pictures (Figure 3.19, e, f).

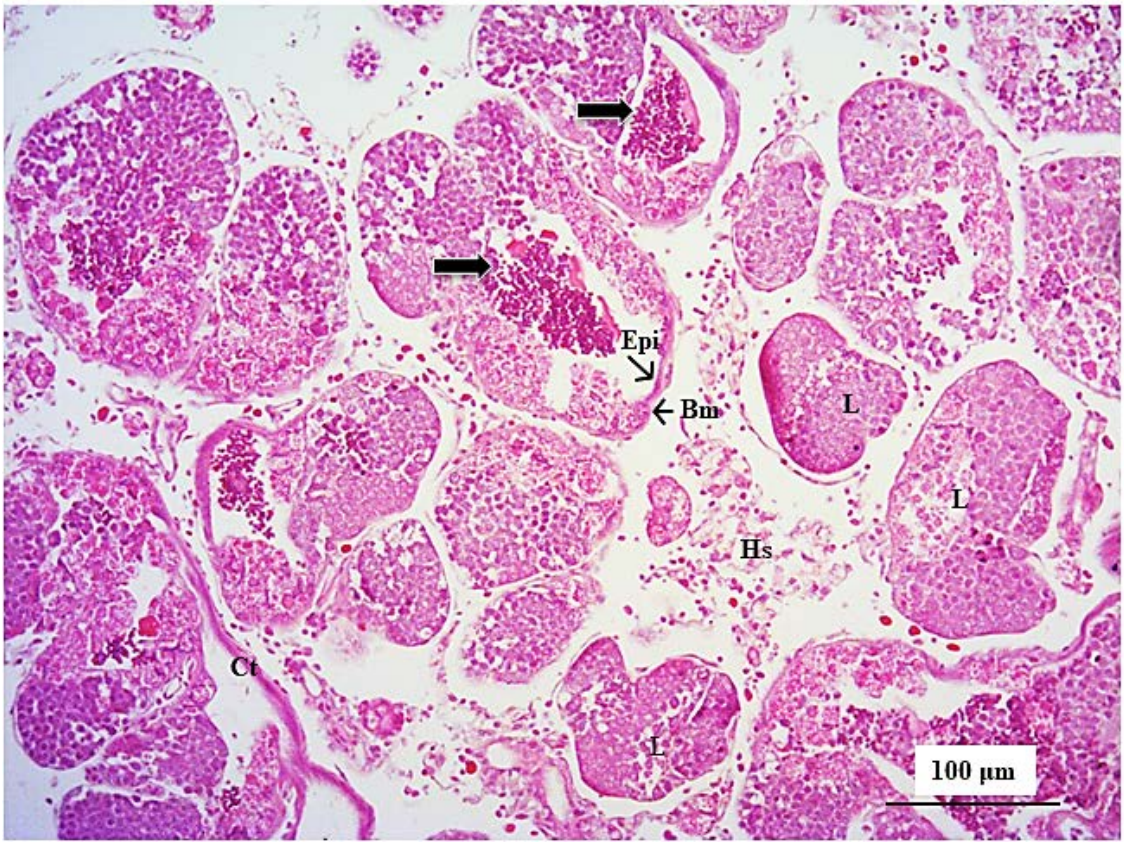

Figure 3.18: Structure of *C. maenas* testis. Histological features of cross section of *C. maenas* testis stained by H & E shows different testicular lobules (L). Layers of connective tissues (Ct) arise from the outer capsule and separate lobules. Lobules are separated by haemal space (Hs), with basement membrane (Bm) enclosing each lobule. Lobules that contain developing spermatocytes or spermatids seem small and compact, while other lobules that contain mature sperm (arrows) are larger and show a central duct lined with epithelium (Epi)

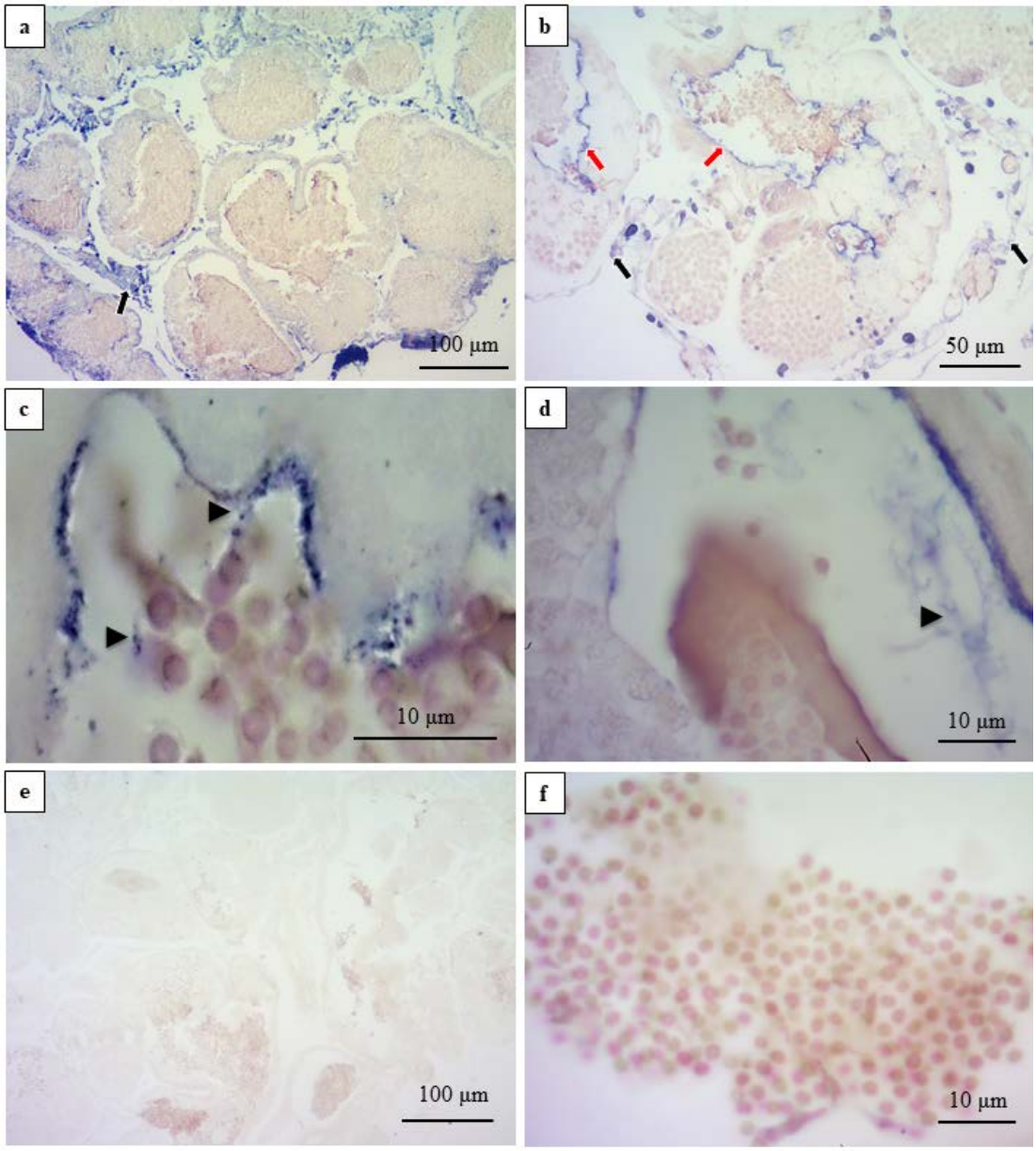

Figure 3.19: Carcinin localisation in testis. (**a**) and (**b**): Low magnification images of testicular cross sections stained with AP tagged carcinin secondary Ab. (**c**) and (**d**): High magnification of testicular sections, stained as above. (**e**) and (**f**): Low and high magnification images of the antisera control. Carcinin is observed in connective tissues (**a**, black arrow) between testicular lobules, while it is absent from the lobules themselves. Note that this area of the section does not show any mature sperm. In testicular section with lobules that have mature sperm (**b**), carcinin is localised in the epithelium that lines the lobular ducts (red arrows), with some faint staining in the loose connective tissues (black arrow) as well. High magnification images (**c**) and (**d**) reveal a thin layer of epithelium with carcinin released from the stained epithelium (arrow heads). Antisera control images reveal the natural colour of the sperm, and confirm the absence of carcinin.

3.4. Discussion

The work described in this chapter confirmed the identification of carcinin in different haemocyte types and identified the protein distribution in tissues of healthy, adult, unchallenged animals, *in vivo*. This revealed that carcinin can be seen on the membrane of some HCs and clarified the localisation of the mature protein in different tissues. This contrasted with previous gene expression studies of crustins (reviewed by Smith and Dyrynda, 2015), which had not shown specific localisation within the various organs. These studies reported that crustin transcripts were detected widely, but not in consistent patterns, in tissues of unchallenged animals. Examples include work on crabs: Yue *et al.* (2010 b) and Mu *et al*. (2010); shrimp: Sun *et al*. (2010) and Anthony *et al*. (2011), as well as crayfish (Yu *et al*., 2016). Such results were interpreted as evidence that the organ or tissue itself expresses the protein. However, in this study, it was confirmed that haemocytes perfusing the tissues are the origin of carcinin, while the tissues themselves, with the exceptions of eyestalk and gonads, did not seem to produce carcinin *de novo*.

3.4.1. Carcinin localisation in circulating and tissue-penetrating haemocytes

Colorimetric and fluorescent immuno-detection was the selected procedure to detect carcinin in separated haemocytes *in vitro*, and in haemocytes penetrating tissues *in vivo*, enabling localisation and visualisation of carcinin in each cell type. Percoll density gradient centrifugation aided in enrichment of individual haemocyte populations, with approximately 90% purity. However, it was not possible with other procedures, like western blotting, to detect if a positive carcinin signal in HCs population, actually originated from the enriched HCs, or from contaminating SGCs. Although western blotting is considered to be a highly sensitive method in detecting and quantifying proteins, it does not enable visualisation of the origin of the detected signal at the cellular and sub-cellular level.

Immune detection revealed high levels of carcinin in the granules of GCs and SGCs, both in circulating haemocytes (either separated or un-separated), and in those infiltrating different tissues. This shows that these two cell types are the main sites for carcinin synthesis, and is consistent with other crustins (Sperstad *et al*., 2009 a) and antimicrobial peptides like penaeidins (Destomioux *et al*., 2000) that were reported to be produced and stored in haemocytes (reviewed by Rosa and Barraco, 2010). GCs

and SGCs exert their action mainly via degranulation, when granule components are secreted to the extracellular domain. This occurs upon microbial stimulation (Smith and Söderhäll, 1983) and serves different biological and physiological roles by releasing proteins such as the components of the pro-PO activation system, the cell adhesion protein peroxinectin, in addition to antimicrobial peptides (Cerenius *et at.*, 2010), of which in the shore crab, carcinin is the most abundant.

Using indirect ICC, images showed degranulating haemocytes releasing granules containing carcinin. Degranulation not only allows direct killing or inhibition of invading microorganisms through the action of antimicrobial peptides, but can also deliver carcinin to other cells that might bind the protein for protective or other purposes. This is strengthened by the detection of carcinin in association with the membrane of some circulating and tissue-penetrating HCs, either at the surface, or slightly diffused to the intracellular domain. As the majority of HCs were devoid of carcinin, it is unlikely that carcinin is produced there. This agrees with the study by Sperstad *et al*, (2010) on the spider crab, *Hyas areneus*, which found that a type I crustin in the granular and semi-granular haemocytes was expressed 2000 fold and 30 fold, respectively, compared with the HCs.

Otherwise, it is possible that HCs receive secreted carcinin when exposed to specific stimulants, indicating a role for the protein in HC functions. The location at the membrane may imply an opsonic role for carcinin to enhance phagocytosis by HCs, something recently reported for another crustin (Liu *et al.*, 2015*)*. Carcinin might also support HCs in trapping invading microorganisms via encapsulation and extracellular trap formation. This could either be via direct antimicrobial activity during peptide release in the developing capsules, or enhancement of cellular adhesion, in a similar manner to peroxinectin (Sritunyalucksana *et al.*, 2001). Alternatively, as there is an association with the cytoplasmic membrane of the HCs, carcinin might contribute to pathogen recognition mechanisms. Havanapan *et al.*, (2014) reported that crustin*Pm*1 in the shrimp *Penaeus monodon* is associated with the cytoplasmic membrane of granular haemocytes and link it to viral recognition pathways. Co-localisation analysis revealed a small amount of carcinin to be infused to the cytoplasmic matrix, while the majority appeared to present on or around the cytoplasmic membrane. If carcinin diffuses from the HC membrane into the cell, the protein might then contribute to

intra-cellular pathways, e.g. those that trigger other protein transcription, or cell death. The fact that carcinin appears to associate with some HCs is highly novel, and has not, to date, reported for any other crustins.

Little is known, to date, of AMP presence in ProHs. Roulston and Smith (2010) were the first to characterize and enrich ProHs from *H. araneus*, finding two types, namely granular and agranular. The same study investigated their possible immunological functions, however, no definite role was detected in the assays used. Similarly, the study by Robb *et al*, (2014) did not report any extracellular trap formation by pro-haemocytes. In the present study, immunocytochemistry revealed carcinin in a small percentage of pro-haemocytes. This further supports the idea that prohaemocytes develop into two cell lineages, with those positive for carcinin becoming granular or SGCs, with the others ultimately developing into HCs, as previously suggested for the spider crab by Roulston and Smith, (2010). Given that direct antimicrobial activity has yet to be demonstrated by pro-haemocytes, it is still unclear if carcinin contributes an antimicrobial function or participates in others, perhaps related to development and differentiation. Certainly, the existence of carcinin in cytoplasmic granules may have use as a marker for different haemocyte types and could also discriminate between separate groups of ProHs.

Immunohistochemistry showed carcinin was present in haemocytes *in vivo*, as well as revealing weaker carcinin signals close to haemocytes. The carcinin appears to have been released by the cells and diffused to adjacent extracellular spaces, such as the gill lamellae, interstitial spaces and connective tissues. This also agrees with the results from the three protein databases searched (Chapter 2), which predicted that carcinin is a secretory (or extracellular) protein. Sites in the tissues might be the ultimate targets for carcinin, where its antimicrobial properties could aid in protection, or the protein could participate in other processes such as encapsulation. Some capsules or nodule-like structures were observed in tissue sections, most extensively in gills, but also in ovaries, heart and hepatopancreas (data not shown), where carcinin was present in the developing capsules (see Chapter 6). As the mature circulating and tissue-penetrating haemocytes are the main immunological effectors in the animal, the dominant presence of carcinin in these cells clearly shows a significant immunological role, while still raising the possibility of having other, non-immunological functions.

3.4.2. Histological localisation of carcinin

There was little indication of carcinin in other cells from most tissues. In the gill, hepatopancreas, heart, and mid-gut caecum, carcinin was only present in haemocytes, apart from some staining in enclosing capsules, connective tissues and epithelia. Outer capsules of organs form essential barriers that encase and protect tissues from any potential pathogens, while epithelial tissues have significant roles in immunity, with numerous AMPs reported there. The first account of antimicrobial activity in animal epithelia was in 1922, when Fleming and Alison discovered lysozyme in human mucus (reviewed by Ganz, 2003). Later on, many AMPs have been described in different types of epithelial cells from various vertebrates (e.g. Zasloff, 1987; Diamond *et al.*, 1991), and in human intestinal epithelium (e.g. Jones and Bevins, 1992; Ouellette and Selsted, 1996). In invertebrates, AMPs were also reported in gut epithelium in insects (Richman and Kafatos, 1996; Richman *et al.*, 1997), before being detected in other taxa, including the crustaceans, when Stoss *et al.* (2004) reported a crustin-like gene, PET-15, to be expressed in epithelium of the olfactory organ of spiny lobsters, *Panulirus argus* (Stoss *et al.*, 2004). Connective tissues are largely permeated with haemocytes, and the release of carcinin there from haemocytes would assist in maintaining the sterility of connective tissues, or allow diffusion to other cell types. It is still not clear if carcinin might be expressed in other cells upon exposure to certain stimulants, or whether greater quantities of the protein would be brought there by haemocytes. It is important to mention that all previous studies on crustins that employed gene expression studies did not use *in situ* hybridization, thus not elucidating where the sites of production are in the tissues.

The most striking results from the immunohistochemistry were observed in the eyestalk and gonads. The localisation observed in the eyestalk is most likely related to moulting. The crustacean cuticle is replaced at every moult, allowing growth bands to form in the eyestalk endocuticle, and is thus related to the age of the animal (Kilada *et al.*, 2012). The presence of carcinin in the eyestalk cuticle growth bands raises the possibility that it might have chitin-binding properties and this idea will be discussed later in chapter 5. It is also important to mention that crustin-like genes have been reported from the eyestalk of *P. trituberculatus*, suggesting that the eyestalk might have an immunological role (Liu *et al*, 2011; Cui *et al*., 2012). This would agree with

the presence of carcinin in the eyestalk endocuticle, with the advantage that the present study allowed more precise localisation of the protein.

The localisation of carcinin in the gonads was very pronounced. In the testes, carcinin was detected in the thin rim of epithelial cells around the lobular ducts, where mature sperm are present, and also in the surrounding connective tissue. Its presence would clearly be important in protecting the testes from infection, but it may have other roles there as well. Recent observations on other AMPs from the mud crab, *Scylla serrata*, have found the peptides in seminal fluid (Qiao *et al,* 2016). These AMPs, mainly scygonadin, plus a second peptide highly similar in sequence to scygonadin, has been proved to be involved in reproductive immunity in both males and females during mating (Xu *et al,* 2011 a & b). It was not possible in the present study to attempt to detect carcinin in the seminal plasma, but whether or not it is present there, it would clearly have potential importance in protecting the genital tracts from possible infection.

With respect to the ovary, carcinin was detected in the capsule, epithelia, connective tissues, and haemocytes. Unexpectedly, it also showed an intriguing presence in some of the developing oocytes, occupying the whole cell, and sometimes also staining strongly in the nucleus. The protein was also in close association with some of the accessory cells surrounding the outer part of the developing oocytes. The presence of carcinin in the oocytes, however, did not follow a consistent pattern, as it occurred in different developmental stages, though not all oocytes from the same stage were stained. The carcinin was mostly detected in the later, vitellogenic oocytes (Oc3, Oc4). The correlation between vitellogenesis and immunity in crustaceans has been reported previously in the crayfish *Pacifastacus leniusculus* (Hall *et al.,* 1995). These authors characterized two lipoproteins, a high density (HDL) and a very low density one (VLDL), and found these to be identical to previously reported immune recognition proteins, namely β-1, 3-glucan binding protein and the clotting protein, respectively (Hall *et al*., 1995).

In addition, Avarre *et al,* (2003) recorded delayed mortality rates in vitellogenic *Penaeus indicus* females upon challenge with *Vibrio penaeicida*, compared with pre-vitellogenic animals. The same study also found a decrease in the total number of

haemocytes in vitellogenic animals and correlated it to bacterial clearance. The lower haemocyte number could be explained by the possible role of haemocytes in oocyte degeneration, something reported previously in shrimp by Browdy, (1988). Oocyte degeneration could result from infection (Liu, 1992), and haemocytes would most likely then migrate to the ovary to attack the infective agents (Avarre *et al*, 2003). It is possible, therefore, that carcinin-positive oocytes may be degenerating, either physiologically since degeneration can occur naturally throughout all developmental stages (Jong-Brink *et al.*, 1983), or due to infection of the ovarian tissue (Liu, 1992). In the latter case, carcinin might enhance the haemocytes' ability to re-absorb degenerated oocytes via phagocytosis (similar to an opsonization effect), or be involved in the apoptotic process of degeneration. Ovarian degeneration occurs when oocytes undergo 'atresia', a controlled apoptotic process resulting in cell death (Perez *et al.*, 1999). It has been studied extensively in bivalves (Dorange and Le Pennec, 1989; Gaulejac *et al.*, 1995, Kim *et al.*, 2014) and transmission electron microscopy has shown oocytes with damaged nuclear envelopes, swollen endoplasmic reticulum and degenerated yolk bodies.

In the present study, some degenerated oocytes were seen in the H & E stained sections, and these showed similar features, namely, vacuolization and absence of nuclei. As atresia involves nuclear membrane damage, and if carcinin is present in atresic oocytes and passes through the damaged nuclear membrane, this might explain the positive signal in the nucleus of some oocytes. Moreover, it has been found that accessory cells, where the carcinin signal was also observed, are involved in atresia as well (Kim *et al.*, 2014). Interestingly, one WFDC-domain containing protein, uromodulin like-1, was reported to accelerate age-related ovarian degeneration in rodents (Wang *et al.*, 2012). The oocytes appeared to be greatly affected by over-expression of the uromodulin like-1 protein, which sent signals to adjacent cells in a way that caused ovarian degeneration (Wang *et al.*, 2012).

Furthermore, another example of a gene encoding a WFDC-domain containing protein in humans, (WFDC-2, also known as human epididymis protein, HE4), was discovered to be over-expressed in cancerous ovarian tissue (Hellström *et al*., 2003, Bingle *et al*., 2006). Another study recently showed that the encoded protein regulates apoptosis thus enhances proliferation of the cancer cells (Chen *et al*., 2013). It is clear from

these reports that WFDC proteins have considerable involvement with developing ovarian cells across different taxa. Certainly, further investigations into the role of carcinin in reproductive tissues are warranted.

This chapter revealed the novel and unusual distribution of carcinin in organs of the shore crab *C. maenas*. These results have provided more information on carcinin localisation in different haemocyte types, shown that the protein is largely absent from organs such as gills and hepatopancreas, but present unexpectedly in the eyestalks and gonads. These findings have expanded our knowledge of carcinin localisation and thus shed more light on its possible biological functions. The presence of carcinin in the eyestalk growth rings, together with its strong signal in the ovaries, implies that carcinin may also be associated with cell development or resorption. The reports of other WFDC-domain containing proteins associated with ovarian cells in other taxa further supports this. The results also indicate that greater caution may be necessary when interpreting data from purely genomic approaches, and emphasizes the importance of native protein isolation, visualization and functional studies based on *in vivo* and *in vitro* proteomic methods. Having established a 'baseline' localisation of the protein in tissues of healthy adult crabs, the next chapter will examine whether carcinin distribution changes with natural events in the life cycle of the animal.

Chapter 4

Changes in Carcinin Localisation During Physiological Changes: Gonad Maturation, Tissue Regeneration, and Moulting

4.1. Introduction

The previous chapter illustrated the distinct localisation of carcinin in different tissues of the shore crab *C. maenas*. Since localisation showed some surprising results in the gonads and eyestalk, subsequent experiments were done to investigate how its localisation might change during major biological changes such as gonad development, tissue regeneration, and moulting. Eyestalk ablation was chosen to induce these as it has been used widely to drive moulting and gonad maturation in various crustaceans, including the spiny lobster, *Panulirus homarus* (Fernandez and Radhakrishnan, 2016), the fiddler crab, *Uca triangularis* (Supriya *et al*., 2016), and the penaeid shrimp, *Penaeus vannamei* (Montoya, *2016*). In addition, it was predicted that the remaining part of the ocular peduncle of the ablated eyestalk would undergo wound repair and regeneration (Desai and Achuthankutty, 2000), thus the role of carcinin in this process could also be studied. Although eyestalk ablation has been used widely in various crustacean studies, no previous studies were reported to employ this process to study crustins or any other AMPs.

The eyestalk of crustaceans contains the main endocrine complex that controls several bioactivities like moulting, metabolism and reproduction. This complex consists of the medulla terminalis ganglionic X-organ (XO) responsible mainly for hormonal synthesis, and the sinus gland (SG) where produced hormones are stored and secreted (the XO/SG complex) (Quackenbush, 1986; Webster, 2012). Multiple hormones are produced by this neuro-secretory system, although the moult-inhibiting hormone (MIH) (Soumoff and O'Connor, 1982; Mattson and Spaziani, 1985), and the gonad-inhibiting hormone (GIH) (Soyez *et al.*, 1991), are the ones responsible for controlling moulting and gonad development, respectively (Figure 4.1).

Crustacean growth is accompanied by moulting (or ecdysis), in which the animal disengages its hard, non-living exoskeleton, expands due to water uptake, and then hardens its newly formed cuticle by calcification (Crothers, 1967; Webster, 2015). This process, which can take place over a year of crab's life, can induce major histological changes in key organs and affects the animals' physiology and biochemistry (Chang, 1995). The use of eyestalk ablation to induce moulting goes back to 1905, when Zeleny noticed that moulting of the fiddler crab *Uca pugilator* accelerated in eyestalk-less animals. Removal of the eyestalk results in depriving the animal of the inhibitory effect

of MIH, thus activating the Y-organ to release ecdysteroids, the principal hormones responsible for moult induction (Figure 4.1). In the present study, in addition to the attempt to activate moulting by eyestalk ablation, a juvenile male crab that naturally moulted was sacrificed immediately after casting off its old exoskeleton. The main organs including gills, hepatopancreas, testis and heart were excised for IHC procedure to map carcinin localisation. This natural moult was defined as the newly moulted/post-moult A_1 stage, according to Crothers, (1967) (Table 4.1), and based on observed morphological features.

Eyestalk ablation has been used to manipulate gonad development after it was first reported by Panouse, (1943) that removal of the eyestalk could increase ovarian size in the shrimp, *Leander serratus* (cited in Fingerman, 1997). Ovarian maturation is mainly manifested by vitellogenesis, the process that leads to the production of the yolk protein, vitellin, which is a complex high-density lipoprotein conjugated with carbohydrates and carotenoids (Subramoniam, 2011). Eyestalk ablation has also been recorded to increase both testis size and sperm numbers in the white shrimp, *Penaeus vannamei* (Leung - Trujillo and Lawrence, 1985). In this study, the use of eyestalk ablation to induce gonadal maturation aimed to address changes in carcinin localisation during the development of the reproductive cells, especially after carcinin showed surprising localisation in both ovary and testis (Chapter 3). Moreover, some reports have pointed to the interactions between reproduction and immunity (Hall *et al*., 1996, Avarre *et al.*, 2002), thus the potential role of carcinin during gonad development is of interest.

The other objective of conducting eyestalk ablation was to investigate a possible role for carcinin in tissue regeneration. In both crustaceans and insects, animals are able to re-grow lost structures, for example limb autotomy, by a complicated process called epimorphic regeneration. The process aims firstly to heal the wound resulting from an injury to restrict bleeding and repair the epidermis. The secretion of a new cuticle by the activated epidermal cells also supports this. The process is then followed by migration of haemocytes to the injured site where they function in melanization, clotting and defense (Hopkins, 2001). Later on, the tissue regeneration proceeds by the formation of blastema, which are the basic undifferentiated cells that develop later into different tissue types by serial mitotic events (Hopkins and Das, 2015). Haemocytes, especially GCs and SGCs, play significant roles in this complicated process (Hopkins

2001; Hopkins and Das, 2015). Carcinin, as a main component of the cytoplasmic granules and due to its intriguing presence in the endocuticle of the eyestalk, as seen in Chapter 3), is highly suspected to play a role in this mechanism.

The aims of this chapter are:

1. Track carcinin localisation changes in maturing gonads as a result of eyestalk ablation.
2. Investigate carcinin localisation in tissues of a naturally moulting crab.
3. Record whether carcinin distribution changes during the eyestalk regeneration process.

Figure 4.1

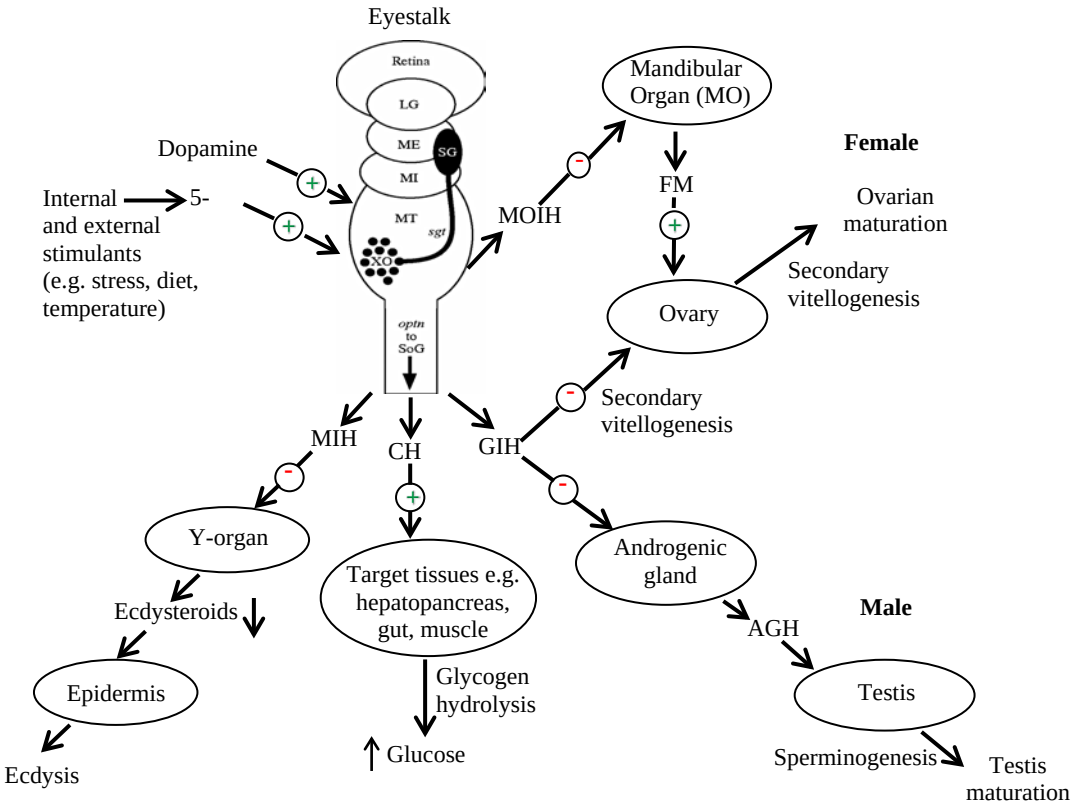

Figure 4.1: Hormonal regulation of metabolism, moulting and reproduction in crustaceans; the endocrinological role of the eyestalk. Crustacean eyestalks contain the main complex responsible for synthesis and secretion of numerous peptide hormones controlling homeostasis, namely the X organ (XO)/ sinus gland (SG) complex. Glands are stimulated by the secretion of neurotransmitters from the brain including 5-hydroxytriptamine (5-HT) and dopamine. Moult-inhibiting hormone (MIH) inhibits the Y-organ (near the mandible external adductor muscles), which suppresses synthesis and secretion of the main ecdysteroids which induce the onset of moulting. Gonad development is driven by secretion of the gonad-inhibiting hormone (GIH). In females, GIH inhibits secondary vitellogenesis, while the mandibular organ (MO) releases methyl farnesoate (MF) that stimulates vitellogenesis but is subject to suppression by mandibular organ-inhibiting hormone (MOIH), also secreted from the XO/SG complex. GIH has an indirect effect on the testis; it inhibits secretion of androgenic gland hormone (AGH), which induces sperminogenesis. CHH= crustaceans hyperglycemic hormone. Adapted from Quackenbush 1986; Khalaila *et al.*, 2002; Webster *et al.*, 2012 and Robert *et al.*, 2016.

Table 4.1: Moult cycle of the shore crab *C. maenas*. Adapted from Crothers (1967).

Stage	Symbol	Description	% Duration of total cycle
Pre-ecdysis	**D_0**	Material absorption from the old cuticle by activated tissues underneath the epidermis. Formation of new cuticle begins.	10
	D_1	New cuticle made under the old, starts to appear in some areas of the 1st maxilliped.	5
	D_2	Tissues of new integument are fully assembled and folded to occupy the space under the old one.	5
Peeler	**D_3**	Appearance of absorption lines on the surface due to the rapid dissolution of material from the old exoskeleton.	3
About to moult	**D_4**	Old cuticle cracks, especially in weak, decalcified areas. Crab begins to swell.	1
Ecdysis	**E**	Total removal of the thin, resorbed old cuticle, crab withdraws backwards due to its swelling.	0.5
Newly moulted /post moult	**A_1**	Crab increases in size greatly. Calcification of new cuticle starts from appendage tips.	0.5
Soft	**A_2**	Crab stops growing. Calcification of the new cuticle proceeds	1.5
Paper shell	**$B_{1\&2}$**	Hardening continues, all tissues of the newly formed integument now complete	8
Hard crab/ Intermoult	**$C_{1\&2}$**	Growth of the main tissues proceeds	15
	C_3	The new integument formation is finalized	15
	C_4	Main inter-moult period, storing of nutrients in the hepatopancreas occurs.	+30
Terminal anecdysis	**C_4T**	Animal moulting stops.	Until death

4.2. Methods

4.2.1. Eyestalk ablation procedure

Animals were collected and kept as in Chapter 2 (Section 2.2.1). A total of 18 crabs (9 males and 9 females) were used in this experiment, and allocated into six groups, each comprising either 3 males or 3 females. The moult stage was defined as inter-moult C_4, according to morphological observations; the crabs had hard cuticles with epibionts present, the carapace colour was brownish-red and there were no signs of moulting, nor of a new cuticle (Vinuesa, 2007). The sexual maturity of gonads was estimated according to observations of Crothers (1967) and Lyons *et al*., (2012), namely that crabs sampled in late summer with carapace widths of 50-59 mm (females) or 60-69 mm (males) are unlikely to have mature gonads. For each group, one animal was subjected to unilateral eyestalk ablation (one eyestalk cut), the second was bilaterally ablated (both eyestalks cut), and the third was not ablated (control). Prior to the procedure, animals were chilled for five minutes (-20 °C) in order to make them quiescent and to reduce blood loss, then the eyestalk was swabbed with 70% ethanol. To ablate, the ocular peduncle of the eyestalk was cut transversely with sterile scissors (Figure 3.11, b). The cut surface was immediately treated with antiseptic cream (10 mg fusidic acid in a sterile base). The crabs recovered for 2 h at 4 ^{o}C in Instant Ocean (Aquarium Systems, Sarrebourg, France) made up in 0.22 μm filtered water, before allowing the temperature to return to the ambient level of 10 ± 3 ^{o}C. Un-ablated control crabs were maintained similarly. After 5 days, during which the tank water was changed every 48 h, the crabs were weighed, and then sacrificed as in Chapter 3 (Section 3.2.4.1). The gonads were examined macroscopically, and then weighed to calculate the gonado-somatic index (GSI) to estimate maturation. The equation used was:

GSI= gonad weight /body weight x 100

Gonad tissues were then subjected to processing for histology as in Chapter 3 (Sections 3.2.4.2 and 3.2.4.3), H & E staining as in Chapter 3 (Section 3.2.5), and immuno-localisation of carcinin as in Chapter 3 (Section 3.2.6).

4.2.2. Eyestalk regeneration

The eyestalk was cut as in Section (4.2.1) and the remaining parts of the cut ocular peduncle of the eyestalks were excised from the experimental crabs using sterile scissors five days post ablation. They were fixed with Davidson solution for 48 hours, and then decalcified for one week by keeping them in EDTA solution (25 g EDTA in 175 mL dH_2O). Ablated tissues were processed for histology and immunohistochemistry, as above, in order to study carcinin distribution during the healing and regeneration of this structure.

4.2.3. Carcinin localisation in immediate post-moult animal tissues

A juvenile male crab (carapace width *ca* 35 mm) was observed among collected stock animals. It was kept in a separate tank and maintained as in Chapter 2. Upon the visible onset of moulting (the animal escaped from its old cuticle and became transparent) it was sacrificed immediately. Pieces of hepatopancreas, heart, gill and testis were removed for immunohistochemical analysis in order to monitor carcinin localisation. Unfortunately, this was the sole animal (among males and females) that was observed to experience moulting, for reasons unknown. The tissues from the male crab were removed and processed for histology and immunostaining, as above.

4.2.4. Statistical analysis

Values of carapace width, body and gonad weight, and GSI were calculated as mean percentage ± standard deviation. The statistical differences in GSI values between control and experimental animals were tested using one way Analysis of Variance (ANOVA) test via R statistical software (Boston, MA, USA) (R Core Team, 2017). Statistical significance was accepted at $P<0.05$, followed by application of Tukey Honestly Significant Difference (Tukey HSD) test for *post hoc* difference analysis.

4.3. Results

4.3.1. Effects of eyestalk ablation

Five days after the eyestalk ablation procedure, no morphological signs of moulting were noticed on either unilaterally or bilaterally ablated animals. The exoskeleton remained hard, there were no signs of new cuticle formation, and crabs looked in a good condition and fed well.

4.3.1.1. Ovaries

Removal of the eyestalk activated ovarian maturation as revealed by comparisons of colour, size (Figure 4.2 and Table 4.2), and histological features between control and experimental animals (Figure 4.3 and Table 4.3). The ovaries became more conspicuous and changed from creamy white to yellow and orange in unilaterally and bilaterally ablated animals, respectively. Oocyte maturation was accompanied by the production of spherical cytoplasmic inclusions called yolk bodies, which support the construction of the developing embryo and comprise glycoproteins, lipids and vitellin. The yolk bodies appeared in the vitellogenic stage and became enlarged with localisation initially at the periphery of Oc3, before they occupy most of the cytoplasm of Oc4 and the mature oocytes. Overall, the effect of eyestalk ablation was much stronger and more pronounced in the individuals in which both eyestalks were removed. These changes were quantifiable using GSI values, rising fivefold between control females and those in the bilateral ablation group (Table 4.2). Statistical analysis illustrated significant differences in GSI values between the control and the bilateral ablation groups ($P < 0.0001$) and the unilateral and bilateral ablation groups ($P < 0.0001$). However, the difference between the control and the unilateral ablation groups was not statistically significant ($P = 0.68$).

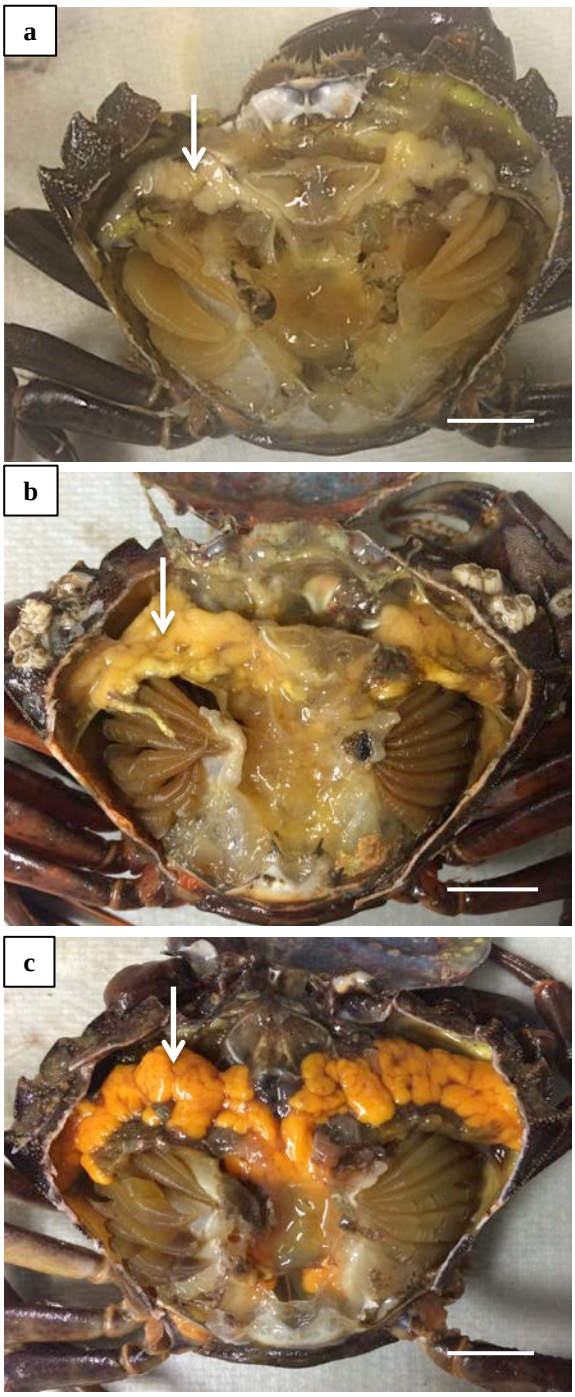

Figure 4.2: Morphological changes in ovary following eyestalk ablation. White arrows indicate ovaries. (**a**) Control, non-ablated crab has smooth, white, creamy ovary. (**b**): Unilateral ablation Ovary is yellow, enlarged, with a more conspicuous lobular structure. (**c**): Bilateral ablation. Ovary is dark orange, much larger and more lobulated, occupying most of the cephalothorax and covering the hepatopancreas. Scale bar: 1 cm.

Table 4.2: Carapace width, body and ovary weights, and calculated GSI for control and experimental female crabs subject to eyestalk ablation. N = 3.

Mean values (± standard deviation)	**Control**	**Unilateral ablation**	**Bilateral ablation**
Carapace width (mm)	55.33 ± 1.52	55.66 ± 1.52	56 ± 1.73
Body weight (g)	83.06 ± 1.90	83.66 ± 0.57	85.33 ± 2.30
Ovary weight (g)	0.89 ± 0.12	1.17 ± 0.03	4.46 ± 0.78
GSI	1.01 ± 0.11	1.31 ± 0.02	5.06 ± 0.74

Accompanying these changes were marked alterations in the histological characteristics of the ovary tissue (Figure 4.3). All oocytes seen in the ovarian cross section of the bilateral ablation group stained with H & E seemed fully mature, with large yolk vesicles dominating the cytoplasmic area and hiding the nucleus (Figure 4.3, c). Haemal spaces between mature oocytes appeared to be diminished or squeezed, with haemocytes seen only rarely in the section (Figure 4.3, c).

Removal of one eyestalk in the female crabs induced some changes in maturation, although these were small in comparison with the bilateral ablation group. Most oocytes in the unilateral ablation group appeared in the vitellogenic and late vitellogenic stage, yet not fully mature. Among all oocytes in the section, a lower percentage of oocytes were pre-vitellogenic (14%), (Figure 4.3, b), while that stage comprised 42% of oocytes in the control non-ablated group, (Figure 4.3, a).

Carcinin localisation changed dramatically with ovarian development (Figures 4.4 and 4.5). There was a marked reduction in its level and presence throughout the ovary in crabs that underwent eyestalk ablation. Carcinin showed similar ovarian localisation in the control group to that detailed previously in Chapter 3 (Figure 4.4, a). However, the signal intensity was weaker in the ovarian capsule, epithelium and some oocytes of animals in the unilateral ablation group, especially in the nucleus (Figure 4.4, c). It was also noticeable in parts of the outer capsule (Figure 4.4, b), but absent from most of the oocyte epithelium. For the bilateral ablation group, carcinin was almost absent from the fully developed oocytes (Figure 4.5, a), although a few oocytes showed weak internal staining (Figure 4.5, d). Carcinin was not seen in association with the surrounding epithelium, although it was present in some interstitial connective tissues (Figure 4.5, b) and parts of the capsule (Figure 4.5, a). Few haemocytes were seen in the vascular spaces outside the oocytes, but those present were well stained (Figure 4.5, c). Apart from this, no traces of carcinin were observed in any other parts of the section.

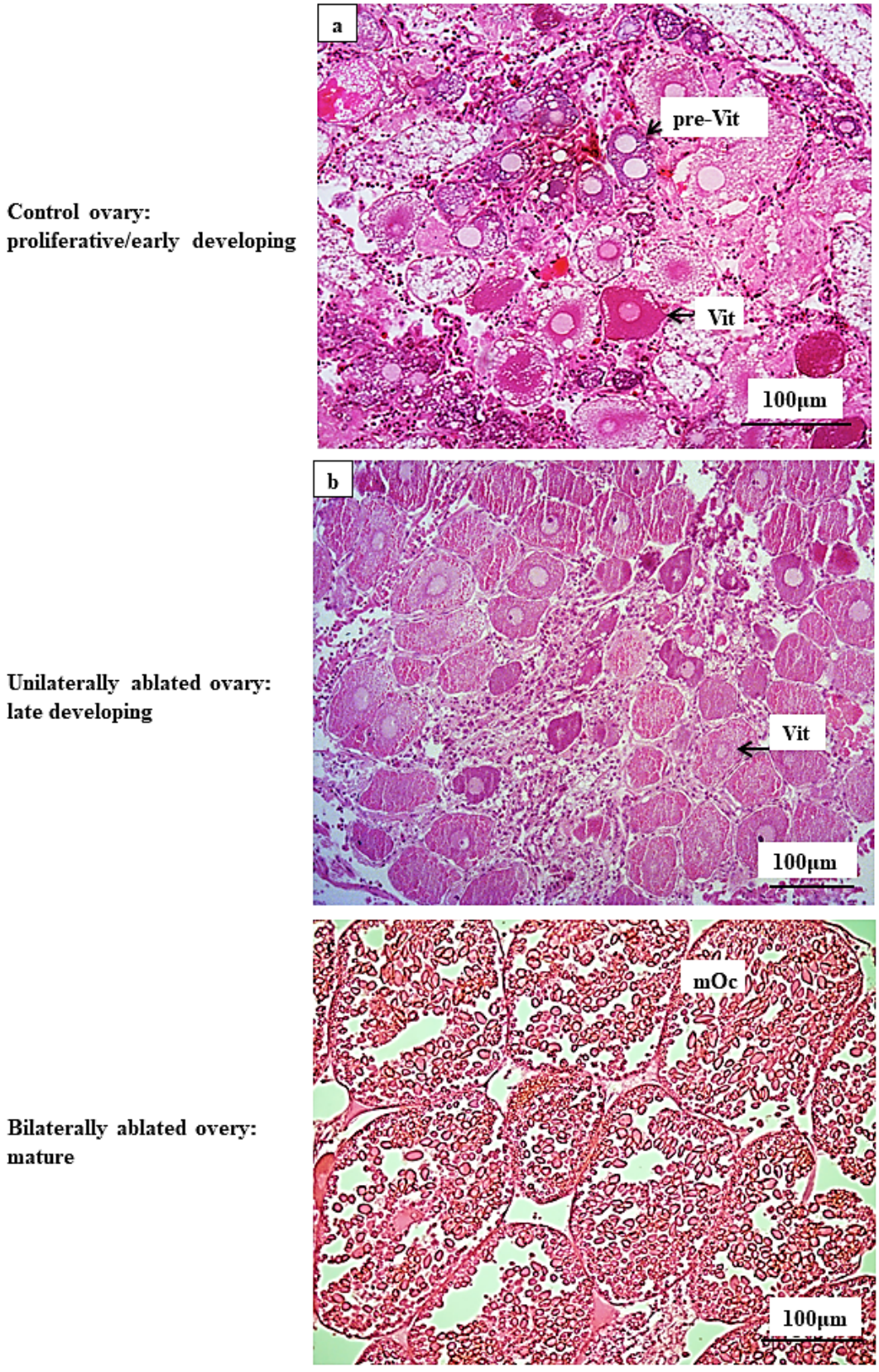

Figure 4.3: Histological characterization of ovarian development induced by eyestalk ablation. All staining by H & E, ovarian cross section from control, non-ablated (**a**), unilaterally (**b**) and bilaterally (**c**) ablated female crabs. H & E stained cross

section of the control reveals developing oocytes: pre-vitellogenic (pre-Vit) have basophilic cytoplasm (*ca* 25-40 μm diameter), vitellogenic (Vit) have more eosinophilic cytoplasm (*ca* 50-80 μm diameter). No oocytes appear fully mature. In the unilateral ablation image (**b**), more vitellogenic oocytes present, with small yolk bodies occupying the cytoplasm, especially near the periphery. Few pre-vitellogenic oocytes are present. In the bilateral ablation image (**c**), the ovary appears completely mature. All mature oocytes (mOc)s are large (*ca.* 140-300 μm diameter), deeply pink-stained and yolk bodies occupy most of the cytoplasm, while the nuclei are obscure.

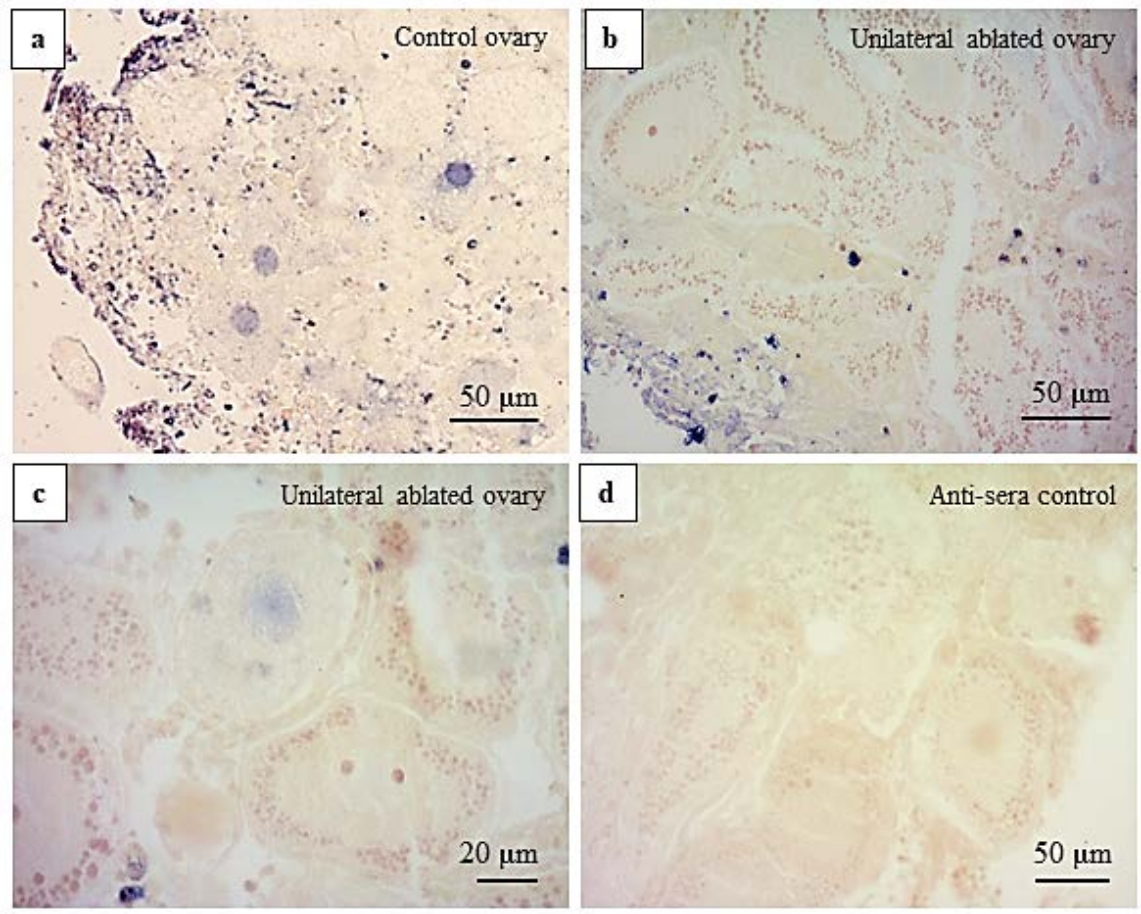

Figure 4.4: Carcinin localisation in ovaries of control and unilaterally ablated crabs. (**a**): Control ovary section. (**b**) and (**c**) Unilateral ablation sections. (**d**): Antisera control. Carcinin localised with alkaline phosphatase tagged secondary Ab, showing stained ovarian capsule and stained oocytes in the control ovary image. In the unilateral ablation image, low magnification (**b**) revealed carcinin staining in ovarian capsule and epithelium, in addition to haemocytes in haemal spaces. None of the

vitellogenic oocytes visible have a signal for carcinin. Some oocytes show faint staining for carcinin in nucleus (**c**), without any in the cytoplasm.

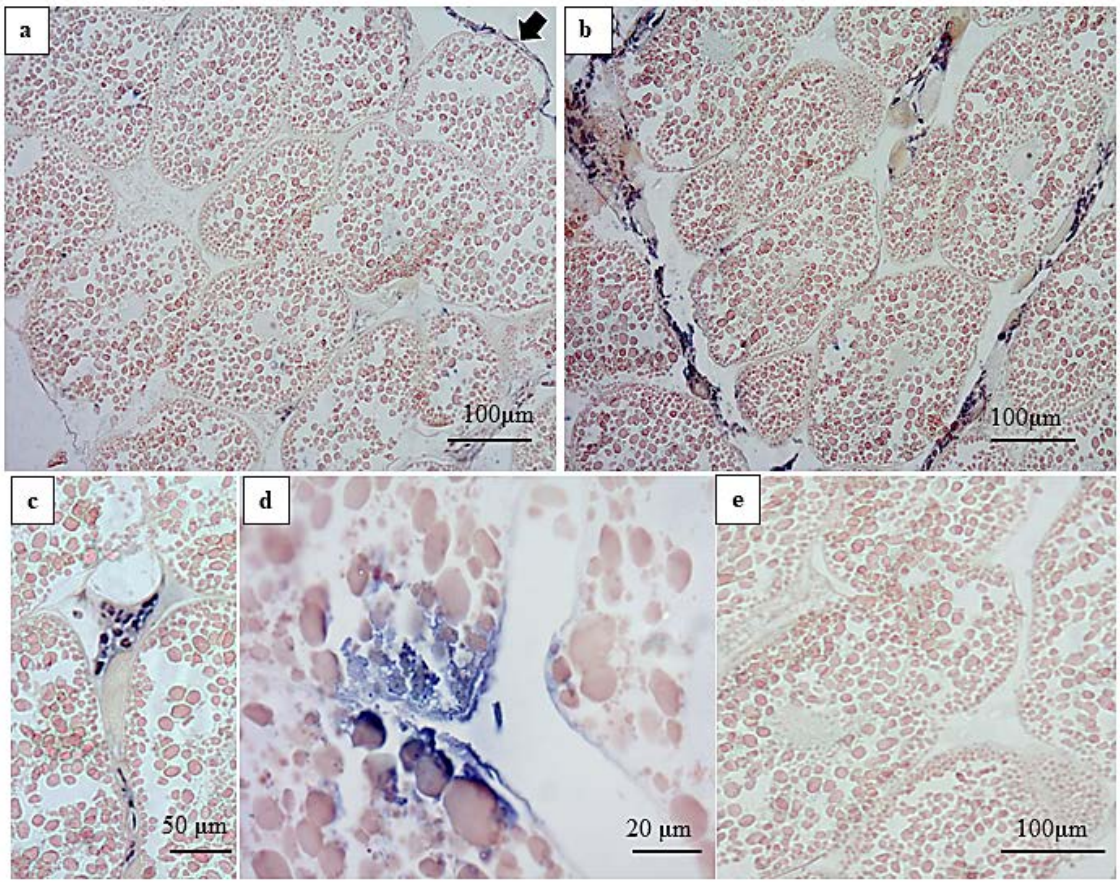

Figure 4.5: Carcinin localisation in ovary of bilaterally ablated crabs. (**a**): Low magnification of ovarian cross section taken from one of the bilateral ablation group. (**b**): Cross section of mature ovarian lobe. (**c**) and (**d**): High magnification from interstitial region of the ovarian section. (**e**): Antisera control. The low magnification image shows thin, stained ovarian capsule (black arrow) with no carcinin signal from the majority of the fully developed oocytes. The image (**b**) shows carcinin staining in parts of connective tissues in interstitial space, where carcinin signal is observed also in the haemocytes (**c**). Carcinin staining is observed occasionally in mature oocytes epithelium and penetrated inside oocytes to surround some of the yolk vesicles, as in (**d**).

Table 4.3: Eyestalk ablation effects on ovarian development and carcinin localisation. N = 3.

	Control	**Unilateral ablation**	**Bilateral ablation**
Macroscopic features	Ovary is creamy white and smooth. Extends parallel to hepatopancreas.	Colour changes to yellow. Covers most of the hepatopancreas	Ovary becomes orange and lobulate. Occupies most of the body cavity.
GSI	1.01 ± 0.11	1.31 ± 0.02	5.06 ± 0.74
Histological features	Oocytes in various developmental stages, with 42% pre-vitellogenic (mean diameter: 30 μm). Follicular cells present in oval-like shape and surround oocytes	More vitellogenic oocytes present in the section (mean diameter 85 μm), with only 14% pre-vitellogenic. Yolk bodies start to appear in vitellogenic oocytes, especially near oocytes periphery. Follicular cells flattened and surround oocytes more extensively	Large fully mature oocytes present in the section (mean diameter 200 μm). Yolk bodies large, predominant and were brownish-orange in their natural colour. Haemocytes and follicular cells are rarely seen.
Carcinin distribution	Carcinin localises in ovarian capsule, epithelium, and stains some oocytes.	Carcinin signal is less intense, but still present in parts of ovarian capsule, haemocytes, and occasionally, faintly in nucleus of oocytes.	Carcinin presence is minimal in oocytes, but apparent in connective tissues, parts of capsule and the few haemocytes present.

4.3.1.2. Testis

Unlike ovaries, eyestalk ablation did not induce notable changes in testicular morphology (Figure 4.6). Testes of both unilateral and bilateral ablation groups had the same morphology in terms of their appearance, size and colour. There was no significant difference in GSI values between control and experimental groups according to ANOVA test ($P = 0.85$) (Table 4.4). It was difficult to define any spermatogenesis or sperminogenesis development after eyestalk ablation using just H & E staining. Most of the developing spermatocytes or spermatids in testicular sections showed very similar cell and nucleus sizes, morphology and pattern of staining (Figure 4.7, a, c and e), which was comparable to what was observed in Chapter 3 (Figure 3.15) and described in Section (3.3.3.7).

Carcinin localisation in the testes of the groups did not change significantly (Figure 4.7, b, d and f). In both the experimental and control animals, carcinin was strongly detected in the connective tissues of the testes and in the testicular capsule. Haemocytes in all experimental and control groups looked abundant and infiltrated the haemal spaces and connective tissues. Though faint traces of soluble carcinin were detected diffusing between the lobules, no evidence of any protein binding to the surface of developing spermatocytes or spermatids was observed. As with all sectioned testes in this experiment, mature sperm were detected in some parts of the lobules, with a thin rim of carcinin positive epithelium surrounding them. All observations matched what was described previously in Section (3.3.3.7). However, the only difference noted was the natural colour of developing spermatocytes/spermatids inside the lobes; this appeared darker in the unilateral eyestalk ablated group (Figure 4.7, d), while it looked rather pale in the bilateral ablated group (Figure 4.7, f), compared with the control animals.

Non eyestalk-ablated testis

Unilaterally eyestalk-ablated testis

Bilaterally eyestalk-ablated testis

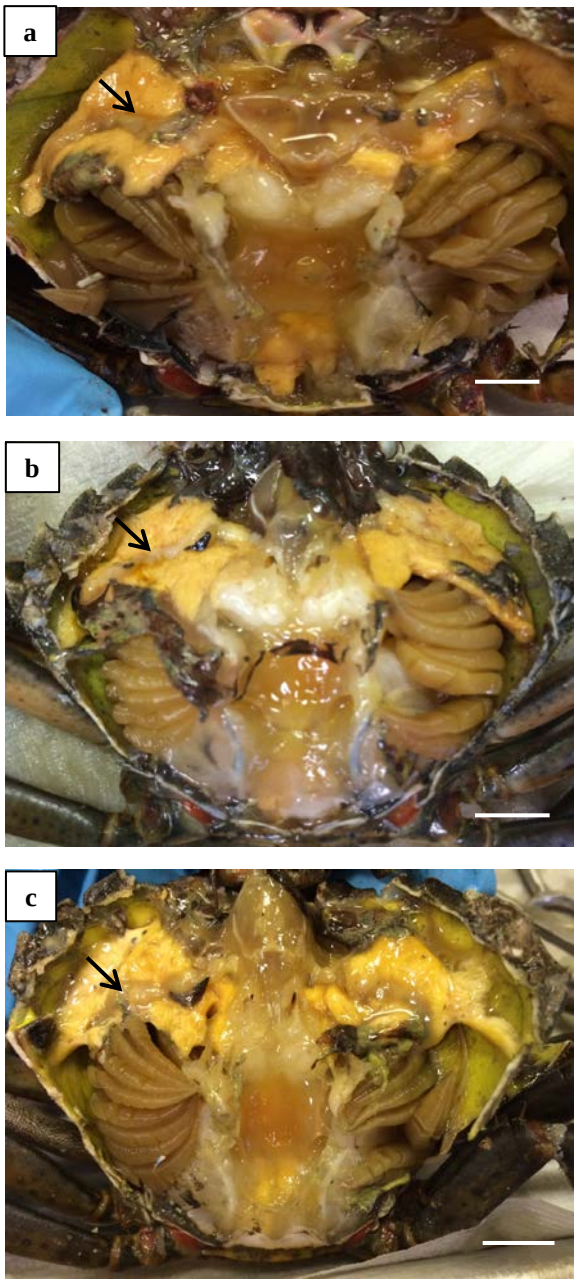

Figure 4.6: Macroscopic features of control and eyestalk-ablated male crabs. (**a-c**) illustrate the morphology of testes (arrows) of control, unilaterally, and bilaterally ablated male crabs, respectively. Neither testis size, colour, nor general appearance differs notably between treatments. Scale bar: 1 cm.

Non eyestalk-ablated testis

Unilaterally eyestalk-ablated testis

Bilaterally eyestalk-ablated testis

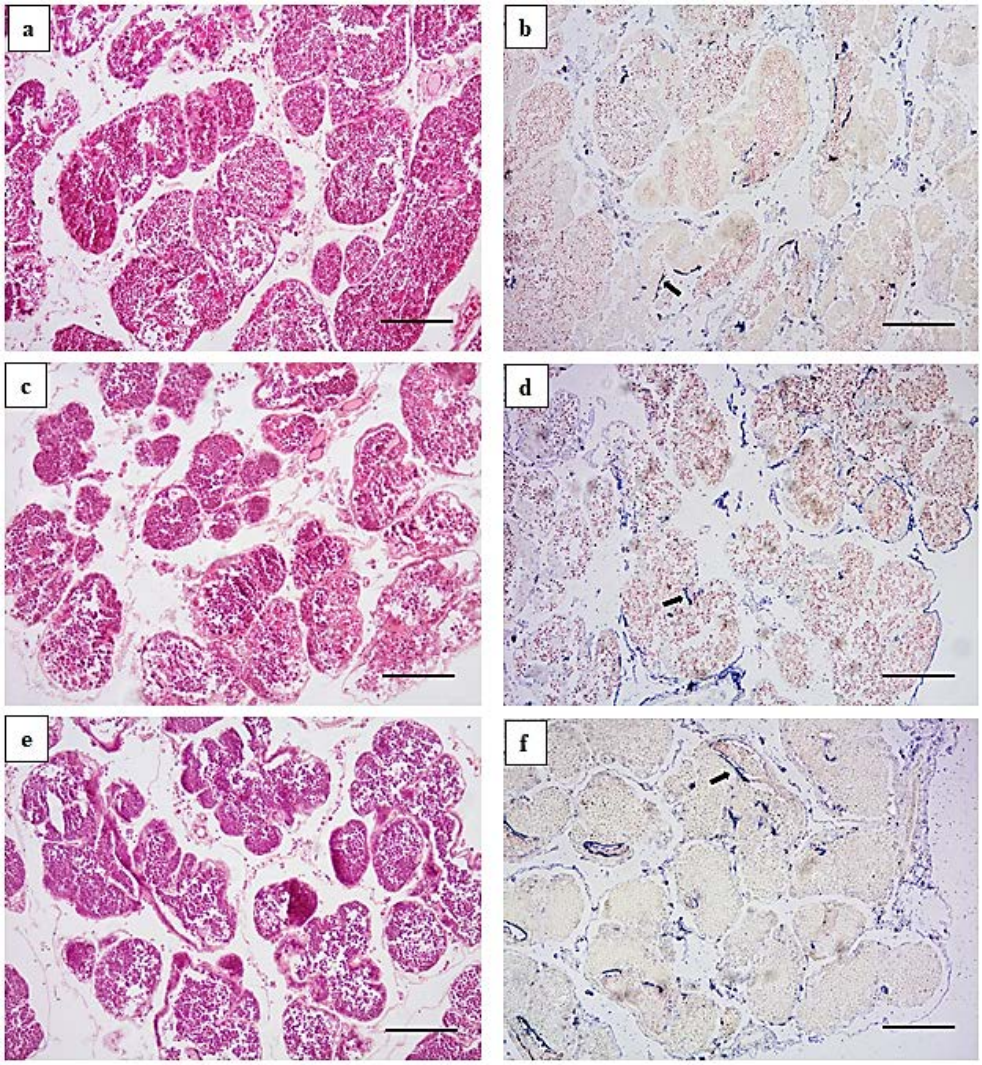

Figure 4.7: Carcinin localisation in testes of control and ablated animals. Histological structure revealed by H & E (**a, c, e**) and carcinin localisation shown by AP staining (**b, d, f**) in non-ablated (**a** and **b**), unilaterally ablated (**c** and **d**) and bilaterally ablated (**e** and **f**) animals. In general, both histological features and carcinin localisation are highly similar in all animals. Testes consist of loose lobes containing spermatocytes, spermatids or mature spermatozoa. AP stained sections reveal carcinin in the haemocytes, connective tissues between lobes, parts of epithelium corresponding with mature sperm and the capsule (black arrows in **b, d** and **f**). In bilaterally ablated crabs, carcinin is present in the testis capsule. Scale bar = 100 µm.

Table 4.4: Carapace width, body and testis weights, and calculated GSI for control and experimental male crabs subject to eyestalk ablation. N = 3.

Mean values (± standard deviation)	**Control**	**Unilateral ablation**	**Bilateral ablation**
Carapace width (mm)	65.7 ± 0.57	66.0 ± 1	65.7 ± 0.57
Body weight (g)	92.2 ± 0.75	92.3 ± 0.25	92.1 ± 1
Testis weight (g)	1.16 ± 0.02	1.14 ± 0.03	1.17 ± 0.01
GSI	1.16 ± 0.05	1.14 ± 0.07	1.15 ± 0.05

4.3.2. Carcinin in regenerating eyestalk tissue

Macroscopic and histological examinations five days following ablation confirmed that the eyestalk underwent wound healing, as the cut surface of the remaining peduncle stub showed visible signs of recovery to the injury, including the emergence of a melanised, regenerating epithelial layer (Figure 4.8, a). Throughout the five days, animals were active, feeding and appeared in good condition.

At the cellular level, the cuticular capsule, although it was ragged and torn with the inner core unstructured and dense (Figure 4.8, b), seemed to be regenerating. Interestingly, the regenerating areas were intensely stained for carcinin (Figure 4.8, c) with almost the entire exo- and endocuticular areas plus the inner cellular matrix strongly staining blue. The re-growing inner tissue was also infiltrated with cells, presumably haemocytes that were strongly positive for carcinin (Figure 4.8, d).

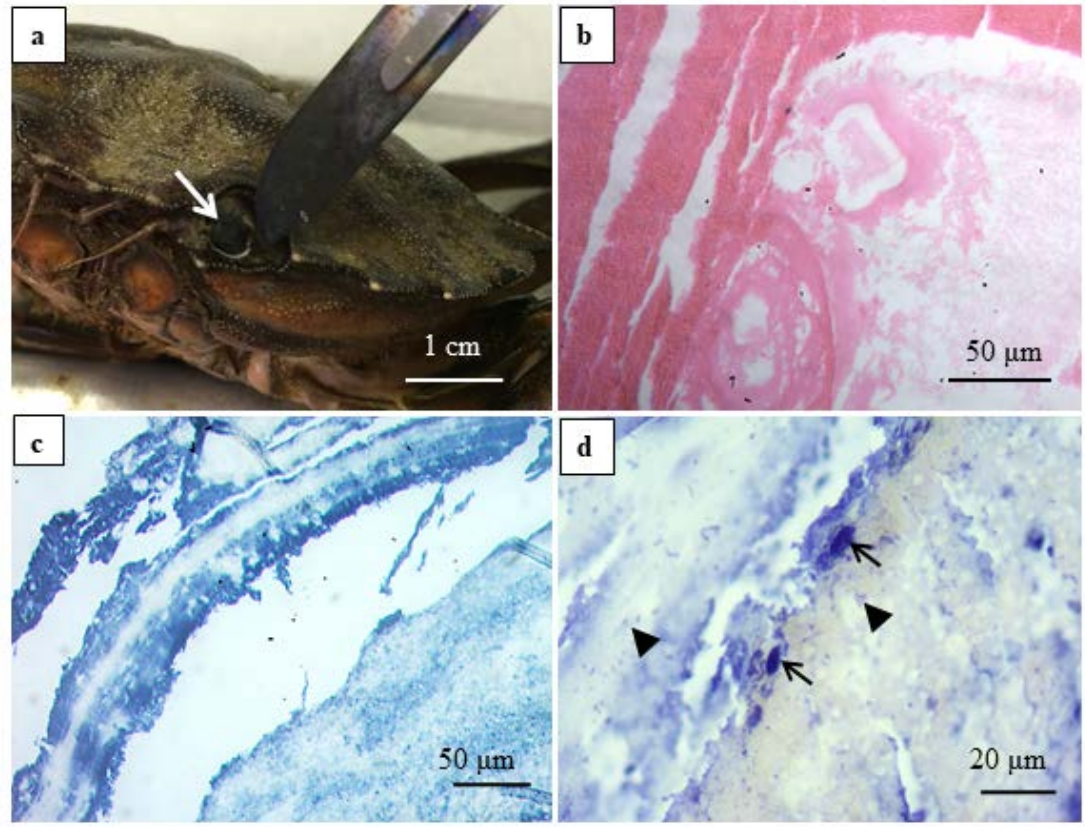

Figure 4.8: Characterization of eyestalk regenerating tissues and carcinin localisation five days post ablation. (**a**): Regenerating area of the eyestalk ocular peduncle five days post-surgery. (**b**): H & E staining of traverse section in the regenerating area. (**c**): Carcinin staining in traverse section of the regenerating area. (**d**): High magnification image of carcinin staining in the regenerating area. Image (**a**) shows wound healing, newly growing layer looks black due to melanisation (white arrow). The image (**b**) features the newly formed cuticle, supporting wound closure. Central tissues appear irregular and diffuse. Carcinin staining in regenerating area (**c**) shows strong presence of carcinin throughout the majority of the section. (**d**): Under high magnification, some carcinin-positive haemocytes are present (arrows), otherwise staining is localised in secreted haemocyte granules (arrow heads).

4.3.3. Effects of moulting on histology and carcinin localisation

4.3.3.1. Gills

Gills excised from the post-moult juvenile male crab stained with H & E showed gill lamellae slightly smaller in size than those described in Chapter 3, Section (3.3.3.1) (Figure 4.9 a and c), mostly due to the early maturation stage of the juvenile crab. Signs of cuticle shedding were observed in many parts of the sectioned gill (Figure 4.9 e and f), where the old cuticle appeared torn. Haemocytes appeared to be clustering mostly in the lamellae (Figure 4.9 e and f), while in the central stem, they showed little or no presence (Figure 4.9 c and d). However, numerous clusters of spindle-shaped cells measuring *ca* 20 μm were observed in the central stem, staining under H & E as a deeper red colour, compared with the haemocytes. The morphology of these cells matched the description of the branchial podocytes/nephrocytes, as recorded by Johnson (1981). The same cells were observed occasionally in the central stem while examining the inter-moult gill tissues (data not shown), but to a lesser degree than that observed in the post-moult gill sections. Podocytes are characterized by their extended pedicels that form an interlocking network facing the basal lamina in gill tissues (Doughtie and Rao, 1981). They serve in ultrafiltration and detoxification processes as well as phagocytosis in the gills, especially at the moulting stage (Doughtie and Rao, 1981).

Carcinin distribution was also observed in a distinct pattern. Podocytes in most parts of the gill stem appeared to be carcinin positive (Figure 4.10, a). However, in other parts they did not show carcinin staining, but their natural pinkish colour (Figure 4.10, b, c and d). Signs of degranulation were observed markedly in the section, as carcinin-stained granules were noticed very close to podocytes (Figure 4.10 c and d). Apart from that, some haemocytes were in the secondary lamellae, where stained stripes of released carcinin were noticed there. Interestingly, carcinin was also detected in parts of the gill wall, especially where signs of shredding and tearing were seen (Figure 4.10, e).

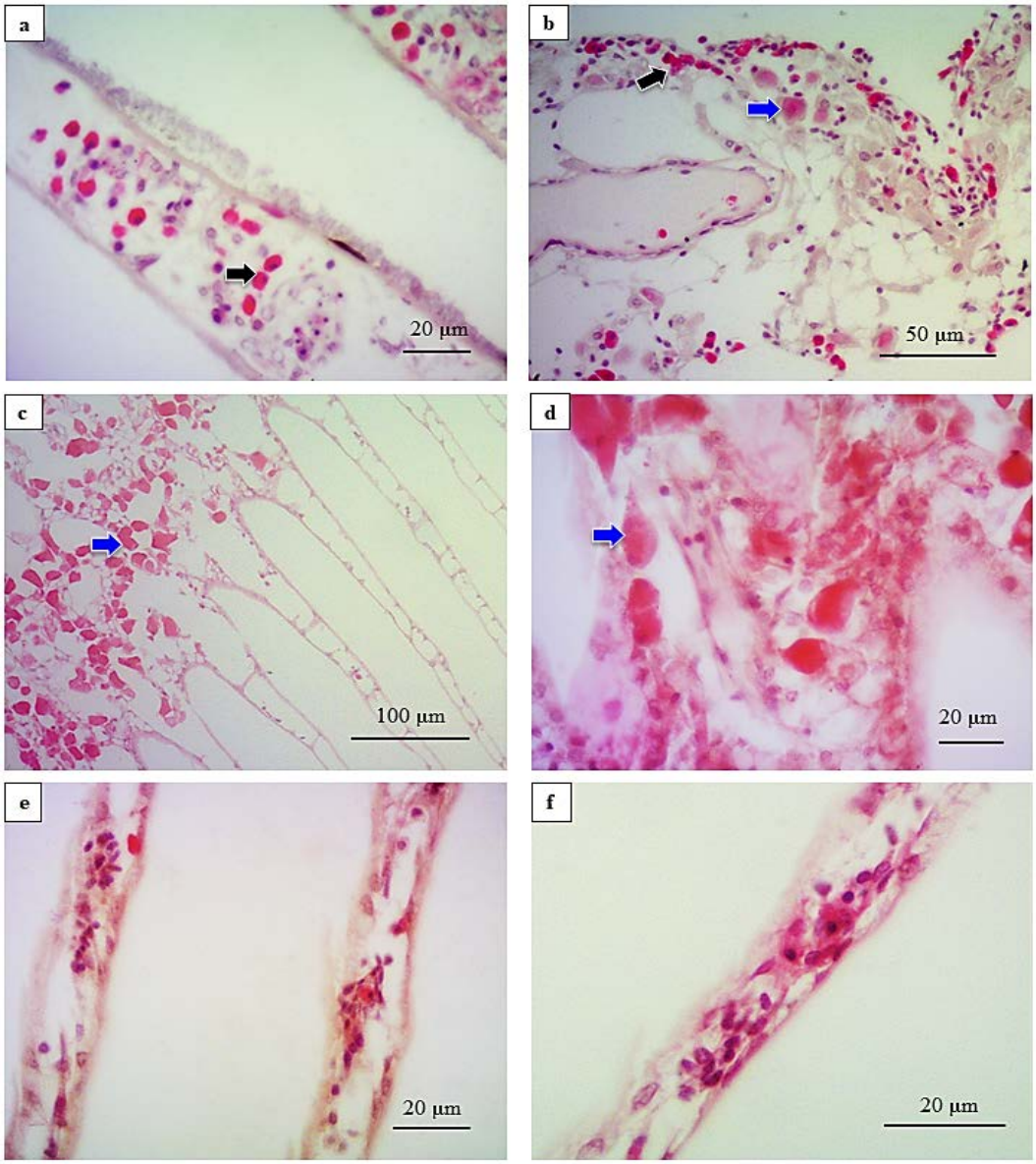

Figure 4.9: Histological features of post moult juvenile gill section compared with inter-moult gill, stained with H & E. (**a)** and **(b**): Inter-moult gill sections. (**c**-**f**): Post moult gill sections. In the inter-mould animal, the structure of a secondary lamellae (**a**) reveals normal gill wall and thick well-defined cuticle, as well as gill central stem (**b**). Haemocytes (black arrows), with their round oval shape and defined purple nucleus are the main cell type that infiltrate inter-moult gill structure. In the post-moult animal (**c**) (low magnification), and (**d**) (high magnification), central stem contained abundant podocytes (blue arrows), seen in deep pink staining due to their inclusions, and measuring more than 20 microns in diameter. Haemocyte numbers were very low in the central stem, possibly due to the high numbers of podocytes hiding them, or degranulation. (**e**) and (**f**): Secondary lamellae of post moult gill, with shredding and peeling signs apparent in gill wall. Haemocytes are present mostly clustering inside the lamellae, rather than the central stem.

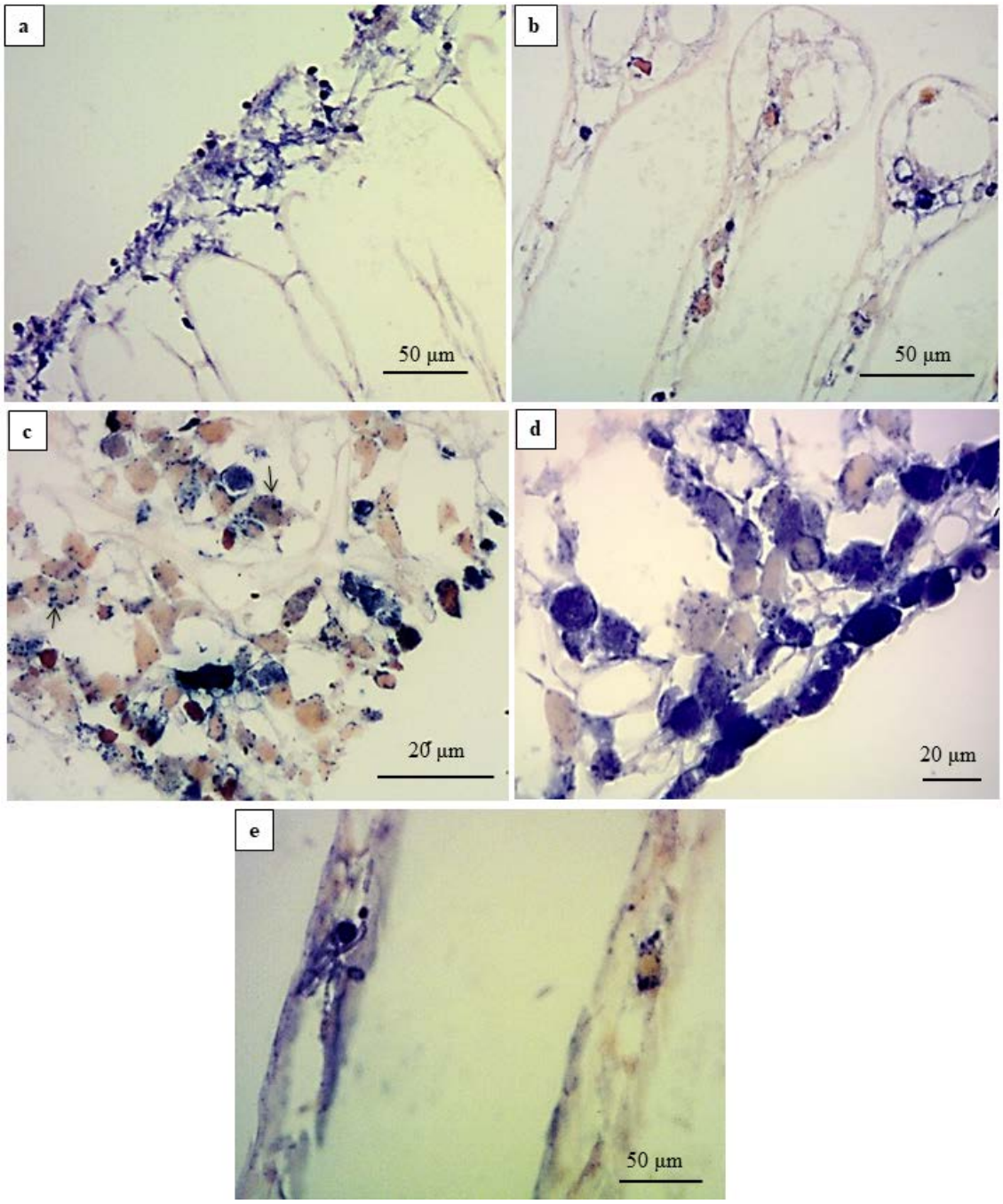

Figure 4.10: Carcinin localisation in post-moult gill section. (**a**) and (**b**): Low magnification of post-moult gill section, stained with AP carcinin secondary Ab. (**c**) and (**d**): High magnification images of post-moult gill sections, stained as above. (**e**): High magnification image of post-moult longitudinal section of gill lamellae, stained as above. Images (**a**), (**c**) and (**d**) show intense carcinin signal in cells located in central stem. High magnification image in (**d**) reveals that stained cells are likely to be podocytes in terms of shape and size. Though in some parts, podocytes were unstained as in (**c**), where granules positive for carcinin (arrows) are observed scattered around very close to podocytes, suggesting that carcinin may be delivered there via degranulating haemocytes, to bind to podocytes and thus stain them. Cells in the base

of the gill (**d**) and lamellae (**e**) appeared positive for carcinin, where some as in (**e**) release carcinin, which was observed to stain areas of gill wall.

4.3.3.2. Hepatopancreas, testis and heart

The hepatopancreas histology differed in the post-moult crab as signs of oedema resulting from water uptake were seen. Haemal spaces appeared enlarged and rather empty in some places. The epithelial cells of tubules lost their inclusions, with no apparent presence of calcium spherules (Figure 4.11, c). Carcinin staining was noticed in the capsule encasing the hepatopancreas and in the connective tissues associated with the haemal space (Figure 4.11, d), where the carcinin signal was intense in some parts (Figure 4.11, e). Apart from that, carcinin was only seen to stain haemocytes that were present in large numbers (Figure 4.11, c, d and e).

In the testes, the lobules appeared in the early development stage (Figure 4.12, a) due to the large nucleus of developing spermatocytes compared with previous observations in Sections (3.3.3.7) and (4.3.1.2), which indicated that the cells were mostly spermatogonia or primary spermatocytes. Little or no spermatozoa were noticed, however, mostly because the tissue was taken from a juvenile male. Little presence of carcinin was detected in parts of testicular capsule and connective tissues, while it looked faint or absent from most areas of the testis (Figure 4.12, b and c).

Heart tissue appeared similar to the normal adult organ (Figure 4.12, d), described in Section (3.3.3.4). Carcinin presence showed a similar pattern to that described earlier, namely staining in the haemocytes in the myocardium and epicardium areas (Figure 4.12 e).

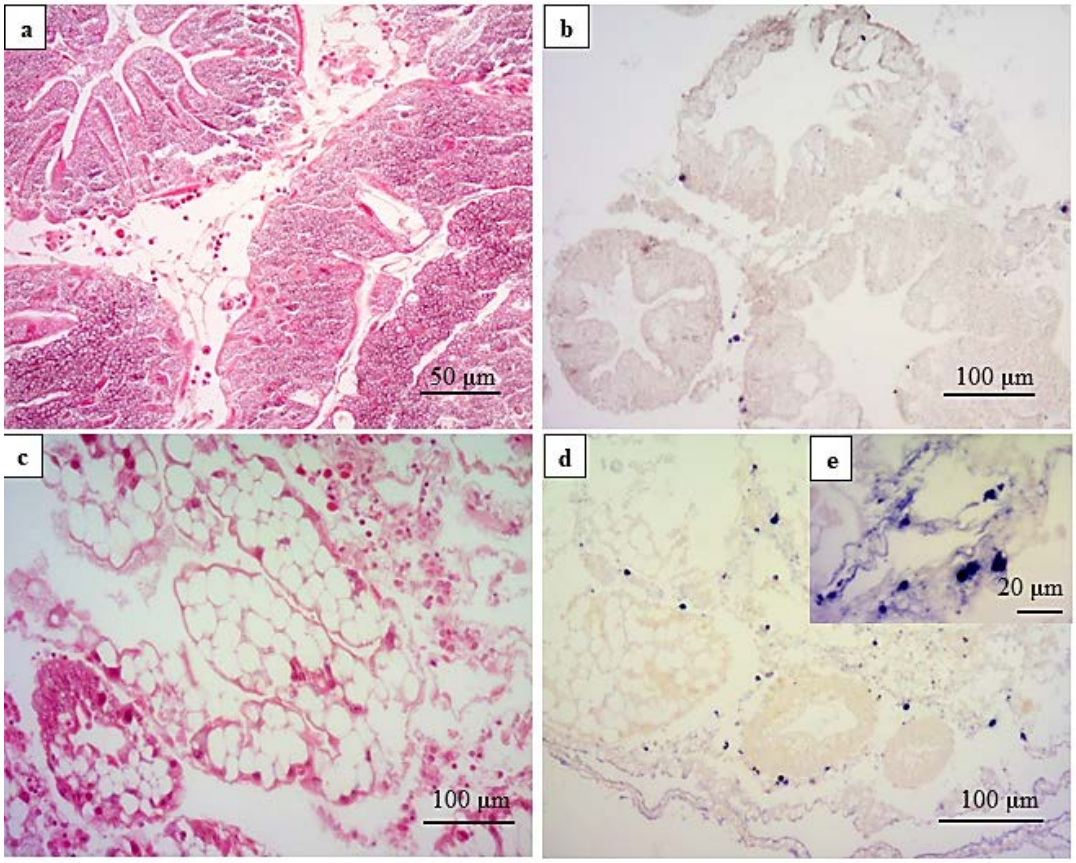

Figure 4.11: Histological features and carcinin localisation of post-moult crab hepatopancreas. (**a**) Inter-moult hepatopancreas sections stained with H & E. (**b**): IHC with AP-tagged secondary Ab. (**c**): Histological features of post-moult hepatopancreas stained with H & E. (**d**) and (**e**): Low and high magnification images of carcinin staining in post-moult hepatopancreas section. Image (**a**) shows thick epithelial cells present in tubules, while image (**b**) reveals carcinin in some haemocytes in the haemal space, with some staining in nearby connective tissues. The post moult image (**c**) reveals signs of oedema and water absorption. Tubule epithelial cells feature spaces and some tubules appear empty. Carcinin is present in the outer capsule (**d**), similarly to before (Chapter 3) but also appears to a large extent in connective tissues with signal intensity appearing stronger in contrast to inter-moult hepatopancreas sections, as highlighted in (**e**).

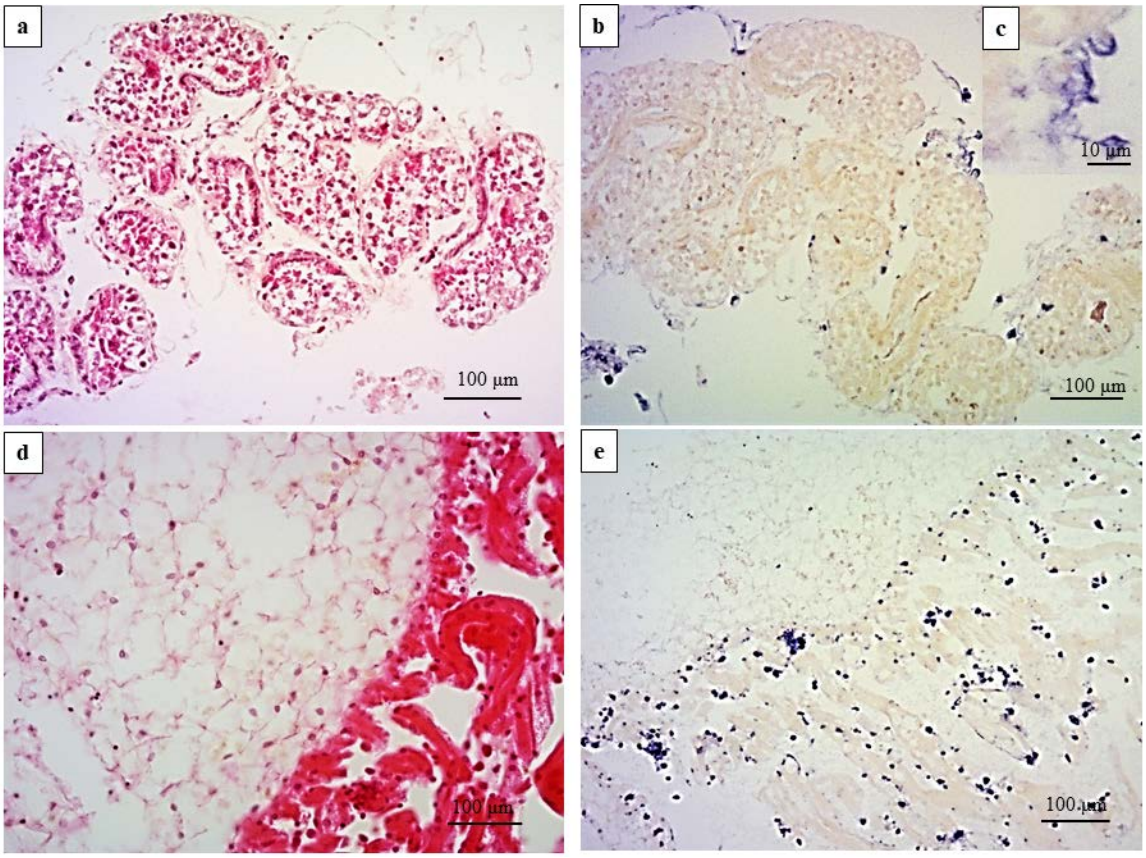

Figure 4.12: Histological features and carcinin localisation in testis and heart tissues of post-moult male crab. (**a-c**): Testicular sections stained with H & E (**a**) and AP tagged secondary Ab (**b** and **c**). (**d)** and **(e**): Post-moult animal heart sections stained with H & E (**d**) and carcinin Ab (**e**). Testicular structure features early development stage with spermatogonia/early spermatocytes in lobes (**a**). Carcinin presence appears less intense than the inter-moult stage seen in Chapter 3 (Fig. 3.16), as seen in (**b**). Few stained haemocytes are seen in haemal spaces, while carcinin is faint/absent in connective tissues. Only limited parts of the capsule are positive for carcinin (**c**). Histological structure of the post-moult heart (**d**) appears very similar to inter-moult animals. Many carcinin-positive haemocytes present (**e**), releasing and diffusing carcinin around the myocardium and epicardium, similarly to that observed in inter-moult animals.

4.4. Discussion

Carcinin localisation differed remarkably in a number of *C. maenas* tissues upon induced physiological changes. While eyestalk ablation stimulated ovarian development, carcinin signal showed a significant decrease there. Such changes were limited to female animals, without any significant alterations in testis morphology, histology or carcinin localisation post eyestalk abaltion. Carcinin exhibits significant deposition in the regenerating tissues of the eyestalk, and in the gill of the moulting juvenile animal, which pointed largely to its contributions in the processes occurring at these stages.

4.4.1. Gonad maturation

Removal of both eyestalks from the female crabs strongly induced vitellogenesis. However, removal of one eyestalk did not influence ovarian maturation to the same extent, judged by the size, GSI and histology of the unilateral ablated female ovaries, presumably because GIH would still be secreted from the remaining eyestalk in adequate amounts to regulate ovarian maturation. The present study could define three developmental stages of the ovary; proliferative/early developing as in the control, non-ablated females, late developing as in the unilaterally ablated females, and the fully mature, as seen in the bilaterally ablated females. This matched previous observations by Lyons *et al.* (2012), and Sherifian *et al.* (2015).

IHC images confirmed observations from Chapter 3 that carcinin is present in the developing ovary, and may be synthesised by ovarian tissues, but not consistently throughout development. In particular, carcinin seemed to be present in oocytes that undergo vitellogenesis, and absent from mature oocytes. The association between vitellogenesis and the synthesis of immune mediators was reported by Hall *et al. (*1995) and Avarre *et al.* (2003) as discussed in Chapter 3. It is possible that at early to late vitellogenesis stages, the oocytes undergo selective maturation, ensuring that only healthy oocytes progress to become mature ova, thus maximizing the production of healthy embryos. While infected or defective oocytes are being eliminated, carcinin might serve either as an antimicrobial agent to prevent infection spreading to other oocytes, or to mark redundant oocytes in order to facilitate their subsequent clearance.

The ablation of the eyestalk in male crabs did not induce dramatic changes. This could be explained by the contribution of the androgenic gland, which is located near the sperm duct (Padmanabhan and Raghavan, 2016). It is known that the effect of GIH on testis development in crustaceans is indirect, but relies on mediation from the sinus gland/androgenic gland/testis axis (Khalaila *et al.*, 2002). There were no apparent changes relating to carcinin signal at the microscopic level among the male groups. This lack of effect in males helps confirm that the considerable changes observed in ablated females were not due to haemolymph loss, otherwise, similar changes would be noticed in the male crabs too. However, since there was no notable change in testicular histology after eyestalk ablation, it was unlikely that major changes in carcinin signal would be noticed.

4.4.2. Tissue regeneration

Observation of the eyestalk injury site five days post-ablation confirmed wound healing had been occurring. The growing site looked dark, most likely from melanisation resulting from the action of the pro-PO system arising from the haemocytes. The strong signal for carcinin in the regenerating tissues indicated large quantities of the protein were present, which is in agreement with the presence of other crustin-like peptide transcripts at regenerating sites in limb (Durica *et al.*, 2006) and the olfactory organ (Stoss *et al.*, 2004).

As SGCs and GCs are the main source of carcinin, a high level of degranulation was assumed to occur at the injured site. It has been shown previously that haemocyte degranulation is essential in wound healing and limb regeneration, as these cells are the source of many important molecules that mediate healing and melanisation (Hopkins, 2001, Hopkins and Das, 2015). Certainly, after wound closure, large numbers of haemocytes migrate to injured sites where they act in important roles like encapsulation of contaminating bacteria, phagocytosis of necrotic tissues, and secretion of cytokine-like molecules that can help the healing process (Hopkins and Das, 2015). Lacking a cuticular barrier, the wound is highly exposed to microbial invasion especially in the first days of injury. Moreover, the secretion of the new cuticle was reported to start early after injury, as the cuticle can support the role of haemocytes in closing the wound (Hopkins and Das, 2015). If carcinin has chitin-binding ability, it may be assumed to attach and support the defence ability of the thin newly formed layer against invading bacteria, thus explaining its intense presence at the injured site (Bachere *et al.*, 2000).

4.4.3. Moulting effects

All crabs used in this experiment did not display any signs of moult five days post ablation, although, eyestalk ablation was shown to induce moulting in the juvenile lobster, *Homarus americanus*, by elevation of ecdysteroids levels in haemocylmph (Chang and Bruce, 1980). It might be possible, as indicated by Chang and Mykles (2011) that the (XO/SG) complex is not the only regulator of moulting, and that other factors, including physiological and environmental, have an influence too. While the aquarium where the crabs were kept is designed to resemble the ambient environment in terms of salinity and temperature, it cannot reproduce exactly many natural conditions. Photoperiod, crowding and stress caused by the surgical procedure might have prevented the initiation of ecdysis as a protection from what is an extreme physiological process (Bliss and Boyer, 1964).

This study revealed interesting results regarding carcinin localisation in post-moult juvenile crab tissues. In the gill, carcinin showed a distinct signal especially in the central stem, where large numbers of carcinin-positive cells were detected, together with noticeable degranulation and release of carcinin-positive granules. In terms of morphology and location, these cells were believed to be podocytes. However, it seems unlikely that these secrete carcinin themselves, as localisation in inter-moult gills only showed carcinin present in the haemocytes. Moreover, not all podocytes in the sections showed a positive carcinin signal, and non-stained ones could be seen with carcinin granules adjacent to them. This may indicate that carcinin released from haemocytes might associate with podocytes, perhaps acting in a protective function in a newly moulted animal.

Podocytes play different roles to haemocytes in the gill, such as participating in mineral absorption, detoxification and removal of foreign particles (Maina, 1998). Moreover, Doughtie and Rao (1981) reported increased phagocytic activity of these cells in the pre-moult, and more remarkably in the early post-moult grass shrimp, *Palaemonetes pugio*. It was assumed that they were responsible for elimination of macro and micro molecules from the haemolymph, and even some cell types, e.g. the epithelial cells in gill walls. Their increased prominence and association with carcinin in the newly moulted animal may therefore relate to clearance of redundant gill material.

Crustaceans at the moulting stage are prone to infection. High mortality rates were reported due to *Vibrio* infections during pre and post moult stages in the shrimps, *Penaeus stylirostris* (Le Moullac *et al.*, 1997), and *Litopenaeus vannamei* (Liu *et al* 2004), due to the absent of hard sclerotized cuticle (Liu *et al* 2004), and the weakening of haemocyte immunological functions like phenoloxidase activity (Le Moullac *et al.*, 1997, Liu *et al.*, 2004), and phagocytosis (Liu *et al.*, 2004). However, the high susceptibility to pathogens at this stage may drive the animal to higher dependency on other defence mechanisms to survive. The possible contribution of carcinin might be either to support defence reactions with its antibacterial effect, or as a mediator of other immunological processes. This could include phagocytosis conducted by podocytes, especially with a carcinin signal detected in association with a large number of these cells. These observations urged more research to be done to investigate how carcinin might affect phagocytosis and other immunological mechanisms, which will be revealed and discussed in the oncoming chapters.

In contrast, the distribution of carcinin in testicular tissues was less than that observed from inter-moult animals. Carcinin in the newly moulted male testis was restricted to a small part of the outer capsule and a small number of haemocytes in the haemal spaces. It was largely absent from connective tissues, and not close to spermatozoa, unlike its strong presence in the inter-moult testis. It is possible that the protective role of carcinin in the reproductive system is not essential during moulting as the male is not expected to mate then. It was reported that mating required strong adult males to compete for the soft-shelled female, thus mating could not accomplished by moulting males (Crothers, 1967).

The observations from this study, however, contradict previous research that reported a considerable deterioration in the main immunological effectors during moulting. For example, Kuballa *et al.* (2011) reported reduction in the gene expression of phenoloxidase activators during moult. Chiou *et al.* (2007) stated that expression of mo-penaeidin in haemocytes of inter-moult animals was significantly higher than the pre-moult of the tiger shrimp, *Penaeus monodon*. However, the first study was limited to investigating the Pro PO system, and its results cannot be generalized to judge other immune effectors on the same way. The second investigated the expression of penaeidin in the circulating haemecytes, which cannot be used to track its changes in

other tissues where it might be also expressed, and neglecting the fact the haemocytes can leave the circulation to other parts like the gills to mediate or support other processes occurring there.

Another important observation was the association of carcinin with parts of the gill wall, where chitin might be exposed due to shredding of the old cuticle. This, in addition to the extensive deposition of carcinin in the regenerating tissues of the eyestalk, indicates that carcinin is attracted to chitin-rich structures. This gives more importance to its vital role as a dynamic molecule participating in various physiological processes taking place throughout the lifespan. The oncoming chapters will shed more light on these contributions, by focusing on immune functions, including phagocytosis, which is one of the most important and conserved immune mechanisms responsible for animal survival.

As a conclusion, carcinin showed distinct presence in different physiological stages of the shore crab *C. maenas*, namely ovarian maturation, moulting and tissue regeneration. This strongly indicates vital roles in reproduction and tissue development and/or differentiation. These roles are consistent with some reported crustins and AMPs, as discussed above, but have never been reported to be influenced by the same peptide. Carcinin was the first crustin AMP to show a strong contribution to a wide range of essential physiological changes. This result does not only emphasize the vital multifunctional role of carcinin, but also indicates to the usefulness of using eyestalk ablation in investigating the association of crustins and other crustaceans AMPs in the key life stages of the animal.

Chapter 5

Functional Study 1: Role of Carcinin as an Anti-bacterial and Opsonic Peptide.

5.1. Introduction

It is crucial to investigate how carcinin can contribute to various immunological processes in *C. maenas*, especially after it showed a distinct presence in the tissues, clearly displaying a role in different reproductive stages (Suleiman *et al*., 2017). Further studies were carried out to elucidate its role in cellular immunity especially in the HCs, as carcinin appeared interestingly to associate with their cytoplasmic membrane.

So far, very little is known about the model by which carcinin can affect bacterial cells, or whether it is involved in other immunological responses. The multifunctionality of carcinin, as suggested by Brockton *et al.* (2008), remains poorly understood. Actually, no research has been conducted to further enlighten the effects of carcinin against bacteria following the publication of an unusual pattern of expression with bacterial challenge (Brockton *et al.*, 2008). Unexpectedly, in the Brockton *et al*. study, carcinin expression did not up-regulate after challenge with *Planococcus citreus*. Moreover, there was instead a decrease in carcinin expression 84 hours after bacterial injection. This was explained by the haematocytopenia, which occurred after depletion of haemocytes from the circulation. In particular, this migration would have been to the gills, to participate in the encapsulation process. This ambiguous pattern of expression led Smith *et al.* in 2008 to describe carcinin and other crustins as an "enigmatic proteins".

Together with the unique tissue distribution of carcinin, illustrated in the previous chapters, an important role is predicted either as a local immunological effector in tissues exposed to microbes, or as a mobile molecule that can be delivered by GCs and SGCs to the area of invasion. Therefore, to understand its roles more deeply, experiments were performed to test the antibacterial and opsonic properties of carcinin.
The aims of this chapter are:

1. To elucidate the interactions of carcinin with Gram-positive and Gram-negative marine bacteria.
2. To investigate the ability of carcinin to interact with or bind to eukaryotic cells
3. To investigate a possible role for carcinin as an opsonin.

5.2. Methods

5.2.1. Carcinin minimum inhibitory concentration (MIC)

As carcinin was first isolated on the basis of its ability to inhibit the growth of the Gram-positive marine bacterium, *Planococcus citreus* (NCIMB 1493) (Relf *et al*., 1999), this was used as one of the test micro-organisms in the present study. MIC procedure was adapted from Fernandez *et al*. (2002). *P. citreus* was cultured on plates of marine agar (Difco), made to the manufacturers' specifications at room temperature. A single colony was inoculated into sterile marine broth and left to grow to mid-log phase (17 hours) in a Thermo Scientific MaxQ^{TM} 3000 benchtop orbital Shaker (Paisley, UK) at room temperature. After growth, the concentration of bacteria was determined by calibrated optical density and washed three times in sterile filtered 3.2% NaCl, by centrifugation at 2000 x *g* for 10 minutes at 4°C. Subsequently, bacteria were re-suspended in sterile marine broth and their count was adjusted to 5×10^5 CFU mL^{-1} (*ca* 0.4 O.D). Serial dilutions of sterile purified carcinin (1.562, 3.125, 6.25, 12.5, 25, 50 nM) were made up with 50 mM sodium phosphate buffer (Chapter 2) with 3% added NaCl. These were adapted from the study by Relf *et al*. (1999), which indicated that the specified osmolarity and pH gave the maximum anti-bacterial efficacy of carcinin. Equal volumes (100 µL) of bacterial suspension were added per well of a 96-well multi-well plate, followed by adding 100 µL of each carcinin dilution in duplicate wells before incubation at room temperature for 24 hours on an orbital shaker (as above). Absorbance was read at 570 nm, and the MIC was defined as the lowest concentration of carcinin that reduced the growth of bacteria by 50%.

5.2.2. Carcinin binding to marine bacteria

The protocol conducted in this study to investigate carcinin capability to interact with bacterial cells was developed by my self. The ability of carcinin to bind to bacterial cells was tested against live and dead *P.citreus* and *Listonella anguillarum*. *Listonella anguillarium* (ATCC 43305), a Gram-negative member of the *Vibrionaceae* that is mildly pathogenic for crabs (Hauton *et al*., 1997). Whilst *L. anguillarum* is killed by haemocyte lysate supernatants from C. maenas (Chisholm and Smith, 1992), its growth is not adversely affected by purified carcinin (Relf *et al*., 1999). It was therefore used as a negative comparator. Both strains were inoculated, grown and washed as above, and after the final wash, the bacterial count was adjusted as before. Bacteria were killed

by incubation in a boiling water bath for 20 minutes. Live and dead bacteria were then stained with FITC, by incubation in 10 mL of 100 μg mL^{-1} FITC for one hour at 4 °C, followed by three washes with 3.2% sterile NaCl by centrifugation (as above). Where live bacteria were used, viability after FITC staining was checked by plating 100 μL of stained bacterial suspension on sterile marine agar plates. No effect on bacterial viability for either species was observed with FITC staining. Purified carcinin (100 μg. mL^{-1}) diluted in 3% NaCl was then added to live and dead FITC-stained bacterial suspensions and incubated for three hours. BSA at the same concentration as carcinin, and 50 mM sodium phosphate buffer with 3% NaCl were used as controls. After incubation, three washes with 3.2% NaCl (10 minutes, 2000 x *g*, 4 °C) were performed. The bacteria were then fixed with 4% PFA for 30 minutes. After three washes as before, 100 μL of bacteria were cyto-centrifuged onto sterile glass slides (56 x *g* for 10 minutes), using a Shandon 3 cytospin, as in Section (3.2.1). Cell permeabilization and ICC procedure were run as in Section (3.2.3) using 1:100 diluted carcinin specific polyclonal Ab, and undiluted Alexa Fluor® 594 goat anti-rabbit secondary Ab (Thermo Fisher Scientific, Paisley, UK). Slides were examined using a Leica (DMIRE2) TCS2 confocal microscope (Leica Microsystems, Milton Keynes, UK) and images were captured via Leica software and processed using Image J (National Institutes of Health, USA).

5.2.3. Scanning electron microscopy

Scanning electron microscopy (SEM) was performed according to the protocol described by Fischer *et al*. (2012) using a Quanta 3D FEG–FEI microscope (FEI UK). *P. citreus* and *L. anguillarum* were prepared as above. Volumes of 50 μL of the prepared live, unlabelled *P. citreus* or *L. anguillarum* suspensions were pipetted onto separate sterile round glass coverslips (diameter 7 mm) pre-coated with a thin carbon conductive layer and placed in wells of a 24-well plate. Bacteria were left to attach for 1 h at room temperature. For pre-coating the coverslips, four conductive carbon discs were first placed in a tube containing 1 mL of acetone and agitated for 2-3 minutes. After removing large particles, the sterile coverslips were immersed in the mixture and left for 2 minutes. The coated coverslips were then placed in 24-well plates where the bacterial suspensions were added. After gentle washing with sterile 3.2% NaCl the experimental bacteria were incubated with 250 or 500 μg mL^{-1} of carcinin in salt amended sodium phosphate buffer (SSPB) for three hours. Bacteria on control

coverslips were similarly treated but with bovine serum albumin (BSA), also at a concentration of 250 or 500 μg mL^{-1} in SSPB, or SSPB alone instead of carcinin. The bacteria were fixed immediately with 2.5% glutaraldehyde in 0.1M sodium cacodylate buffer overnight at 4 °C. After washing 3 × 5 minutes with 0.1M sodium cacodylate, dehydration of bacterial cells was carried out using an increasing graded series of ethanol (10%, 35%, 50%, 70%, 90%, 95%, 100%). This was followed by chemical critical point drying using hexamethyldisilazane (HMDS); the first incubation was 1:2 then 2:1 diluted in ethanol, and completed with absolute HMDS, each incubation for 20 minutes. Finally, the bacterial cells were left to dry before gold sputter coating using Polaron SC502 sputter coater (Quorum Technologies LTD, Kent, UK) for 45 second at 17.5 mA, and imaging.

5.2.4. Protease inhibitory assay

Anti-protease activity was investigated using a chromogenic substrate method adapted from Amparyup *et al*. (2008 b) and Suthianthong *et al*. (2012) testing four proteases; trypsin, α-chymotrypsin, subtilisin and elastase, and their chromogenic substrates, namely: N- Benzoyl-Phe-Val-Arg-*p* nitroanilide N Succinyl-Ala-Ala-Pro-Phe-*p* nitroanilide, N-Benzoyl-Phe-Val-Arg-*p* nitroanilide, and N-Succinyl-Ala-Ala-Ala-*p* nitroanilide, respectively. All enzymes and substrates were diluted with 50 mM Tris-HCl; pH 8. Proteases were prepared to obtain 1 nM solutions and protease:carcinin ratios from 1:1.562 up to 1:50 were used. Carcinin was prepared in serial dilutions as in MIC assay. Substrates of trypsin, α-chymotrypsin, subtilisin and elastase were used in concentration of 125, 17.5, 225, and 22.5 μM, respectively. Enzyme, substrate and carcinin solutions (50 μL of each) were added to each well of a 96-well plate. The ultimate concentrations for proteases were 0.33 nM, while for carcinin the final concentrations were 0.52, 1.04, 2.08, 4.16, 8.33 and 16.66 nM, and substrate concentrations were 41.66, 5.83, 75,and 7.5 μM for trypsin, α-chymotrypsin, subtilisin and elastase, respectively. The reaction was initiated by adding enzymes to the substrates and carcinin mixtures. Plates were incubated at 37 °C for 15 min after brief shaking, and the reactions were stopped by adding 50 μL of 50% acetic acid, diluted in 50 mM Tris-HCl buffer. Optical density of the released *p*-nitroaniline was read at 405 nm. Three replicas were performed for each enzyme-substrate reaction. The protease activity was considered as 100% in negative control wells (sodium phosphate buffer

with no carcinin). The remaining activity in all test wells was calculated as the following: (OD test well/OD Control well) x 100.

5.2.5. Interaction of carcinin with eukaryotic cells

Possible interactions with eukaryotic cells were assessed by incubating carcinin with: (i) isolated HCs from *C. maenas*, (ii) haemocytes from the blue mussel *Mytilus edulis* (another marine species from a different phylum) and (iii) a marine eukaryotic microorganism, the thraustochytrid, *Schizochytrium* species. A trypan blue dye exclusion viability test was used to evaluate cell survival after incubation with 250 and 500 µg mL^{-1} of carcinin. In addition, any haemolytic activity of carcinin was investigated by testing lysis of sheep erythrocytes following incubation with serial dilutions of carcinin for 30 minutes at 37 °C (Section 5.2.5.4).

5.2.5.1.Haemolymph sampling and cell culture preparation

C. maenas were collected and maintained as in Chapter 2 (Section 2.2.1). *M. edulis* were collected from Cramond (Edinburgh, Scotland) and kept under the same aquarium conditions as *C. maenas,* but were fed with the marine green alga, *Tetraselmis suecica*. Bleeding of *C. maenas* and separation of HCs was according to Söderhäll and Smith, (1983), as in Section (3.2.2). HCs were finally re-suspended in ML-15 medium made up in 0.4 M NaCl. *M. edulis* haemocytes were extracted according to the method of Wootton *et al.* (2003). Briefly, 0.2 ml of *M. edulis* haemolymph was withdrawn from the posterior adductor muscle using a syringe containing 0.3 mL of anticoagulant buffer (0.05 M Tris-HCl, 2% glucose, 2% NaCl, 0.5% EDTA; pH 7.6; Coles *et al*., 1995). The cell suspension was centrifuged at 500 x *g* for 5 minutes at 4 °C, before removing the supernatant and re-suspending cells in ML-15 medium, as above.

5.2.5.2.Thaustochytrid culture and preparation

A strain (NBRC 102616: *Schizochytrium* sp. (SEK345) (Genus *Schizochytrium*/ family Thraustochytriaceae) was cultured at 15 °C in sterile Mar Chiquita—brain heart broth (MC-BHB) medium (glucose 0.1%, peptone 0.05%, yeast extract 0.05%, monosodic glutamate 0.05%, gelatine hydrolysate 0.1%, corn steep liquor 0.05% v/v, brain heart infusion 1.75%, agar 2%, 50% sea water, 50% dH2O; pH 7 (Rosa *et al.*, 2011) with

help from Mr. Loris Fossier and advice from Dr. Jane Polglase (Heriot-Watt University). *Schizochytrium* cells (10 mL 25,000 cells. mL^{-1}) were sampled aseptically into a sterile falcon tube, then subjected to three washes in 3.2% NaCl by centrifugation (500 x *g*, 5 minutes, 4 °C). Subsequently, the supernatant was discarded and the cells were re-suspended in ML-15 medium.

5.2.5.3.Carcinin incubation

Three duplicates of 0.5 mL of each cell cultures (30 000 cells mL^{-1}) were placed in 24-well plates and incubated with 0.5 mL of carcinin (250 and 500 µg mL^{-1} in SSPB) , or BSA (same concentrations), and SSPB as controls. Plates were incubated for 3 hours at 10 °C. Cells were then washed by 3.2% NaCl three times, each for 5 minutes, and re-suspended finally in ML-15 medium, either for trypan blue viability check, or for cyto-centrifuge preparation. The experiments were repeated three times, and triplicate cultures set up per treatment, per time point.

5.2.5.4. Cyto-centrifuge preparations and ICC procedure

Cyto-centrifuge preparations protocol was run as in Robb *et al*. (2014). Cell suspensions (200 µL) of the haemocytes and thraustochytrids incubated with carcinin were cyto-centrifuged on sterile slides as in Chapter 3 (Section 3.2.1), at 7 x *g*, 3 minutes for *C. maenas* cells and *M. edulis* haemocytes and 22 x *g* for 8 minutes for *Schizochytrium*. All slides were then fixed immediately with 4% PFA in 0.2% NaCl for 30 minutes. After washing three times each for 5 minutes with PBS, cells were permeabilized and ICC procedure was run as in Chapter 3 (Section 3.2.3) using carcinin specific polyclonal Ab and secondary Ab mix (1:100 FITC-tagged goat anti-rabbit Ab + 5 µM DRAQ5 ^{TM} + 0.15 µM rhodamine phalloidin). Slides were mounted with Vectashield and examined using a Leica (DMIRE2) TCS2 confocal microscope as in Section 5.2.2.

5.2.5.5.Haemolysis assay

The haemolytic activity of carcinin was assessed using sheep erythrocytes, using a protocol adapted from Fernandez *et al*. (2002). Erythrocytes were obtained from Thermo Scientific^{TM} (Paisley, UK) by centrifugation at 500 x *g* for 10 minutes at 4°C,

then washed with PBS containing 0.9% NaCl three times. Erythrocytes were then sedimented by centrifuging at 800 x *g* for 10 minutes. Serial dilutions of carcinin were prepared as in Section (5.2.1), with BSA used as a negative control, and 0.1% Triton X-100 as a positive control. The test solutions (100 μL) were added to each well of a 96-well plate and packed erythrocytes were added to each dilution and the controls to obtain a final concentration of 5% erythrocytes. The plate was incubated at 37 °C for one hour. After incubation, visual examination was made to assess any haemolytic and/or agglutination activity.

5.2.6. Involvement of carcinin in haemocyte-bacterial interactions

The reaction of haemocytes upon challenge with carcinin-incubated Gram-positive and Gram-negative marine bacteria was addressed for HCs and SGCs, via a protocol adapted from Smith and Ratcliffe, (1978). *P. citreus* and *L. anguillarum* were cultured, harvested, stained with FITC and incubated with carcinin as in Section (5.2.2). After carcinin incubation, bacteria were washed with *Carcinus* saline (NaCl 0.57 M**,** KCl 0.012 M**,** CaCl2.6H2O 0.012 M**,** MgCl2.6H2O 0.026 M**,** Na2HPO4.12H2O 0.0005 M, Tris (hydroxymethyl) methylamine 0.05 M**,** 1 M HCl 42.5 ml**,** dH2O up to 1 litre, pH: 7.4; Smith and Ratcliffe, 1978). HCs and SGCs were separated as in Chapter 3 (Section 3.2.2), washed with *Carcinus* saline and adjusted to 25,000 cells mL^{-1}. Cell monolayers were prepared by adding 200 μL of cell suspension to sterile glass slides and leaving to attach for 30 minutes in moist chambers at room temperature. After three times gentle washing with *Carcinus* saline, cells were challenged with carcinin-incubated, FITC-stained bacterial suspensions over three hours in moist chambers at room temperature.

Subsequently, the slides were washed three times with *Carcinus* saline to remove unattached bacteria. Fluorescence from any remaining extracellular bacteria was quenched by incubating for five minutes with 200 μL of 0.1mg mL^{-1} trypan blue and slides were washed to remove unattached particles, followed by immediate fixing with 4% PFA plus 2% NaCl. Slides were mounted with Vectashield and examined the next day via fluorescence and phase contrast microscopy. Where phagocytosis was detected, the percentages of haemocytes having one or more intracellular particles were calculated (percentage phagocytosis), and the phagocytic index recorded, namely, the number of ingested bacteria per phagocytic haemocyte. A total of ten animals were used for each challenge, with three replicas examined for each animal. To address any

association of carcinin with ingested bacteria, the previous procedure was repeated and followed by ICC procedure. After the application of fixative, ICC was run as in Section (5.2.2). In other slides, to test whether challenging with bacteria caused cell death, DNA staining was carried out after fixation, by applying DAPI solution (Partec CyStain UV Ploidy, Münster, Germany) on fixed, permeabilized, monolayer preparations for 30 minutes. The slides were then washed three times with PBS, mounted with Vectashield and examined using a Zeiss fluorescence and phase contrast microscope as before.

5.2.7. Statistical analysis

Percentage phagocytosis and phagocytic indices are presented as mean ± standard deviation. Data were transformed into arc sine values before statistical testing. Percentage phagocytosis data were loaded into R Statistical Software and tested for homogeneity via the Bartlett test. One way ANOVA was run using the same software to assess the statistical significance of percentage phagocytosis between control and experimental groups, and significance was accepted at $P< 0.05$. Where ANOVA showed a statistically significant difference, a *post hoc* test for difference analysis was performed using Tukey HSD test. The difference between control and treatment groups in phagocytic index values was evaluated via the Chi-square test, considering $P<0.05$ as significant.

5.3.Results

5.3.1. Carcinin interaction with marine bacteria

Carcinin showed variations when binding to marine bacteria, differing according to both viability and Gram type (Figures 5.1, 5.2 and 5.3). When carcinin was added to live bacteria, it bound to the Gram-positive *P. citreus*, mostly in association with the periphery (Figure 5.1, b and c). In contrast, no carcinin signal was detected with the Gram-negative *L. anguillarum* (Figure 5.3, b). Interestingly, it was observed that in some instances carcinin caused major alterations in the cellular conformation of *P. citreus*, with some carcinin-positive cells appearing fainter than the intact cells, with some having lost their round shape. In addition, some bacterial cells looked damaged and disfigured (Figure 5.1, d, e and f). Occasionally, the carcinin signal was associated with some indistinct material, probably remains of burst bacterial cells (Figure 5.1 e and g). It was also observed that carcinin caused a moderate degree of aggregation of *P. citreus*, with noticeable co-localisation between carcinin and the bacterial cluster, evidenced by ICC image and co-localisation analysis scatter plot (Figure 5.1 h).

Adding carcinin to heat-killed bacteria did not result in the same binding pattern as with live ones. Carcinin bound to both types, without causing any apparent damage to the cellular structure of either. All *L. anguillarum* cells retained their rod-like shape, while *P. citreus* preserved their round firm structure, unlike the disfigured cells evident following carcinin incubation with live bacteria (Figures 5.2 and 5.3). However, carcinin was associated with visible bacterial aggregates of both heat-killed *P. citreus* (Figure 5.2, b and c) and *L. anguillarum* (Figure 5.3, e and f). Co-localization was also indicated by the percentage values from pixel analysis (Figures 5.2 d and 5.3 g). The bacterial cells appeared rather clumped and clustered, although, the appearance of individual cells appeared undisrupted in both Gram-positive and Gram-negative strains.

However, the current study could not define the MIC of carcinin against Gram-positive bacterial cells. *P. citreus* incubated with carcinin serial dilutions up to 50 nM did not show any decrease in bacterial growth, as detected by spectrophotometry Bacterial growth, as measured by optical density, recorded largely similar values between different concentrations of carcinin and controls.

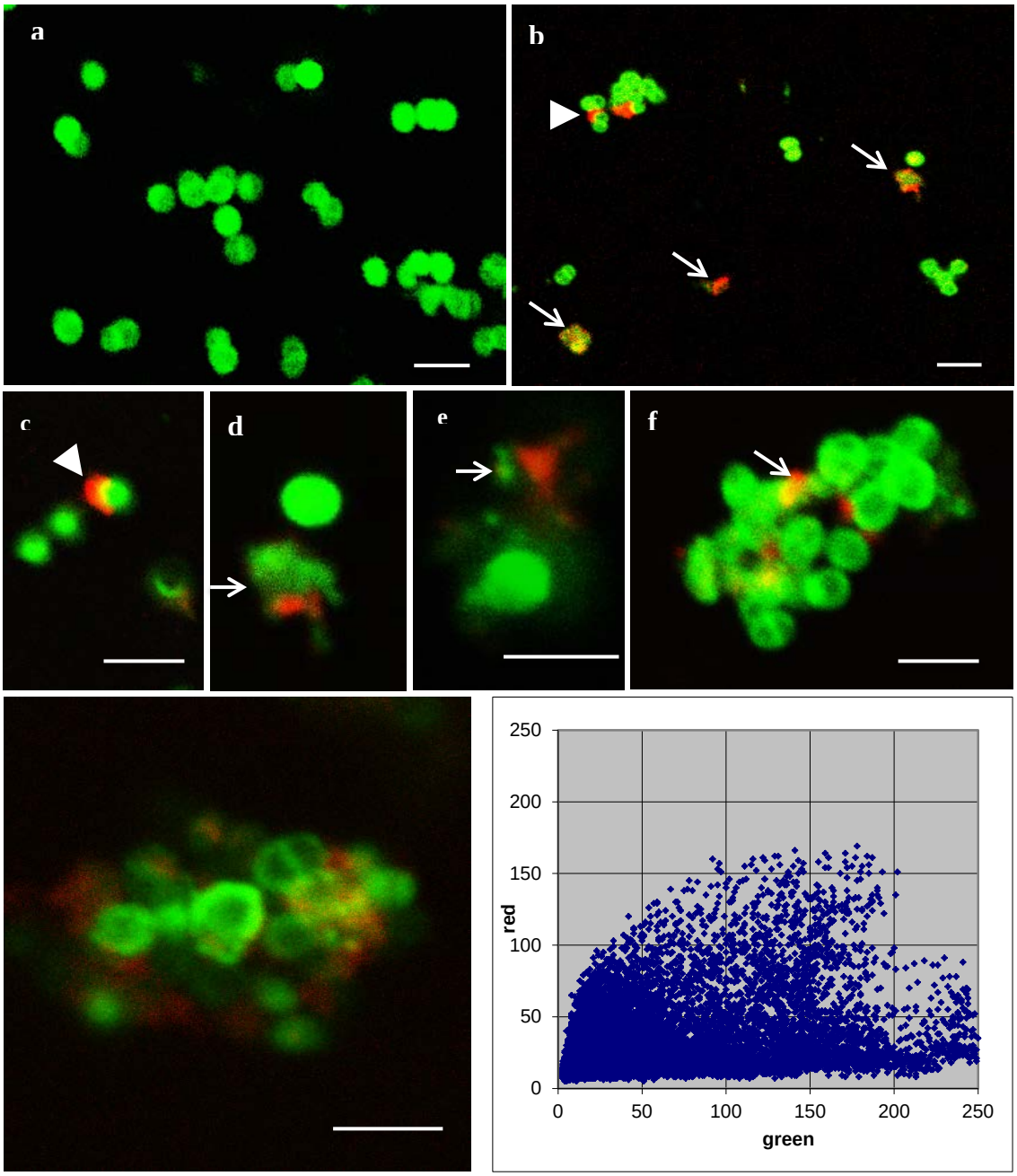

Total no. of pixels:	Green	Red	Yellow	Black	Total
	3620	765	1460	10539	16384
	61.9%	13.1%	25%		
Total pixel intensity:	G only	G in Y		R only	R in Y
	408414	173920		49428	125208
	70%	30%		28.3%	71.7%

Figure 5.1: Carcinin interaction with live *P. citreus* bacteria. (**a**): Cyto-centrifugation preparation of FITC-stained *P. citreus* incubated with BSA (representative control). (**b-g**): ICC images of cyto-centrifugation preparations of FITC-stained *P. citreus* after 3 hours incubation with carcinin, visualized with carcinin specific Ab and Alexa-fluor 594 tagged secondary Ab (red staining). (**h**): Scatter plot of distribution of red and green pixels of image (**g**). In the control image (**a**), bacterial cells appear intact, with normal coccus shape and defined circular edges. Carcinin interaction with the Gram-positive marine bacterium is either by sticking to the outer edge of the bacterial cells, without visible alteration of the shape of the bacteria (**b** and **c**, arrow heads), or by associating and altering bacterial cell shape, as some appear degraded (**b** and **d,** white arrows). In some instances, (**e**, white arrow), only small traces of bacterial debris are seen associated with carcinin. (**f**) and (**g**): Bacterial cells to which carcinin was seen to be bound were occasionally aggregated to a moderate degree (10-15 bacterial cells), in (**g**) the cluster is formed mainly by damaged bacterial cells. Scale bar: 2 μm. The scatter plot illustrates partial co-localisation (71%) between carcinin and bacterial cells, as indicated in the correspondent table.

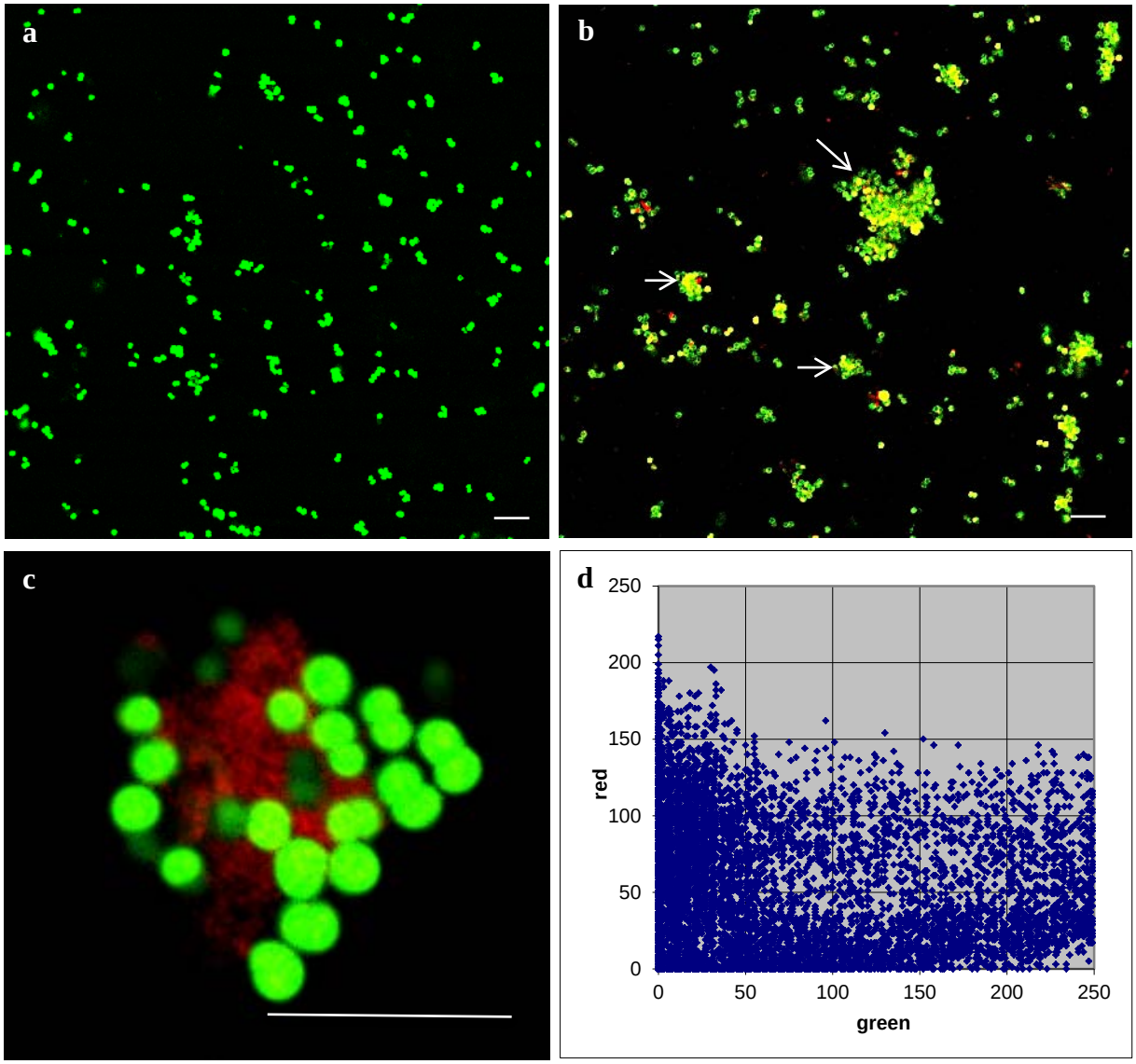

Total no. of pixels:	Green	Red	Yellow	Black	Total
	3580	3766	3963	5075	16384
	31.6%	33.3%	35.%		
Total pixel intensity:	G only	G in Y		R only	R in Y
	597760	862867		363451	321542
	40.9%	59.1%		53%	47%

Figure 5.2: Carcinin interaction with dead *P. citreus.* (**a**): Cyto-centrifugation preparations of heat-killed, FITC-stained *P. citreus* incubated with BSA (representative control). (**b**): Low magnification of cyto-centrifugation preparation of heat killed *P.citreus* incubated with carcinin for 3 hours and visualized as above. (**c**): High magnification of one bacterial cluster. (**d**): Analysis of pixel distribution in the image (**c**). The control image in (**a**) reveals normal looking cocci, occurring either alone or in pairs, heaps or tetrads. After three hours of carcinin incubation (**b**), dead stain of *P. citreus* binds carcinin, which causes bacterial cells to form large aggregates (20-70 bacterial cells) (white arrows). The high magnification image (**c**) reveals carcinin as red patches in-between and around bacterial cells, which appear intact with no changes on their normal configuration. Scale bar = 5 μm. Scatter plot reveals 47% of carcinin to co-localise with bacterial cells.

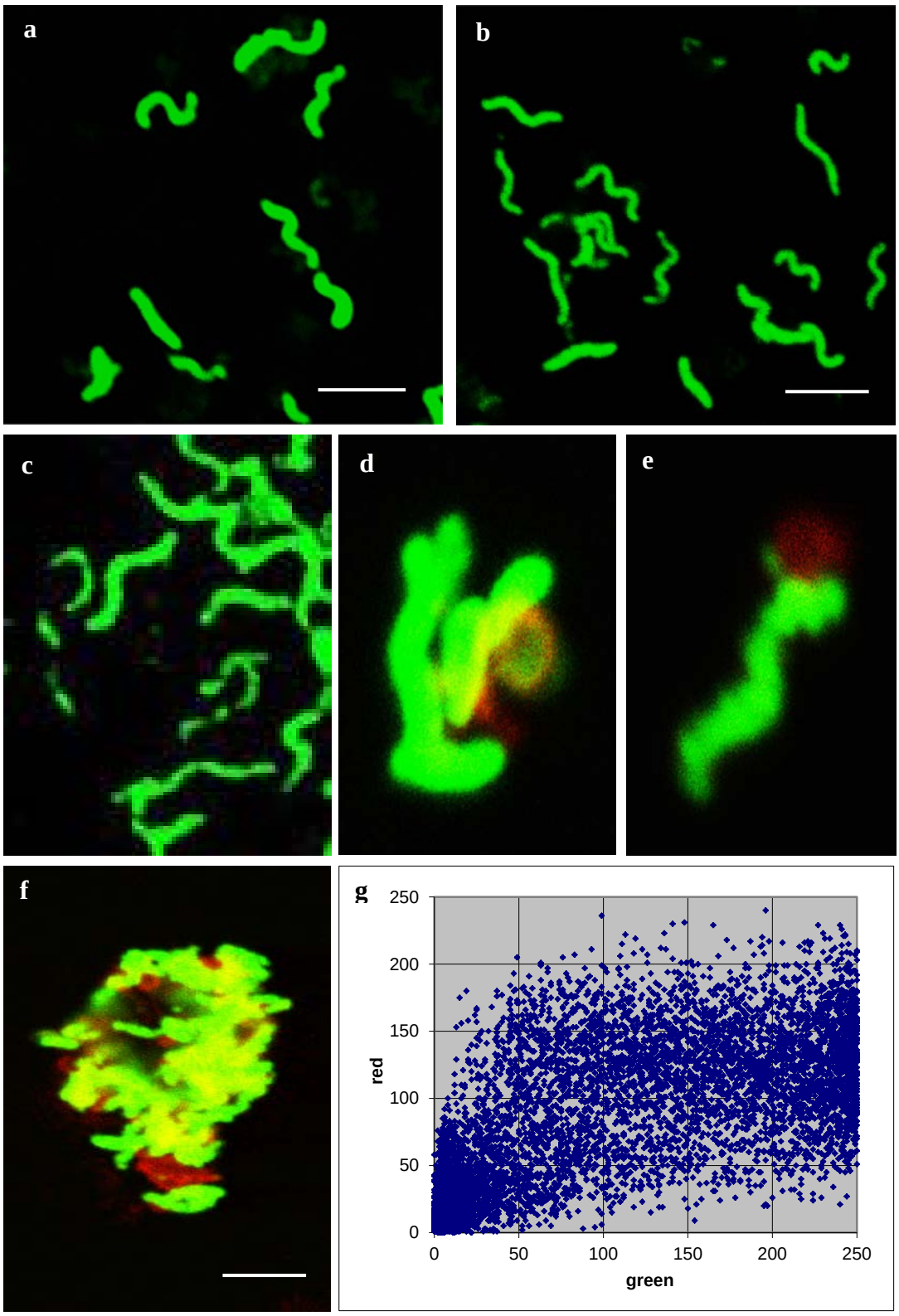

Tot no. of pixels:	Green	Red	Yellow	Black	Total
	398	624	5558	9804	16384
	6.05%	9.48%	84.47%		
Tot pixel intensity:	G only	G in Y		R only	R in Y
	43263	1055956		52571	704815
	3.94	96.06		6.94	93.06

Figure 5.3: Carcinin interaction with *Listonella anguillarum*. (**a**): Cyto-centrifugation preparation of live *L. anguillarum* stained with FITC, and incubated with BSA (as representative control). (**b**): The same live *L. anguillarum* preparation but incubated with carcinin. (**c)**: Heat-killed *L. anguillarum* incubated with BSA. (**d-f**): Heat-killed *L. anguillarum* incubated with carcinin. (**g**): Scatter plot analysis of pixel distribution in the overlay image (**f**). The control live *L. anguillarum* illustrate intact rod-like bacteria measuring *ca* 2-5 μm.length. Carcinin does not seem to affect live *L. anguillarum* as revealed in image (**b**). When incubated with the heat killed *L. anguillarum*, carcinin signal is observed in all the pictures (**d-f**), either surrounding bacterial cells, or co-localising. In some preparations, as in (**f**), carcinin seems to cause bacterial cell aggregation. Scale bar = 2 μm. Pixel distribution plot in (**g**) reveals high degree of co-localisation, where 93% of carcinin in the image co-localises with FITC-stained bacteria.

5.3.2. Scanning electron microscopy

Carcinin was confirmed by SEM to remarkably affect *P. citreus* cell walls, with greater degrees of damage seen at the higher carcinin concentration. The walls of *P. citreus* seemed perforated in some regions (Figure 5.4, c and d), suggesting that the visible pore-like structures had been formed following incubation with carcinin. Other cells seemed to be either swollen (Figure 5.4, e) with wrinkles (Figure 5.4, f) or flattened (Figure 5.4, g), or even totally destroyed (collapsed) as seen in (Figure 5.4, h). Such changes were not observed after incubation of Gram-positive bacterial cells with BSA (Figure 5.4, a) or sodium phosphate buffer (Figure 5.4), since these controls showed bacteria with smooth, intact cell walls. Carcinin incubation with Gram-negative bacterial cells did not appear to cause any similar morphological changes, as *L. anguillarum* cells were mostly seen intact (Figure 5.4, h, i and j).

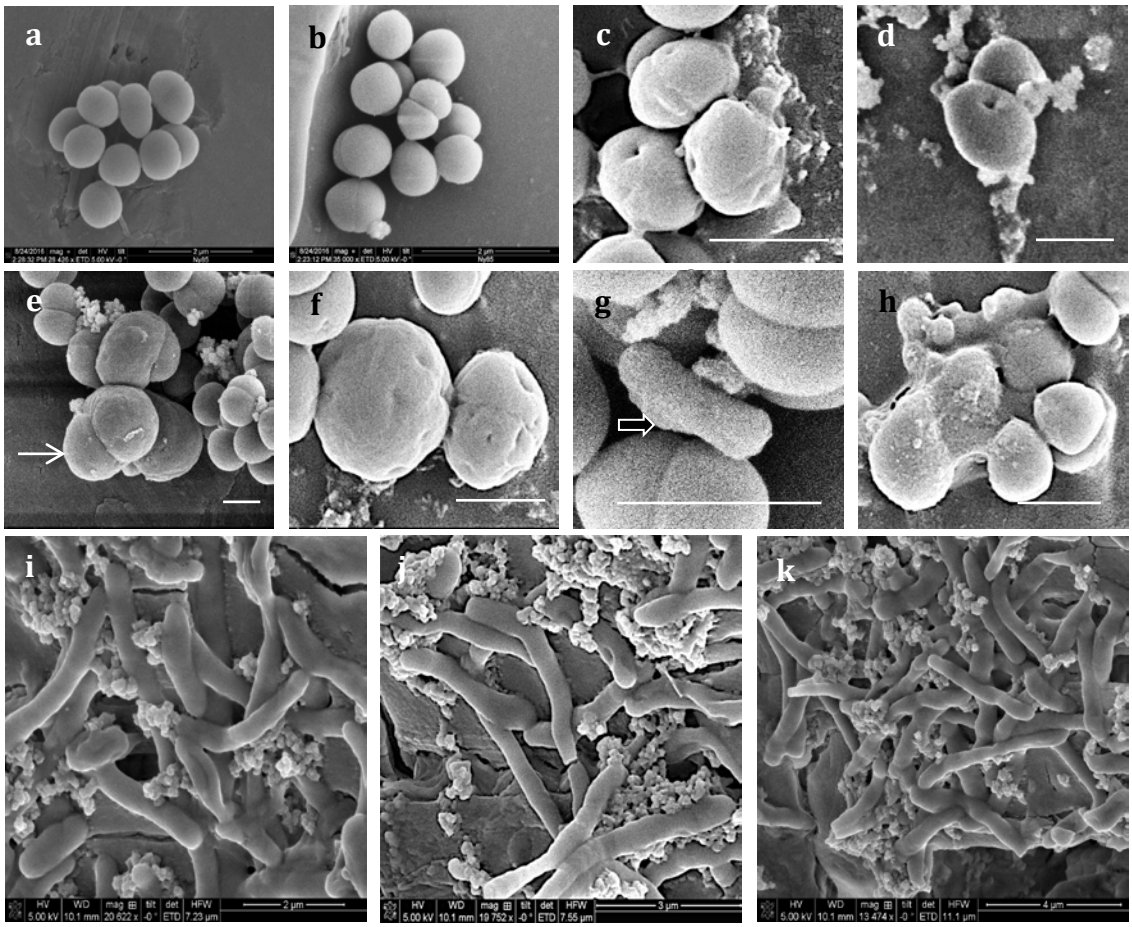

Figure 5.4: Scanning electron microscopy images of carcinin interaction with bacterial cells. (**a**) and (**b**): The normal, intact *P. citreus* after incubation with SSPB or BSA, respectively as control, showing round cells with smooth surface. (**c-h**): *P. citreus* cells after incubation with carcinin, revealing extensive signs of damage. Pores were seen on the bacterial wall as in (**c**) and (**d**), or with wrinkled surface as in (**c**) and (**f**), while in other areas, the bacterial cells appeared enlarged as in (**e**), white arrow), or shrunken as in (**g**, black arrow) indicating that carcinin is affecting permeabilization of bacterial envelope. Sometimes bacterial cells were seen largely disfigured with debris related to burst cells, as in (**h**). Scale bar = 1 μm. (**i-k**): Images of *L. anguillarum*, where (**i**) and (**j**) are bacterial cells incubated with SSPB or BSA, respectively. (**k**): *L. anguillarum* incubated with carcinin. No differences are observed between the controls and carcinin incubated cells, with no visible damage to the Gram-negative bacteria.

5.3.3. Protease inhibitory effect

The protease inhibitory assay revealed no obvious inhibitory effect of carcinin against the tested proteases within the used concentrations. In all experimental and control wells, catalytic activity was detected for all four proteases, evidenced by developing of purple colour resulted from proteolysis and release of *p*-nitroaniline (Figure 5.5).

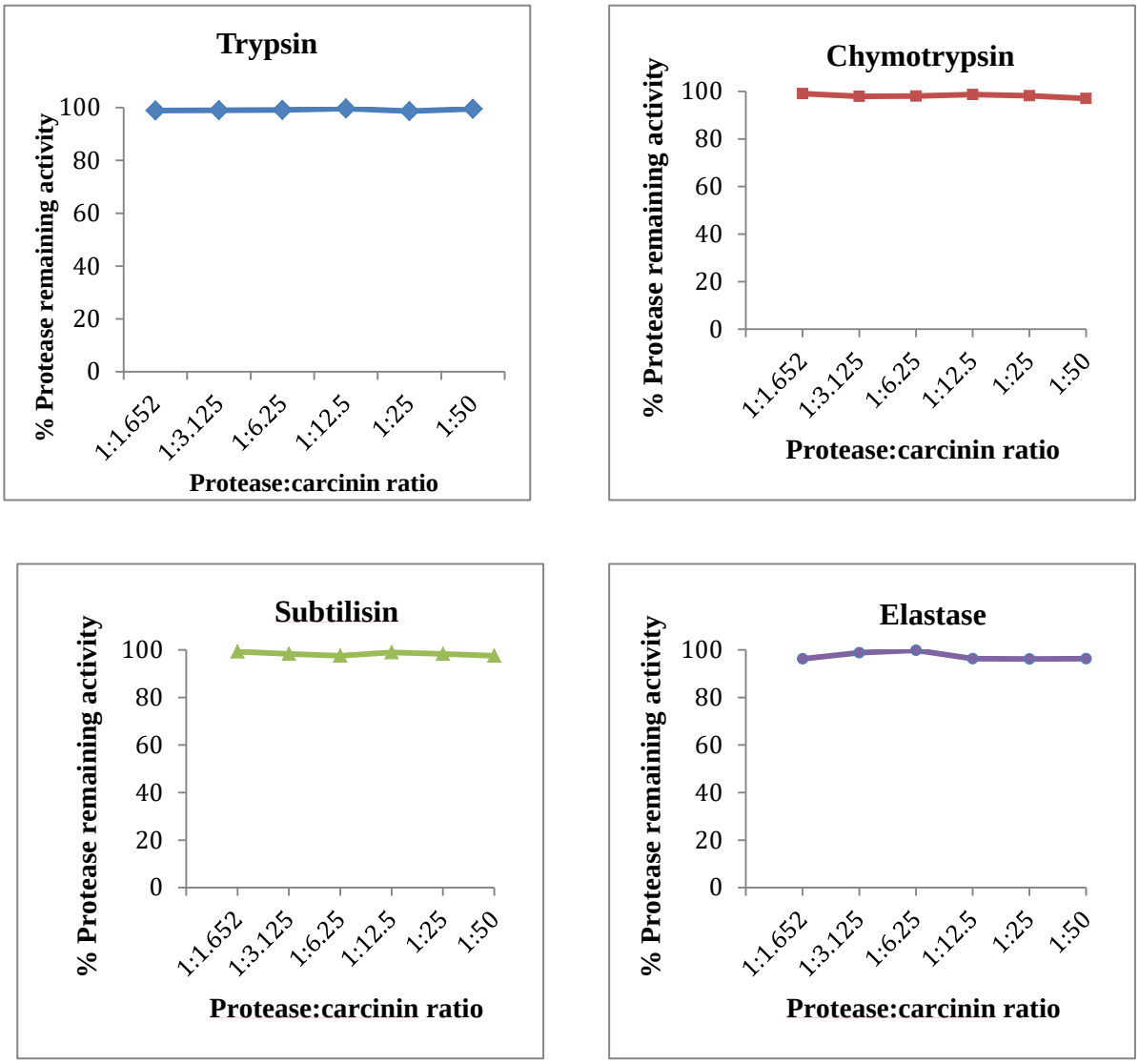

Figure 5.5: Effect of carcinin on the enzymatic activity of four proteases: trypsin, chymotrypsin, subtilisin and elastase. Charts represent percentages of proteases remaining activity against protease:carcinin ratio. For all tested proteases, carcinin does not seem to affect catalytic activity, evidenced by 100% remaining activity of enzymes after incubation with different carcinin concentrations.

5.3.4. Carcinin interaction with eukaryotic cells

Incubation of separated HCs with added carcinin for 3 hours *in vitro* resulted in an increase in the number of carcinin-positive HCs, where around 30% showed a green rim of FITC signal around their periphery (Figure 5.6, a-d). This agrees with results in Chapter 3 that carcinin is mainly associated with the HC cytoplasmic membrane, with little co-localisation with F-actin. This suggests that even if carcinin binds to or diffuse inside HCs, it remains at the peripheral region very close to the cytoplasmic membrane. Addition of carcinin did not affect cell viability, as the trypan blue test confirmed that all HCs were still viable after 3 hours incubation with 250 µg of carcinin. Carcinin showed no interaction with other eukaryotic cells used in this experiment, as it was not detected in association with either *M. edulis* haemocytes, nor thraustochytrid cells. Again, no effect was observed on cell viability. These findings indicated that carcinin binding capability is specific to *C. maenas* HCs, and supported our previous finding *in vivo*, that carcinin might be secreted from granular and SGCs of the shore crab, to bind to HCs, as ICC images showed.

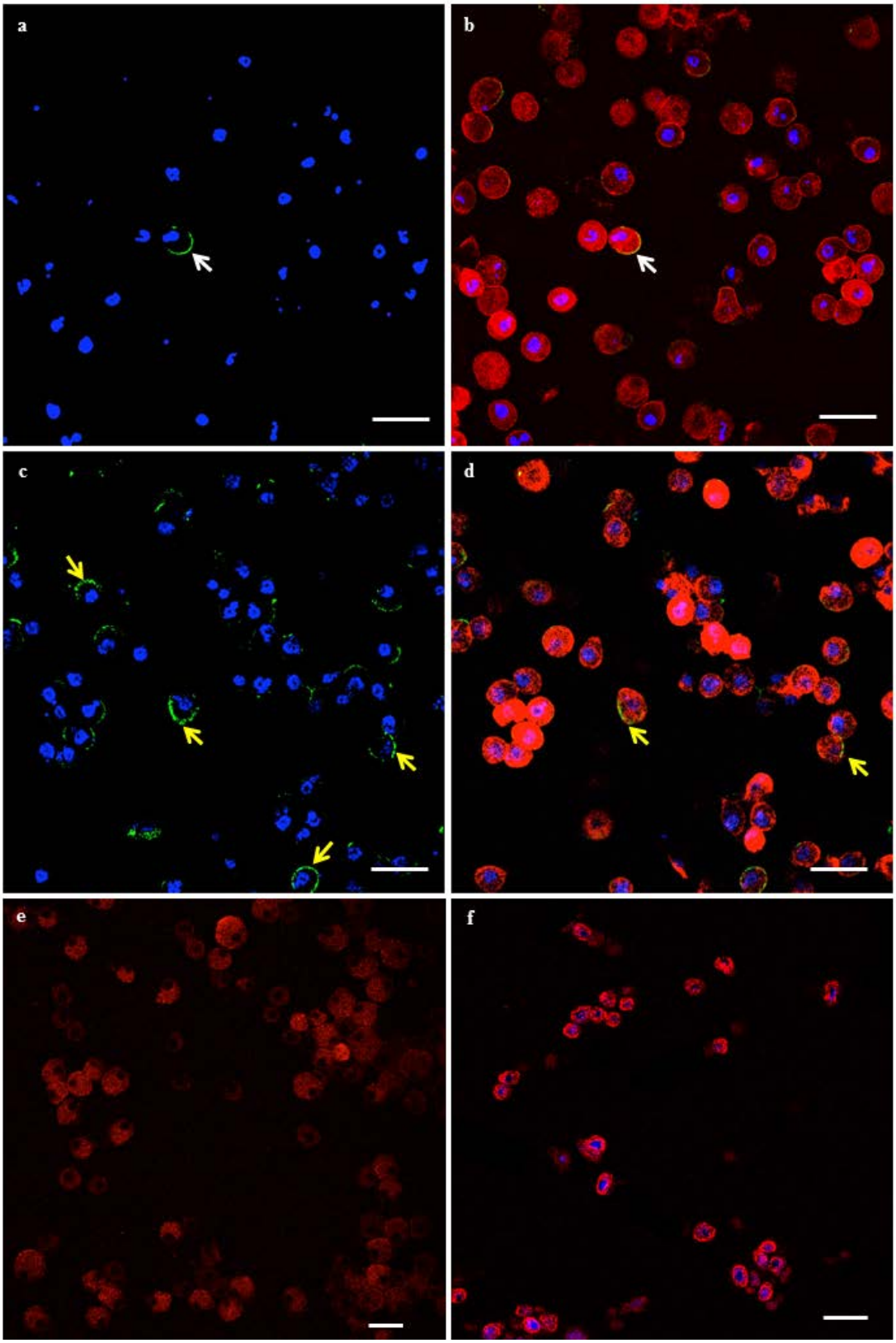

Figure 5.6: Carcinin binding ability to eukaryotic cells. (**a**-**d**): Images of HC populations from *C. maenas*. (**a**) and (**c**) are the overlay images of carcinin, detected by goat-anti rabbit Ab labelled with FITC (green) and DRAQ5™ for DNA staining (blue

pseudo-colour). (**b**) and (**d**) are overlay images as before, in addition to rhodamine phalloidin for f-actin (red). In BSA-incubated populations (**a**) and (**b**), the white arrow indicates where one HC appears to have carcinin associated with the cytoplasmic membrane. In carcinin-incubated population (**c**) and (**d**), the HCs population shows more carcinin-positive HCs (yellow arrows) confirming its ability to associate with their cytoplasmic membrane. Carcinin is not detected to bind to any of the other eukaryotic cells used in the experiment, neither in any of the isolated haemocytes from *M. edulis* (**e**), nor *Schizochytrium* cells (**f**), both incubated with the same amount of carcinin, and stained as above. Scale bar = 20 μm.

5.3.5. Role of carcinin in haemocyte-bacteria interactions

HCs exhibited phagocytosis when challenged with bacteria (Figure 5.7), whereas SGCs reacted via cell degranulation (Figure 5.8). Most of the challenged SGCs burst upon bacterial challenge, and cell debris was observed widely in addition to clumps of bacterial cells in both experimental (carcinin-treated) and control (BSA and buffer treated) bacterial groups (Figure 5.8, e and f). It is possible that bacterial clumping might result from secretion of internal carcinin from the SGCs upon degranulation.

For HCs, however, differences were observed between challenges with the Gram-positive bacteria *P.citreus* or Gram-negative bacteria *L. anguillarum*. While the role of carcinin was not discernible when HCs were incubated with *L. anguillarum*, a notable effect could be seen when HCs were challenged with carcinin-incubated *P. citreus*. ANOVA showed statistically significant differences in percentage phagocytosis between carcinin-treated and BSA-treated bacteria ($P< 0.0001$) and carcinin-treated and buffer-treated bacteria ($P< 0.0001$), while there was no significant difference between the two control groups ($P=1$) (Figure 5.9). Moreover, bacterial cells incubated with carcinin showed significantly higher phagocytic indices in terms of the number of ingested bacteria. The ingestion of three or more bacterial cells was at the maximum values when bacteria were pre-incubated with carcinin (Figure 5.10) (Figure 5.7, a), (Figure 5.8, a-d). Phagocytic indices were significantly higher when *P. citreus* had been incubated with carcinin ($P=0.042$ and $P=0.008$, when comparing with the BSA and buffer-incubated groups, respectively). In particular, the difference was more remarkable when comparing the percentages of HCs ingesting more than three bacteria

(*P*= 0.002 when comparing carcinin and BSA treated groups, and *P*=0.00018 when comparing the carcinin and the buffer only treated groups). There was no statistically significant difference between the two control groups (Figure 5.10). Carcinin was further confirmed to have an important role when it was observed to be stuck to some bacterial cells inside the cytoplasm of a phagocytic HC (Figure 5.8, d).

When challenged with *L. anguillarum* after three hours, many HCs died (Figure 5.11). Dead cells could be seen where the nuclei remained intact (Figure 5.11, b), showing signs of apoptotic-like irregular nuclear shape (Figure 5.11, c), but ETotic cells were also present, as indicated by the expulsion of extracellular chromatin (Figure 5.11, d). Rarely, intact HCs were found with ingested *L. anguillarum* as in (Figure 5.11, a). No noticeable effect of carcinin was observed following challenge with *L. anguillarum*, as all interactions observed were seen in both experimental and control groups.

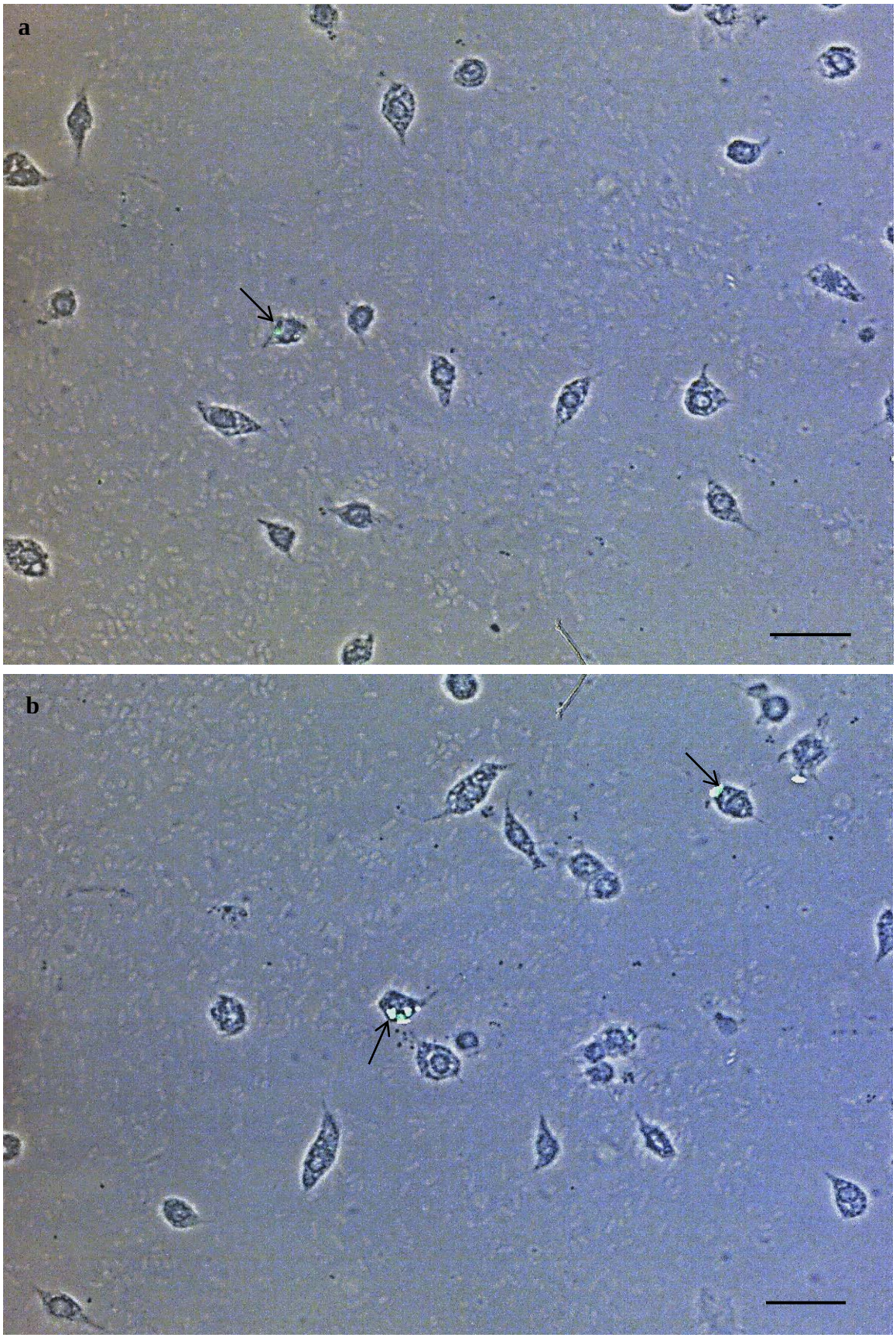

Figure 5.7: Carcinin role in phagocytosis. (**a**): Low magnification control image reveals HCs challenged with BSA-incubated, FITC-stained *P. citreus.* (**b**): Low magnification of HCs challenged with carcinin-incubated, FITC stained *P. citreus*.

Although phagocytosis is detectable in the control image, most phagocytic HCs have only ingested one particle, as indicated by the arrow. More HCs are seen to ingest bacterial cells (arrows) after incubation with carcinin (**b**), with some having more than two bacterial cells in their cytoplasmic inclusions (arrows). Scale bar = 15 μm

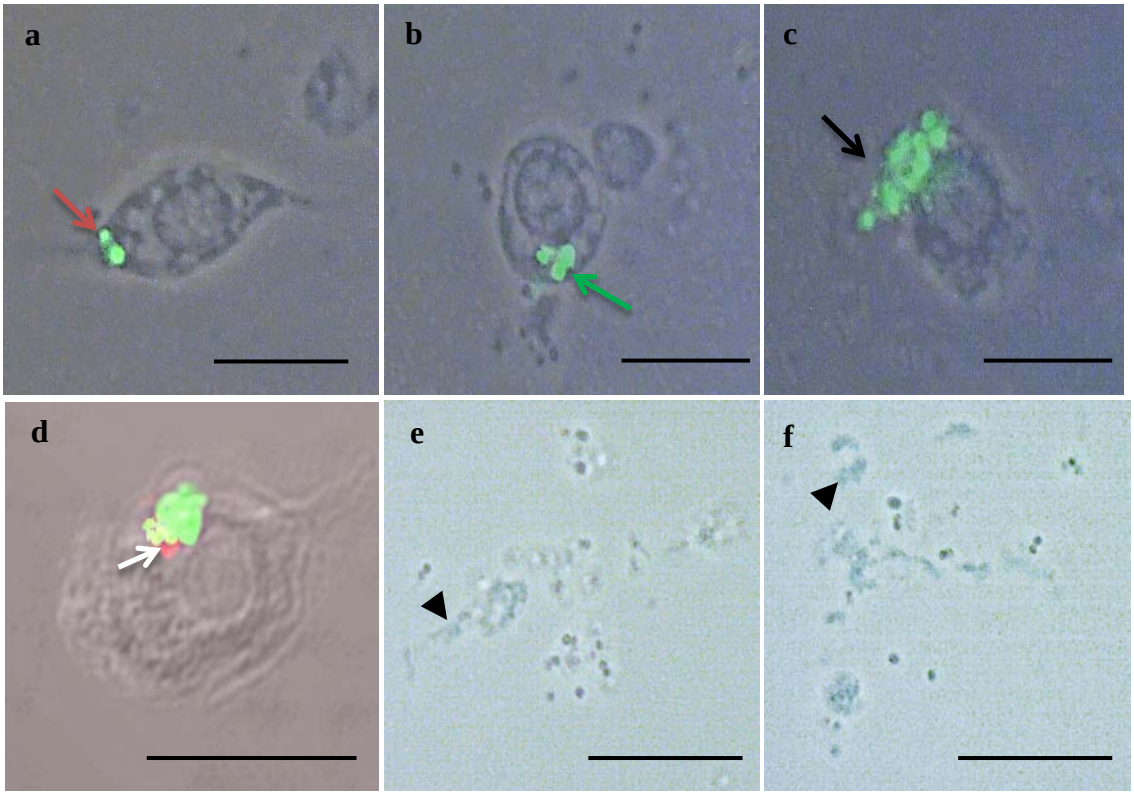

Figure 5.8: Carcinin role in response of HCs and SGcs upon challenge with *P. citreus.* (**a**), (**b**), (**c**) and (**d**): High magnification of some phagocytic HCs challenged with carcinin incubated *P. citreus*. (**e**) and (**f**): SGCs challenged with *P. citreus*, incubated with carcinin (**e**) or BSA (**f**). The HCs are seen to engulf two (**a,** red arrow), three (**b,** green arrow) and even more (**c,** black arrow) of the *P. citreus* cells, with (**d**) ICC image showing carcinin, indicated by Alexa fluor 594-tagged goat-anti-rabbit secondary Ab (red colour), where it is associated with some bacterial cells inside the cytoplasm of the HC (white arrow). No differences are observed between the two SGCs images, with bacterial challenge apparently causing degranulation of SGCs, as only cell debris (arrow heads) is seen associated with *P. citreus* cells. Scale bar = 15 μm.

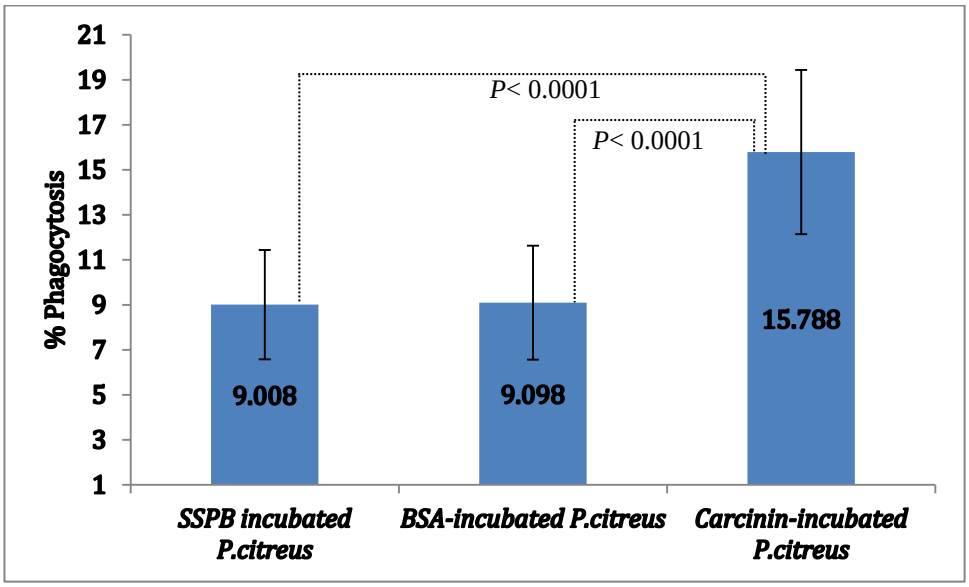

Figure 5.9: Percentage phagocytosis of isolated HCs of *C. maenas*. Mean of percentage phagocytosis for the ten animals used in this study is illustrated on each group column (N = 10).

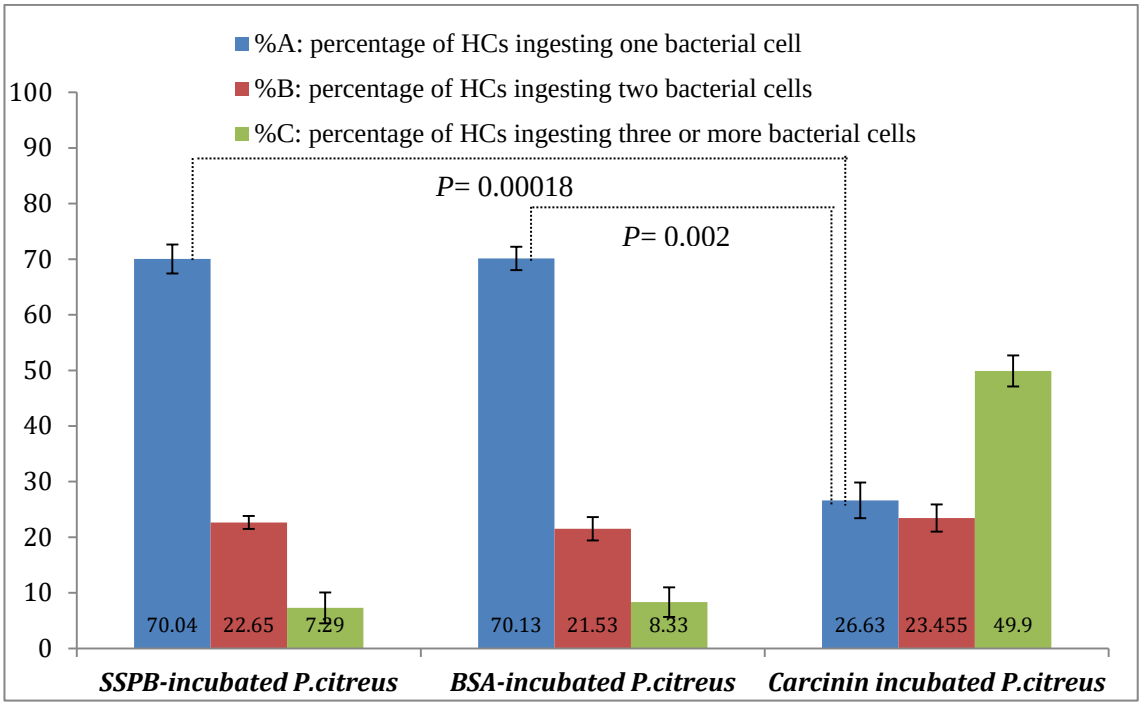

Figure 5.10: Phagocytic indices, showing percentage of haemocytes ingesting one, two or three-plus bacteria per haemocyte. An average of 49.9±2.78% of HCs are able to ingest three and more bacterial cells when incubated with carcinin, which is significantly higher than the percentage of the buffer and BSA incubated control groups whereas the majority (*ca*. 70%) of phagocytic HCs of the control groups are able to engulf one bacterial cell compared with 26.63 ± 3.2 % in carcinin-treated group.

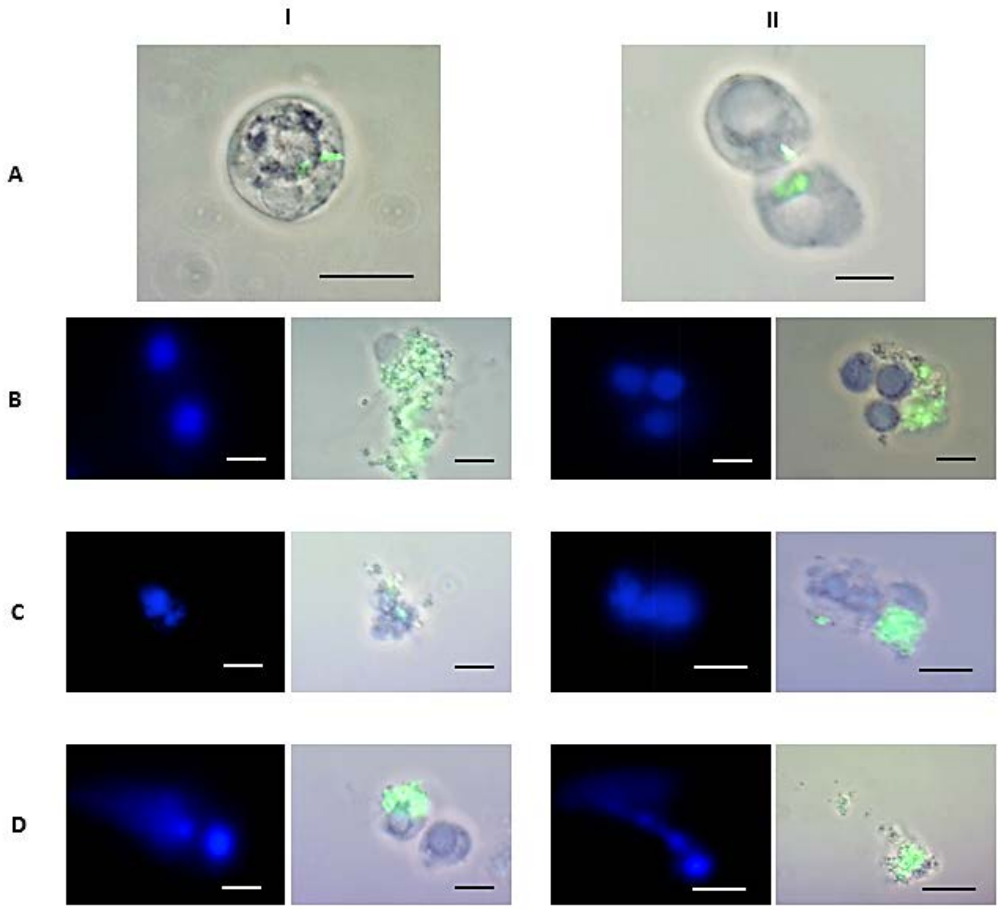

Figure 5.11: Response of HCs upon challenge with *L. anguillarum*. HCs have been challenged with FITC-stained bacteria, which have been incubated with either BSA (representative control) (**i**), or carcinin (**ii**). DNA is visualised by staining with DAPI (blue staining). Corresponding overlay images of FITC-stained bacteria (green) taken by fluorescence microscopy and HCs taken by phase contrast microscopy are shown as well. Phagocytosis was only rarely observed (**a**), where bacterial cells are seen inside a phagocytic HC. Mostly, *L. anguillarum* caused HC lysis (**b**), leaving the nucleus (DAPI) as a normal shape, and cellular debris. Some features of apoptosis are detected as well, as in (**c**), where cells look irregular, with nuclear fragmentation. ETotic cells appeared occasionally (**d**), where chromatin is extruded to the extracellular domain where it can trap bacteria. No significant differences were observed between the control (**i**) and carcinin (**ii**) groups, as both showed similar types of HC responses. Scale bar = 10 μm.

5.4. Discussion

AMPs are widely expressed molecules present in immune cells and epithelial surfaces. Many have been reported as multifunctional molecules (Lai and Gallo, 2009), acting through multiple mechanisms, and beyond their direct antimicrobial effect. As revealed in previous chapters, carcinin was found not only in haemocytes, but also in some key organs as an extracellular molecule. This raised the question whether carcinin acts via other mechanisms rather than the directly antimicrobial properties originally discovered by Relf *et al.* (1999) and Brockton *et al.* (2008). In order to consider this further, it was important to investigate how carcinin interacts with bacterial cells, and how it might influence bacterial activity.

5.4.1. Anti-bacterial mechanisms of action

In the current study, carcinin showed specific activity against the live Gram-positive bacteria *P. citreus* , but not the Gram-negative bacteria *L. anguillarum*. This was expected from Relf *et al*. (1999), who reported carcinin to have selective antibacterial effects against Gram-positive bacteria. In its interaction, carcinin was expected to act according to the classic pattern of most AMPs: i) attracted to the anionic groups of the lipid bilayer of the bacterial cell wall due to its positive net charge, ii) attachment to the bacterial surface, which was confirmed in the present study by ICC images where carcinin was seen associated with *P. citreus* outer membrane, then iii) damage the structure of Gram-positive bacteria as seen from ICC images, where some cells incubated with carcinin were seen largely disorganised.

However, this was not enough to define precisely carcinin's mechanism of action, as AMPs can either affect bacterial envelope permeabilization, or penetrate inside the bacterial cells to suppress certain cellular processes (Brogden, 2005). The SEM results confirmed that carcinin-incubated *P. citreus* had pores on the cellular wall. The present study also showed that carcinin did not bind or induce any visible effects on live Gram-negative bacteria, although some binding was observed with dead Gram-negative cells. This could reflect the fact that *L. anguillarum* is a mild pathogen for several marine and aquatic organisms, including *C. maenas*, and thus live cells may have effective evasion strategies of host defences. The binding to dead cells might be due to protein denaturation caused by the high temperature of heat-killing, in which the tertiary

structure of certain proteins structured in the outer membrane might be altered, revealing the lipo-bilayered groups and allowing the interaction of carcinin.

In fact, most crustin AMPs have been recorded to be active primarily against Gram-positive bacteria (reviewed by Smith and Dyrynda 2015). The inability of the AMP to affect the Gram-negative bacteria can be explained by the presence of the outer membrane, an extra layer characteristic of Gram-negative bacteria, which can protect against AMPs. This outer membrane contains phospholipids on its inner leaflet, while the outer leaflet is composed of glycolipids, like the lipopolysaccharides, in addition to proteins. The outer membrane represents the main obstacle that obscures the negatively charged lipids and thus prevents binding of AMPs (Silhavy *et al*., 2010). While the majority of crustin studies have been directed at studying gene expression variations following immune challenge, few of them have aimed to establish the mechanism of action by which these antimicrobials interact with their targets. Examples of those where pore formation model were reported include the recombinant crustin *Pm*7, which created pores in the bacterial wall of *V. harveyi* (Krusong *et al.,* 2012). In addition, the recombinant s*Mj*Cru1 from *M. japonicus* caused membrane perforations in *Klebsiella pneumoniae* cells (Liu *et al.,* 2015).

Carcinin did not show any anti-protease effect against the four proteases tested, in peptide concentrations up to 50 nM. This might indicate that its ability to damage the bacterial cells depends mainly on pore formation ability. It is still possible, however, that carcinin might affect other proteases or only have an inhibitory effect at higher concentrations, which this study unfortunately could not address. Crustins reported to have protease inhibitory effects were mostly type III, e.g. the recombinant *Fc*-SWD from the fleshy prawn *F. chinensis* against subtilisin and protein K (Jia *et al.,* 2008), the recombinant *Pc*SWD from red swamp crayfish, *Procambarus clarkia* against the secretory proteases from *B. subtilis* and *P. aeruginosa* (Du *et al.,* 2010), and the crustin from *P. monodon* with both antimicrobial and protease inhibitory roles (Amparyup *et al* 2008 b). Anti-protease activities were also detected from type IV crustins, for example *Mj*-DWD from the shrimp *M. japonicas,* (Chen *et al.,* 2008), and the recombinant *Fc*-DWD from the Chinese white shrimp, *F. chinensis,* both against the secretory proteases from *B. subtilis*, and for the latter, *P. aeruginosa* as well (Du *et al.,* 2009) (reviewed by Smith 2011; Smith and Dyrynda 2015).

The previous studies showed how the ability of microbial killing can relate to the protease inhibitory effect. This however, contradicts the assumption made by Ota *et al*. (2002) that protease inhibition requires the presence of a methionine residue next to the second cysteine in the 4DSC domain, which actually crustins lack. Nevertheless, another assumption might arise that crustin antiproteases are mostly Type III and IV, as this was also presumed by Smith and Dyrynda (2015), especially since a study on two Type I crustins (*Pl*crustin1 and *Pl*crustin2) from the crayfish *Pacifastacus leniusculus* revealed them not to have this property (Donpudsa *et al*., 2010).

Unfortunately, this study could not detect an MIC for carcinin against *P. citreus*, despite the same concentrations causing visible damage to the bacteria under SEM, as discussed above. This might suggest that with the concentrations used in this study, the effect of carcinin was still reversible, which means it was not enough to overwhelm the repairing mechanisms by which the bacterial cells try to amend the harmful effects of the AMP. However, the reported MIC values for different crustins are notably higher than other AMPs. For example, the crustin Cru*Ha*1 from the spider crab, *H. araneus* has a MIC of 1.6 µM against the Gram-positive bacterium *Corynebacterium glutamicum* (Sperstad *et al.*, 2009 a). This is the lowest value of MIC published amongst all crustins and it is still 30 times higher than the maximum carcinin concentration tested in the current study.

5.4.2. Opsonic activity

The idea of carcinin having an opsonic effect emerged after the protein showed an ability to bind bacteria and cause bacterial agglutination. In addition, carcinin was detected in specific association with the HC membrane. This was confirmed by *in vitro* experiments, where added carcinin bound to higher numbers of HCs than the control. In addition, carcinin is selective in its binding to HCs among the other eukaryotic ones tested in this study. It is believed though that carcinin becomes associated with HCs in a different manner to bacterial cells. In fact, eukaryotic cells lack a surface negative charge, since lipid bilayers are hidden in the inner side of the cytoplasmic membrane, while the exposed side has no charge (Silhavy *et al*., 2010). This presumably explains why carcinin did not cause noticeable cytotoxic effects on the eukaryotic cells tested in the present study, since these surface neutral phospholipids prevent carcinin from being integrated into cellular membrane structure electrostatically.

It was then confirmed that the phagocytic ability of HCs could indeed be enhanced when challenged with Gram-positive bacteria that been incubated with carcinin. Percentage phagocytosis increased significantly, also, higher phagocytic indices were recorded when bacteria was treated with carcinin. This provided strong evidence that carcinin enhances phagocytosis in HCs, possibly in a similar way to the complement C3b in mammals (Hartung and Hadding, 1983), by attracting bacterial cells electrostatically, and at the same time binding to a receptor on HCs, thus connecting the HCs with their targets and facilitating phagocytosis.

A number of crustacean AMPs' have been reported to bind bacterial cells, e.g. Krusong *et al.* (2012), Du *et al.* (2015), Jiang *et al.* (2015) and Liu *et al.* (2015). Though, the ability to enhance phagocytosis was only studied by Jiang *et al.* (2015) and Liu *et al*. (2015). Liu *et al*. (2015) stated that a type I crustin (*Mj*Cru I-1) was able to elevate phagocytosis by haemocytes of *M. japonicus*. The method used, however, could be criticized in many ways. The study used indirect *in vivo* method to test opsonization ability of the tested crustin, merely enumerating recovered bacteria from cells. Therefore they did not score uptake by the haemocytes directly. Another thing was that Liu *et al*. (2015) employed whole haemolymph samples rather than separated haemocyte populations, overlooking the fact that not all haemocyte types are phagocytic, and neglecting the possible secretion of molecules from non-phagocytic haemocytes that might interact with the crustin activity. It also did not consider the loss of haemocytes upon injection, which might occur as a result of encapsulation, chromatin extracellular trap formation, degranulation, or even other cell death pathways. Finally, it utilized recombinant rather than the native protein, which might not display equal efficacy.

The fact that carcinin attached to both viable and dead bacterial cells showed its efficacy in the clearance process. It is possible that carcinin is able to bind dead bacteria more easily than live ones, allowing them to be removed from haemolymph. It is important to argue as well that carcinin binding to HCs could relate to two possibilities, namely: (i): carcinin might enhance HC phagocytosis, as discussed above, or (ii): carcinin might bind to HCs showing signs of degradation, to mediate the recognition of other phagocytic HCs in order to remove them from circulation. This

property of carcinin being able to bind HCs and whether it can facilitate defective cell elimination is quite novel, as none of the opsonic crustins, mentioned above nor other WFDC proteins, were reported to act in a similar manner.

This finding is consistent with observations of carcinin localisation in the previous chapters. A signal for carcinin was detected in some ovarian oocytes, where carcinin is believed to bind to degenerating oocytes to aid their removal (Chapter 2). In addition, carcinin was found to bind to a proportion of gill podocytes, for which the roles of phagocytosis, removal of different dead tissues, and control of osmolarity of the crab during moulting was reported by Doughtie and Rao (1981) and Maina (1998).

In conclusion, carcinin was shown to be a highly effective element of the crab immune system, acting by a dual mode. Firstly, carcinin shows the ability to destroy bacterial cells by forming pores on the Gram-positive bacterium *P. citreus*, and being one of the few crustins studied by SEM. Secondly, it has an opsonic effect, as it can cause bacterial cell agglutination and enhance the ability of HCs to phagocytose. While this had been suggested previously by researchers, the present study is the first to confirm this by a direct method. Furthermore, carcinin was revealed to effectively bind dead Gram-positive and Gram-negative bacterial cells, which strongly points to its opsonic effect being of great importance for bacterial clearance by the animal. This binding ability is unique, to date, among crustins, and is key to understanding crustins' mechanism of action. In addition, this study specifically revealed carcinin capability to bind both live and dead bacterial strains, suggesting that even if carcinin does not destroy certain bacterial strains by a direct bactericidal effect, it still has a significant role in their elimination, thus contributing effectively to cell-mediated immune responses.

Chapter 6

Functional Study 2: Association of Carcinin with Invertebrate Extracellular Phagocyte Traps (InEPTs)

6.1. Introduction

It has been shown that ETosis serves effectively in conquering microbial infections in mammals, whether bacterial (Brinkmann *et al*., 2004), fungal like *Candida albicans* (Urban *et al*., 2006) and *Aspergillus nidulans* (Bianchi *et al*., 2011), parasites such as *Toxoplasma gondii* (Abi Abdallah *et al*., 2012), or even against the human immunodeficiency virus -1 (HIV-1) (Saitoh *et al*., 2012). The antimicrobial activity of extracellular traps is thought to arise from a combination of factors: (i) the presence of antimicrobial molecules, most importantly histones, in addition to defensins and calgranulin (Urban *et al*., 2009; Bianchi *et al*., 2011); (ii) the enhanced activity of these effectors due to the high local concentration (Brinkmann *et al*., 2004), and (iii) the presence of enzymes such as elastase (Brinkmann *et al*., 2004), cathepsin G and proteinase 3 (Averhoff et al., 2008) that cleave and inactivate virulence factors of some bacteria. As yet, no research has been published investigating the role of different AMPs in InEPTs formation (Figure 6.1; von Köckritz-Blickwede and Nizet, 2009).

In the last chapter, carcinin was shown to cause pores in the bacterial wall of *P. citreus*. Moreover, carcinin showed a distinct property to stick to bacterial cells, and aid the phagocytic capability of hyaline cells. The cationic property of carcinin triggered the question about its ability to stick to negatively charged nucleic acid (DNA), and if so, a possible association with InEPTs. As an antibacterial protein produced and stored in the cytoplasmic haemocyte granules, it is also considered possible that carcinin might be localized on the extracellular traps, since in mammalian ETosis, nuclear and cytoplasmic components integrate and decorate the chromatin thus participating in bacterial killing.

It is conceivable that carcinin may have other involvements with extracellular trap formation besides that of bactericidal activity. SLPI is a WFDC-domain-containing protein stored in cytoplasmic granules of human neutrophils, which serves both as an antibacterial molecule and a protease inhibitor (Sallenave *et al*., 1997), (Chapter 1). Recently, another role of SLPI was reported in ETosis due to its neutrophil elastase inhibitory property (Zabieglo *et al*., 2015). Since elastase is a key enzyme in chromatin decondensation (Brinkmann *et al*., 2004), SLPI can counteract this mechanism by its anti-elastase activity (Zabieglo *et al*., 2015) and thus have a controlling effect on extracellular trap formation. Given that both SLPI and carcinin are WFDC-domain

containing proteins, this raises the question of whether carcinin might also influence InEPT formation.

This chapter aims to:

1. Investigate the localisation of carcinin on InEPTs stimulated in HCs and SGCs *in vitro*.
2. Examine carcinin association with InEPTs formed via encapsulation *in vivo.*

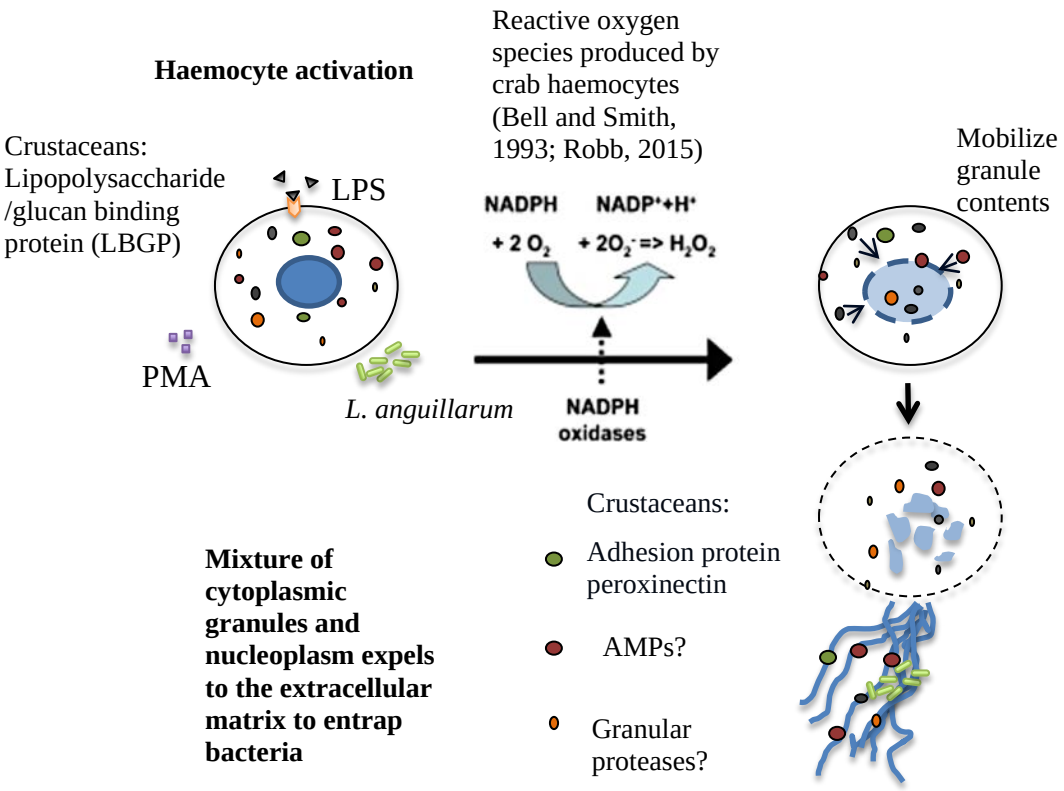

Figure 6.1: Systematic diagram of extracellular trap formation. Similarly to mammalian cells, extracellular chromatin can be induced in crab HCs and SGs by different stimuli, such as PMA, LPS and the bacterium *L. anguillarum*, resulting in formation of reactive oxygen species (ROS) by nicotinamide adenine dinucleotide phosphate (NADPH) oxidase. This triggers events in the stimulated cell characterized by disruption of the nuclear membrane allowing mixing of nuclear and cytoplasmic granule contents. The later disruption of the cytoplasmic membrane causes discharging of extracellular chromatin associated granular peptides, probably AMPs, which can entrap and kill microbes. '?' indicates aspects currently unknown in crustaceans. Adapted from von Köckritz-Blickwede and Nizet, (2009).

6.2. Methods

6.2.1. Effect of carcinin on viability of *C. maenas* haemocytes

Preliminary experiments were performed to detect any cytotoxic or apoptotic effects of carcinin on whole haemocytes. Haemolymph was extracted as in Chapter 2 (Section 2.2.3.1) and the haemocytes were washed and re-suspended, as in Chapter 3 (Section 3.2.1). Haemocyte samples (1 mL containing 6×10^5 cells) were placed in each well of a 24-well plate. Carcinin (1.562, 3.125, 6.25, 12.5, 25, 50 nM) was added to the haemocytes, with BSA substituted for carcinin in control wells. After 1, 3 or 24 hour incubation periods, cells were removed from the wells, and viability was checked immediately with the trypan blue exclusion test. After gentle washing by centrifugation (3 times, at 500 × *g* for 5 min, at 4 °C) and re-suspension in 3.2% NaCl, cyto-centrifugation preparations were prepared as in Chapter 3 (Section 3.2.1). Haemocytes were fixed and permeabilised with methanol for 1 min, followed by staining with Diff-Quik™ (VWR, Leicestershire, UK) red for 1.5 min, then Diff-Quik blue for 1 min. Slides were mounted with DePeX mountant and examined using a Zeiss Axiophot bright field microscope to visualize any apoptotic haemocytes (Robb, 2015).

6.2.2. Localisation of Carcinin on InEPTs, *in vitro*

To generate InEPTs *in vitro*, HCs and SGCs were separated as in Chapter 3 (Section 3.2.2). Cell viability after re-suspension in ML-15 medium was measured using the trypan blue exclusion test (as above) and the cell count adjusted to 25,000 cells mL^{-1}. Sterile round cover slips (7 mm, Agar Scientific) were placed in each well of a 24-well plate. Separated HCs and SGCs (1 mL volume) were seeded gently on top of the cover slips and allowed to attach for 1 hour at 10° C, as in Section 5.2.5.1. ETosis was stimulated by incubation with 1 nM PMA (diluted in ML-15 medium) for either 16 or 24 hours at 10° C. Controls substituted ML-15 instead of PMA. After incubation, the experiment was either stopped by removing the media and immediately fixing with 4% PFA in PBS with added NaCl (both HCs and SGCs), or continued by incubation with 1 mL of carcinin (100 µg mL^{-1} solution) for three hours at 10 $^{\circ}$C, before being washed with 3.2% NaCl and fixed, as above (HCs only). The further incubation with carcinin following PMA stimulation was done to replicate the likely degranulation of SGCs and GCs *in vivo*, which would thus release carcinin extracellularly.

For all treatments, the cells were subjected to ICC procedure as in Chapter 3 (Section 3.2.3**)**, using carcinin specific primary Ab. The secondary Ab mix consisted of FITC-tagged goat anti-rabbit secondary Ab against carcinin and and DRAQ5^{TM} for DNA staining.

Due to the fragile nature of the extracellular traps, extremely careful manipulation and washing was required throughout the procedure, therefore this was modified from before (Chapter 3, Section 3.2.3). A parafilm sheet was placed on a test tube rack and pressed to form pore holes (or mini wells). The wells were filled with roughly 300 µL of PBS. A pair of fine curved-end forceps was used to lift the round coverslips from the culture plate and invert them on top of the PBS drop. This was repeated three times, each wash lasting five minutes, by moving the coverslips to fresh PBS each time. After finishing the final wash, coverslips were lifted carefully and inverted on top of Vectashield mounting medium placed on a sterile microscope slide. After 24 hours at room temperature to allow the mountant to set, the slides were examined using a Leica Confocal microscope, as before.

6.2.3. Carcinin association with InEPTs during encapsulation *in vivo*

This experiment was carried out jointly with Dr. Calum Robb (Centre for Inflammation Research, University of Edinburgh). Crabs were injected with LPS and the gills removed and fixed after either 1, 3, or 24 hours, as in Robb *et al.* (2014). In order to achieve a final concentration of 0.1 µg mL^{-1} LPS within the haemocoel, each crab was injected with 100 µL of 20 µg mL^{-1} of LPS from *Escherichia coli* serotype 0111:B4 in sterile 3.2% NaCl. Control crabs were each administered 100 µL of 0.22 µm filtered sterile 3.2% NaCl instead of LPS. Both groups were kept separately in the aquarium until sampling at 1, 3, or 24 hours when they were sacrificed as described in Robb *et al*. (2014). LPS treatment, tissue processing and sectioning were done by Dr. Calum Robb (as detailed in Robb *et al.,* 2014). The immunohistochemistry procedure was carried out by myself using carcinin specific antibody and goat anti-rabbit alkaline phosphatase tagged secondary antibody, as in Chapter 3 (Section 3.2.6).

Image processing and analysis of fluorescence microscopy images was carried out as in Chapter 3 (Section 3.2.4).

6.3. Results

6.3.1. Effect of carcinin on *C. maenas* haemocyte viability

Carcinin did not affect the viability of haemocytes as neither the trypan blue exclusion test, nor examination of cyto-centrifugation preparations revealed any significant difference on the viability or appearance of haemocytes (Appendix. 3). The viability was consistently at 98% (± 1.5%) and no indications of apoptosis were observed from examination of the haemocyte nuclei. There was therefore no sign that carcinin incubation caused death of *C. maenas* haemocytes at any of the time intervals used in these experiments.

6.3.2. Localisation of Carcinin on InEPTs, *in vitro*

Incubation with PMA resulted in the generation of InEPTs and also produced a greater degree of cell clumping/aggregation than in the controls, however, ICC images did not reveal carcinin to decorate InEPTs *in vitro*. Separated HCs stimulated with PMA either for 16 or 24 hours did not show carcinin co-localising with the extracellular chromatin (Figure 6.2, ii, Figure 6.3). Carcinin was detected in the control as seen before, associated with the cytoplasmic membrane of *ca* 10% of H cells (Figure 6.2, i). The amount of carcinin detected in most of the 16-hour ETotic hyaline cell images was small (Figure 6.2, ii), with no evidence of association with the decondensed chromatin. After 24 hours incubation, more HCs had become ETotic (Figure 6.3, i) but only minimal indications of carcinin were observed. The traces of carcinin present had probably arisen from membrane debris after ETosis, or from granules released from a few contaminating SGCs that burst upon PMA stimulation. However, still no carcinin was detected in association with the chromatin (Figure 6.3, i, c). This was also confirmed by using image analysis to quantify colocalization of blue and green pixels (Fig. 6.3, ii).

i

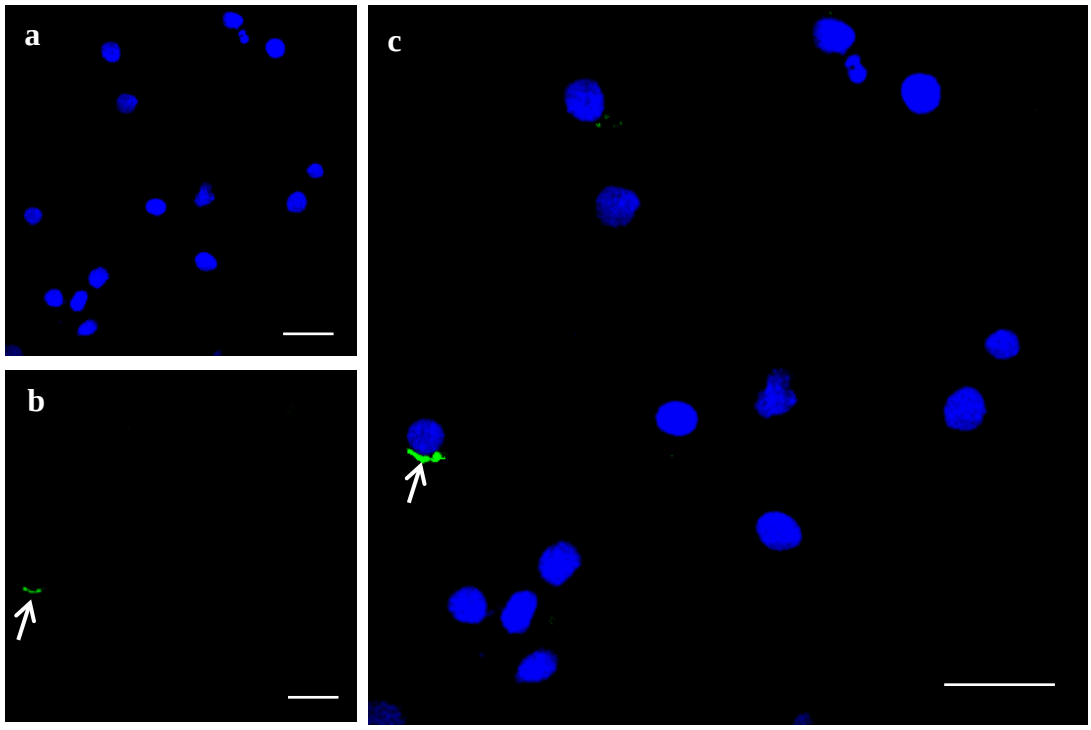

ii

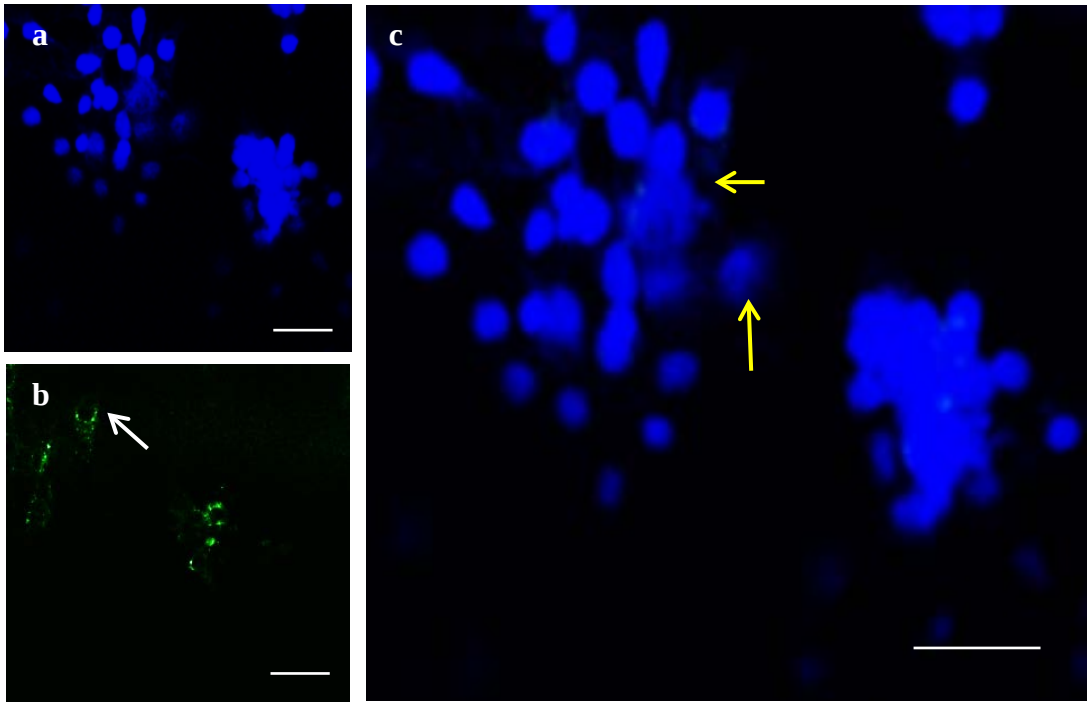

iii

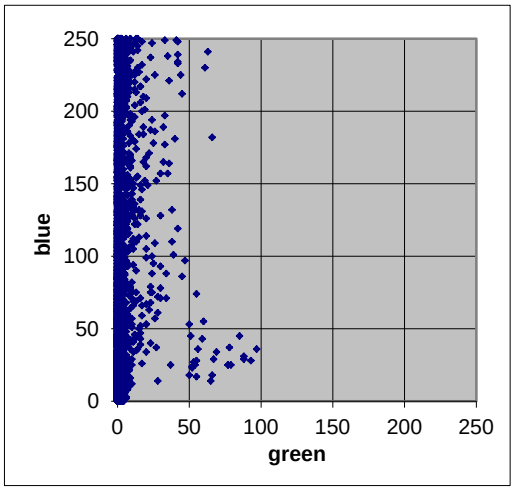

	Green	Blue	Cyan
Total no. of pixels:	23	2148	6
	1%	98.6%	0.3%
	G only	G in C	
Total pixel intensity:	1566	355	
	81.5%	18.5%	

Figure 6.2: Carcinin localisation in ETotic HCs 16 hours post PMA stimulation. HCs were treated with PMA to stimulate ETosis and monitored after 16 hours. Visualization of nuclear material was via DRAQ5^{TM} staining (blue **i** and **ii, a**). Carcinin was localised using FITC-tagged secondary Ab (green, **i** and **ii, b**) with overlay images depicted in **i, ii** (**c**). (**iii**): Scatter plot of co-localisation analysis. Control (**i**) was run by incubating the same cell population with ML-15 instead of PMA. Control images show normal stained HCs with intact nuclei. Carcinin is limited to small areas of the HC peripheral membrane (**i,** white arrow). Incubation for 16-hours with PMA (**ii**) caused the onset of ETosis in a number of hyaline cells, mostly demonstrated by the 'puff ball' appearance (**ii, a** and **c,** yellow arrows). Very little carcinin is observed (**ii**, **b,** white arrow), and that present does not bind the decondensed chromatin (**ii, c**, overlay image). Scale bar = 10 µm. The scatter plot shows the distribution of blue and green pixels, where majority of pixels in the overlay image are blue, green alone pixels are 1%, and cyan pixels are very low (0.28%). However only 18% of carcinin in the image co-localises with the nuclear material, which is considered as weak co-localisation.

i

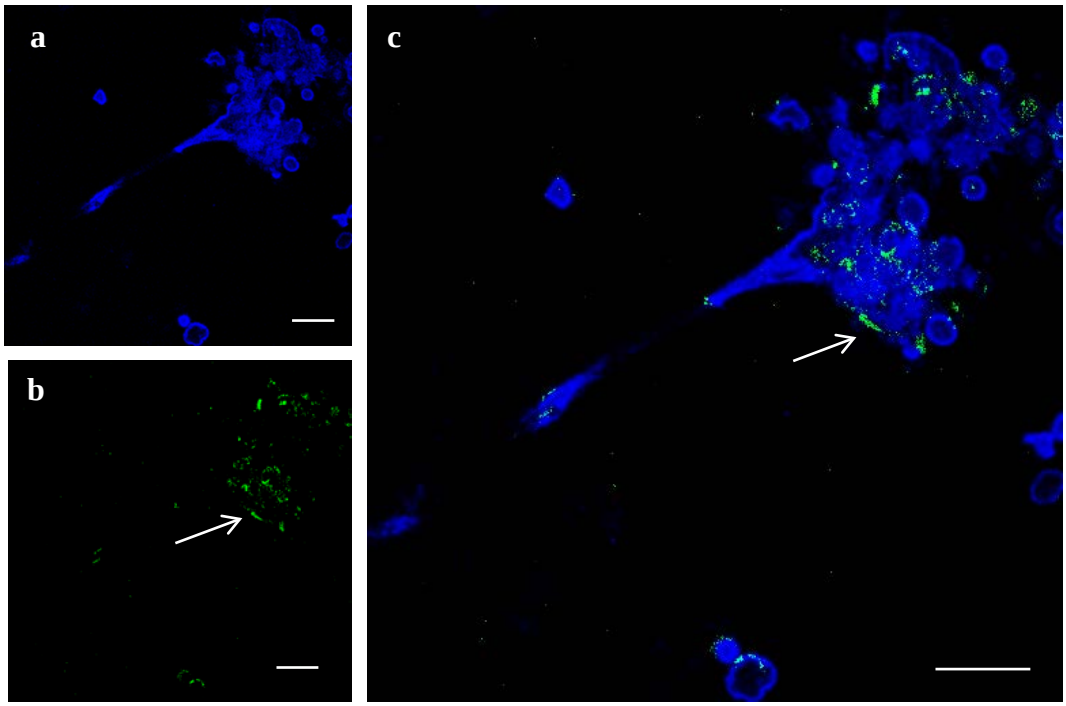

ii

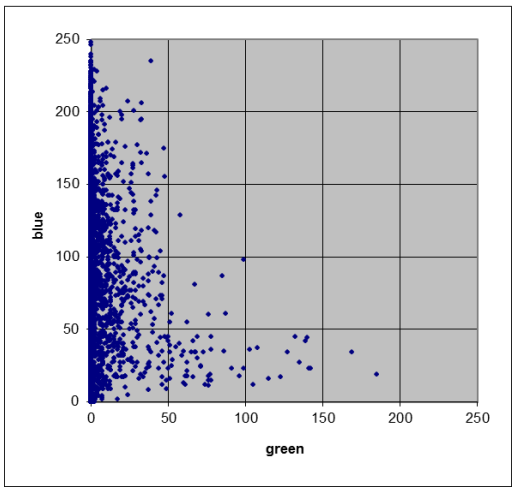

	Green	Blue	Cyan
Total no. of pixels:	55	4829	9
	1.1%	98.7%	0.18%
	G only	G in C	
Total pixel intensity:	4603	637	
	87.8	12.2	

Figure 6.3: Carcinin localisation in ETotic HCs 24 hours post PMA stimulation. HCs were treated with PMA to stimulate ETosis and monitored after 24 hours (**i**): ICC images of the 24-hour ETotic HCs, stained as above. (**ii**): Scatter plot to analyse carcinin co-localisation with the extracellular chromatin. ICC images feature extracellular strands of chromatin (**i, a** and **c**). Carcinin is detected scattering around and in-between cells (**i**, **b**, white arrows), with no obvious association with the extracellular chromatin (**i**, **c**, overlay image). Scale bar = 20 µm. The scatter plot reveals that almost all pixels are blue, with only a few cyan (0.18% of total pixels). Only 12% of the green pixels are present in the combination colour, pointing to no significant co-localisation.

With SG cells, carcinin localisation was still not associated with the nuclear material, despite the presence of carcinin in the granules of this cell type. Sixteen hours after PMA stimulation, chromatin was first seen to be decondensed and starting to diffuse outside the nucleus, while the carcinin signal was present in granules close to the cell periphery (Figure 6.4, ii). Twenty-four hours after PMA stimulation, more SG cells were showing signs of ETosis, yet very little carcinin signal was detected, and like the HCs, none was seen in association with the chromatin (Figure 6.5, i and ii). The only apparent traces of carcinin are believed to come from the remaining granules after SGC degranulation.

Where carcinin was added to stimulated HCs, a remarkable increase in carcinin signal associated with hyaline cells was detected after 16 hours of PMA stimulation, compared with the control (non ETotic) (Figure 6.6, i, ii). The carcinin signal was considerably more intense in the PMA-stimulated HCs, with *ca* 90% of these staining positively for carcinin on the membrane, versus *ca* 30% of the control HCs. HC clusters could also be observed in which some cells were showing the first signs of ETosis. The addition of carcinin resulted in the protein being associated on HC cell membranes and on the outside of HC clusters, but with no diffusion inside the core of the cluster or any colocalization with chromatin (Figure 6.6, ii).

At 24 hours, and as more single cells could be seen with extensive extracellular chromatin strands (Figure 6.7, ii), added carcinin was still detectable, but without obvious co-localisation with the extracellular chromatin strands (Figure 6.7, ii, c). Remarkably, unstimulated cells after 24 hours showed to associate with carcinin in a higher degree, with approximately 60% cells showed carcinin around their edge (Figure 6.7, i).

i

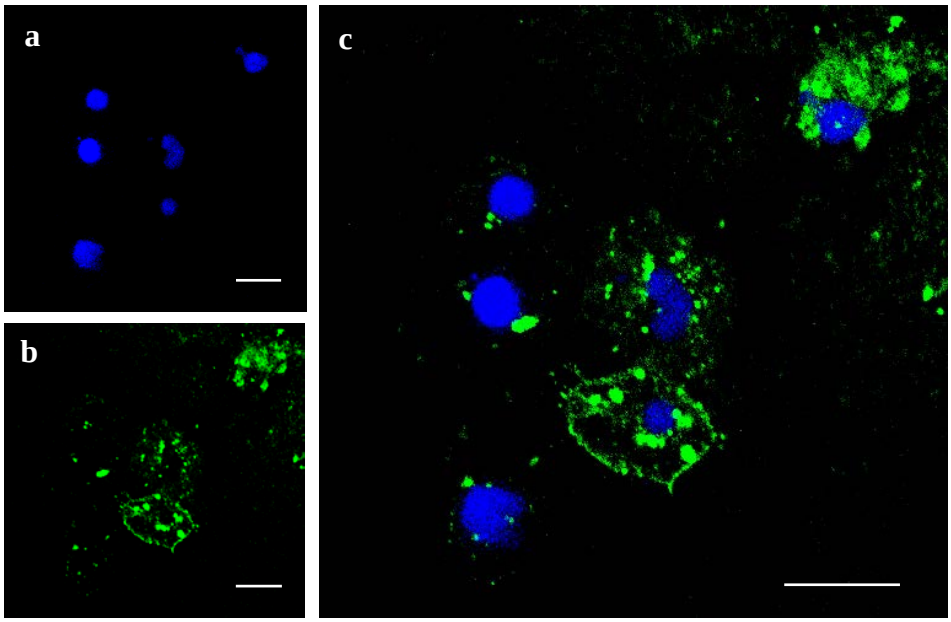

ii

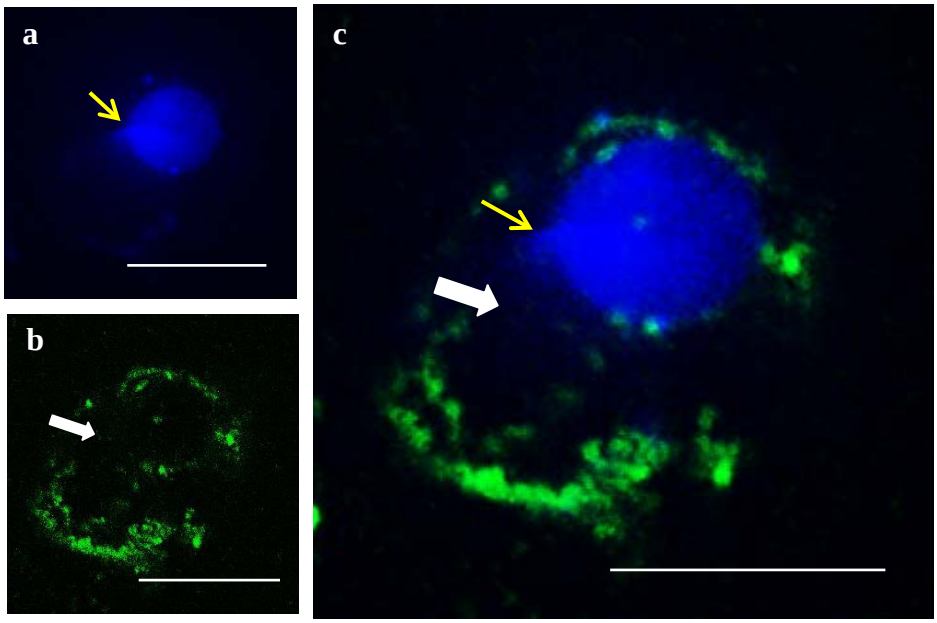

iii

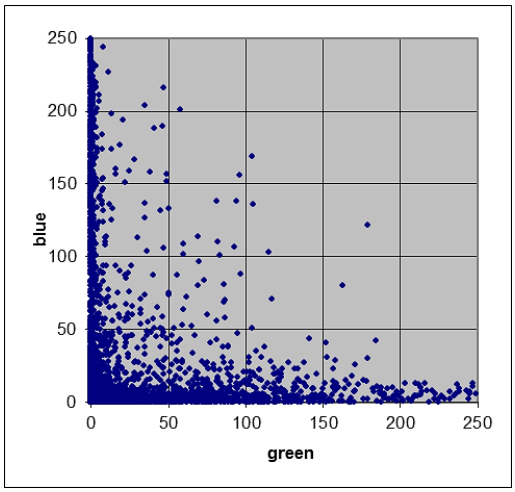

	Green	Blue	Cyan
Total no. of pixels:	684	697	36
	48.3%	49.2%	2.5%
	G only	G in C	
Total pixel intensity:	72730	2980	
	96%	3.9%	

Figure 6.4: Carcinin localisation in ETotic SGs 16 hours post PMA stimulation. Separated SGs incubated with ML-15 (control) (**i**), and PMA (**ii**) for ETosis stimulation, stained with DRAQ 5^{TM} for DNA (**i-iii**, **a**) and FITC-tagged secondary Ab for carcinin (**i-iii**, **b**). (**iii**): Analysis of pixel distribution in the overlay image. (**i**) Shows normal non-ETotic SG, carcinin present throughout the cell in the cytoplasmic granules. (**ii**): Images were taken after 16-hour PMA incubation, nucleus shows first signs of ETosis where chromatin density in the nucleus appears uneven and begins to extend to the cytoplasmic domain (**ii**, **a**, yellow arrow). No co-localisation is detected between the expelled chromatin outside the nucleus and carcinin granules still in the cytoplasm (**ii**, **c**, overlay image). Scale bar = 10 µm. The scatter plot reveals higher amount of carcinin in the image compared with HCs figures, indicated by percentages of green pixels, at 48%. However, cyan pixels are low (2.5% of total pixels), whereupon carcinin only co-localised by 4% with the nuclear material.

i

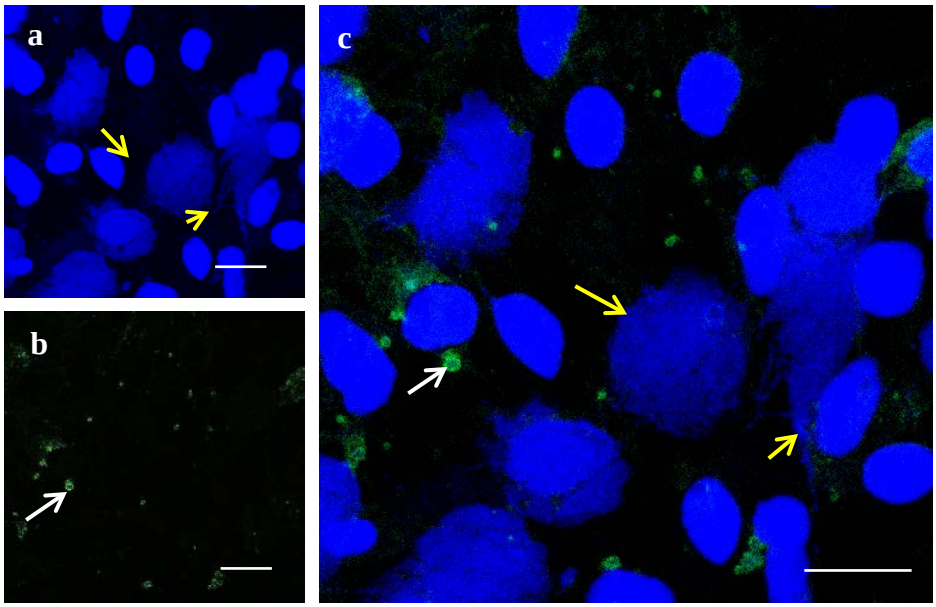

ii

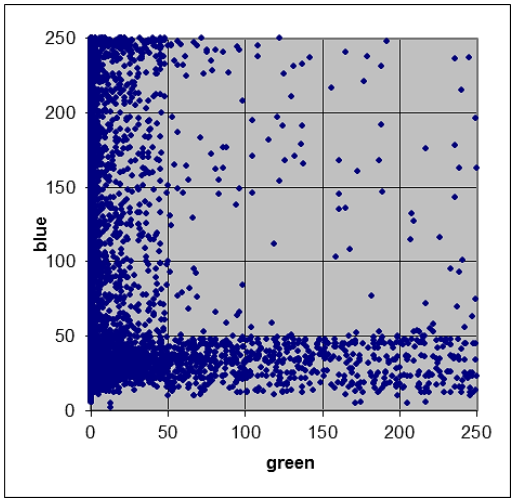

	Green	Blue	Cyan
Total no. of pixels:	680	6987	141
	8.7%	89.5%	1.8%
	G only	G in C	
Total pixel intensity:	89616	18358	
	83%	17%	

Figure 6.5: Carcinin localisation in ETotic SGs 24 hours post PMA stimulation. (**i**): Images taken after 24-hour PMA stimulation, and stained as above. (**ii**): Analysis of the 24-hour PMA stimulation overlay image. Nucleus is seen decondensed, either as 'puff ball' shapes or strands outside the cellular domain (**i, a** and **c,** yellow arrows). Surprisingly, carcinin signal diminishes to only some granules detected in the extracellular domain (**i**, **b**, white arrows), with no remarkable binding to the extracellular chromatin, as seen in (**i**, **c**, overlay image). Scale bar = 10 µm. The scatter plot reveals very little carcinin in the image (8.7% of total pixels) and little co-localisation, with only 1.8% of the total pixels in the image being cyan, and 17% of those are in the combination colour.

i

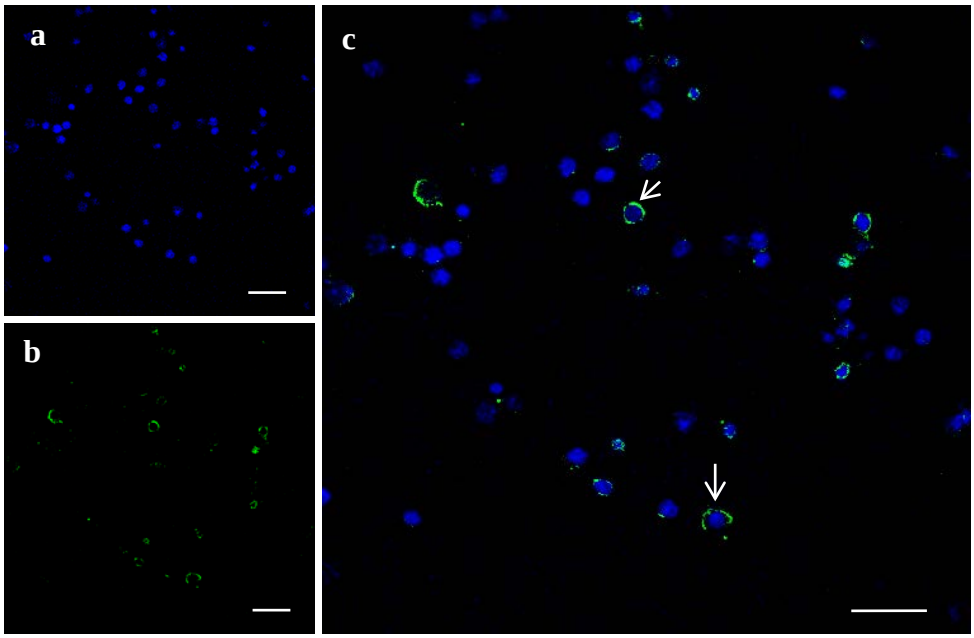

ii

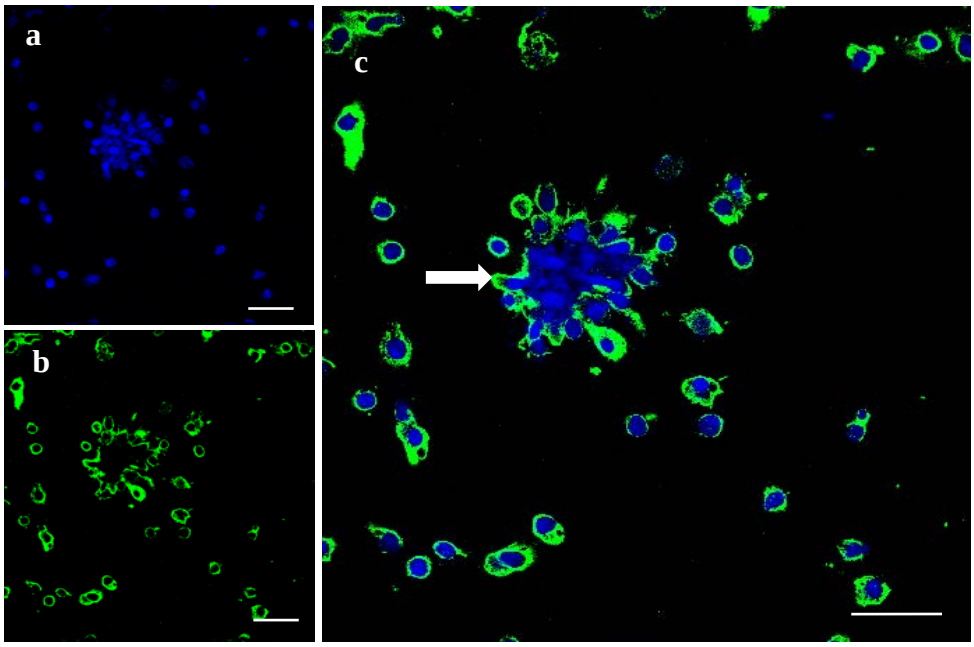

iii

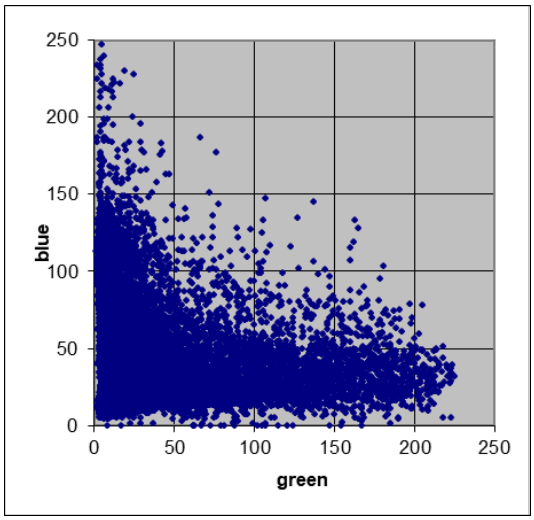

	Green	Blue	Cyan
Total no. of pixels:	2953	3741	672
	40.1%	50.8%	9.1%
	G only	G in C	
Total pixel intensity:	324531	67779	
	82.7%	17.3%	

Figure 6.6: The effect of additional carcinin post-PMA stimulation. PMA was used to stimulate ETosis in isolated hyaline cells. (**i**): Cells were incubated with ML-15 instead of PMA in control. (**ii**): Carcinin was added after 16 hours stimulation. (**iii**): Scatter plot for distribution of pixels in the overlay image in (**ii**, **c**). Distinct binding of carcinin (green) to stimulated HCs was observed after 16 hours of PMA stimulation, with 90% of HCs staining positively for carcinin (**ii**, **b** and **c**), while only 30% of non ETotic HCs bind carcinin (**i,** white arrows). In (**ii**), clusters of HCs at 16-hours post-stimulation shows the added carcinin binding to the periphery of the cluster (**ii**, white thick arrow), with none being diffused inside the ETotic core. Scale bar = 20 µm. Scatter plot reveals 9.1% of the pixels are cyan, while 17.3% of the green carcinin pixels are present in co-localisation with nuclear material.

i

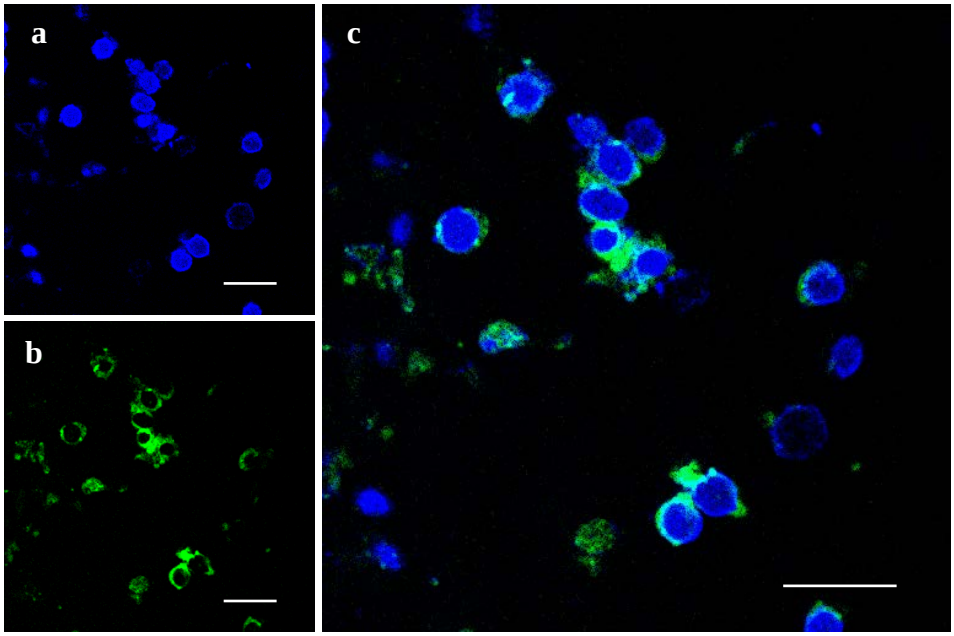

ii

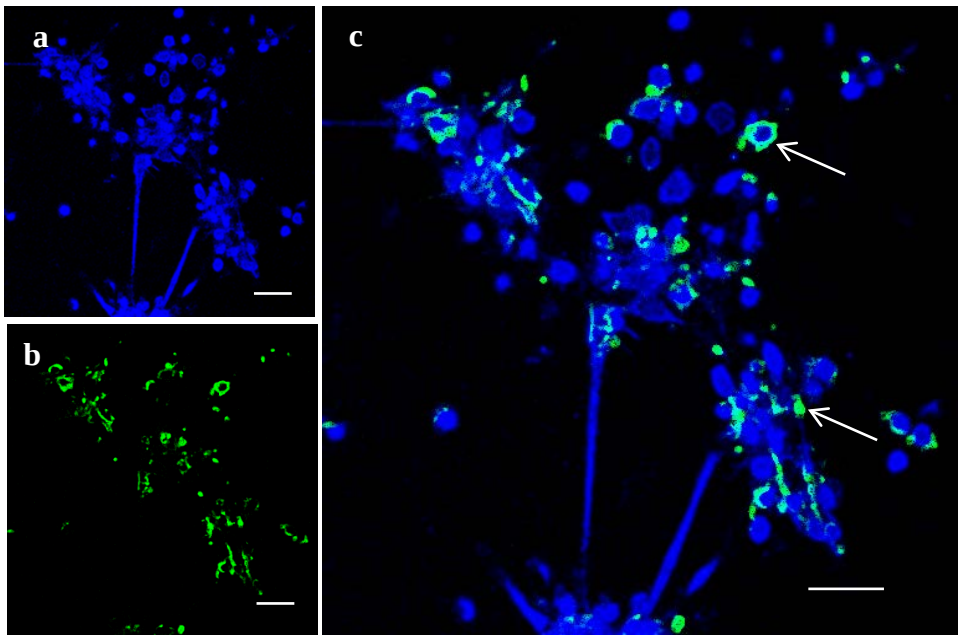

iii

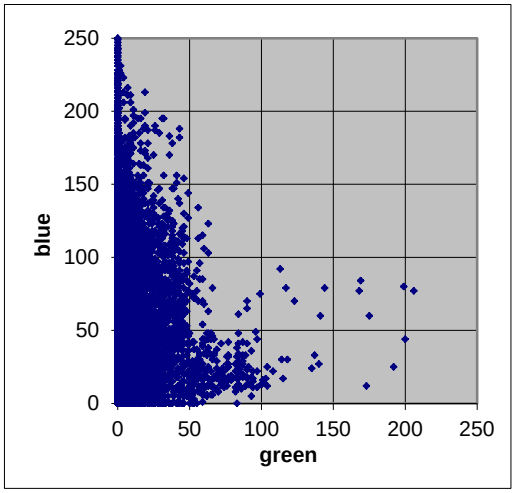

	Green	Blue	Cyan
Total no. of pixels:	235	4187	36
	5.3%	93.9%	0.8%
	G only	G in C	
Total pixel intensity:	16788	3182	
	84.1%	15.9%	

Figure 6.7: The effect of additional carcinin post-PMA stimulation. (**i**): Control ICC images of 24-hour PMA unstimulated HCs, with added carcinin. (**ii**): 24-hour PMA stimulated HCs, with added carcinin. (**iii**): Scatter plot of pixel analysis of the overlay image in (**ii**). ML-15-incubated HCs after 24 hours seem to bind more carcinin than observed in the 16 hour ML-15 control (**i**, **b** and **c**). (**ii**): In 24-hour ETotic HCs, extracellular chromatin strands are seen in the images, with carcinin detected scattering around and between the ETotic cells (**ii**, **b** and **c**, white arrows). Co-localisation with the extracellular chromatin is not present in the overlay image (**ii**, **c**). Scale bar = 10 µm. (**iii**): Scatter plot of pixel distribution of PMA-stimulated HCs, with added carcinin. Cyan pixels comprise 0.81% of the total, of which 16% is related to carcinin (green pixels in the combination colour), pointing to no significant co-localisation between carcinin and the extracellular chromatin.

6.3.3. Carcinin associated with encapsulation *in vivo*

As described by Robb *et al.* (2014), LPS injection stimulated the formation of capsules, which were highly similar to those formed in response to bacterial injection (Smith and Ratcliffe, 1980), and after injection of certain glucans (Smith *et al.*, 1984). In the present study, haemocytes were observed to form small, loosely compacted groups inside gill lamellae within the first hour post treatment (Figure 6.8, b-d). SGCs and GCs were seen frequently at this stage, however, high percentages of these cells were degranulating, especially where the haemocytes were beginning to assemble (Figure 6.8, b and d). At this stage, carcinin was observed especially scattering around the early-stage clumps (Figure 6.8, c and d). Neither degranulation nor clumping was observed in the controls (Figure 6.8, a). Remarkably, the carcinin signal was also detectable in parts of the gill walls, as seen in (Figure 6.8, e, f).

After 3 hours, haemocytes were seen to form larger, more compacted clumps. Carcinin was diffused inside the cellular cluster, with some still being detected around or close to the clumps (Figure 6.9, a and b). In addition, larger areas of the inner walls of some gill lamellae were seen to have carcinin staining (Figure 6.9, c). In the 24-hours post-injection samples (Figure 6.9, d), the haemocytes were tightly compacted and the capsules fully developed. Carcinin was still present inside the capsule, though it was difficult to define if it had been secreted or was still inside the haemocytes, due to the tightly compacted nature of the structure at this stage.

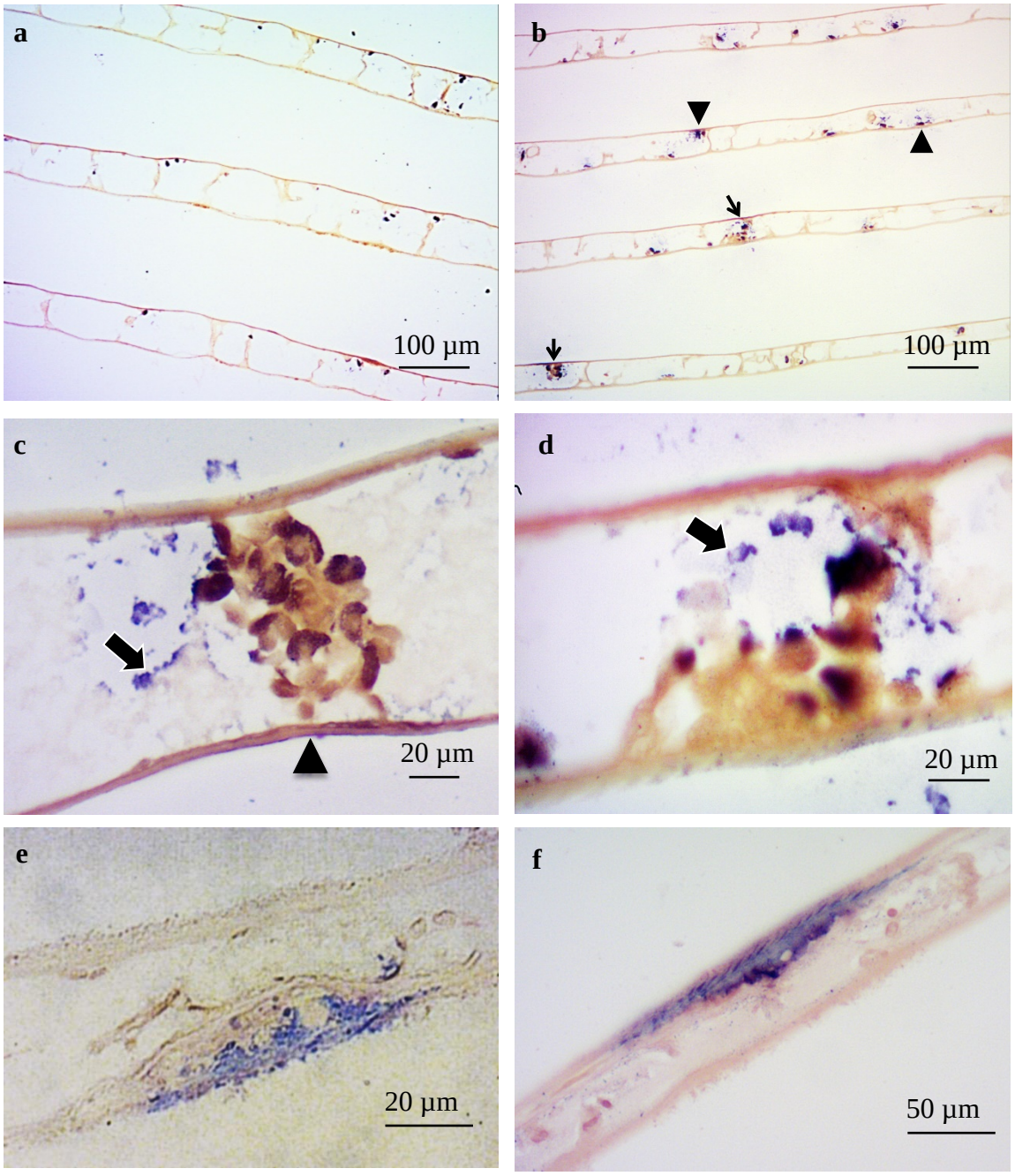

Figure 6.8: Carcinin in crab gill, 1-hour post-injection with LPS. Carcinin was detected using AP-tagged secondary Ab (purple staining). (**a**): Gill image of control crab injected with saline. (**b**): Low magnification image of crab gill section 1 hour post-injection of LPS. (**c**) and (**d**): Details of 1-hour post-injection haemocyte clumps. (**e**) and (**f**): Carcinin associated with parts of the gill wall with details of staining in thickened areas of gill wall. In the image (**a**), haemocytes seem scattered in gill lamellae and stained for carcinin in a similar manner to that observed for healthy, un-injected crabs (Chapter 3). Black arrows in image (**b**) indicate early haemocyte clumps, with degranulation activity apparent nearby. Arrowheads (**b**) point to degranulating

haemocytes close to the gill wall, with carcinin signal also detectable in the adjacent part of the gill lamella. In (**c**) and (**d**), arrows point to carcinin released by haemocyte degranulation and located around the early capsules. In (**c**), arrowhead indicates carcinin associated with the gill wall.

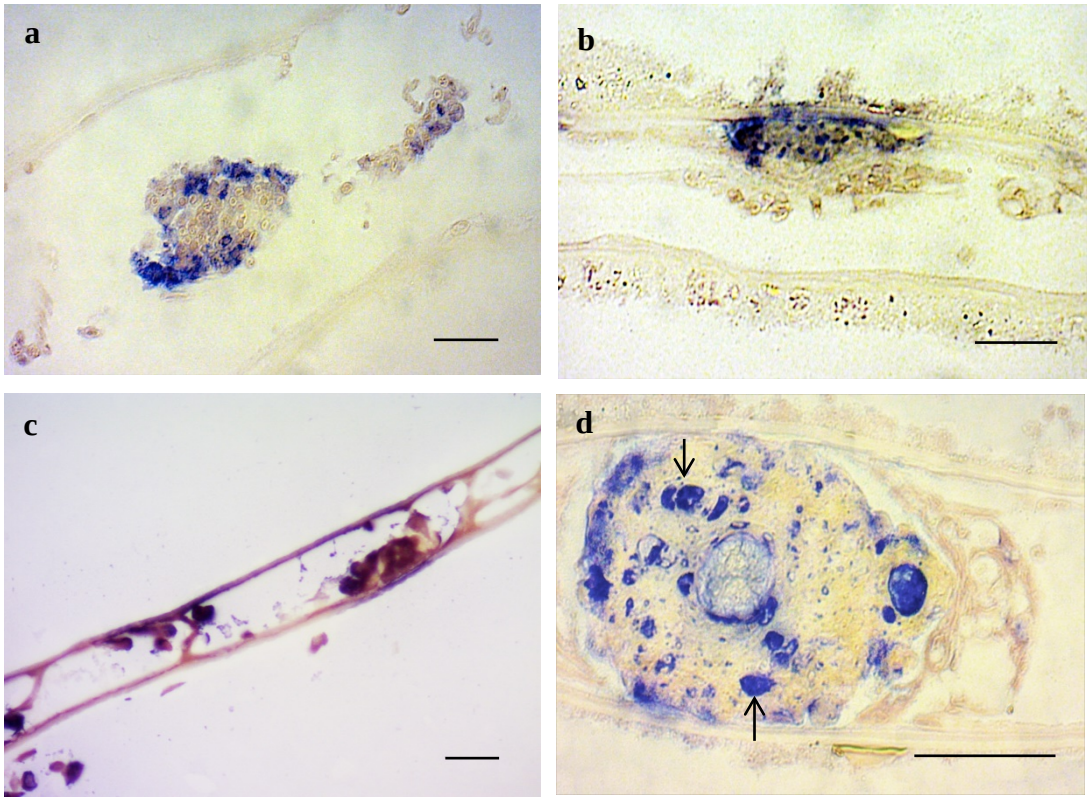

Figure 6.9: Carcinin in crab gill at 3 and 24-hour post-LPS injection. (**a**) and (**b**): Detail of the crab gill at 3-hour post-injection with LPS. Carcinin signal is shown with AP-tagged secondary Ab. (**c**): Image of gill lamellae (3 hours) showed extensive staining along the gill wall. (**d**): Fully developed capsule lodged inside gill lamellae 24 hours post LPS injection. After three hours of LPS injection, carcinin reveals stronger intensity, with more peptide diffusing inside the developing capsule. In (**b**), soluble carcinin appears to spread inside and extend to the adjacent area of the gill wall. The 24-hour LPS injection mage (**d**) shows high amount of carcinin in areas inside the capsule and close to its core. Some staining may indicate carcinin inside some intact haemocytes (arrows). Scale bar = 50 µm.

6.4. Discussion

This chapter aimed to establish whether carcinin is associated with extracellular trap formation in the crab, as the first crustin to be investigated for this purpose. Although ETosis was reported to occur in many invertebrates including shrimp species, as stated earlier, no role for crustins or other crustacean AMPs has yet been investigated. The secretion of AMPs is likely to augment this process, either when occurring in circulation or associating with encapsulation in crab gills (Robb *et al.*, 2014). In the previous chapters, carcinin appeared as a major part of the cytoplasmic granules in SGCs, and associated with some hyaline cell membranes, both of which cell types were shown to undergo ETosis in the present study as well as Robb *et al*., (2014).

However, ICC performed on PMA-stimulated HCs and SGCs *in vitro* did not reveal any significant binding of carcinin to the extracellular chromatin. Despite the absence of carcinin on the InEPTs, it was still detectable on some HC membranes. When carcinin was added post-PMA stimulation, it showed an ability to bind the stimulated hyaline cells and to attach to the outside of cell clumps. In the *in vivo* experiment, carcinin was detected in capsules at all stages of development, presumably arising from release by the SGC and GCs. This led to speculation of other possible contributions of carcinin to this process, despite no apparent localisation on the extracellular chromatin structures themselves.

In mammals, numerous proteases and other peptides have been confirmed to decorate extracellular traps (Urban *et al*., 2009), some decoration coming from cationic antimicrobial peptides believed to interact with DNA electrostatically. However, this raised an argument that binding extracellular chromatin might reduce the effectiveness of AMP activity as binding might neutralize the AMPs' net charge, limiting their ability to interact and affect bacterial cells (Sørensen and Borregaard, 2016). Alternatively, binding of AMPs to bacterial cells might mask the bacterial cell surface charge, and minimize the chance of bacteria being captured by chromatin traps. In fact, it has been reported that some pathogens can change their surface charge in order to escape NETs (Wartha *et al*., 2007, reviewed by Brinkmann and Zychlinsky, 2012). Accordingly, carcinin as a cationic AMP, if bound to negatively charged DNA, might lose its ability to interact electrostatically with bacteria, or might disguise bacterial cells, and thus fail

to support this process. This led to speculation that in the mammalian system, that AMPs in general might act more effectively independently of ETosis.

It is also important to consider that peptides contributing to this mechanism in mammals were mostly of cytoplasmic or granular origin, and definitely not delivered from the extracellular environment (Brinkmann *et al*., 2004; Urban *et al*., 2009). Carcinin, though a predominant component of the cytoplasmic granules of SGCs and GCs, is certainly not present in the cytoplasm of the HCs, that have few, if any, granules. In the present study, carcinin was confirmed as a protein secreted from SGCs and GCs. The present study also showed that carcinin was associated with the membrane of some HCs, although there was no firm evidence that it is present in or can diffuse inside HCs. ETosis as reported in human neutrophils involved mixing of cytoplasmic and nuclear components, with cytoplasmic peptides stored in granules being able to associate with chromatin, before expulsion to the extracellular domain. If InEPT formation in crustaceans follows this pattern, carcinin, as a SGC and GC derived protein that associates with the HC cytoplasmic membrane, is not likely to become attached to the discharged HC chromatin. Carcinin is thus unlikely to contribute to the regulation or decoration the extracellular chromatin trap in HCs. Since the process in crustaceans mirrors that of NET formation in mammals, then the contribution of intra-, not extracellular proteins, is key.

As seen in the Section 6.3.2, there is no evidence that carcinin decorates the extracellular chromatin. It is therefore unlikely to play a part in controlling ETosis in a similar way to that of SLPI, especially since carcinin did not show any protease inhibition activity. Data from an EST library of *C. maenas*, however, revealed the likelihood that an elastase-like protein exists in different tissues of *C. maenas* (dbEST Id: 28380988; Towle and Smith, 2006). If this enzyme, and possibly other proteases, decorate ETotic structures similarly to those of mammals, then carcinin is likely to be degraded due to their secretion after onset of ETosis.

However, despite the lack of carcinin localisation with InEPT structures, carcinin may have other possible functions related to the process. After extracellular trap formation, there are questions about their fate, and what kind of clearance processes may occur. It was reported that expelled chromatin might present a ‘danger signal’ to stimulate innate

immune responses in mammals (Seong and Matzinger, 2004). Interestingly, Farrera and Fadeel (2013) stated that NETs are cleared via phagocytic activity of monocytes, and that this activity was aided by opsonisation of the complement component Cq1, with pre-processing by DNase I (Farrera and Fadeel, 2013). If extracellular traps in invertebrates are similarly degraded after conducting their role in sequestering infection, clearance is likely to be done by phagocytes and supported by an opsonic agent. In the previous chapter, the adherence of carcinin to bacteria was shown and its opsonic effect was demonstrated by the *in vitro* phagocytosis experiments. Carcinin was also inferred to play a role in phagocytosis by podocytes in the moulting crab gill, as it showed ability to attach there (Chapter 4). It was also seen associated with oocytes that were suspected to be degenerating and thus might attract phagocytic haemocytes for their elimination (Chapter 3). This points to a possible role of carcinin in extracellular chromatin clearance. Especially that, notably, higher proportions of HC cells bound carcinin when stimulated with PMA. It was also supported when more carcinin was seen in the 24-hours unstimulated HCs with extra added carcinin. Robb (2015) reported significantly increasing mortality of unstimulated HCs throughout 24 hours in culture. The percentages of dead HCs ranged from ca. 15% after 4 hours in cultures, to >30% at 6 hours and >50% at 24 hours (Robb, 2015), either through ETotic or other types of cell death. This, combined with the increased percentage of carcinin-positive control HCs with time in the present study, gives a further indication to the possible association of carcinin with dying or degenerating cells.

The same attractant effect of carcinin was also speculated from the *in vivo* experiment using LPS injection. Carcinin being released from LPS-stimulated GCs and SGCs, would be in line with observations by Smith and Ratcliffe (1980), who noted extensive degranulation upon LPS stimulation. In the present study, secreted carcinin appeared to attach to HCs *in vivo*, especially to those cells on the periphery of the early developing capsule. Considering the *in vitro* observations of the present study, when more carcinin attached to PMA-stimulated HCs (Figure 6.5), it might be reasonable to speculate that both PMA and LPS-stimulation increase carcinin association with HCs. Therefore, carcinin might bind more cells towards the clumping area, and might aid in cellular attachment mediated by adhesive proteins such as peroxinectin. Such an attractant effect, although not illustrated previously with any crustins, was shown by a penaedin

from *P. monodon*, which attracted haemocytes towards injured areas (Li and Song, 2010).

During capsule formation, especially at 1 and 3 hours post-LPS injection, carcinin was seen associated with parts the of gill wall, presumably discharged from haemocytes. This signal indicated that carcinin might be able to bind chitin present in the cuticle. This tallied with observations made in Chapter 3, where carcinin was detected in the eyestalk endocuticle, which is chitin-rich. The external cuticle, also a chitin-rich structure, is a strong defence barrier in *C. maenas* against pathogens in the marine environment. The defence role of the gill cuticle comes mainly from the presence of chitin, which is also present in the crustacean exoskeleton and gives it the hardness as part of a complex with calcium carbonate.

Chitin is also a component of fungal cell walls, thus chitin-binding proteins are important anti-fungal molecules (Hemmi *et al.,* 2003). A number of arthropod AMPs are already known to have chitin binding activity, e.g tachycitin, from horseshoe crab haemocytes (Kawabata *et al.,* 1996*),* and penaedins from the haemocytes of the shrimp *P. vannamei* (Destoumieux *et al.,* 2000). Both peptides were speculated to have a role in the healing of damaged tissues due to their chitin-binding ability. This assumption came after Bachère *et al*, (2000) identified a chitin-binding motif in different peptides exhibiting this binding ability. The motif is located at the C-terminus and is rich in cysteine residues, thus in some injured sites where chitin becomes exposed, the peptides may aid in regeneration and recovery.

The possibility that carcinin might have this region was revealed from the software PROSITE. The interrogation of the PROSITE search engine (http://prosite.expasy.org/) when carcinin amino acid sequence was scanned against the sequence of the chitin-binding motif resulted in a matching hit on one sequence. The matching output gave an expected frequency of a random match to the chitin-binding motif of 8.2 in 100,000 sequences (based on a sequence length of 500 amino acid residues), which is considered to be high frequency (Ref: PMID 11535175) (Appendix. 4). This makes it likely that carcinin might have chitin-binding properties, and be able to attach to exposed chitin in areas of damage in the gill walls. This gives further support to the idea that carcinin

may play a role in tissue regeneration and repairing, and supports the previous finding in Chapter 4 where carcinin was detected extensively in regenerating eyestalk tissue.

The present study showed that carcinin appeared to penetrate inside the developing capsule and had a continued presence after 24-hours throughout the mature capsule, including the melanised core. Although visualization was difficult in some fully-formed capsules, there are still appeared to be some intact haemocytes at the edges of the capsule which are positive for carcinin. It is unlikely that active phagocytosis occurs within haemocyte capsules (Smith VJ, pers comm), although phagocytes containing bacteria opsonised with carcinin might well be present in the capsule matrix. Elimination of capsules during the moult indicates that additional clearance processes in the gills are unnecessary.

In this chapter, further indication of the crucial role of carcinin in innate immune processes of the crab was revealed. The patterns of carcinin localisation in association with cells undergoing ETosis indicate an alternative role for carcinin, rather than decoration of the extracellular traps themselves. The increased localisation of carcinin with PMA-stimulated HC cells, as well as with those spending longer in incubation, is highly novel and may indicate association with cells undergoing changes such as dying, as suggested in Chapter 3 for oocytes. A potential role in tissue repair is also supported by the presence of a chitin-binding motif, which although was reported for penaedins, has never been reported for any of the studied crustins. Therefore, these findings further sustain the notion of crustins' multifuctionality, and highlight the necessity of investigating crustins' contribution in more immune responses. This would not only help understand crustin multifunctionality, but also assist in further elucidation of the mechanisms by which potential pathogens may be eliminated.

Chapter 7

General Discussion

7.1. General Discussion

This project studied carcinin, a WFDC domain-containing protein and a Type I crustin from the shore crab *C. maenas*. The purified, native peptide was used in all experiments and to generate a carcinin-specific rabbit polyclonal Ab. Carcinin localisation in cells and tissues was investigated *in vitro* and *in vivo* using ICC and IHC procedures. These techniques were also used to track changes in carcinin distribution through different life events, such as sexual maturation, tissue regeneration, and moulting. Experiments were also performed using the native protein in a number of *in vitro* biological assays. The findings have added greatly to the understanding of carcinin's biological function, as well as shedding more light on mechanisms of host immune responses in crustaceans.

The purification process described in Chapter 2 was a modified method from Relf *et al*. (1999), using FPLC instead of HPLC. The method was optimised in order to increase the amount of the purified peptide. FPLC enabled better yields of carcinin to be purified more quickly, which was an important advantage over using the HPLC technique, given the frequent use of the pure protein in these experiments. In fact, FPLC has been used in preference for purifying of biomolecules since it avoids harsh conditions that might harm protein structure (Runde, 2016). As a result, the purified carcinin appeared in a slightly different way to the original report by Relf *et al*. SDS/PAGE revealed two very close bands from FPLC purification, which were both confirmed by mass spectrometry to be carcinin. The paper by Brockton *et al*., (2007) found several putative carcinin isoforms from gene sequence data, and the results from the present study strengthen the possibility that isoforms of the native protein occur naturally in the animals. However, the appearance of the closely migrated bands might also be due to individual differences in alternative splicing and/or carcinin breaking down, as discussed in chapter 2. Given that around 40-60% of all eukaryotic cell genes undergo alternative splicing (Modrek and Lee, 2001) and that the functional diversity of proteins might be affected by the extent of this process (Graveley, 2001), future work on the molecular, phylogenetic and functional analysis of carcinin isoforms would be very valuable. This could include high-resolution separation of the bands via two-dimensional gel electrophoresis with subsequent amino acid sequencing and phylogenetic study. Thus, more confirmation about isoform identity and its occurrence in different species or populations could be gained. Mapping isoform variation at the

gene level via *in situ* hybridization on haemocytes and tissues could also provide useful data, contributing further to understanding carcinin multi-functionality.

More information regarding the role of carcinin would have been gained in the present study if larger yields of the purified protein had been possible. Sadly, some loss occurred from the purified fractions due to carcinin adhesion on dialysis membranes and ultrafiltration concentration methods. While FPLC proved more effective than HPLC in the present study, it would be recommended for future work to use more crabs at the initial stage for haemolymph extraction. Higher concentrations of protein in the crude HLS would increase yield of the purified protein. One advantage of this would be the provision of enough carcinin to enable its three dimensional structure to be confirmed via protein crystallography.

It is possible that other researchers have experienced similar difficulties in purifying crustins, particularly when using decapod species with smaller quantities of haemolymph and/or lower numbers of circulating cells. This may be a factor in the large number of studies choosing to use recombinant proteins rather than native ones. The drawbacks to this, however, are that peptides produced by bacterial expression systems may not have identical properties to their native equivalents. Recombinant peptides do not undergo phosphorylation, acetylation and acylation, or might not be folded in the same ways as the native ones. This further emphasizes the important advantage of using the native, rather than the recombinant peptides, especially for functional studies, where protein structure is a key. Many recent approaches aimed to produce recombinant peptides via insect or mammalian expression systems that mimic the post-translational modifications occurring on the natural peptide (Fernandez and Hoeffler, 1999). It is possible that alternative expression systems might yield recombinant carcinin in high quantities and with greater similarity to the native protein, thus enabling its use for structural and biological elucidation.

Many reports have stated that DNA sequencing is not sufficient for the full elucidation of proteins' biological functions. The majority of crustins reported in the literature have antibacterial properties, however, their spectrum of activity is mainly limited to Gram-

positive bacteria (as reviewed by Smith *et al.*, 2008, and Smith and Dyrynda, 2015). Thus in general, most crustins are considered to be weak disinfectants with no other functions definitely proven, despite their abundance in haemolymph. Mammalian AMPs exhibit multiple functions (Lai and Gallo, 2009), however, this has not been investigated in invertebrates to any significant degree. Nevertheless, a few crustins, primarily Type IIIs, have been indicated to have proteinase inhibitory properties (Jia *et al*., 2008; Du *et al.*, 2010). It is perhaps unusual that so few of this large WFDC-domain containing protein family act as proteinase inhibitors, unlike the majority of the vertebrate WFDC-domain proteins. Among the few studies addressing other functions of carcinin, some Type IIs are reported to be involved in haematopoiesis (Fagutao *et al*., 2012; Chang *et al*., 2013), in addition to one of the Type I group presented recently as an opsonin (Liu *et al*., 2015). Few existing studies have reported protein localisation in the animals, thus this project aimed to localise carcinin both *in vitro* in haemocytes and *in vivo* in tissues as a first step in uncovering its biological role.

From the localisation of carcinin in pro- and mature haemocytes (Chapter 3; Figure 7.1), carcinin appears to be present in haemocyte granules from an early stage, since it was detected in the cytoplasmic granules of some ProHs, believed to be the precursors of SGCs and GCs (Roulston and Smith, 2011). Based on these results, it is possible that carcinin or other crustins could act as indicators for different ProH types in studies of haemopoiesis in crustaceans. It was clear as well that the granular haemocytes are the vehicles that carry and release carcinin via degranulation to act mainly in the extracellular domain, when needed. Localisation of carcinin in SGC and GCs would be expected, however, the membrane staining of HCs was unusual and had not been previously recorded. As described in Chapter 3, degranulation activity was observed close to tissues such as connective tissues and epithelial cells that showed some carcinin localisation. What represents an important asset of using immune staining rather than studying gene expression for localisation studies, is that carcinin appears not to be generated inside these tissues, but is deposited there by haemocytes. In addition, localisation in organs such as the eyestalk and gonads showed that carcinin exists in certain structures, but not throughout the whole tissue in question, which gives further insights into its functions

The distinct localisation of carcinin in gonads, especially in the ovaries, tallies with the findings of Zhang *et al*. (2007 a) and Sun *et al*. (2010), who reported expression of crustin genes in the ovary of untreated shrimp. In the present study, carcinin positive oocytes appeared vacuolated and fragmented, thus its occurrence may be linked to oocyte degeneration or clearance of redundant ones. More evidence is required to substantiate this. Therefore experiments involving induction of apoptosis in oocytes followed by monitoring of carcinin signals would contribute to further understanding this mechanism. In crab's testicular tissues, carcinin was also seen to deposit in epithelial cells surrounding mature sperm. However, it was not possible in this study to investigate further association of carcinin with sperm development or mating, as this would need additional procedures, e.g. extraction of seminal fluid from males. It is important to mention that some WFDC-domain containing proteins in mammals, particularly eppin, occur in the testes and/or ovary (Trexler *et al*., 2002; Yenugu *et al*., 2004). A recent study further supports the idea that carcinin may be linked to dying/degenerating cells, as it was shown in mammals that the WFDC-domain containing protein, WFDC-2, enhances proliferation of cancer cells by regulating apoptosis (Chen *et al*., 2013).

Inaccurate localisation of peptides inside specific organs, as stated in the majority of crustin studies, can lead not only to an erroneous understanding of the role of crustins, but also the organ function as a whole. For example, Liu *et al*., (2011) claimed that the eyestalk of the swimming crab, *Portunus trituberculatus*, has an immunological function as crustin transcripts were detected there. In fact, carcinin was seen in the present study in the eyestalk of the shore crab, but was confined to the haemocytes in addition to the growth rings of the endocuticle, which is highly likely to receive the peptide from haemocytes. There is not enough evidence, as yet, that the eyestalk contributes directly to the immunological response of the crab. This illustrates a gap in many crustin reports, and thus more caution is required when considering data from genomic studies. It is also emphasizing the need to utilise the native peptides in functional studies. It is now fully recognised that the change in one gene does not necessarily reflect a change in the mature peptide, as important modifications on gene transcripts occur at the post-translational level (Pandey and Mann, 2000).

More insight into carcinin function was revealed in Chapter 4. Carcinin showed significant roles in different life stages of the animal. During gonad development, carcinin appeared to be associated with redundant and defective oocytes in the ovaries that are subject to clearance. While it did not show a similar appearance in the testis, carcinin changes seemed to relate to vitellogenesis occurring in ovaries of the female crabs, to support the development of healthy ova, which is vital to ensure healthy reproductive function of the animal. It also gave an additional clue of carcinin's role as an opsonin to mediate the clearance of the defective oocytes. Additional evidence of this role came after carcinin was detected in association with podocytes in the gills of a moulting animal. This pointed to another contribution of carcinin in the important clearance process conducted by these cells (Doughtie and Rao, 1981). Carcinin is thought also to be delivered not generated inside these cells, thus its association with podocytes also resulted from its adhesive property. Another target of carcinin binding was the regenerating parts of the moulting gill wall, which was the first indication of its ability to bind chitin. A further indication was carcinin's extensive presence in the regenerating tissues of the eyestalk. Carcinin was believed to be secreted there by granular haemocytes, where it is largely assumed to support wound healing and tissue regenerating, either by binding chitin, or facilitating phagocytosis of necrotic and damaged tissues. The ability of carcinin to bind chitin was further revealed in Chapter 6, and will be discussed later. Given the associations of carcinin with clearance and/or regeneration, together with possible chitin-binding, it would be of interest to localise the protein in the earlier larval stages of *C. maenas*, which go several stages of metamorphosis with extreme changes in body size and morphology.

From all results of this carcinin localisation study, and as carcinin specific mapping in tissues and organs was revealed, it is important to emphasize the importance of immune-staining to track the studied peptide. Most crustin studies built insight on the possible functional roles by tracing crustin transcripts in tissues of the animal, which showed weaknesses as discussed above. However, a few studies aimed to use the immune staining approach, by raising an antiserum against the recombinant peptide (Du *et al*., 2015, Yu *et al*., 2016). This approach, however, is debatable as recombinant peptides do not exactly resemble their native versions present in tissues. Thus antibodies produced against recombinant peptides may not be interacting with the same epitope present in the native peptide.

The experiments described in Chapter 5 used further novel methods to investigate carcinin interaction with its possible targets. Showed that carcinin discharged from haemocytes affected bacteria in two ways. Firstly, carcinin has the ability to attach to *P. citreus* bacterial cells and destabilise them by inducing pore formation in the bacterial cell wall. Secondly, carcinin through its capability to bind bacterial cells and associate with HCs, supports HC phagocytosis as an opsonin (Figure 7.1). While some crustacean AMPs, such as penaeidins, are released directly into phagosomes to kill engulfed bacteria (Destoumieux *et al*., 2000), this appeared not to be the case for carcinin, as shown by immunocytochemical co-localisation. Normally, the site of microbial killing would be the open circulation of the crab, where the efficacy of carcinin depends largely on its *in vivo* MIC and half-life, or inside infected tissues. According to this study, the MIC of carcinin *in vitro* is higher than 50 nM. It is important also to consider that even if the tested *P. citreus* was resistant to carcinin concentrations used in this study, other Gram-positive marine bacteria might be sensitive. It might be worth then assessing carcinin MIC using species of Gram-positive marine bacteria.

The importance of carcinin being deposited in certain tissues, e.g. immunological barriers like the outer capsules of organs, epithelial cells, and chitin-rich tissues, is quite essential to achieve required concentration for bacterial killing, giving that Brockton *et al*. (2007) predicted it to have a short half-life based on *in silico* observation and the quick cleavage of the recombinant carcinin, which may impact on killing in open circulation.

The *in vitro* phagocytosis assay was the definite evidence of carcinin's role as an opsonin (Figure 7.1), and supported previous observations of its association with phagocytic cells such as HCs and moulting gill podocytes on one hand, and unwanted cells or non-self particles such as bacteria, redundant oocytes, or damaged tissues. However, it might be useful to run the same assay, but with hyaline cells that been pre-incubated with carcinin, in addition to control hyaline cells without carcinin. This would give stronger evidence that carcinin, by its interaction with hyaline cells, is actually participating directly in the cellular responses, and mimicking the action of factors such as complement 3b in mammals (Hartung and Hadding, 1983). The ability

of carcinin to act as an opsonin is unique and it is the only crustin, to date, to show this activity via a direct assay using isolated phagocytes *in vitro.*

Carcinin was also found to be associated with some connective tissues (Chapter 4). In addition, more carcinin was seen deposited on cell surfaces after immune stimulation and injury, as seen in the 16-hours PMA-stimulated HC clusters, the outer layer of the one-hour, early developing capsules in the gill, and regenerating tissues of the eyestalk. This gave rise to the idea that the released carcinin upon stimulation might act as a chemoattractant, bringing more haemocytes to injured or infected areas, and thus playing a role in tissue connectivity and cell-cell signalling. This was detected in one of the proline-rich penaeidins (Li and Song, 2010), but not in other crustins or WFDC containing peptides, which indicated that the WFDC domain is unlikely to be the key mediator of this function. An increased carcinin signal was also detected in the gills; in particular, carcinin-positive podocytes were of great interest. This pointed to another contribution of carcinin to the important clearance process conducted by these cells (Doughtie and Rao, 1981). Carcinin is thought also to be delivered, not generated, inside these cells, thus its association with podocytes could result from an adhesive property. Actually, the positive net charge of carcinin allows it to interact with many negatively charged surfaces, like bacterial cell walls. However, carcinin's ability to stick to cells such as HCs and podocytes raised the question whether a specific receptor for carcinin exists on these surfaces. The opsonisation effect of carcinin is also linked with its adhesive property that enabled it to attach to both bacterial cells and HCs. This further highlights the value of establishing the three-dimensional structure of carcinin and how this relates to its functions. This would help identify other functional domains present in the carcinin structure, and whether any resemblance exists with other proteins such as complement 3b, thus aiding in explanation of the importance and unique adhesion capability of this peptide.

The chitin-binding property of carcinin, as speculated from PROSITE software, is implicated in its anti-infection ability, tissue regeneration and chitin synthesis. The presence of carcinin in regenerating tissues and in gills of the moulting animal supported this idea. Apart from it being able to protect the soft animal and/or enhance podocyte function at the moulting stage, in addition, carcinin would also protect the

injured, cuticle-free site of the ablated eyestalk. The presence of carcinin in moulting tissues might also support the formation of new cuticle, especially since carcinin signal showed some increase in the hepatopancreas of the moulting animal, which plays an important metabolic role in this stage. However, the chitin-binding ability might be further confirmed via a chitin-binding assay *in vitro*, using the purified native carcinin. In addition, chitin-binding proteins were reported to be anti-fungal (Koo *et al*., 1998), therefore it would be of value to test the ability of carcinin to bind and/or fight fungi, in order to confirm this property as well.

It is also important that although ETosis has been recorded in a number of invertebrate species including the shrimp, carcinin is the only crustin, to date, to be studied during ETosis, despite a large number of AMPs recorded from shrimp species. Although this study could not assign carcinin a major contributory role in ETosis, it gave indications as to its further possible influence in the process.

However, carcinin association with cell death mechanisms remains vague. Carcinin was not shown to bind the extracellular chromatin expelled from ETotic haemocytes *in vitro*. Otherwise, it was detected with the outer membrane of HCs (Figure 7.1), which came in line with its opsonic effect as here too it might function in the clearance of ETotic haemocytes, and supports its association with elimination of damaged and/or defected tissues.

Carcinin in different parts of this project reinforces it as an important molecule for immunity in the crab (Figure 7.1). Its wide distribution and presence varies in critical states of the animal's life. Localisation studies in particular unveiled carcinin's role to a large extent, highlighting the efficiency and value of the methodology conducted in of this study.

However, more confirmation is needed. Carcinin gene silencing could be one approach to assess its biological contribution to different aspects of crustacean immunity. RNA interference (RNAi) has gained more interest recently in studying crustaceans' genes.

Double-stranded RNA (dsRNA)-based RNAi is used for a wide range of immunity studies in shrimp (reviewed by Sagi *et al.*, 2013), most importantly for immunity against viruses (Hirono *et al.*, 2011, Lin *et al.*, 2013), and occasionally to study antibacterials (De la Vega *et al.*, 2008). Some studies have involved silencing of crustin genes in order to elucidate its function *in vivo* (Shockey *et al.*, 2009). The injection of the dsRNA was the main delivery method in this paper, so it might be possible to use the same approach for crab species, after optimization according to organism size. This kind of research would be very useful e to unveil functions of novel peptides, like carcinin.

Finally, this project achieved essential knowledge on the vital role of carcinin for immunity and survival of the animal, and gave more insight of the multifunctionality of WFDC protein as a whole. The utilised methods that depend on the native peptide aided greatly to specifically understand its biological role, in wider and more comprehensive scope than other studied crustins.

The main outcomes of this project can be summarized as the following:

1. Carcinin is an anti-bacterial peptide, produced and stored in granules of the SGCs and GCs of the shore crab *C. maenas*. This project confirmed its role as a secreted protein, released from granulated haemocytes via excocytosis upon exposure to certain immune stimulants.
2. Carcinin exerts its action in the extracellular domain. This study succeeded in identifying the some important targets of its action, most importantly immunological tissues.
3. It is certain from this study that a proportion of immature, pro-haemocytes are positive for carcinin, giving support to the hypothesis that there are two distinct cell lineages.
4. Carcinin revealed a potential significant role in reproductive immunity, most notably in ovaries of the female crabs, and contributes to the sterile and healthy embryonic development.
5. Carcinin was shown to be able to affect the Gram-positive bacteria, *P. citreus*, by inducing pore formation in bacterial cells wall.

6. An important function of carcinin was revealed in this study; carcinin's antibacterial effect is supported by its ability to associate with phagocytic cells such as HCs and podocytes. It also showed a potential role in clearance processes of foreign and defective particles such as bacteria and infected/damaged cells/tissues.
7. An *in vitro* phagocytosis assay confirmed that carcinin acts as an opsonin.
8. The identification of a chitin-binding motif and the localisation of carcinin in chitin-rich structures supports the suggestion that carcinin may participate in formation of new cuticle.

Figure 7.1

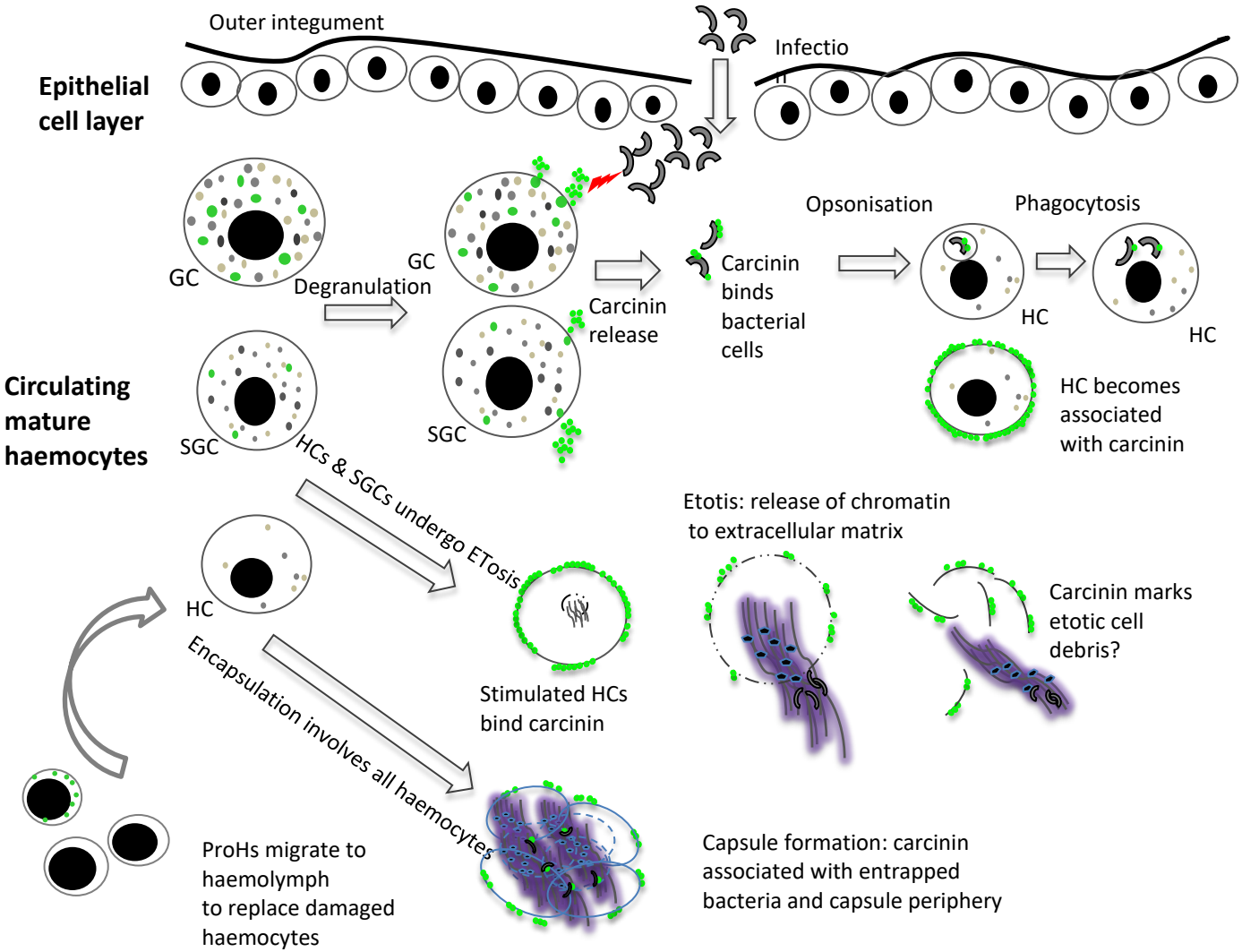
Outer integument
Epithelial cell layer
Infectio
n
GC
Degranulation
GC
Carcinin release
SGC
SGC
Circulating mature haemocytes
Carcinin binds bacterial cells
Opsonisation
Phagocytosis
HC
HC
HC becomes associated with carcinin
HCs & SGCs undergo ETosis
Etotis: release of chromatin to extracellular matrix
HC
Stimulated HCs bind carcinin
Carcinin marks etotic cell debris?
Encapsulation involves all haemocytes
ProHs migrate to haemolymph to replace damaged haemocytes
Capsule formation: carcinin associated with entrapped bacteria and capsule periphery

Figure (7.1): Schematic diagram summarizing the contribution of carcinin to host defence in *C. maenas* haemocytes, according to results from the current project. Following injury, bacterial cells enter circulation and induce degranulation of GCs and SCs, thus releasing carcinin, as well as other proteins. While carcinin can directly attack bacteria and induce pore formation, it also binds bacterial cells and interacts with HCs to increase phagocytosis as an opsonin. Infection also stimulates HCs and SGCs to form extracellular traps. Although carcinin does not decorate the traps themselves, it was observed to bind to the membrane of stimulated HCs. Following the release of extracellular chromatin that traps bacterial cells, carcinin may associate with cellular debris as a possible marker to guide and support phagocytes. Where encapsulation occurs in the gill, all haemocyte types participate in capsule formation to ensnare bacteria. Carcinin is present at all stages of capsule formation, most importantly in the early stages, it deposits on the outer edges of the capsules. In mature capsules, carcinin is present extensively within the capsule, most probably acting as a directly microbicidal agent in the confined area of the structure. Induced by haemocytopenia, immature ProHs migrate to circulation as precursors of HCs, SGCs and GCs. Adapted from Smith and Dyrynda, 2015.

Abi Abdallah, D. S., Lin, C. Y., Ball, C. J., King, M. R., Duhamel, G. E. and Denkers, E. Y. (2012) *Toxoplasma gondii* triggers release of human and mouse neutrophil extracellular traps, *Infection and Immunity*, 80, 768–777.

Afsal, V., Antony, S. P., Sathyan, N. and Philip, R. (2011) Molecular characterization and phylogenetic analysis of two antimicrobial peptides: anti-lipopolysaccharide factor and crustin from the brown mud crab, *Scylla serrata*, *Results in Immunology*, 1(1), 6-10.

Afsal, V., Antony, S. P., Bright, A. R. and Philip, R. (2013) Molecular identification and characterization of Type I crustin isoforms from the hemocytes of portunid crabs, *Scylla tranquebarica* and *Portunus pelagicus*, *Cellular Immunology*, 284(1), 45-50.

Ahyong, S. T., Lowry, J. K., Alonso, M., Bamber, R. N., Boxshall, G. A., Castro, P., Gerken, S., Karaman, G.S., Goy, J. W. and Jones, D. S. (2011) Subphylum Crustacea Brünnich, 1772. In Zhang, Z. Q. *Animal Biodiversity: An Outline of Higher-Level Classification and Survey of Taxonomic Richness*, Auckland, Magnolia Press, 165–191.

Amparyup, P., Kondo, H., Hirono, I., Aoki, T. and Tassanakajon, A. (2008 a) Molecular cloning, genomic organization and recombinant expression of a crustin-like antimicrobial peptide from black tiger shrimp *Penaeus monodon*, *Molecular Immunology*, 45(4), 1085-1093.

Amparyup, P., Donpudsa, S. and Tassanakajon, A. (2008 b) Shrimp single WAP domain (SWD)-containing protein exhibits proteinase inhibitory and antimicrobial activities, *Developmental & Comparative Immunology*, 32(12), 1497-1509.

Andersson, M., Boman, A. and Boman, H. G. (2003) Ascaris nematodes from pig and human make three antibacterial peptides: isolation of cecropin P1 and two ASABF peptides, *Cellular and Molecular Life* Sciences, 60, 599–606.

Andres, E. and Dimarcq, J. L. (2004) Cationic antimicrobial peptides: update of clinical development, *Journal of Internal Medicine*, 255, 519–520.

Andreu, D. and Rivas, L. (1998) Animal antimicrobial peptides: an overview, *Biopolymers,* 47, 415–433.

Antony, S. P., Singh, I. B. and Philip, R. (2010) Molecular characterization of a crustin-like, putative antimicrobial peptide, *Fi*-crustin, from the Indian white shrimp, *Fenneropenaeus indicus*, *Fish & Shellfish Immunology,* 28(1), 216-220.

Antony, S. P., Philip, R., Joseph, V. and Singh, I. B. (2011a) Anti-lipopolysaccharide factor and crustin-III, the anti-white spot virus peptides in *Penaeus monodon*: control of viral infection by up-regulation, *Aquaculture,* 319(1), 11-17.

Antony, S. P., Singh, I. B., Sudheer, N., Vrinda, S., Priyaja, P. and Philip, R. (2011b) Molecular characterization of a crustin-like antimicrobial peptide in the giant tiger shrimp, *Penaeus monodon*, and its expression profile in response to various immunostimulants and challenge with WSSV, *Immunobiology,* 216(1), 184-194.

Arayamethakorn, S., Supungul, P., Tassanakajon, A. and Krusong, K. (2017) Characterization of molecular properties and regulatory pathways of Crustin*Pm*1 and Crustin*Pm*7 from the black tiger shrimp *Penaeus monodon*, *Developmental and Comparative Immunology*, 67, 18-29.

Arockiaraj, J., Gnanam, A. J., Muthukrishnan, D., Gudimella, R., Milton, J., Singh, A., Muthupandian, S., Kasi, M. and Bhassu, S. (2013) Crustin, a WAP domain containing antimicrobial peptide from freshwater prawn *Macrobrachium rosenbergii*: immune characterization, *Fish & Shellfish Immunology,* 34(1), 109-118.

Aspán, A. and Söderhäll, K. (1991) Purification of prophenoloxidase from crayfish blood cells, and its activation by an endogenous serine proteinase, *Insect Biochemistry and Molecular Biology*, 21, 363-373.

Avarre, J.-C., Saulnier, D., Labreuche, Y., Ansquer, D., Tietz, A. and Lubzens, E. (2003) Response of *Penaeus indicus* females at two different stages of ovarian development to a lethal infection with *Vibrio penaeicida*, *Journal of Invertebrate Pathology,* 82(1), 23-33.

Averhoff, P., Kolbe, M., Zychlinsky, A. and Weinrauch, Y. (2008) Single residue determines the specificity of neutrophil elastase for *Shigella* virulence factors, *Journal of Molecular Biology*, 377, 1053–1066.

Bachère, E., Destoumieux, D. and Bulet, P. (2000) Penaeidins, antimicrobial peptides of shrimp: a comparison with other effectors of innate immunity, *Aquaculture*, 191, 71–88.

Banerjee, D., Maiti, B., Girisha, S. K., Venugopal, M. N. and Karunasagar, I. (2015) A crustin isoform from black tiger shrimp, *Penaeus monodon* exhibits broad spectrum anti-bacterial activity, *Aquaculture Reports*, 2, 106-111.

Baranger, K., Zani, M-L., Chandenier, J., Dallet-Choisy, S. and Moreau, T. (2008) The antibacterial and antifungal properties of trappin-2 (pre-elafin) do not depend on its protease inhibitory function, *The FEBS Journal*, 275, 2008–2020.

Bartlett, T. C., Cuthbertson, B. J., Shepard, E. F., Chapman, R. W., Gross, P. S. and Warr, G. W. (2002) Crustins, homologues of an 11.5-kDa antibacterial peptide, from two species of penaeid shrimp, *Litopenaeus vannamei* and *Litopenaeus setiferus*, *Marine Biotechnology*, 4(3), 278-293.

Battison, A. L., Summerfield, R. and Patrzykat, A. (2008) Isolation and characterisation of two antimicrobial peptides from haemocytes of the American lobster *Homarus americanus*, *Fish & Shellfish Immunology*, 25(1), 181-187.

Bechinger, B. (1999) The structure, dynamics and orientation of antimicrobial peptides in membranes by multidimensional solid-state NMR spectroscopy, *Biochimica et Biophysica Acta*, 1462, 157–183.

Bianchi, M., Hakkim, A., Brinkmann, V., Siler, U., Seger, R. A., Zychlinsky, A. and Reichenbach, J. (2009) Restoration of NET formation by gene therapy in CGD controls aspergillosis, *Blood*, 114, 2619–2622.

Bierbaum, G. and Sahl, H. G. (1987) Autolytic system of *Staphylococcus simulans* 22: influence of cationic peptides on activity of N-acetylmuramoyl-L-alanine amidase, *Journal of Bacteriology*, 169, 5452–5458.

Binder, J. X., Pletscher-Frankild, S., Tsafou, K., Stolte, C., O'Donoghue, S. I., Schneider, R. and Jensen, L. J. (2014) COMPARTMENTS: unification and visualization of protein subcellular localization evidence, *Database*, 2014, bau012.

Bingle, C. D. and Vyakarnam, A. (2008) Novel innate immune functions of the whey acidic protein family, *Trends in Immunology*, 29, 444–453.

Bingle, C. D. (2011) Towards defining the complement of mammalian WFDC-domain-containing proteins, *Biochemical Society Transactions*, 39, 1393–1397.

Bingle, L., Tetley, T. D. and Bingle, C. D. (2001) Cytokine-mediated induction of the human elafin gene in pulmonary epithelial cells is regulated by nuclear factor-kappaB, *American Journal of Respiratory Cell and Molecular Biology*, 25, 84–91.

Bingle, L., Singleton, V. and Bingle, C. D. (2002) The putative ovarian tumour marker gene HE4 (WFDC2), is expressed in normal tissues and undergoes complex alternative splicing to yield multiple protein isoforms, *Oncogene*, 21, 2768–2773.

Bingle, L., Cross, S. S., High, A. S., Wallace, W. A., Rassl, D., Yuan, G., Hellstrom, I., Campos, M. A. and Bingle. C. D. (2006) WFDC2 (HE4): a potential role in the innate immunity of the oral cavity and respiratory tract and the development of adenocarcinomas of the lung, *Respiratory Research*. 7, 61.

Bliss, D. E. and Boyer, J. R. (1964) Environmental regulation of growth in the decapod crustacean *Gecarcinus lateralis*, *General and Comparative Endocrinology*, 4, 15–41.

Bodén, M. and Hawkins, J. (2005) Prediction of subcellular localisation using sequence-biased recurrent networks, *Bioinformatics*, 21(10), 2279-2286,

Boman, H. G. (1995) Peptide antibiotics and their role in innate immunity, *Annual Review of Immunology*, 13, 61–92.

Bradford, M. M. (1976) A rapid and sensitive method for the quantitation of microgram quantities of protein utilizing the principle of protein-dye binding, *Analytical Biochemistry*, 72(1-2), 248-254.

Briggs, D. (1978) The morphology, mode of life, and affinities of *Canadaspis perfecta* (Crustacea: Phyllocarida), Middle Cambrian, Burgess Shale, British Columbia, *Philosophical Transactions of the Royal Society B,* 281(984), 439–487.

Brinkmann, V., Reichard, U., Goosmann, C., Fauler, B., Uhlemann, Y. and Weiss, D. S. (2004) Neutrophil extracellular traps kill bacteria, *Science,* 303, 1532–1535.

Brinkmann, V. and Zychlinsky, A. (2012) Neutrophil extracellular traps: is immunity the second function of chromatin?, *Journal of Cell Biology,* 198(5), 773–783.

Brites, D., McTaggart, S., Morris, K., Anderson, J., Thomas, K., Colson, I., Fabbro, T., Little, T.J., Ebert, D. and Du Pasquier, L. (2008) The Dscam homologue of the crustacean *Daphnia* is diversified by alternative splicing like in insects, *Molecular Biology and Evolution,* 25, 1429–1439.

Brockton, V., Hammond, J. A. and Smith, V. J. (2007) Gene characterisation, isoforms and recombinant expression of carcinin, an antibacterial protein from the shore crab, *Carcinus maenas*, *Molecular Immunology,* 44(5), 943-949.

Brockton, V. and Smith, V. J. (2008) Crustin expression following bacterial injection and temperature change in the shore crab, *Carcinus maenas, Developmental & Comparative Immunology,* 32(9), 1027-1033.

Brogden, K. A., De Lucca, A. J., Bland, J. and Elliott, S. (1996) Isolation of an ovine pulmonary surfactant-associated anionic peptide bactericidal for *Pasteurella haemolytica, Proceedings of the National Academy of Sciences of the United States of America,* 93, 412–416.

Brogden, K. A. (2005) Antimicrobial peptides: pore formers or metabolic inhibitors in bacteria?, *Nature Reviews Microbiology,* 3(3), 238-250.

Brotz, H., Bierbaum, G., Leopold, K., Reynolds, P. E. and Sahl, H. G. (1998) The lantibiotic mersacidin inhibits peptidoglycan synthesis by targeting lipid II, *Antimicrobial Agents and Chemotherapy*, 42, 154–160

Browdy, C.L., (1988) Aspects of the reproductive biology of *Penaeus semisulcatus de Haan*' (Crustacea; Decapoda; Penaeidae), Ph.D. Thesis, Tel Aviv University, Israel, 138 p.

Burgess, R. R., Richard, R. B. and Murray, P. D. (2009) Refolding solubilized inclusion body proteins, *Methods in Enzymology*, 463(11), 259-282.

Campos, A., Puerto, M., Prieto, A., Camean, A., Almeida, A. M., Coelho, A. V. and Vasconcelos, V. (2013) Protein extraction and two-dimensional gel electrophoresis of proteins in the marine mussel *Mytilus galloprovincialis*: an important tool for protein expression studies, food quality and safety assessment, *Journal of the Science of Food and Agriculture*, 93(7), 1779-87.

Casadio, R., Martelli, P. L., Pierleoni, A. (2008) The prediction of protein subcellular localization from sequence: a shortcut to functional genome annotation, *Briefings in Functional Genomics & Proteomics*, 7(1), 63-73.

Cavallaro, A. S., Mahony, D., Commins, M., Mahony, T. J. and Mitter, N. (2011) Endotoxin-free purification for the isolation of Bovine Viral Diarrhoea Virus E2 protein from insoluble inclusion body aggregates, *Microbial Cell Factories*, 10(1), 57.

Cerenius, L, Söderhäll, K. (2004) The prophenoloxidase-activating system in invertebrates', *Immunological Reviews*, 198, 72-82.

Cerenius, L., Jiravanichpaisal, P., Liu, H. and Söderhäll, I. (2010) Crustacean immunity, In Söderhäll, K. *Invertebrate Immunity*, New York, Landes Biosciences/Springer Biosciences+Business Media: 239-259.

Chandramouli, K. (2016) Marine Proteomics: Challenges and Opportunities, *Journal of Data Mining in Genomics and Proteomics*, 7, e122.

Chang, E. S. and Bruce, M. J. (1980) Ecdysteroid titers of juvenile lobsters following molt induction, *Journal of Experimental Zoology*, 214(2), 157-160.

Chang, E. S. (1995) Physiological and biochemical changes during the molt cycle in decapod crustaceans: an overview, *Journal of Experimental Marine Biology and Ecology*, 193(1), 1-14.

Chang, E. S. and Mykles, D. L. (2011) Regulation of crustacean molting: a review and our perspectives, *General and Comparative Endocrinology*, 172(3), 323-330.

Chang, Y.-T., Lin, C.-Y., Tsai, C.-Y., Siva, V.S., Tsai, H.-J. and Song, Y.-L. (2013) The new face of the old molecules: crustin *Pm*4 and transglutaminase Type I serving as RNPs down-regulate astakine-mediated hematopoiesis, *PLoS One* 2793.

Chen, D., He, N. and Xu, X. (2008) *Mj*-DWD, a double WAP domain-containing protein with antiviral relevance in *Marsupenaeus japonicus*, *Fish & Shellfish Immunology*, 25(6), 775-781.

Chen, J. Y., Chuang, H., Pan, C. Y. and Kuo, C. M. (2005) cDNA sequence encoding an antimicrobial peptide of chelonianin from the tiger shrimp, *Penaeus monodon*, *Fish & Shellfish Immunology*, 18, 179–183

Chen, Y., Mu, X., Wang, S., Zhao, L., Wu, Y., Li, J. and Li, M. (2013) WAP four-disulfide core domain protein 2 mediates the proliferation of human ovarian cancer cells through the regulation of growth-and apoptosis-associated genes, *Oncology Reports*, 29, 288-296.

Cheung, R. C. F., Ng, T, B. and Wong, J. H. (2015) Marine peptides: bioactivities and applications, *Marine Drugs*, 13, 4006–4043.

Chhikara, N., Saraswat, M., Tomar, A. K., Dey, S., Singh, S. and Yadav, S. (2012) Human epididymis protein-4 (HE-4): a novel cross-class protease inhibitor, *PLoS One*, 7, e47672.

Chiou, T.-T., Lu, J.-K., Wu, J.-L., Chen, T. T., Ko, C.-F. and Chen, J.-C. (2007) Expression and characterisation of tiger shrimp *Penaeus monodon* penaeidin (mo-penaeidin) in various tissues, during early embryonic development and moulting stages, *Developmental & Comparative Immunology*, 31(2), 132-142.

Chisholm, J.R.S. and Smith, V. J. (1992) Antibacterial activity in the haemocytes of the shore crab, *Carcinus maenas, Journal of the Marine Biological Association of the United*
Kingdom, 72, 529–542.

Chou, P.-H., Chang, H.-S., Chen, I.-T., Lin, H.-Y., Chen, Y.-M., Yang, H.-Y. and Wang, K.C. (2009) The putative invertebrate adaptive immune protein *Litopenaeus vannamei* Dscam (*Lv*Dscam) is the first reported Dscam to lack a transmembrane domain and cytoplasmic tail, *Developmental and Comparative Immunology*, 33, 1258–1267.

Chou, P.-H., Chang, H.-S., Chen, I.-T., Lee, C.-W., Hung, H.-Y. and Wang, K.C. (2011) *Penaeus monodon* Dscam (*Pm*Dscam) has a highly diverse cytoplasmic tail and is the first membrane-bound shrimp Dscam to be reported, *Fish & Shellfish Immunology*, 30, 1109–1123.

Christie, A. E., Rus, S., Goiney, C. C., Smith, C. M., Towle, D. W. and Dickinson, P. S. (2007) Identification and characterization of a cDNA encoding a crustin-like, putative antibacterial protein from the American lobster *Homarus americanus*, *Molecular Immunology*, 44, 3333-3337.

Clark, K. F., Acorn, A. R. and Greenwood, S. J. (2013) Differential expression of American lobster (*Homarus americanus*) immune related genes during infection of *Aerococcus viridans var. homari*, the causative agent of Gaffkemia, *Journal of Invertebrate Pathology*, 112, 192-202.

Clark, K., Karsch-Mizrachi, I., Lipman, D. J., Ostell, J. and Sayers, E. W. (2016) GenBank. *Nucleic Acids Res*. 44(D1):D67-72.

Clauss, A., Lilja, H. and Lundwall, A. (2002) A locus on human chromosome 20 contains several genes expressing protease inhibitor domains with homology to whey acidic protein, *Biochemical Journal*, 368, 233–242.

Coles, J. A., Farley, S. R. and Pipe, R. K. (1995) Alteration of the immune response of the common marine mussel *Mytilus edulis* resulting from exposure to cadmium, *Diseases of Aquatic Organisms*, 22, 59–65.

Couto, M. A., Harwig, S. S. L. and Lehrer, R. I. (1993) Selective inhibition of microbial serine proteases by eNAP-2, an antimicrobial peptide from equine neutrophils, *Infection and Immunity*, 61, 2991-2994.

Covich, A. P. and Thorp, J. H. (1991) Crustacea: Introduction and Peracarida, In James, H. Thorp, J. H. and Covich, A. P., *Ecology and Classification of North American Freshwater Invertebrates* (1st ed.), San Diego, Academic Press, 665–722.

Crothers, J.H. (1967) The biology of the shore crab *Carcinus maenas* (L.) 1. The background-anatomy, growth and life history, *Field Studies*, 2, 407-434.

Crothers, J.H. (1968) The biology of the shore crab *Carcinus maenas* (L.) 2. The life of the adult crab, *Field Studies*, 2, 579-614.

Cui, Z., Song, C., Liu, Y., Wang, S., Wang, Q.L. and Li, X. (2012) Crustins from eyestalk cDNA library of swimming crab Portunus trituberculatus: molecular characterization, genomic organization and expression analysis, *Fish & Shellfish Immunology*, 33, 937–945.

Curvelo, J. A., Barreto, A. L., Portela, M. B., Alviano, D. S., Holandino, C., Souto-Padrón, T. and Soares, R. M. (2014) Effect of the secretory leucocyte proteinase inhibitor (SLPI) on *Candida albicans* biological processes: A therapeutic alternative?, Archives of Oral Biology, 59 (9), 928-937.

De Castro E., Sigrist, C. J. A., Gattiker, A., Bulliard, V., Langendijk-Genevaux, P. S., Gasteiger, E., Bairoch, A. and Hulo, N. (2006) ScanProsite: detection of

PROSITE signature matches and ProRule-associated functional and structural residues in proteins, *Nucleic Acids Research*, 1;34.

De la Vega, E., O'Leary, N. A., Shockey, J. E., Robalino, J., Payne, C., Browdy, C. L., Warr, G. W. and Gross, P. S. (2008) Anti-Lipopolysaccharide factor in *Litopenaeus vannamei* (*Lv*ALF): A broad spectrum antimicrobial peptide essential for shrimp immunity against bacterial and fungal infection, *Molecular Immunology*, 45, 1916–1925.

De Pourcq, K., De Schutter, K. and Callewaert, N. (2010) Engineering of glycosylation in yeast and other fungi: current state and perspectives, *Applied Microbiology and Biotechnology*, 87(5), 1617-1631.

Desai, U. M. and Achuthankutty, C. Y. (2000) Complete regeneration of ablated eyestalk in penaeid prawn, *Penaeus monodon*, *Current Science*, 79, 10-11.

Desbois, A. P. and Smith, V. J. (2010) Antibacterial free fatty acids: activities, mechanisms of action and biotechnological potential, *Applied Microbiology and Biotechnology*, 85, 1629–1642.

Destoumieux, D., Bulet, P., Loew, D., van Dorsselaer, A., Rodriguez, J. and Bachère, E. (1997) Penaeidins, a new family of antimicrobial peptides isolated from the shrimp *Penaeus vannamei* (decapoda). *Journal of Biological Chemistry*, 272, 28398–28406.

Destoumieux, D., Muñoz, M., Cosseau, C., Rodriguez, J., Bulet, P., Comps, M., Bachère, E. (2000) Penaeidins, antimicrobial peptides with chitin-binding activity, are produced and stored in shrimp granulocytes and released after microbial challenge, *Journal of Cell Science*, 113, 461-469.

Destoumieux-Garzon, D., Rosa, R. D., Schmitt, P., Barreto, C., Vidal-Dupiol, J., Mitta, G., Gueguen, Y. and Bachère, E. (2016) Antimicrobial peptides in marine invertebrate health and disease, *Philosophical Transactions of the Royal Society B*, 371, 20150300.

Diamond, G., Zasloff, M., Eck, H., Brasseur, M., Maloy, W. L. and Bevins, C. L. (1991) Tracheal antimicrobial peptide, a cysteine-rich peptide from mammalian tracheal

mucosa: peptide isolation and cloning of a cDNA, *Proceedings of the National Academy of Sciences*, 88(9), 3952-3956.

Doley, R., Pahari, S., Resa, M. A., Mackessy, S. P. and Kini, R. M. (2010) The gene structure and evolution of ku-wap-fusin (Kunitz waprin fusion) protein, a novel evolutionary intermediate of the Kunitz serine protease inhibitors and waprins from *Sistrurus catenatus* (Massasauga rattlesnake) venom glands, *The Open Evolution Journal*, 4, 31–41.

Donpudsa, S., Rimphanitchayakit, V., Tassanakajon, A., Söderhäll, I. and Söderhäll, K. (2010) Characterization of two crustin antimicrobial peptides from the freshwater crayfish *Pacifastacus leniusculus*, *Journal of Invertebrate Pathology*, 104, 234–238.

Donpudsa, S., Visetnan, S., Supungul, P., Tang, S., Tassanakajon, A. and Rimphanitchayakit, V. (2014) Type I andType II crustins from *Penaeus monodon*, genetic variation and antimicrobial activity of the most abundant crustin *Pm*4, *Developmental and Comparative Immunology*, 47, 95–103.

Dorange G, Le Pennec MLE (1989) Ultrastructural study of oogenesis and oocytic degeneration in *Pecten maximus* from the Bay of St. Brieuc, *Marine Biology*, 103, 339-348.

Doughtie, D. G. and Rao, K. R. (1981) The syncytial nature and phagocytic activity of the branchial podocytes in the grass shrimp, *Palaemonetes pugio*, *Tissue and Cell*, 13(1), 93-104.

Du, Z.-Q., Ren, Q., Zhao, X.-F. and Wang, J.-X. (2009) A double WAP domain (DWD)-containing protein with proteinase inhibitory activity in Chinese white shrimp, *Fenneropenaeus chinensis*, *Comparative Biochemistry and Physiology Part B: Biochemistry and Molecular Biology*, 154(2), 203-210.

Du, Z.-Q., Li, X.-C., Wang, Z.-H., Zhao, X.-F. and Wang, J.-X. (2010) A single WAP domain (SWD)-containing protein with antipathogenic relevance in red swamp crayfish, *Procambarus clarkii*, *Fish & Shellfish Immunology*, 28(1), 134-142.

Du, Z.-Q., Yuan, J. J. and Ren, D-A. (2015) A novel single WAP domain-containing protein isoform with antibacterial relevance in *Litopenaeus vannamei*, *Fish & Shellfish Immunology*, 44, 478–484.

Durica, D. S., Kupfer, D., Najar, F., Lai, H., Tang, Y., Griffin, K., Hopkins, P. M. and Roe, B. (2006) EST library sequencing of genes expressed during early limb regeneration in the fiddler crab and transcriptional responses to ecdysteroid exposure in limb bud explants, *Integrative and Comparative Biology*, 46(6), 948-964.

Duvic, B. and Söderhall, K. (1990) Purification and characterization of a beta-1,3-glucan binding-protein from plasma of the crayfish *Pacifastacus leniusculus*, *Journal of Biological Chemistry*, 265, 9327-9332.

Ehrenstein, G. and Lecar, H. (1977) Electrically gated ionic channels in lipid bilayers, *Quarterly Reviews of Biophysics*, 10, 1–34.

Eisenberg, S.P., Hale, K. K., Heimdal, P. and Thompson, R. C. (1990) Location of the protease-inhibitory region of secretory leukocyte protease inhibitor, *Journal of Biological Chemistry*, 265, 7976–7981.

Emes, R. D., Goodstadt, L., Winter, E. E., Ponting, C. P. (2003) Comparison of the genomes of human and mouse lays the foundation of genome zoology, *Human Molecular Genetics*, 12, 701–709

Fagutao, F. F., Maningas, M. B. B., Kondo, H., Aoki, T. and Hirono, I. (2012) Transglutaminase regulates immune-related genes in shrimp, *Fish & Shellfish Immunology*, 32, 711–715.

Fahey, J. V., and Wira, C. R. (2002) Effect of menstrual status on antibacterial activity and secretory leukocyte protease inhibitor production by human uterine epithelial cells in culture, *The Journal of Infectious Diseases*, 185, 1606-1613.

Fahrner, R. L, Dieckmann, T., Harwig, S. S., Lehrer, R. I., Eisenberg, D. and Feigot, J. (1996) Solution structure of protegrin-1, a broad-spectrum antimicrobial peptide from porcine leukocytes, *Chemistry & Biology*, 3, 543-550

Farrera, C. and Fadeel, B. (2013) Macrophage clearance of neutrophil extracellular traps is a silent process, *Journal of Immunology*, 191, 2647-2656.

Fernandes, J. M., Molle, M. G. and Smith, V. J. (2002) Anti-microbial properties of histone H2A from skin secretions of rainbow trout, *Oncorhynchus mykiss*, *Biochemical Journal*, 368(2), 611-620.

Fernandez, R. and Radhakrishnan, E. (2016) Effect of bilateral eyestalk ablation on ovarian development and moulting in early and late intermoult stages of female spiny lobster *Panulirus homarus* (Linnaeus, 1758), *Invertebrate Reproduction & Development*, 60(3), 238-242.

Ferreira, Z., Seixas, S., Andrés, A. M., Kretzschmar, W. W., Mullikin, J. C., Cherukuri, P. F., Cruz, P., Swanson, W. J., Clark, A. G., Green, E. D. and Hurle. B. (2013) Reproduction and immunity-driven natural selection in the human WFDC locus, *Molecular Biology and Evolution*, 30, 938–950.

Fingerman, M. (1997) Roles of neurotransmitters in regulating reproductive hormone release and gonadal maturation in decapod crustaceans, *Invertebrate Reproduction & Development*, 31(1-3), 47-54.

Fischer, E. R., Hansen, B. T., Nair, V., Hoyt, F. H. and Dorward, D. W. (2012) Scanning Electron Microscopy, *Current Protocols in Microbiology*, 25:B:2B.2:2B.2.1–2B.2.47..

Fleming, A. and Allison, V. (1922) Observations on a bacteriolytic substance (‘lysozyme’) found in secretions and tissues, *British Journal of Experimental Pathology*, 3(5), 252.

Forest, J., Laurent, M. de S., McLaughlin, P. A. and Lemaitre, R. (2000) The marine fauna of New Zealand: Paguridea (Decapoda: Anomura) exclusive of the Lithodidae. Wellington, New Zealand: *National Institute of Water and Atmospheric Research*.

Francart, C., Dauchez, M., Alix, A. J. and Lippens, G. (1997) Solution structure of R-elafin, a specific inhibitor of elastase, *Journal of Molecular Biology*, 268, 666–677.

Frohm, M., Gunne, H., Bergman, A-C., Agerberth, B., Bergman, T., Boman, A., Liden, S., Jornvall, H., Boman, H. G. (1996) Biochemical and antibacterial analysis of human wound and blister fluid, *European Journal of Biochemistry*, 237, 86–92.

Fu, H., Karlsson, J., Bylund, J., Movitz, C., Karlsson, A. and Dahlgren, C. (2006) Ligand recognition and activation of formyl peptide receptors in neutrophils, *Journal of Leukocyte Biology*, 79(2), 247-256.

Galgano, M. T., Hampton, G. M. and Frierson, H. F. (2006) Comprehensive analysis of HE4 expression in normal and malignant human tissues, *Modern Pathology*, 19, 847-853.

Ganz, T., Selsted, M. E., Szklarek, D., Harwig, S. S, Daher, K., Bainton, D. F. and Lehrer, R. I. (1985) Defensins. Natural peptide antibiotics of human neutrophils, *The Journal of Clinical Investigations*, 76 (4), 1427-1435.

Ganz, T. (2003) The role of antimicrobial peptides in innate immunity, *Integrative and Comparative Biology*, 43(2), 300-304.

García, J. C., Reyes, A., Salazar, M. and Granja, C. B. (2009) Differential gene expression in White Spot Syndrome Virus (WSSV)-infected naïve and previously challenged Pacific white shrimp *Penaeus (Litopenaeus) vannamei*, *Aquaculture*, 289, 253–258.

Gaulejac de, J., Henry, M., Vicente, N. (1995) An ultrastructural study of gametogenesis of the marine bivalve *Pinna nobilis* (Linnaeus,1758) 1. Oogenesis, *Journal of Molluscan Studies*, 6, 375-392.

Graveley, B. R. (2001) Alternative splicing: increasing diversity in the proteomic world, *Trends in Genetics*, 17, 100–107.

Guezennec, J., Simon-Colin, C., Kouzayha, A., Gueguen, Y. and Bachere, E. (2013) Nucleus coated with a film-forming coating having antibacterial and cicatrizing properties and the method for obtaining same, *U.S. Patent*, 20130152865.

Guyot, N., Zani, M.-L., Maurel, M-C., Dallet-Choisy, S. and Moreau, T. (2005) Elafin and its precursor trappin-2 still inhibit neutrophil serine proteinases when they are covalently bound to extracellular matrix proteins by tissue transglutaminase, *Biochemistry*, 44, 15610–15618.

Hall, M., Vanheusden, M. and Söderhäll, K. (1995) Identification of the major lipoproteins in crayfish hemolymph as proteins involved in immune recognition and clotting, *Biochemical and Biophysical Research Communications*, 216(3), 939-946.

Hallock, K. J., Lee, D. K. and Ramamoorthy, A. (2003) MSI-78, an analogue of the magainin antimicrobial peptides, disrupts lipid bilayer structure via positive curvature strain, *Biophysical Journal*, 84, 3052–3060.

Harrison, R. L. and Jarvis, D. L. (2006) Protein N-glycosylation in the baculovirus-insect cell expression system and engineering of insect cells to produce ‘mammalianized’ recombinant glycoproteins, *Advances in Virus Research*, 68, 159-191.

Hartung. H. P. and Hadding. U. (1983) Complement components in relation to macrophage function, *Agents and Actions*, 13(5-6), 415-28.

Hassan, M. A., Butty, V. and Jensen, K. D. (2014) The genetic basis for individual differences in mRNA splicing and APOBEC1 editing activity in murine macrophages, *Genome Research*, 24, 377-389.

Hauton, C., Williams, J. A. and Hawkins, L. E. (1997) The effects of a live *in vivo* pathogenic infection on aspects of the immunocompetence of the common shore crab, *Carcinus maenas* (L.) *Journal of Experimental Marine Biology and Ecology*, 211 (1), 115-128.

Hauton, C., Brockton, V. and Smith, V. (2006) Cloning of a crustin-like, single whey-acidic-domain, antibacterial peptide from the haemocytes of the European lobster, *Homarus gammarus*, and its response to infection with bacteria, *Molecular Immunology*, 43(9), 1490-1496.

Hauton, C. (2012) The scope of the crustacean immune system for disease control, *Journal of Invertebrate Pathology*, 111(1), 251-260.

Havanapan, P.-O., Taengchaiyaphum, S., Bourchookarn, A., Ketterman, A. J. and Krittanai, C. (2014) Yellow head virus binding to cell surface proteins from *Penaeus monodon* hemocytes, *Fish & Shellfish Immunology,* 41(2), 126-136.

He, S. H., Chen, P. and Chen, H. Q. (2003) Modulation of enzymatic activity of human mast cell tryptase and chymase by protease inhibitors, *Acta Pharmaceutica Sinica B*, 24, 923-929.

Heath, J. and Barnes, H. (1970) Some changes in biochemical composition with season and during the moulting cycle of the common shore crab, *Carcinus maenas* (L.), *Journal of Experimental Marine Biology and Ecology*, 5(3), 199-233.

Hellström, I., Raycraft, J., Hayden-Ledbetter, M., Ledbetter, J. A., Schummer, M., McIntosh, M., Drescher, C., Urban, N. and Hellström, K.E. (2003) The HE4 (WFDC2) protein is a biomarker for ovarian carcinoma, *Cancer Research*, 63, 3695-3700.

Hemmi, H., Ishibashi, J., Tomie, T. and Yamakawa, M. (2003) Structural basis for new pattern of conserved amino acid residues related to chitin-binding in the antifungal peptide from the coconut rhinoceros beetle *Oryctes rhinoceros*, *Journal of Biological Chemistry*, 278(25), 22820-22827.

Hennighausen, L. G. and Sippel, A. E. (1982) Mouse whey acidic protein is a novel member of the family of 'four-disulfide core' proteins, *Nucleic Acids Research*, 10(8), 2677-2684.

Hipolito, S. G., Shitara, A., Kondo, H. and Hirono, I. (2014) Role of *Marsupenaeus japonicus* crustin-like peptide against *Vibrio penaeicida* and white spot syndrome virus infection, *Developmental & Comparative Immunology*, 46(2), 461-469.

Hirono, I., Fagutao, F. F., Kondo, H. and Aoki, T. (2011) Uncovering the mechanisms of shrimp innate immune response by RNA interference, *Marine Biotechnology*, 13, 622–628.

Hirsch, J. G. (1956) Phagocytin: a bactericidal substance from polymorphonuclear leucocytes, *Journal of Experimental Medicine*, 103, 589–611.

Hirsch, J. G. (1958) Bactericidal action of histone, *Journal of Experimental Medicine*, 108, 925–944.

Hofman, F. M. and Taylor, C. R. (2013). Immunohistochemistry. *Current Protocols in Immunology*. 103 (21), 1–21.

Hong, M. L. W., Jiang, N., Gopinath, S. and Chew, F. T. (2006) Proteomics technology and therapeutics, *Clinical and Experimental Pharmacology and Physiology*, 33(5-6), 563-568.

Hopkins, P. M. (2001) Regeneration in crustaceans and insects, http://www.els.net .

Hopkins, P. M. and Das, S. (2015) Regeneration in Crustaceans, *The Natural History of the Crustacea*, 4, 168-198.

Hossler, P., Khattak, S. F. and Li, Z. J. (2009) Optimal and consistent protein glycosylation in mammalian cell culture, *Glycobiology*, 19, 936-949.

Hua, L., Liu, Y., Zhen, S., Wan, D., Cao, J. and Gao, X. (2014) Expression and biochemical characterization of recombinant human epididymis protein 4, *Protein Expression and Purification*, 102, 52–62.

Huang, H. W. (2004) Molecular mechanism of peptide induced pores in membranes, *Physical Review Letters*, 92, 198304-1 – 198304-4.

Huang, T. S., Wang, H., Lee, S. Y., Johansson, M. W., Söderhäll, K. and Cerenius, L. (2000) A cell adhesion protein from the crayfish, *Pacifastacus leniusculus*, a serine proteinase homologue similar to *Drosophila* masquerade, *Journal of Biological Chemistry*, 275, 9996-10001

HUGO Gene Nomenclature Committee at the European Bioinformatics Institute, https://www.genenames.org

Idiris, A., Tohda, H., Kumagai, H. and Takegawa, K. (2010) Engineering of protein secretion in yeast: strategies and impact on protein production, *Applied Microbiology and Biotechnology*, 86(2), 403-417.

Imjongjirak, C., Amparyup, P., Tassanakajon, A. and Sittipraneed, S. (2009) Molecular cloning and characterization of crustin from mud crab *Scylla paramamosain*, *Molecular Biology Reports*, 36(5), 841-850.

Inagaki, H. (2015) Snake venom protease inhibitors: enhanced identification, expanding biological function and promising future. In: Gopalakrishnakone, P., Inagaki, H., Vogel, C-W., Mukherjee, A. K., Rahmy, T. R. *Snake Venoms*. Dordrecht: Springer Netherlands. 161-186.

Janeway, C. A. Jr. and Medzhitov, R. (2002) Innate immune recognition, *Annual Review of Immunology*, 20, 197–216.

Jayesh, P., Sruthy, K., Singh, I. B. and Philip, R. (2016) Recombinant expression and functional characterization of antimicrobial peptide crustin from *Artemia salina*, *Fish & Shellfish Immunology*, 53, 119.

Jia, Y.-P., Sun, Y.-D., Wang, Z.-H., Wang, Q., Wang, X.-W., Zhao, X.-F. and Wang, J.-X. (2008) A single whey acidic protein domain (SWD)-containing peptide from fleshy prawn with antimicrobial and proteinase inhibitory activities, *Aquaculture*, 284(1), 246-259.

Jiang, H., Sun, C., Wang, T., Zhao, X. and Wang, J. (2013) A single whey acidic protein domain containing protein (SWD) inhibits bacteria invasion and dissemination in shrimp *Marsupenaeus japonicas*, *Fish & Shellfish Immunology*, 35, 310-318.

Jiang, H.-S., Zhang, Q., Zhao, Y.-R., Jia, W.-M., Zhao, X.-F. and Wang, J.-X. (2015) A new group of anti-lipopolysaccharide factors from *Marsupenaeus japonicas* functions in antibacterial response. *Developmental and Comparative Immunology*, 48, 33–42.

Jiravanichpaisal, P., Lee, B. L. and Söderhäll, K. (2006) Cell-mediated immunity in arthropods: hematopoiesis, coagulation, melanization and opsonization, *Immunobiology*, 221 (4), 231-236.

Jiravanichpaisal, P., Lee, S. Y., Kim, Y. A., Andren, T. and Söderhäll, I. (2007) Antibacterial peptides in hemocytes and hematopoietic tissue from freshwater crayfish *Pacifastacus leniusculus*: characterization and expression pattern, *Developmental and Comparative Immunology*, 31, 441–455.

Johansson, M. W. and Söderhäll, K. (1988) Isolation and purification of a cell adhesion factor from crayfish blood cells, *Journal of Cell Biology*, 106, 1795-1803

Johansson, M. W. and Söderhäll, K. (1989) Cellular immunity in crustaceans and the proPO system, *Parasitology Today*, 5, 171-176

Johansson, M. W, Lind, M. I., Holmbald, P., Thörnqvist, P. O. and Söderhäll, K. (1995) Peroxinectin, a novel cell adhesion protein from crayfish blood, *Biochemical and Biophysical Research Communications*, 216, 1079-1087.

Johansson, M.W. (1999) Cell adhesion molecules in invertebrate immunity, *Developmental & Comparative Immunology*, 23, 303–315.

Johnson, P. T. (1980) The histology of the blue crab *Callinectes sapidus*, a model for the decapoda, New York, Praeger Publishers.

Jong-Brink, M., Boer, H. H. and Joosse, J. (1983) Mollusca, In: Adiyodi, K. G., Adiyodi, R. G. *Reproductive Biology of Invertebrates*. Vol. 1. John Wiley & Sons Ltd, New York, 297–355.

Jones, D. E. and Bevins, C. L. (1992) Paneth cells of the human small intestine express an antimicrobial peptide gene, *Journal of Biological Chemistry*, 267(32), 23216-23225.

Kamei, M., Yamashita, S.-I., Tokuishi, K., Hashioto, T., Moroga, T., Suehiro, S., Ono, K., Miyawaki, M., Takeno, S., Yamamoto, S. and Kawahara, K. (2010) HE4 expression can be associated with lymph node metastases and disease-free survival in breast cancer, *Anticancer Research*, 30, 4779–4783.

Kang, S., Park, S., Mishig-Ochir, T. and Lee, B. (2014) Antimicrobial peptides: therapeutic potentials, *Expert Review of Anti-infective Therapy*, 12, 1477–1486.

Kawabata, S.-i., Nagayama, R., Hirata, M., Shigenaga, T., Agarwala, K. L., Saito, T., Cho, J., Nakajima, H., Takagi, T. and Iwanaga, S. (1996) Tachycitin, a small granular component in horseshoe crab hemocytes, is an antimicrobial protein with chitin-binding activity, *Journal of Biochemistry*, 120(6), 1253-1260.

Khalaila, I., Manor, R., Weil, S., Granot, Y., Keller, R. and Sagi, A. (2002) The eyestalk–androgenic gland–testis endocrine axis in the crayfish *Cherax quadricarinatus*, *General and Comparative Endocrinology*, 127(2), 147-156

Kilada, R., Sainte-Marie, B., Rochette, R., Davis, N., Vanier, C. and Campana, S. (2012) Direct determination of age in shrimps, crabs, and lobsters, *Canadian Journal of Fisheries and Aquatic Sciences*, 69(11), 1728-1733.

Kim, B., Kim, M., Kim, A. R., Yi, M., Choi, J-H., Park, H., Park, W. and Kim, H. W. (2013) Differences in gene organization between type I and type II crustins in the morotoge shrimp, *Pandalopsis japonica*, *Fish & Shelfish Immunology*, 35, 1176-1184.

Kim, M., Jeon, J.-M., Oh, C.-W., Kim, Y. M., Lee, D. S., Kang, C.-K. and Kim, H.-W. (2012) Molecular characterization of three crustin genes in the morotoge shrimp,

Pandalopsis japonica, *Comparative Biochemistry and Physiology Part B: Biochemistry and Molecular Biology*, 163(2), 161-171.

Kim, S. H., Chung, E.-Y. and Lee, K.-Y. (2014) Oocyte degeneration associated with follicle cells in female *Mactra chinensis* (Bivalvia: Mactridae), *Development & Reproduction*, 18(4), 321-327.

Kobayashi, M. M., Johansson, M. W. and Söderhäll, K. (1990) The 76 kDa cell adhesion factor from crayfish hemocytes promotes encapsulation *in vitro*, *Cell and Tissue Research*, 260, 13-18.

Kollewe, C. and Vilcinskas, A. (2013) Production of recombinant proteins in insect cells, *American Journal of Biochemistry and Biotechnology*, 9(3), 255-271.

Koo, J. C., Lee, S. Y., Chun, H. J., Cheong, Y. H., Choi, J. S., Kawabata, S., Miyagi, M., Tsunasawa, S., Ha, K. S., Bae, D. W., Han, C. D., Lee, B. L. and Cho, M. J. (1998) Two hevein homologs isolated from the seed of *Pharbitis nil* L. exhibit potent antifungal activity, *Biochimica et Biophysica Acta*, 1382, 80–90.

Krusong, K., Poolpipat, P., Supungul, P. and Tassanakajon, A. (2012) A comparative study of antimicrobial properties of crustinPm1 and crustinPm7 from the black tiger shrimp *Penaeus monodon*, *Developmental and Comparative Immunology*, 36 (1), 208-215.

Kuballa, A. V. and Elizur, A. (2008) Differential expression profiling of components associated with exoskeletal hardening in crustaceans, *BMC Genomics*, 9:575.

Kuwata, H., Yip, T. T., Yip, C. L., Tomita, M. and Hutchens, T. W. (1998) Bactericidal domain of lactoferrin: detection, quantitation, and characterization of lactoferricin in serum by SELDI affinity mass spectrometry, *Biochemical and Biophysical Research Communications*, 245, 764–773.

Ladokhin, A. S. and White, S. H. (2001) 'Detergent-like' permeabilization of anionic lipid vesicles by melittin, *Biochimica et Biophysica Acta*, 1514, 253–260.

Lai, R., Liu, H., Hui, Lee, W. and Zhang, Y. (2002) An anionic antimicrobial peptide from toad *Bombina maxima*, *Biochemical and Biophysical Research Communications*, 295, 796–799.

Lai, Y. and Gallo, R. L. (2009) AMPed up immunity: how antimicrobial peptides have multiple roles in immune defense, *Trends in Immunology*, 30, 131-141.

Lange, M. K., Penagos-Tabare, F., Muñoz-Caro1, T., Gärtner, U., Mejer, H., Schaper, R., Hermosilla, C. and Taubert, A. (2017) Gastropod-derived haemocyte extracellular traps entrap metastrongyloid larval stages of *Angiostrongylus vasorum*, *Aelurostrongylus abstrusus* and *Troglostrongylus brevior*, *Parasites & Vectors*, 10, 50.

Larsen, M., Ressler, S. J., Gerdes, M. J., Bing, L., Byron, M., Lawrence, B. J. and Rowley, D. R. (2000) The WFDC1 gene encoding ps20 localizes to16q24, a region of LOH in multiple cancers, *Mammalian Genome*, 11, 767–773.

Lee, S. Y., Wang, R. and Söderhäll, K. (2000) A Lipopolysaccharide- and β-1,3-glucan-binding protein from hemocytes of the freshwater crayfish *Pacifastacus leniusculus*, purification, characterization, and cDNA cloning, *Journal of Biological Chemistry*, 275, 1337-1343.

Le Moullac, G., Le Groumellec, M., Ansquer, D., Froissard, S. and Levy, P. (1997) Haematological and phenoloxidase activity changes in the shrimp *Penaeus stylirostrisin* relation with the moult cycle: protection against vibriosis, *Fish & Shellfish Immunology*, 7(4), 227-234.

Leung-Trujillo, J. K. and Lawrence, A. L. (1985) The effect of eyestalk ablation on spermatophore and sperm quality in *Penaeus vannamei*, *Journal of the World Mariculture Society*, 16(1-4), 258-266.

Li, C. Y. and Song, Y. L. (2010) Proline-rich domain of penaeidin molecule exhibits autocrine feature by attracting penaeidin-positive granulocytes toward the wound-induced inflammatory site, *Fish & Shellfish Immunology*, 29, 1044–1052.

Li, F., Wang, L., Qui, L., Zhang, H., Gai, Y. and Song, L. (2012) A double WAP domain-containing protein from Chinese mitten crab *Eriocheir sinensis* with antimicrobial activities against Gram-negative bacteria and yeast, *Developmental and Comparative Immunology*, 36, 183–190.

Li, S., Jin, X., Guo, X., Yu, A., Wu, M., Tan, S., Zhu, Y., Li, W. and Wang, Q. (2013) A double WAP domain-containing protein *Es*-DWD1 from *Eriocheir sinensis* exhibits antimicrobial and proteinase inhibitory activities, *PLoS One*, 8 (8), e73563.

Lin, M-C., Lin, S-B., Lee, S-C., Lin, C-C., Hui, C-F. and Chen, J-Y. (2010 a) Antimicrobial peptide of an anti-lipopolysaccharide factor modulates of the inflammatory response in RAW264.7 cells, *Peptides*, 31, 1262–1272.

Lin, M-C., Lin, S-B., Chen, J-C., Hui, C-F. and Chen, J-Y. (2010 b) Shrimp anti-lipopolysaccharide factor peptide enhances the antitumor activity of cisplatin *in vitro* and inhibits HeLa cells growth in nude mice, *Peptides*, 31, 1019–1025

Lin, X. and Söderhäll, I. (2011) Crustacean hematopoiesis and the astakine cytokines, *Blood*, 117, 6417–6424.

Lin, Y. C., Chen, J. C., Chen, Y. Y., Liu, C. H., Cheng, W., Hsu, C. H. and Tsui, W. C. (2013) Characterization of white shrimp *Litopenaeus vannamei* integrin β and its role in immunomodulation by dsRNA-mediated gene silencing, *Developmental & Comparative Immunology*, 40, 167–179.

Liu, C-H., Yeh, S-T., Cheng, S-Y. and Chen, J-C. (2004) The immune response of the white shrimp *Litopenaeus vannamei* and its susceptibility to *Vibrio* infection in relation with the moult cycle, *Fish & Shellfish Immunology*, 16, (2), 151-161.

Liu, N., Lan, J. F., Sun, J. J., Jia, W. M., Zhao, X. F. and Wang, J. X. (2015) A novel crustin from *Marsupenaeus japonicus* promotes hemocyte phagocytosis, *Developmental & Comparative Immunology*, 49(2), 313-22.

Liu, N., Zhang, R-R., Fan, Z-X., Zhao, X-F. and Wang, X-W. (2016) Characterization of a type-I crustin with broad-spectrum antimicrobial activity from red swamp crayfish *Procambarus clarkia*, *Developmental and Comparative Immunology*, 61, 145-153.

Liu, T. P. (1992) Oöcytes degeneration in the queen honey bee after infection by *Nosema apis*, *Tissue and Cell*, 24 (1), 131-138.

Liu, Y., Cui, Z., Song, C., Wang, S. and Li, Q. (2011) Multiple isoforms of immune-related genes from hemocytes and eyestalk cDNA libraries of swimming crab *Portunus trituberculatus*, *Fish & Shellfish Immunology*, 31(1), 29-42.

Lyons, L. J., O'Riordan, R. M., Cross, T. F. and Culloty, S. C. (2012) Reproductive biology of the shore crab *Carcinus maenas* (Decapoda, Portunidae): a macroscopic and histological view, *Invertebrate Reproduction & Development*, 56(2), 144-156.

Maina, J. (1998) Locations, ultrastructural morphology, and putative functions of the branchial podocytes of the fresh water crab *Potamon niloticus*—Savigy (Crustacea, Decapoda, Potamonidae), *Tissue and Cell*, 30(5), 562-572.

Mann, M. and Jensen, O. N. (2003) Proteomic analysis of post-translational modifications, *Nature Biotechnology*, 21(3), 255-261.

Matsuzaki, K., Murase, O., Fujii, N. and Miyajima, K. (1996) An antimicrobial peptide, magainin 2, induced rapid flip-flop of phospholipids coupled with pore formation and peptide translocation, *Biochemistry*, 35, 11361–11368.

Mattanovich, D., Branduardi, P., Dato, L., Gasser, B., Sauer, M. and Porro, D. (2012) Recombinant protein production in yeasts, *Methods in Molecular Biology*, 824, 329-358.

Mattson, M.P. and Spaziani, E., 1985. Characterization of molt-inhibiting hormone (MIH) action on crustacean Y-organ segments and dispersed cells in culture and a bioassay for MIH-activity, *Journal of Experimental Zoology*, 236, 93-101.

McAlhany, S. J., Ressler, S. J., Larsen, M., Tuxhorn, J. A., Yang, F., Dang, T. D. and Rowley, D. R. (2003) Promotion of angiogenesis by ps20 in the differential reactive stroma prostate cancer xenograft model, *Cancer Research*. 63, 5859–5865.

McCrudden, M. T. C., Dafforn, T. R., Houston, D. F., Turkington, P. T. and Timson, D. J. (2008) Functional domains of the human epididymal protease inhibitor, EPPIN, *FEBS Journal*, 275, 1742–1750.

McKnight, R. A., Burdon, T., Pursel, V.G., Shamany, A., Wall, R. J. and Hennighausen, L. G. (1991) The whey acidic protein, In: Dickson, R.E., Lippman, M.E. *Genes, Oncogenes, and Hormones: Advances in Cellular and Molecular Biology of Breast Cancer*. Kluwer Academic, Boston, 399-412.

Medzhitov, R. and Janeway Jr, C. A. (2002) Decoding the patterns of self and nonself by the innate immune system, *Science*, 296, 298–300.

Mihaila, A. and Tremblay, G. M. (2001) Human Alveolar Macrophages Express Elafin and Secretory Leukocyte Protease Inhibitor *Zeitschrift für Naturforschung C*, 56c, 291-297

Mikami, Y., Iwase, T., Komiyama, Y., Matsumoto, N., Oki, H. and Komiyama. K. (2015) Secretory leukocyte protease inhibitor inhibits expression of polymeric immunoglobulin receptor via the NF-κB signaling pathway, *Molecular Immunology*, 67, 568-574.

Modrek, B. and Lee, C. (2002) A genomic view of alternative splicing, *Nature Genetics*, 30, 13–19.

Montoya, J. A. (2016) Preliminary evaluation of eyestalk ablation and thoracic ganglion implantation on spermatophore quality and molting of male *Penaeus vannamei*, Uniciencia, 9(1), 7-12.

Moreau, T., Baranger, K., Dadé, S., Dallet-Choisy, S., Guyot, N. and Zani, M-L. (2008) Multifaceted roles of human elafin and secretory leukocyte proteinase inhibitor (SLPI), two serine protease inhibitors of the chelonianin family, *Biochimie*, 90, 284–295

Mu, C., Zheng, P., Zhao, J., Wang, L., Zhang, H., Qiu, L., Gai, Y. and Song, L. (2010) Molecular characterization and expression of a crustin-like gene from Chinese mitten crab, *Eriocheir sinensis*, *Developmental & Comparative Immunology*, 34(7), 734-740.

Mu, C., Zheng, P., Zhao, J., Wang, L., Qiu, L., Zhang, H., Gai, Y. and Song, L. (2011) A novel Type III crustin (Crus*Es*2) identified from Chinese mitten crab *Eriocheir sinensis*, *Fish & Shellfish Immunology*, 31(1), 142-147.

Mygind, P. H., Fischer, R. L., Schnorr, K. M., Hansen, M. T., Sönksen, C. P., Ludvigsen, S., Raventós, D., Buskov, S., Christensen, B., De Maria, L., Taboureau, O., Yaver, D., Elvig-Jørgensen, S. G., Sørensen, M. V., Christensen, B. E., Kjærulff, S., Frimodt-Moller, N., Lehrer, R. I., Zasloff, M. and Kristensen, H-H. (2005) Plectasin is a peptide antibiotic with therapeutic potential from a saprophytic fungus, *Nature*, 437, 975–980.

Nair, D. G., Fry, B. G., Alewood, P., Kumar, P. P. and Kini, R. M. (2007) Antimicrobial activity of omwaprin, a new member of the waprin family of snake venom proteins, *Biochemical Journal*, 402, 93–104.

Ng, H. T., Chang, S., Wu, M. and Wang, H. (2013) Shrimp hemocytes release extracellular traps that kill bacteria, *Developmental & Comparative Immunology*, 41, 644-651.

Ng, H. T., Hung, H. Y., Chiang, Y-A., Lin, J-H., Chen, Y-N., Chiang, Y-C. and Wang, H-C. (2014) WSSV-induced crayfish Dscam shows durable immune behavior, *Fish & Shelfish Immunology*, 40 (1), 78-90.

Nico, S. and Endo, Y. (1997) Krill Fisheries of the World, Fisheries Technical Paper. 367. Food and Agriculture Organization. ISBN 978-92-5-104012-6.

Nukumi, N., Iwamori, T., Kano, K., Naito, K. and Tojo, H. (2007a) Whey acidic protein (WAP) regulates the proliferation of mammary epithelial cells by preventing serine protease from degrading laminin, *Journal of Cellular Physiology*, 213, 793-800.

Nukumi, N., Iwamori, T., Kano, K., Naito, K. and Tojo, H. (2007b) Reduction of tumorigenesis and invasion of human breast cancer cells by whey acidic protein (WAP), *Cancer Letters*, 252, 65-74.

O'Neal, R. L., Nam, K. T., LaFleur, B. J., Barlow, B., Nozaki, K., Lee, H-J., Kim, W. H., Yang, H-K., Shi, C., Maitra, A., Montgomery, E., Washington, M. K., El Rifai, W., Drapkin, R. I. and Goldenring, J. R. (2013) Human epididymis protein 4 is up-regulated in gastric and pancreatic adenocarcinomas, *Human Pathology*, 44, 734–742

O'Rand, M. G., Widgren, E. E., Wang, Z. and Richardson, R.T. (2006) Eppin: an effective target for male contraception, *Molecular and Cellular Endocrinology*, 250, 157–162

O'Rand, M. G., Widgren, E. E., Beyler, S. and Richardson, R.T. (2009) Inhibition of human sperm motility by contraceptive anti-eppin antibodies from infertile male monkeys: effect on cAMP, *Reproductive Biology*, 80, 279–285

Oren, Z. and Shai, Y. (1998) Mode of action of linear amphipathic α-helical antimicrobial peptides, *Biopolymers*, 47, 451–463.

Orfanelli, T., Jayaram, A., Doulaveris, G., Forney, L. J., Ledger, W. J. and Witkin, S. S. (2014) Human epididymis protein 4 and secretory leukocyte protease inhibitor in vaginal fluid: relation to vaginal components and bacterial composition, *Reproductive Sciences*, 21, 538–542.

O'Rourke, N. A., Meyer, T. and Chandy, G. (2005) Protein localization studies in the age of 'Omics', *Current Opinion in Chemical Biology*, 9(1), 82-87.

Ota, Y., Shimoya, K., Zhang, Q., Moriyama, A., Chin, A. and Murata, Y. (2002) The expression of secretory leukocyte protease inhibitor (SLPI) in the fallopian tube: SLPI protects the acrosome reaction of sperm from inhibitory effects of elastase, *Human Reproduction*, 17, 2517–2522.

Ouellette, A. J. and Selsted, M. E. (1996) Paneth cell defensins: endogenous peptide components of intestinal host defense, *The FASEB Journal*, 10(11), 1280-1289.

Pacor, S., Giangaspero, A., Bacac,M., Sava, G. and Tossi, A. (2002) Analysis of the cytotoxicity of synthetic antimicrobial peptides on mouse leucocytes: implications for systemic use, *Journal of Antimicrobial Chemotherapy*, 50, 339–348.

Padmanabhan, L. N. and Raghavan, S. D. A. (2016) Impact of eyestalk ablation on androgenic gland activity in the freshwater crab *Travancoriana schirnerae* Bott, 1969 (Decapoda: Gecarcinucidae), *Brazilian Journal of Biological Sciences*, 3(5), 121-134.

Pahari, S., MacKessy, S. P. and Kini, R. M. (2007) The venom gland transcriptome of the desert *Massasauga rattlesnake* (Sistrurus catenatus edwardsii): towards an understanding of venom composition among advanced snakes (Superfamily Colubroidea), *BMC Genomics*, 8, 115–132

Pandey, A. and Mann, M, (2000) Proteomics to study genes and genomes, *Nature*, 405(6788), 837-846.

Panouse, J. B. (1943). Influence de I'ablation du peduncle oculaire sur la croissancedel'ovairechezla Crevette *Lecrnderserrarus*, *Comptes Rendus de l'Académie des Sciences* Paris, 217, 553-555.

Park, C. B., Kim, H. S. and Kim, S. C. (1998) Mechanism of action of the antimicrobial peptide buforin II: buforin II kills microorganisms by penetrating the cell membrane and inhibiting cellular functions, *Biochemical and Biophysical Research Communications*, 244, 253–257.

Patrzykat, A., Friedrich, C. L., Zhang, L., Mendoza, V. and Hancock, R. E. (2002) Sublethal concentrations of pleurocidin-derived antimicrobial peptides inhibit macromolecular synthesis in *Escherichia coli*, *Antimicrobial Agents and Chemotherapy*, 46, 605–614.

Perez, G. I., Tao, X.-J. and Tilly, J. L. (1999) Fragmentation and death (aka apoptosis) of ovulated oocytes, *Molecular Human Reproduction*, 5(5), 414-420.

Pickering, T. R. and Quijón, P. A. (2011) Potential effects of a non-indigenous predator in its expanded range: assessing green crab, *Carcinus maenas*, prey preference in a productive coastal area of Atlantic Canada, *Marine Biology*, 158, 2065-2078.

Piletz, J. E., Heinlin, M. and Ganshow, R. E. (1981) Biochemical characterization of a novel whey protein from murine milk, *Journal of Biological Chemistry*, 256, 11509-11516.

Pisuttharachai, D., Fagutao, F. F., Yasuike, M., Aono, H., Yano, Y., Murakami, K., Kondo, H., Aoki, T. and Hirono, I. (2009) Characterization of crustin antimicrobial proteins from Japanese spiny lobster *Panulirus japonicus*, *Developmental & Comparative Immunology*, 33(10), 1049-1054.

Poirier, A. C., Schmitt, P., Rosa, R. D., Vanhove, A. S., Kieffer-Jaquinod, S., Rubio, T. P., Charrière, G. M. and Destoumieux-Garzón, D. (2014) Antimicrobial histones and DNA traps in invertebrate immunity. Evidences in *Crassostrea gigas*, *The Journal of Biological Chemistry*, 289, 24821-24831

Protein Blotting Guide. A Guide to Transfer and Detection (pdf). *Third Edition*. Bio-Rad. Available at www.bio-rad.com

Ohashi, K., Niwa, M., Nakamura, T., Morita, T. and Iwanaga, S. (1982) Anti-LPS factor in the horseshoe crab, *Tachypleus tridentatus*–its haemolytic activity on the red blood cells ensitized with lipopolysaccharide. *FEBS Letters*, 176, 207–210.

Qiao, K., Xu, W.F., Chen, H.Y., Peng, H., Zhang, Y.Q., Huang, W.S., Wang, S.P., An, Z., Shan, Z.G., Chen, F.Y. and Wang, K.J. (2016) A new antimicrobial peptide SCY2 identified in *Scylla paramamosain* exerting a potential role of reproductive immunity, *Fish & Shellfish Immunology*, 51, 251-62.

Quackenbush, L. S. (1986) Crustacean endocrinology, a review, *Canadian Journal of Fisheries and Aquatic Sciences*, 43(11), 2271-2282.

R core Team (2017) R: a language and environment for statistical computing, *R Foundation for Statistical Computing*, Vienna, Austria, https://www.R-project.org

Ranganathan, S., Simpson, K. J., Shaw, D. C. and Nicholas, K. R. (1999) The whey acidic protein family: a new signature motif and three-dimensional structure by comparative modeling, *Journal of Molecular Graphics and Modelling*, 17, 106–113.

Rattanachai, A., Hirono, I., Ohira, T., Takahashi, Y. and Aoki, T. (2004) Cloning of kuruma prawn *Marsupenaeus japonicas* crustin-like peptide cDNA and analysis of its expression, *Fisheries Science*, 70, 765–771

Relf, J. M., Chisholm, J. R., Kemp, G. D. and Smith, V. J. (1999) Purification and characterization of a cysteine-rich 11.5-kDa antibacterial protein from the granular haemocytes of the shore crab, *Carcinus maenas*, *European Journal of Biochemistry*, 264(2), 350-357.

Richardson, R. T, Sivashanmugam, P., Hall, S. H, Hamil, K. G., Moore, P. A., Ruben, S. M., French, F. S. and O'Rand, M. (2001) Cloning and sequencing of human EPPIN: a novel family of protease inhibitors expressed in the epididymis and testis, *Gene*, 270, 93–102.

Richman, A. M. and Kafatos, F. C. (1996) Immunity to eukaryotic parasites in vector insects, *Current Opinion in Immunology*, 8, 14–19.

Richman, A. M., G. Dimopoulos, G., Seeley, D. and Kafatos, F. C (1997) *Plasmodium* activates the innate immune response of *Anopheles gambiae* mosquitoes, *EMBO Journal*, 16, 6114–6119.

Robb, C. T., Dyrynda, E. A., Gray, R. D., Rossi, A. G. and Smith, V. J. (2014) Invertebrate extracellular phagocyte traps show that chromatin is an ancient defence weapon, *Nature Communications*, 5, 4627.

Robb, C. T. (2015) Cell death processes in immune cells of the shore crab, *Carcinus maenas*, Ph.D Thesis, Heriot-Watt University, UK.

Robert, A., Monsinjon, T., Delbecque, J. P., Olivier, S., Poret, A., Le Foll, F., Durand, F. and Knigge, T. (2016) Neuroendocrine disruption in the shore crab *Carcinus maenas*:

Effects of serotonin and fluoxetine on chh-and mih-gene expression, glycaemia and ecdysteroid levels, *Aquatic Toxicology*, 175, 192-204.

Rodrìguez-Rojas, A., Makarova, O. and Rolff, J. (2014) Antimicrobials, stress and mutagenesis, *PLoS Pathogens*, 10, e1004445.

Rosa, R. D., Bandeira, P. T. and Barracco, M. A. (2007) Molecular cloning of crustins from the hemocytes of Brazilian penaeid shrimps, *FEMS Microbiology Letters*, 274(2), 287-290.

Rosa, R. D. and Barracco M. A. (2010) Antimicrobial peptides in crustaceans, *Invertebrate Survival Journal*, 7, 262-284.

Rosa, R.D., Vergnes, A., Lorgeril, J., Goncalves, P., Perazzolo, L. M., Sauné, L., Romestand, B., Fievet, J., Gueguen, Y., Bachère, E. and Destoumieux-Garzón, D. (2013) Functional divergence in shrimp anti-lipopolysaccharide factors (alfs): from recognition of cell wall components to antimicrobial activity, *PLoS One*, 8, e67937.

Rosa, S. M., Galvagno, M. A. and Vélez, C. G. (2011) Adjusting culture conditions to isolate *thraustochytrids* from temperate and cold environments in southern Argentina, *Mycoscience*, 52(4), 242-252.

Rossong, M. A., Williams, P. J., Comeau, M., Mitchell, S. C. and Apaloo, J. (2005) Agonistic interactions between the invasive green crab, *Carcinus maenas* (Linnaeus) and juvenile American lobster, *Homarus americanus* (Milne Edwards), *Journal of Experimental Marine Biology and Ecology*, 329(2), 281-288.

Roulston, C. and Smith, V. J. (2011) Isolation and *in vitro* characterisation of prohaemocytes from the spider crab, *Hyas araneus* (L.), *Developmental & Comparative Immunology*, 35(5), 537-544.

Runde, S. (2016) FPLC versus Analytical HPLC: Two Methods, One Origin, Many Differences, *LCGC magazine*, 12(15), 12-16. http://www.chromatographyonline.com/fplc-versus-analytical-hplc-two-methods-one-origin-many-differences-0?pageID=2

Ryan, E. P. (1967) Structure and function of the reproductive system of the crab *Portunus sanguinolentus* (Herbst) (Brachyura: Portunidae). II. The female system, *Proceedings of the Symposium on Crustacea Part 2*, 522-544.

Sagi, A., Manor, R. and Ventura, T. (2013) Gene silencing in crustaceans: from basic research to biotechnologies, *Genes*, 4, 620-645.

Saitoh, T., Komano, J., Saitoh, Y., Misawa, T., Takahama, M., Kozaki, T., Uehata, T., Iwasaki, H., Omori, H., Yamaoka S., Yamamoto, N. and Akira, S. (2012) Neutrophil extracellular traps mediate a host defense response to human immunodeficiency virus-1, *Cell Host & Microbe*, 12, 109–116.

Sallenave, J. M., Shulmann, J., Crossley, J., Jordana, M. and Gauldie, J. (1994) Regulation of secretory leukocyte proteinase inhibitor (SLPI) and elastase-specific inhibitor (ESI/elafin) in human airway epithelial cells by cytokines and neutrophilic enzymes, *American Journal of Respiratory Cell and Molecular Biology*, 11, 733–741.

Sallenave, J. M., Si Tahar, M., Cox, G., Chignard, M. and Gauldie, J. (1997) Secretory leukocyte proteinase inhibitor is a major leukocyte elastase inhibitor in human neutrophils, *Journal of Leukocyte Biology*, 61, 695–702.

Sallenave, J. M. (2010) Secretory leukocyte protease inhibitor and elafin/trappin-2: versatile mucosal antimicrobials and regulators of immunity, *American Journal of Respiratory Cell and Molecular Biology*, 42, 635–643.

Sawyer T. K., MacLean S. A., Ziskowski J. (1976) A report on *Ephelota* sp. (*Ciliata, Suctorida*) as an epibiont on the gills of decapod crustaceans, *Transactions of the American Microscopical Society*, 95, 712–717.

Schägger, H. and Von Jagow, G. (1987) Tricine-sodium dodecyl sulfate-polyacrylamide gel electrophoresis for the separation of proteins in the range from 1 to 100 kDa, *Analytical Biochemistry*, 166(2), 368-379.

Schittek, B., Hipfel, R., Sauer, B., Bauer, J., Kalbacher, H., Stevanovic, S., Schirle, M., Schroeder, K., Blin, N., Meier, F., Rassner, G. and Garbe1, C. (2001) Dermcidin: a novel human antibiotic peptide secreted by sweat glands, *Nature Immunology*, 2, 1133–1137

Schnapp, D., Kemp, G. D. and Smith, V. J. (1996) Purification and characterization of a proline-rich antibacterial peptide, with sequence similarity to bactenecin-7, from the haemocytes of the shore crab, *Carcinus maenas*, *European Journal of Biochemistry*, 240, 532–539.

Schummer, M, Ng, W. V., Bumgarner, R. E., Nelson, P. S., Schummer, B., Bednarski, D. W., Hassell, L., Baldwin, R. L, Karlan, B. Y. and Hood, L. (1999) Comparative hybridization of an array of 21,500 ovarian cDNAs for the discovery of genes overexpressed in ovarian carcinomas, *Gene*, 238, 375-385.

Seemuller, U., Arnhold, M., Fritz, H., Wiedenmann, K., Macleidt, W., Heinzel, R., Appelhans, H., Gassen, H.-G. and Lottspeich, F. (1986) The acid stable proteinase inhibitor of human mucus secretions (HUSI-I) antileukoprotease, *FEBS Letters*, 199, 43–48

Seong, S. Y. and Matzinger, P. (2004) Hydrophobicity: an ancient damage-associated molecular pattern that initiates innate immune response, *Nature Reviews Immunology*, 4, 469–478.

Shai, Y. (1999) Mechanism of the binding, insertion and destabilization of phospholipid bilayer membranes by alphahelical antimicrobial and cell non-selective membrane-lytic peptides, *Biochimica et Biophysica Acta*, 1462, 55–70.

Sharifian, S., Kamrani, E. and Safaie, M. (2015) Oogenesis and ovarian development in the freshwater Crab *Sodhiana iranica* (Decapoda: Gecarcinuaidae) from the south of Iran, *Tissue and Cell*, 47(2), 213-220.

Shen, X., Belcher, A. M., Handman, P. K., Stucky, G. D. and Morse, D.E. (1997) Molecular cloning and characterzation of lustrin A, a matrix protein from shell and pearl nacre of *Haliotis rufescens*, *Journal of Biological Chemistry*, 272, 32472–32481

Shevchenko, A., Wilm, M., Vorm, O. and Mann, M. (1996) Mass spectrometric sequencing of proteins from silver-stained polyacrylamide gels, *Analytical Chemistry*, 68(5), 850-858.

Shields, J. D. and Boyd, R. A. (2014) Atlas of Lobster Anatomy and Histology. *Special Papers in Marine Science No. 9*. Virginia Institute of Marine Science, College of William and Mary. http://doi.org/10.21220/V5001R

Shockey, J. E., O'Leary, N. A., de la Vega, E., Browdy, C. L., Baatz, J. E. and Gross, P. S. (2009) The role of crustins in *Litopenaeus vannamei* in response to infection with shrimp pathogens: an *in vivo* approach, *Developmental & Comparative Immunology*, 33(5), 668-673.

Silhavy, T. J., Kahne, D. and Walker, S. (2010) The bacterial cell envelope, *Cold Spring Harbor Perspectives in Biology*, 2(5), a000414.

Simpson, A. J., Maxwell, A. I., Govan, J. R. W., Haslett, C. and Sallenave, J.-M. (1999) Elafin (elastase-specific inhibitor) has antimicrobial activity against Gram-positive and Gram-negative respiratory pathogens, *FEBS Letters*, 452, 309–313

Sivakamavalli, J., Nirosha, R. and Vaseeharan, B. (2015) Purification and characterization of a cysteine-rich 14-kDa antibacterial peptide from the granular hemocytes of mangrove crab *Episesarma tetragonum* and its antibiofilm activity, *Applied Biochemistry and Biotechnology*, 176(4), 1084-101.

Small, D. M., Doherty, D. F., Dougan, C. M., Weldon, S. and Taggart, C. C. (2017) The role of whey acidic protein four-disulfide-core proteins in respiratory health and disease, *Biological Chemistry*, 398 (4), 425-440.

Smith, V. J. and Ratcliffe, N. (1978) Host defence reactions of the shore crab, *Carcinus maenas* (L.), *in vitro*, *Journal of the Marine Biological Association of the United Kingdom*, 58(02), 367-379.

Smith, V. J. and Ratcliffe, N. (1980) Cellular defense reactions of the shore crab, *Carcinus maenas*: *in vivo* hemocytic and histopathological responses to injected bacteria, *Journal of Invertebrate Pathology*, 35(1), 65-74.

Smith, V.J., Söderhäll, K., Hamilton, M. (1984) β-1,3 glucan induced cellular defence reactions in the shore crab, *Carcinus maenas*, *Comparative Biochemistry and Physiology Part A: Physiology* 77, 635–639.

Smith, V. J. and Chisholm, J. R. (2001) Antimicrobial proteins in crustaceans, *Advances in Experimental Medicine and Biology*, 484, 95–112.

Smith, V. J., Brown, J. H. and Hauton, C. (2003) Immunostimulation in crustaceans: does it
really protect against infection? *Fish & Shellfish Immunology*, 15, 71–90.

Smith, V. J., Fernandes, J. M., Kemp, G. D. and Hauton, C. (2008) Crustins: enigmatic WAP domain-containing antibacterial proteins from crustaceans, *Developmental & Comparative Immunology*, 32(7), 758-772.

Smith, V. J., Desbois, A. P. and Dyrynda, E. A. (2010) Conventional and Unconventional Antimicrobials from Fish, Marine Invertebrates and Micro-algae, *Marine Drugs*, 8, 1213-1262.

Smith, V. J. (2011) Phylogeny of whey acidic protein (WAP) four-disulfide core proteins and their role in lower vertebrates and invertebrates, *Biochemical Society Transactions*, 39, 1403–1408.

Smith, V. J. and Dyrynda, E. A. (2015) Antimicrobial proteins: From old proteins, new tricks, *Molecular immunology*, 68(2), 383-398.

Smith, V. J. (2016) Immunology of Invertebrates: Cellular, *Encyclopaedia of Life Sciences (ELS)* On-line Library. John Wiley & Sons, Ltd.

Söderhäll, K. and Smith, V. J. (1983) Separation of the haemocyte populations of *Carcinus maenas* and other marine decapods, and prophenoloxidase distribution, *Developmental & Comparative Immunology*, 7(2), 229-239.

Söderhäll, K., Cerenius, L. and Johansson, M. W. (1994) The prophenoloxidase activating system and its role in invertebrate defence, *Annals of the New York Academy of Sciences*, 712, 155-161.

Söderhäll, K. and Cerenius, L. (1998) Role of the prophenoloxidase-activating system in invertebrate immunity, *Current Opinion in Immunology*, 10 (1), 23-28.

Song, Y.-L. and Li, C.Y. (2014) Shrimp immune system. Special focus on penaeidin, *Journal of Marine Science and Technology*, 22, 1–8.

Soonthornchai, W., Rungrassamee, W., Karoonuthaisiri, N., Jarayabhand, P., Klinbunga, S., Söderhäll, K. and Jiravanichpaisal, P. (2010) Expression of immune-related genes in the digestive organ of shrimp, *Penaeus monodon*, after an oral infection by *Vibrio harveyi*, *Developmental and Comparative Immunology*, 34, 19–28.

Sørensen, O. E. and Borregaard, N. (2016) Neutrophil extracellular traps — the dark side of neutrophils, *The Journal of Clinical Investigation*, 126(5), 1612–1620.

Soumoff, C. and O'Connor, J. D (1982) Repression of Y-organ secretory activity by moult inhibiting hormone in the crab *Pachygrapsus crassipes*, *General and Comparative Endocrinology*, 48, 432 -439.

Sousa, L. G., Cuartas, E. I. and Petriella, A. M. (2005) Fine structural analysis of the epithelial cells in the hepatopancreas of *Palaemonetes argentinus* (Crustacea, Decapoda, Caridea) in intermoult, *Biocell*, 29 (1), 25-31.

Soyez, D., Le Caer, J., Noel, P. and Rossier, J. (1991) Primary structure of two isoforms of the vitellogenesis inhibiting hormone from the lobster *Homarus americanus*, *Neuropeptides*, 20(1), 25-32.

Sperstad, S. V., Haug, T., Paulsen, V., Rode, T. M., Strandskog, G., Solem, S. T., Styrvold, O. B. and Stensvåg, K. (2009 a) Characterization of crustins from the hemocytes of the spider crab, *Hyas araneus*, and the red king crab, *Paralithodes camtschaticus*, *Developmental & Comparative Immunology*, 33(4), 583-591.

Sperstad, S. V., Haug, T., Vasskog, T. and Stensvåg, K. (2009 b) Hyastatin, a glycine-rich multi-domain antimicrobial peptide isolated from the spider crab (*Hyas araneus*) hemocytes, *Molecular Immunology*, 46(13), 2604-2612.

Sperstad, S. V., Smith, V. J. and Stensvåg, K. (2010) Expression of antimicrobial peptides from *Hyas araneus* haemocytes following bacterial challenge *in vitro*, *Developmental & Comparative Immunology*, 34(6), 618-624.

Sritunyalucksana, K., Wongsuebsantati, K., Johansson, M. and Söderhäll, K. (2001) Peroxinectin, a cell adhesive protein associated with the proPO system from the black tiger shrimp, *Penaeus monodon*, *Developmental & Comparative Immunology*, 25(5), 353-363.

Steiner, H., Hultmark, D., Engstrom, A., Bennich, H. and Boman, H. G. (1981) Sequence and specificity of two antibacterial proteins involved in insect immunity, *Nature*, 292, 246–248.

Stoss, T. D., Nickell, M. D., Hardin, D., Derby, C. D. and McClintock, T. S. (2004) Inducible transcript expressed by reactive epithelial cells at sites of olfactory sensory neuron proliferation, *Journal of Neurobiology*, 58(3), 355-368.

Strategies for Protein Purification Handbook (pdf). GE Healthcare. Available at www.gelifesciences.com

Subbalakshmi, C. and Sitaram, N. (1998) Mechanism of antimicrobial action of indolicidin *FEMS Microbiology Letters*, 160, 91–96.

Subramoniam, T. (2011) Mechanisms and control of vitellogenesis in crustaceans, *Fisheries Science*, 77(1), 1-21.

Suleiman, S., Smith, V. J. and Dyrynda, E. A. Unusual tissue distribution of carcinin, an antibacterial crustin, in the crab, *Carcinus maenas*, reveals its multi-functionality, *Developmental and Comparative Immunology*, 76, 274-284.

Sun, C., Du, X.-J., Xu, W.-T., Zhang, H.-W., Zhao, X.-F. and Wang, J.-X. (2010) Molecular cloning and characterization of three crustins from the Chinese white shrimp, *Fenneropenaeus chinensis*, *Fish & Shellfish Immunology*, 28(4), 517-524.

Sun, J., Xu, J., Liu, Z., Liu, Q., Zhao, A., Shi, T., Li, Y. (2005) Refined phylogenetic profiles method for predicting protein-protein interactions, *Bioinformatics*, 16, 3409-15.

Supriya, N. T., Sudha, K., Krishnakumar, V. and Anilkumar, G. (2016) Molt and reproduction enhancement together with hemolymph ecdysteroid elevation under eyestalk ablation in the female fiddler crab, *Uca triangularis* (Brachyura: Decapoda), *Chinese Journal of Oceanology and Limnology*, 1-13.

Supungul, P., Tang, S., Maneeruttanarungroj, C., Rimphanitchayakit, V., Hirono, I., Aoki, T. and Tassanakajon, A. (2008) Cloning, expression and antimicrobial activity of crustin*Pm*1, a major isoform of crustin, from the black tiger shrimp *Penaeus monodon*, *Developmental & Comparative Immunology*, 32(1), 61-70.

Suthianthong, P., Donpudsa, S., Supungul, P., Tassanakajon, A. and Rimphanitchayakit, V. (2012) The N-terminal glycine-rich and cysteine-rich regions are essential for antimicrobial activity of crustin*Pm*1 from the black tiger shrimp *Penaeus monodon*, *Fish & Shellfish Immunology*, 33, 977-983.

Taggart, C. C., Greene, C. M., McElvaney, N. G. and O'Neill S. (2002) Secretory leucoprotease inhibitor prevents lipopolysaccharide-induced IκBα degradation without affecting phosphorylation or ubiquitination, *Journal of Biological Chemistry*, 277, 33648–33653.

Taggart, C. C., Cryan, S. A., Weldon, S., Gibbons, A., Greene, C. M., Kelly, E., Low, T. B., O'neill, S. J. and McElvaney, N. G. (2005) Secretory leucoprotease inhibitor binds to NF-kappaB binding sites in monocytes and inhibits p65 binding, *Journal of Experimental Medicine*, 202 (12), 1659-1668.

Tanaka, S., Nakamura, T., Morita, T. and Iwanaga, S. (1982) Limulus anti-LPS factor: ananticoagulant which inhibits the endotoxin mediated activation of Limulus coagulation system. *Biochemical and Biophysical Research Communications*, 105, 717–723.

Tassanakajon, A., Amparyup, P., Somboonwiwat, K. and Supungul, P. (2011) Cationic antimicrobial peptides in penaeid shrimp. *Marine Biotechnology*, 12, 487–505.

Tatanavicharn, T., Supungul, P., Puanglarp, N., Yingvilasprasert, W. and Tassanakajon, A. (2009) Genomic structure, expression pattern and functional characterization of crustin*Pm*5, a unique isoform of crustin from *Penaeus monodon*, *Comparative Biochemistry and Physiology Part B: Biochemistry and Molecular Biology*, 153(3), 244-252.

Thompson, R. C. and Ohlsson, K. (1986) Isolation, properties, and complete amino acid sequence of human secretory leukocyte protease inhibitor, a potent inhibitor of leukocyte elastase, *Proceedings of the National Academy of Sciences of the United States of America*, 83, 6692-6696.

Thörnqvist, P. O., Johansson, M. W. and Söderhäll, K. (1994) Opsonin activiy of cell adhesion protein and β-1,3-glucan binding protein from two crustaceans, *Developmental and Comparative Immunology*, 18, 279-302.

Torres, A. M., Wong, H. Y., Desai, M., Moochhala, S., Kuchel, P. W. and Kini, R. M. (2003) Identification of a novel family of proteins in snake venoms: purification and structural characterization of nawaprin from *Naja nigricollis* snake venom, *Journal of Biological Chemistry*, 278, 40097–40104

Towle, D. W. and Smith, C. M. (2006) Gene discovery in *Carcinus maenas* and *Homarus americanus* via expressed sequence tags, *Integrative and Comparative Biology*, 46, 912-918.

Treccani, L., Mann, K., Heinemann, F. and Fritz, M. (2006) Perlwapin, an abalone nacre protein with three four-disulphide core (whey acidic protein) domains, inhibits the growth of calcium carbonate crystals, *Biophysical Journal*, 91, 2691–2608.

Trexler, M., Bányai, L. and Patthy, L. (2002) Distinct expression pattern of two related human proteins containing multiple types of protease-inhibitory modules, *Journal of Biological Chemistry*, 383, 223-228.

Urban, C. F., Reichard, U., Brinkmann, V. and Zychlinsky, A. (2006) Neutrophil extracellular traps capture and kill *Candida albicans* yeast and hyphal forms, *Cellular Microbiology*, 8, 668–676.

Urban, C. F., Ermert, D., Schmid, M., Abu-Abed, U., Goosmann, C., Nacken, W., Brinkmann V., Jungblut, P. R. and Zychlinsky, A. (2009) Neutrophil extracellular traps contain calprotectin, a cytosolic protein complex involved in host defense against *Candida albicans*, *PLoS Pathogens*, 5.

van de Braak, C. B. T., Botterblom, M. H. A., Liu, W., Taverne, N., van der Knaap, W. P. W. and Rombout, J. H. W. M. (2002) The role of the haematopoietic tissue in haemocyte production and maturation in the black tiger shrimp, *Penaeus monodon*. *Fish and Shellfish Immunology*. 12, 253e272.

Vargas-Albores, F., Yepiz-Plascencia, G., Jiménez-Vega, F. and Ávila-Villa, A. (2004) Structural and functional differences of *Litopenaeus vannamei* crustins, *Comparative Biochemistry and Physiology Part B: Biochemistry and Molecular Biology*, 138(4), 415-422.

Vatanavicharn, T., Supungul, P., Puanglarp, N., Yingvilasprasert, W. and Tassanakajon, A. (2009) Genomic structure, expression pattern and functional characterization of crustin*Pm*5, a unique isoform of crustin from *Penaeus monodon*, *Comparative Biochemistry and Physiology - Part B: Biochemistry & Molecular Biology*, 153, 244–252.

Vaz Gomes, A., de Waal, A., Berden, J. A. and Westerhoff, H. V. (1993) Electric potentiation, cooperativity and synergism of magainin peptides in protein-free liposomes, *Biochemistry*, 32, 5365–5372.

VGNC Vertebrate Gene Nomenclature Committee at European Bioinformatics Institute, https://vertebrate.genenames.org

Vinuesa, J. H. (2007) Molt and reproduction of the European green crab *Carcinus maenas* (Decapoda: Portunidae) in Patagonia, Argentina, *Revista de Biologia Tropical*, 55(1), 49-54.

Visetnan, S., Supungul, P., Tassanakajon, A., Donpudsa, S. and Rimphanitchayakit, V. (2017) A single WAP domain-containing protein from *Litopenaeus vannamei* possesses antiproteinase activity against subtilisin and antimicrobial activity against AHPND-inducing *Vibrio parahaemolyticus*, *Fish & Shellfish Immunology*, 68, 341-348.

von Köckritz-Blickwede, M. and Nizet, V. (2009) Innate immunity turned inside-out: antimicrobial defense by phagocyte extracellular traps, *Journal of Molecular Medicine*, 87(8), 775–783.

Walsh, G. and Jefferis, R. (2006) Post-translational modifications in the context of therapeutic proteins, *Nature Biotechnology*, 24(10), 1241-1252.

Wang, G., Li, X. and Wang, Z. (2016) APD3: the antimicrobial peptide database as a tool for research and education, *Nucleic Acids Research*, 44, D1087-D1093.

Wang, W., Tang, Y., Ni, L., Kim, E., Jongwutiwes, T., Hourvitz, A., Zhang, R., Xiong, H., Liu, H. and Rosenwaks, Z. (2012) Overexpression of Uromodulin-like1 accelerates follicle depletion and subsequent ovarian degeneration, *Cell Death & Disease*, 3(11), e433.

Wang, Y., Chang, P. and Chen, H. (2008) Differential time-series expression of immune-related genes of Pacific white shrimp *Litopenaeus vannamei* in response to dietary inclusion of β-1,3-glucan, *Fish & Shellfish Immunology*, 24, 113-121

Wang, Z., Widgren, E. E., Sivashanmugam, P., O'Rand, M. G. and Richardson, R. T. (2005) Association of Eepin with semenogelin on human spermatozoa, *Reproductive Biology*, 72, 1064–1070

Wang, Z., Widgren, E. E., Richardson, R. T. and O'Rand, M. G. (2007a) Characterization of an eppin protein complex from human semen and spermatozoa, *Reproductive Biology*, 77, 476–484

Wang, Z., Widgren, E. E., Richardson, R. T. and O'Rand, M. G. (2007b) Eppin: a molecular strategy for male contraception, *Journal of Reproduction and Fertility. Supplement*, 65, 535–542.

Ward, P. A. (1999) Regulatory effects of endogenous protease inhibitors in acute lung inflammatory injury, *Journal of Immunology*, 162, 3653-3662

Wartha, F., Beiter, K., Albiger, B., Fernebro, J., Zychlinsky, A., Normark, S. and Henriques-Normark, B. (2007) Capsule and D-alanylated lipoteichoic acids protect *Streptococcus pneumoniae* against neutrophil extracellular traps, *Cellular Microbiology*, 9, 1162–1171.

Watthanasurorot, A., Jiravanichpaisal, P., Liu, H., Söderhäll, I. and Söderhäll, K. (2011) Bacteria-induced Dscam isoforms of the crustacean, *Pacifastacus leniusculus*, *PLoS Pathogens*, 7, e1002062.

Watthanasurorot A, Jiravanichpaisal P, Liu H, Söderhäll I, Söderhäll K (2016). Retraction: Bacteria-Induced Dscam Isoforms of the Crustacean, *Pacifastacus leniusculus*. *PLoS Pathogens*, 12(5): e1005630.

Webster, S. G., Keller, R. and Dircksen, H. (2012) The CHH-superfamily of multifunctional peptide hormones controlling crustacean metabolism, osmoregulation, moulting, and reproduction, *General and Comparative Endocrinology*, 175(2), 217-233.

Webster, S. G. (2015) Endocrinology of molting, In: Chang, E. S., Thiel, M. *Physiology, The Natural History of Crustacea*. 4th ed. New York: Oxford University Press. 1-35.

Wetie, A. G. N., Sokolowska, I., Woods, A. G., Roy, U., Deinhardt, K. and Darie, C. C. (2014) Protein–protein interactions: switch from classical methods to proteomics and bioinformatics-based approaches, *Cellular and Molecular Life Sciences,* 71(2), 205-228.

Wen, F. S., White, G. J., Van Etten, H. D., Xiong, Z. G. and Hawes, M. C. (2009) Extracellular DNA is required for root tip resistance to fungal infection, *Plant Physiology*, 151(2), 820-829.

White, K. N. and Ratcliffe, N. A. (1982) The segregation and elimination of radio and fluorescent-labelled marine bacteria from the haemolymph of the shore crab, *Carcinus maenas, The Journal of the Marine Biological Association of the United Kingdom,* 62, 819–833.

Wiedow, O., Schroeder, J.-M., Gregory, H., Young, J.A. and Christophers, E. (1990) Elafin: an elastase-specific inhibitor of human skin. Purification, characterization, and complete amino acid sequence, *Journal of Biological Chemistry*, 265, 14791–14795

Wiedow, O., Harder, J., Bartels, J., Streit, V. and Christophers, E. (1998) Antileukoprotease in human skin: an antibiotic peptide constitutively produced by keratinocytes, *Biochemical and Biophysical Research Communications*, 248, 904–909.

Williams, S. E., Brown, T. I., Roghanian, A. and Sallenave, J. (2006) SLPI and elafin: one glove, many fingers, *Clinical Science*, 110 (1), 21-35.

Wootton, E.C., Dyrynda, E.A., Ratcliffe, N.A. (2006) Interaction between non-specific electrostatic forces and humoral factors in haemocyte attachment and encapsulation in the edible cockle, *Cerastoderma edule*, *Journal of Experimental Biology,* 209, 1326–1335.

Xu, W.-F., Qiao, K., Huang, S.-P., Peng, H., Huang, W.-S., Chen, B., Chen, F.-Y., Bo, J. and Wang, K.-J. (2011 a) Quantitative gene expression and *in situ* localization of

scygonadin potentially associated with reproductive immunity in tissues of male and female mud crabs, *Scylla paramamosain*, *Fish & Shellfish Immunology*, 31(2), 243-251.

Xu, W.-F., Qiao, K., Huang, S.-P., Peng, H., Huang, W.-S., Chen, F.-Y., Zhang, N., Wang, G.-Z. and Wang, K.-J. (2011 b) The expression pattern of scygonadin during the ontogenesis of *Scylla paramamosain* predicting its potential role in reproductive immunity, *Developmental & Comparative Immunology*, 35(10), 1078-1090.

Yang, L., Harroun, T. A., Weiss, T. M., Ding, L. and Huang, H.W. (2001) Barrel-stave model or toroidal model? A case study on melittin pores, *Biophysical Journal*, 81, 1475–1485.

Yenugu, S., Richardson, R. T., Sivashanmugam, P., Wang, Z., Michael, G., French, F. S. and Hall, S. H. (2004) Antimicrobial activity of human EPPIN, an androgen-regulated, sperm-bound protein with a whey acidic protein motif, *Biology of Reproduction*, 71, 1484-1490.

Yu, A.-Q., Shi, Y.-H. and Wang, Q. (2016) Characterisation of a novel type I crustin involved in antibacterial and antifungal responses in the red claw crayfish, *Cherax quadricarinatu*', *Fish & Shellfish Immunology*, 48, 30-38.

Yu, C. S., Chen, Y. C., Lu, C. H. and Hwang, J. K. (2006) Prediction of protein subcellular localization, *Proteins: Structure, Function and Bioinformatics*, 64, 643-651.

Yue, F., Pan, L., Xie, P., Zheng, D. and Li, J. (2010 a) Immune responses and expression of immune-related genes in swimming crab *Portunus trituberculatus* exposed to elevated ambient ammonia-N stress, *Comparative Biochemistry and Physiology Part A*, 157, 246–251.

Yue, F., Pan, L., Miao, J., Zhang, L. and Li, J. (2010 b) Molecular cloning, characterization and mRNA expression of two antibacterial peptides: crustin and anti-lipopolysaccharide factor in swimming crab *Portunus trituberculatus*, *Comparative Biochemistry and Physiology Part B: Biochemistry and Molecular Biology*, 156(2), 77-85.

Zabieglo, K., Majewski, P., Majchrzak-Gorecka, M., Wlodarczyk, A., Grygier, B., Zegar, A., Kapinska-Mrowiecka, M., Naskalska, A., Pyrc, K., Dubin, A., Wahl, S.M. and Cichy, J. (2015) The inhibitory effect of secretory leukocyte protease inhibitor (SLPI) on formation of neutrophil extracellular traps, *Journal of Leukocyte Biology*, 98(1), 99-106.

Zasloff, M. (1987) Magainins, a class of antimicrobial peptides from *Xenopus* skin: isolation, characterization of two active forms, and partial cDNA sequence of a precursor, *Proceedings of the National Academy of Sciences*, 84(15), 5449-5453.

Zeleny, C. (1905) Compensatory regulation, *Journal of Experimental Zoology*, 2, l-102.

Zhang, J., Li, F., Wang, Z. and Xiang, J. (2007 a) Cloning and recombinant expression of a crustin-like gene from Chinese shrimp, *Fenneropenaeus chinensis*, *Journal of Biotechnology*, 127(4), 605-614.

Zhang, J., Li, F., Wang, Z. and Xiang, J. (2007 b) Expression, purification, and characterization of recombinant Chinese shrimp crustin-like protein (Cru*Fc*) in *Pichia pastoris*, *Biotechnology Letters*, 29(5), 813-817.

Zhang, X., Zhuchenko, O., Kuspa, A. and Soldati, T. (2016) Social amoebae trap and kill bacteria by casting DNA nets, *Nature Communications*, 7, 10938.

Zhang, Y., Söderhäll, I., Söderhäll, K. and Jiravanichpaisal, K. (2010) Expression of immune-related genes in one phase of embryonic development of freshwater crayfish, *Pacifastacus leniusculus*, *Fish & Shellfish Immunology*, 28, 649-653.

Zhang, Z. and Zhu, S. (2012) Comparative genomics analysis of five families of antimicrobial peptide-like genes in seven ant species, *Developmental and Comparative Immunology*, 38, 262–274.

Zhu, J. and Hatton, D. (2016) New Mammalian Expression Systems, In: *Advances in Biochemical Engineering/Biotechnology*. Springer, Berlin, Heidelberg.

Zinchuk, V., Zinchuk, O. and Okada, T. (2007) Quantitative colocalization analysis of multicolor confocal immunofluorescence microscopy images: pushing pixels to explore biological phenomena, *Acta Histochemica et Cytochemica*, 40 (4): 101–111